March 2022

THE THERMOELECTRIC, THERMORESISTIVE, AND HYGRORESISTIVE PROPERTIES AND APPLICATIONS OF VAPOR PRINTED PEDOT-CL

Linden K. Allison
University of Massachusetts Amherst

THE THERMOELECTRIC, THERMORESISTIVE, AND HYGRORESISTIVE PROPERTIES AND APPLICATIONS OF VAPOR PRINTED PEDOT-CL

A Dissertation Presented

by

LINDEN KOHLER ALLISON

Submitted to the Graduate School of the

University of Massachusetts Amherst in partial fulfillment

of the requirements for the degree of

DOCTOR OF PHILOSOPHY

February 2022

Chemistry

THE THERMOELECTRIC, THERMORESISTIVE, AND HYGRORESISTIVE PROPERTIES AND APPLICATIONS OF VAPOR PRINTED PEDOT-CL

A Dissertation Presented

By

LINDEN KOHLER ALLISON

Approved as to style and content by:

_____

Trisha L. Andrew, Chair

_____

Dhandapani Venkataraman, Member

_____

Ricardo B. Metz, Member

_____

Zlatan Aksamija, Member

_____

Ricardo B. Metz, Department Head

Department of Chemistry

DEDICATION

To my family and my found family for being my greatest support system and giving me the motivation to achieve this momentous life goal.

ACKNOWLEDGEMENTS

I would like to thank my advisor, Trisha L. Andrew, for providing me with the opportunity to do this work. Because of her, I was able to become an independent researcher and a skilled scientist. She has truly taught me how to be a strong woman in the STEM field, which is the most valuable thing I could have gained from graduate school. Trisha, your intelligence, tenacity, and creativity are an inspiration and my time in your lab has helped mold the person that I am today. I am so thankful for all she has helped me accomplish.

I would also like to thank my committee members: Professor Dhandapani Venkataraman, Professor Ricardo B. Metz, and Professor Zlatan Aksamija. Your constructive critiques and experimental suggestions during each of my candidacy milestones has greatly strengthened my research. I am thankful for all of the time and energy you put into my work to help guide me down the path of success.

During my time in graduate school, I had the pleasure of working with members of the Sensor Lab run by Professor Deepak Ganesan. I would especially like to thank Soha Rostaminia, who worked with me to gain a large understanding of the properties of my work, and Ali Kiaghadi, who was essential in providing the technology for me to do our collaborative work.

I would like to thank the members of the DV lab who provided me with the equipment to take all of my thermoelectric measurements. Especially to Dr. Connor Boyle, Emily Smith, and Michael Lu-Diaz who gave me frequent help and guidance on my

research. And to Emily Smith and Hamza Javaid for acting as participants in my experiments.

Thank you to Kristine Isherwood who gave me the fantastic opportunity to take my research to the next level and create prototypes of my work. Your patience and passion allowed me to make great scientific strides and I am very appreciative for your trust and confidence in my science.

I was very fortunate to work with amazing people in the Wearable Electronics Laboratory. Without their support I would not be where I am today. They have taught me how to work closely and collaboratively with people every single day. Together, they created a kind and compassionate environment where I felt I could really thrive and shine. I am so thankful for all of the help, advice, and especially the tea. I can only hope I was able to return a fraction of the support they gave to me during my time in the lab. Thank you, from the bottom of my heart.

I have an incredible amount of gratitude towards my friends, both here at UMass and those scattered across the country. Laurel Watkins, you have instilled a sense of wonder in me that I carry into every part of my life. Haley Chandler, your compassion, support, and humor have gotten me through my hardest and happiest moments. Stevie Kitching, you have given me a sense of adventure that is one of the brightest parts of my life. And lastly, Emily Smith, I don't have enough words to describe how important you are to me and my journey. I would not have gotten through this experience without you.

I would like to give a huge thank-you to my family. My sister, Clara, and my brother, Braden, have given me the inspiration and drive that led me to pursue higher education. My parents, Amy and Steve, have instilled me with a sese of pride in my work.

My entire family has pushed me to challenge myself intellectually for my entire life, and I would never have made it to grad school if it were not for them. Thank you, so much.

Finally, I would like to thank my cat, Gus. Who didn't really contribute anything to my research, but I love him very much.

ABSTRACT

THE THERMOELECTRIC, THERMORESISTIVE, AND HYGRORESISTIVE PROPERTIES AND APPLICATIONS OF VAPOR PRINTED PEDOT-CL

FEBRUARY 2022

LINDEN KOHLER ALLISON

B.S., JUNIATA COLLEGE

Ph.D., UNIVERSITY OF MASSACHUSETTS AMHERST

Directed by: Professor Trisha L. Andrew

Wearable electronics are a valuable tool to increase consumer access to real-time and long-term health care monitoring. The development of these technologies can also lead to major advancements in the field, such as self-charging systems that are completely removed from the electrical grid. However, much of the wearable technology available commercially contain rigid components, use unsustainable synthetic methods, or undesirable materials. The field has thus been moving towards wearables that mimic textiles or use textiles as a substrate. Herein, we discuss the use of oxidative chemical vapor deposition (oCVD) to produce textiles coated with poly(3,4-ethylenedioxythiophene) known as PEDOT-Cl. We evaluate the thermoelectric, thermoresistive, and hygroresistive properties of these PEDOT-Cl fabrics. We also explore the applications of these properties by creating humidity sensors, temperature sensors, and thermoelectric generators integrated with clothing. In general, we discuss the process of designing a wearable to best accommodate the desired application.

TABLE OF CONTENTS

Page

LIST OF FIGURES

Figure Page

Chapter 1

INTRODUCTION

1.1 Introduction to Wearable Electronics

The advancement of wearable technologies and their integration with long-term and continuous health monitoring has created a promising nascent means for in-home health care.[1–8] Providing people with a way of monitoring their health without the restraints of being in a medical facility allows for a functional option for providing healthcare to a large variety of patients.[9] Sensors, energy harvesters, and power delivery lines have been creatively miniaturized for the purpose of creating self-charging systems that are removed from the power grid entirely, however translating these circuit components into a comfortable and wearable form still proves challenging.[4,10–16] Much of the available wearable technologies on the market still include bulky or rigid components, which can cause discomfort for the consumer.[17–24]

In recent years, the field has started to investigate wearable electronics that either mimic fabrics and fibers or are produced directly on the surface of textiles providing a promising method of increasing consumer comfort.[25–61] However, incorporation of electronic materials into fabric has still proven to be a significant challenge. For example, Grunlan et.al. used a solution spinning technique to produce fibers out of carbon nanotubes (CNT). These fibers demonstrated ultrahigh conductivity (16 ± 3 MS m^{-1}) which enabled a very high thermoelectric efficiency (14 ± 5 mW m^{-1} K^{-2}), shown in Figure 1.1 a.[61] However, CNTs have recently been added to the Substitute In Now (SIN) list due to associated health risks with causing lung cancer.[62] Thus, CNTs should be avoided in

applications such as wearables where users will be in contact with this material. The biocompatibility of the spun CNT fibers has not been reported.

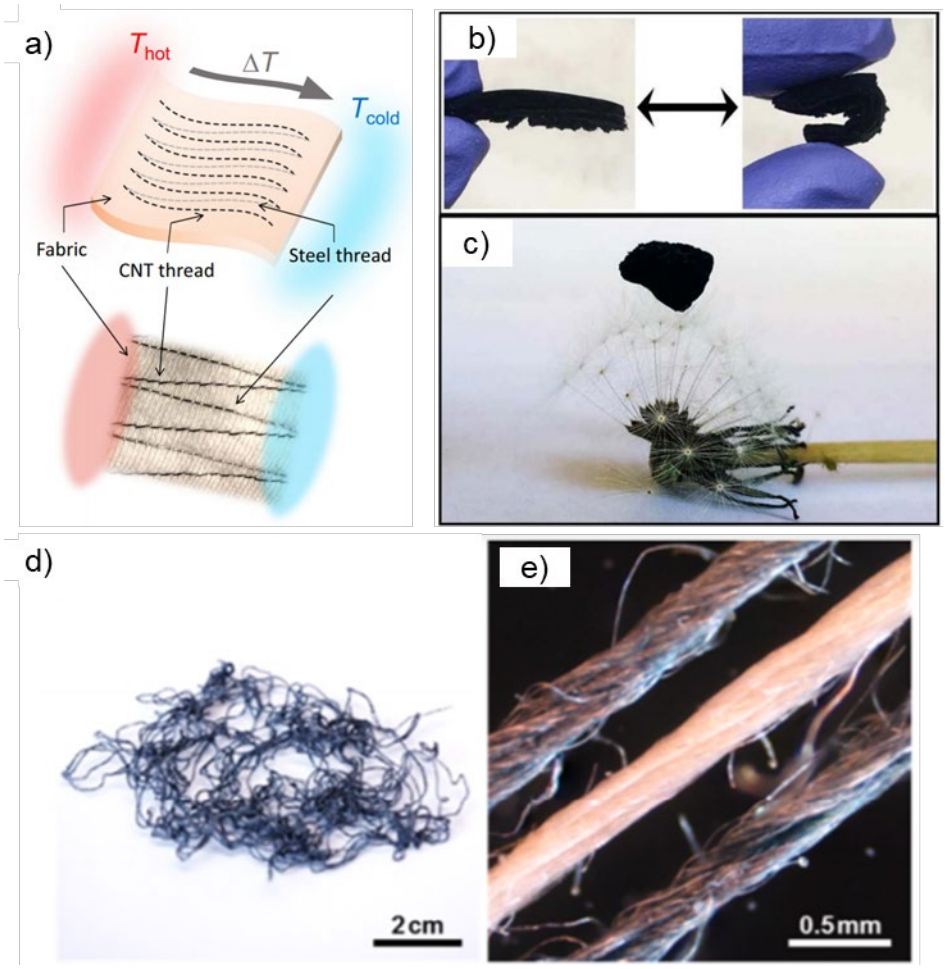

Figure 1.1. a) Thermoelectric Generator design of CNT threads and steel threads reported by Grunlan et.al. b and c) images of PEDOT:PSS aerogel reported by Urban et.al. d and e) bundle and optical microscopy image of PEDOT:PSS dyed silk yarns, respectively, reported by Muller et.al.

Urban et.al. synthesized an aerogel from Poly(3,4-ethylenedioxythiophene), polystyrene sulfonate (PEDOT:PSS) that mimics a porous textile, such as a felt or foam, shown in Figure 1.1 b-c. These aerogels exhibited high thermoelectric power factors (6.8

$\mu W\ m^{-1}\ K^{-2}$) that indicate the efficiencies are not depended on the macroscopic structure. Although, the mechanical and wash stability was not reported and is imperative to create functional electronic textiles.[63]

Alternatively, Muller et.al. reported an electronically enabled textiles through dyeing silk yarn with PEDOT:PSS with a conductivity of 14 S cm^{-1} shown in Figure 1.1 d-e. In order to create the multilayer film on the fibers, a time consuming process of dipping the yarns into acidic (pH 2) solutions of PEDOT:PSS was used. The process was also attempted on cotton fibers, however these samples suffered hydrolysis of the cellulose in the acidic solution and became too brittle to handle.[33] Because of this the scalability and versatility of this technique is quite limited.

It is evident from these issues that a technique is needed to create robust and efficient electronic fabrics that can be made into comfortable wearable devices such as sensors and energy harvesters. This technique should be versatile enough to facilitate the coating of many types of materials and substrates for various applications. Herein, we discuss the fabrication of electronic textiles through chemical vapor deposition (CVD).

1.2 Conductive Polymers

One viable means of creating electronic textiles is to coat or impregnate a textile with a conductive polymer. While many polymers have been studied, the most widely explored is currently PEDOT:PSS. PEDOT:PSS is produced through the polymerization of EDOT in the presence of an aqueous polyelectrolyte (PSS) creating a polymer with a small molecule counterion and enabling the final polymer to be dispersed in water.[64] By

utilizing a conductive polymer that can be dispersed in water, one can use traditional textile processing methods, such as dyeing to create a polymer coating on a textile.[26,33,41,59,60,65]

PEDOT:PSS shares many similar properties and applications to the polymer explored in this work, PEDOT-Cl. PEDOT:PSS exhibits hygroresistive, thermoresistive, and thermoelectric properties.[66–70] It is characterized as a mixed ionic-electronic conductor as a portion of its conductivity is derived from an ionic conductivity.[71]

PEDOT:PSS has been coated onto textiles using a dip-coating technique, that requires multiple coating to be applied to the textile and can be time consuming. These polymer-coated textiles result in non-uniform coatings, agglomeration of the polymer between the textile fibers, and can be prone to microcrack and delamination upon bending or abrasion. Furthermore, PEDOT:PSS contains acidic moieties that can lead to skin irritation and degradation of natural fibers.[31]

Additionally, it is important to consider the environmental impacts of creating these PEDOT:PSS coated textiles on a large scale. The textile industry already produces a significant amount of chemical waste during the processing of fabrics.[72,73] Most dip-coating techniques require several layers of PEDOT:PSS coating and specific pre-treatment or post-treatment of the coated textile. When scaled up these techniques will add a significant amount of chemical waste to this process.

Using PEDOT that is synthesized through different techniques can allow us to obtain a highly efficient polymer without the need of insulating counterions such as PSS. Techniques like chemical vapor deposition can functionalize fabrics with PEDOT coatings not containing insulating molecules. Thus, we can study the characteristics of PEDOT coated fabrics without the drawbacks associated with PEDOT:PSS. The CVD technique is

easily scaled up and produces less chemical waste than dyeing techniques, allowing for a more environmentally friendly way of producing conductive textiles.[74–80]

1.3 Electronic Properties of PEDOT

Conductive polymers have electronic, mechanical, photovoltaic, and thermoelectric properties that make them attractive for both academic research and use in industry. PEDOT is one of the most popular conductive polymers when it comes to applications due to its high conductivity. The polymer has also been found to be stable in ambient conditions and thus an ideal choice for developing robust products.[81]

PEDOT demonstrates properties making them suitable for use in health monitoring applications, such as having a temperature dependent resistance, known as thermoresistivity, and a moisture dependent resistance, known as hygroresistivity. It is also capable of generating a thermopower through the thermoelectric nature of the polymer. This work will concentrate on exploring these three properties and their applications.

1.4 The Thermoelectric Effect

Before discussing the experimental findings of the work, it is important to first understand the fundamental principles on which some devices in this work rely upon. The thermoelectric effect is a phenomenon that occurs in materials with high electrical conductivities and low thermal conductivities. When these materials are exposed to a temperature gradient a migration of charges is induced to balance the energy dispersion,

resulting in an electromotive force referred to as the Seebeck voltage. The Seebeck coefficient can be defined by :

Equation 1.1

$$S = \left(\frac{dV}{dT}\right)_{I=0} \qquad where\ \ \Delta T = T_H - T_C$$

where *dV* is the measured voltage output and *dT* is the difference in temperature between the hot side (T_H) and the cold side (T_C) of the material being measured. Furthermore, the efficiency can be expanded upon through the power factor (PF):

$$PF = S^2\sigma$$

where σ is the conductivity of the material. The PF provides a more observable value when evaluating the material's thermoelectric efficiencies.

When two types of thermoelectric materials with different efficiencies are connected, they form a device called a thermoelectric generator (TEG) (Figure 1.2) which can be used to harvest the charges accumulating at the ends of the thermoelectric material, creating a power source.[82–98]

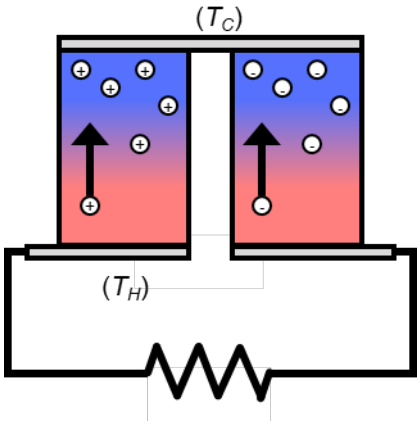

1.5 Dissertation Overview

The goal of this thesis work is to investigate the properties and applications of robust conductive fabrics for use in a variety of wearable health monitoring systems. Chapter 2 describes the synthesis of the conductive polymer PEDOT-Cl on the surface of textiles using CVD. Next, Chapter 3 depicts the hygroresistive properties, the humidity dependent resistance, of the polymer coated fabrics, wherein a humidity sensor is created and integrated into a face mask to enable respiration monitoring. Following this, Chapter 4 describes the thermoresistive properties, the temperature dependent resistance, of the polymer coated fabrics and details how these properties can be tuned through substrate choice. Finally, Chapter 5 shows the thermoelectric properties of the polymer coated fabrics, which are then used to create energy harvesting devices and subsequently integrated into a variety of garments.

1.6 References

(1) Patel, S.; Park, H.; Bonato, P.; Chan, L.; Rodgers, M. A Review of Wearable Sensors and Systems with Application in Rehabilitation. J. NeuroEngineering Rehabil. 2012, 9, 21. https://doi.org/10.1186/1743-0003-9-21.

(2) Herbert, R.; Jeong, J.-W.; Yeo, W.-H. Soft Material-Enabled Electronics for Medicine, Healthcare, and Human-Machine Interfaces. Materials 2020, 13 (3), 517. https://doi.org/10.3390/ma13030517.

(3) Son, D.; Lee, J.; Qiao, S.; Ghaffari, R.; Kim, J.; Lee, J. E.; Song, C.; Kim, S. J.; Lee, D. J.; Jun, S. W.; Yang, S.; Park, M.; Shin, J.; Do, K.; Lee, M.; Kang, K.; Hwang, C. S.; Lu, N.; Hyeon, T.; Kim, D.-H. Multifunctional Wearable Devices for Diagnosis and Therapy of Movement Disorders. Nat. Nanotechnol. 2014, 9 (5), 397–404. https://doi.org/10.1038/nnano.2014.38.

(4) Jung, S.; Hong, S.; Kim, J.; Lee, S.; Hyeon, T.; Lee, M.; Kim, D.-H. Wearable Fall Detector Using Integrated Sensors and Energy Devices. Sci. Rep. 2015, 5 (1), 17081. https://doi.org/10.1038/srep17081.

(5) Merritt, C. R.; Troy Nagle, H.; Grant, E. Fabric-Based Active Electrode Design and Fabrication for Health Monitoring Clothing. IEEE Trans. Inf. Technol. Biomed. 2009, 13 (2), 274–280. https://doi.org/10.1109/TITB.2009.2012408.
(6) Pang, Y.; Jian, J.; Tu, T.; Yang, Z.; Ling, J.; Li, Y.; Wang, X.; Qiao, Y.; Tian, H.; Yang, Y.; Ren, T.-L. Wearable Humidity Sensor Based on Porous Graphene Network for Respiration Monitoring. Biosens. Bioelectron. 2018, 116, 123–129. https://doi.org/10.1016/j.bios.2018.05.038.
(7) Dinh, T.; Nguyen, T.; Phan, H.-P.; Nguyen, N.-T.; Dao, D. V.; Bell, J. Stretchable Respiration Sensors: Advanced Designs and Multifunctional Platforms for Wearable Physiological Monitoring. Biosens. Bioelectron. 2020, 166, 112460. https://doi.org/10.1016/j.bios.2020.112460.
(8) Wang, Y.; Zhang, L.; Zhang, Z.; Sun, P.; Chen, H. High-Sensitivity Wearable and Flexible Humidity Sensor Based on Graphene Oxide/Non-Woven Fabric for Respiration Monitoring. Langmuir 2020, 36 (32), 9443–9448. https://doi.org/10.1021/acs.langmuir.0c01315.
(9) Hughes-Riley, T.; Dias, T.; Cork, C. A Historical Review of the Development of Electronic Textiles. Fibers 2018, 6 (2), 34. https://doi.org/10.3390/fib6020034.
(10) Pu Xiong; Hu Weiguo; Wang Zhong Lin. Toward Wearable Self-Charging Power Systems: The Integration of Energy-Harvesting and Storage Devices. Small 2017, 14 (1), 1702817. https://doi.org/10.1002/smll.201702817.
(11) Fan Feng Ru; Tang Wei; Wang Zhong Lin. Flexible Nanogenerators for Energy Harvesting and Self-Powered Electronics. Adv. Mater. 2016, 28 (22), 4283–4305. https://doi.org/10.1002/adma.201504299.
(12) Kim, M. K.; Kim, M. S.; Jo, S. E.; Kim, H. L.; Lee, S. M.; Kim, Y. J. Wearable Thermoelectric Generator for Human Clothing Applications. In 2013 Transducers Eurosensors XXVII: The 17th International Conference on Solid-State Sensors, Actuators and Microsystems (TRANSDUCERS EUROSENSORS XXVII); 2013; pp 1376–1379. https://doi.org/10.1109/Transducers.2013.6627034.
(13) Hussain, A. M.; Ghaffar, F. A.; Park, S. I.; Rogers, J. A.; Shamim, A.; Hussain, M. M. Metal/Polymer Based Stretchable Antenna for Constant Frequency Far-Field Communication in Wearable Electronics. Adv. Funct. Mater. 2015, 25 (42), 6565–6575. https://doi.org/10.1002/adfm.201503277.
(14) Vilkhu, R.; Thio, W. J.-C.; Das Ghatak, P.; Sen, C. K.; Co, A. C.; Kiourti, A. Power Generation for Wearable Electronics: Designing Electrochemical Storage on Fabrics. IEEE Access 2018, 6, 28945–28950. https://doi.org/10.1109/ACCESS.2018.2839078.
(15) Vilkhu, R.; DeLong, B.; Kiourti, A.; Das Ghatak, P.; Mathew-Steiner, S.; Sen, C. K. Power Harvesting for Wearable Electronics Using Fabric Electrochemistry. In 2017 IEEE International Symposium on Antennas and Propagation USNC/URSI National Radio Science Meeting; 2017; pp 213–214. https://doi.org/10.1109/APUSNCURSINRSM.2017.8072149.
(16) Li, J.; Xin, M.; Ma, Z.; Shi, Y.; Pan, L. Nanomaterials and Their Applications on Bio-Inspired Wearable Electronics. Nanotechnology 2021, 32 (47), 472002. https://doi.org/10.1088/1361-6528/abe6c7.

(17) Wu, H.; Huang, Y.; Xu, F.; Duan, Y.; Yin, Z. Energy Harvesters for Wearable and Stretchable Electronics: From Flexibility to Stretchability. Adv. Mater. 2016, 28 (45), 9881–9919. https://doi.org/10.1002/adma.201602251.
(18) Siddique, A. R. M.; Mahmud, S.; Heyst, B. V. A Review of the State of the Science on Wearable Thermoelectric Power Generators (TEGs) and Their Existing Challenges. Renew. Sustain. Energy Rev. 2017, 73, 730–744. https://doi.org/10.1016/j.rser.2017.01.177.
(19) Lugoda, P.; Hughes-Riley, T.; Morris, R.; Dias, T. A Wearable Textile Thermograph. Sensors 2018, 18 (7). https://doi.org/10.3390/s18072369.
(20) Fan, X.; Liu, B.; Ding, J.; Deng, Y.; Han, X.; Hu, W.; Zhong, C. Flexible and Wearable Power Sources for Next-Generation Wearable Electronics. Batter. Supercaps 2020, 3 (12), 1262–1274. https://doi.org/10.1002/batt.202000115.
(21) Zhong, J.; Zhang, Y.; Zhong, Q.; Hu, Q.; Hu, B.; Wang, Z. L.; Zhou, J. Fiber-Based Generator for Wearable Electronics and Mobile Medication. ACS Nano 2014, 8 (6), 6273–6280. https://doi.org/10.1021/nn501732z.
(22) Zeng, W.; Shu, L.; Li, Q.; Chen, S.; Wang, F.; Tao, X.-M. Fiber-Based Wearable Electronics: A Review of Materials, Fabrication, Devices, and Applications. Adv. Mater. 2014, 26 (31), 5310–5336. https://doi.org/10.1002/adma.201400633.
(23) Qiu, Q.; Zhu, M.; Li, Z.; Qiu, K.; Liu, X.; Yu, J.; Ding, B. Highly Flexible, Breathable, Tailorable and Washable Power Generation Fabrics for Wearable Electronics. Nano Energy 2019, 58, 750–758. https://doi.org/10.1016/j.nanoen.2019.02.010.
(24) Ling, Y.; An, T.; Yap, L. W.; Zhu, B.; Gong, S.; Cheng, W. Disruptive, Soft, Wearable Sensors. Adv. Mater. 2020, 32 (18), 1904664. https://doi.org/10.1002/adma.201904664.
(25) Qu, H.; Semenikhin, O.; Skorobogatiy, M. Flexible Fiber Batteries for Applications in Smart Textiles. Smart Mater. Struct. 2015, 24 (2), 025012. https://doi.org/10.1088/0964-1726/24/2/025012.
(26) Wu, Q.; Hu, J. Waterborne Polyurethane Based Thermoelectric Composites and Their Application Potential in Wearable Thermoelectric Textiles. Compos. Part B Eng. 2016, 107, 59–66. https://doi.org/10.1016/j.compositesb.2016.09.068.
(27) Hu, E.; Kaynak, A.; Li, Y. Development of a Cooling Fabric from Conducting Polymer Coated Fibres: Proof of Concept. Synth. Met. 2005, 150 (2), 139–143. https://doi.org/10.1016/j.synthmet.2005.01.018.
(28) Leonov, V. Thermoelectric Energy Harvesting of Human Body Heat for Wearable Sensors. IEEE Sens. J. 2013, 13 (6), 2284–2291. https://doi.org/10.1109/JSEN.2013.2252526.
(29) Jafar-Zanjani, S.; Salary, M. M.; Mosallaei, H. Metafabrics for Thermoregulation and Energy-Harvesting Applications. ACS Photonics 2017, 4 (4), 915–927. https://doi.org/10.1021/acsphotonics.6b01005.
(30) Zhang, L.; Baima, M.; Andrew, T. L. Transforming Commercial Textiles and Threads into Sewable and Weavable Electric Heaters. ACS Appl. Mater. Interfaces 2017, 9 (37), 32299–32307. https://doi.org/10.1021/acsami.7b10514.
(31) Allison, L.; Hoxie, S.; Andrew, T. L. Towards Seamlessly-Integrated Textile Electronics: Methods to Coat Fabrics and Fibers with Conducting Polymers for

Electronic Applications. Chem. Commun. 2017, 53 (53), 7182–7193. https://doi.org/10.1039/C7CC02592K.

(32) Zhang Lushuai; Fairbanks Marianne; Andrew Trisha L. Rugged Textile Electrodes for Wearable Devices Obtained by Vapor Coating Off-the-Shelf, Plain-Woven Fabrics. Adv. Funct. Mater. 2017, 27 (24), 1700415. https://doi.org/10.1002/adfm.201700415.

(33) Ryan, J. D.; Mengistie, D. A.; Gabrielsson, R.; Lund, A.; Müller, C. Machine-Washable PEDOT:PSS Dyed Silk Yarns for Electronic Textiles. ACS Appl. Mater. Interfaces 2017, 9 (10), 9045–9050. https://doi.org/10.1021/acsami.7b00530.

(34) Wawro, D.; Stęplewski, W. Producing of Continuous Cellulose Fibres Modified with Plant Proteins. Fibres Text. East. Eur. 2010, Nr 6 (83).

(35) Knittel, D.; Schollmeyer, E. Electrically High-Conductive Textiles. Synth. Met. 2009, 159 (14), 1433–1437. https://doi.org/10.1016/j.synthmet.2009.03.021.

(36) Ding, Y.; Invernale, M. A.; Sotzing, G. A. Conductivity Trends of PEDOT-PSS Impregnated Fabric and the Effect of Conductivity on Electrochromic Textile. ACS Appl. Mater. Interfaces 2010, 2 (6), 1588–1593. https://doi.org/10.1021/am100036n.

(37) Lee, J. A.; Aliev, A. E.; Bykova, J. S.; Andrade, M. J. de; Kim, D.; Sim, H. J.; Lepró, X.; Zakhidov, A. A.; Lee, J.-B.; Spinks, G. M.; Roth, S.; Kim, S. J.; Baughman, R. H. Woven-Yarn Thermoelectric Textiles. Adv. Mater. 2016, 28 (25), 5038–5044. https://doi.org/10.1002/adma.201600709.

(38) Jung, S.; Lauterbach, C.; Strasser, M.; Weber, W. Enabling Technologies for Disappearing Electronics in Smart Textiles. In 2003 IEEE International Solid-State Circuits Conference, 2003. Digest of Technical Papers. ISSCC.; 2003; pp 386–387 vol.1. https://doi.org/10.1109/ISSCC.2003.1234347.

(39) Glampedaki, P.; Calvimontes, A.; Dutschk, V.; Warmoeskerken, M. M. C. G. Polyester Textile Functionalization through Incorporation of PH/Thermo-Responsive Microgels. Part II: Polyester Functionalization and Characterization. J. Mater. Sci. 2012, 47 (5), 2078–2087. https://doi.org/10.1007/s10853-011-6006-6.

(40) Husain, M. D.; Kennon, R.; Dias, T. Design and Fabrication of Temperature Sensing Fabric. J. Ind. Text. 2014, 44 (3), 398–417. https://doi.org/10.1177/1528083713495249.

(41) Lee, J.-W.; Han, D.-C.; Shin, H.-J.; Yeom, S.-H.; Ju, B.-K.; Lee, W. PEDOT:PSS-Based Temperature-Detection Thread for Wearable Devices. Sensors 2018, 18 (9). https://doi.org/10.3390/s18092996.

(42) Castano, L. M.; Flatau, A. B. Smart Fabric Sensors and E-Textile Technologies: A Review. Smart Mater. Struct. 2014, 23 (5), 053001. https://doi.org/10.1088/0964-1726/23/5/053001.

(43) Bhat, N. V.; Seshadri, D. T.; Nate, M. M.; Gore, A. V. Development of Conductive Cotton Fabrics for Heating Devices. J. Appl. Polym. Sci. 2006, 102 (5), 4690–4695. https://doi.org/10.1002/app.24708.

(44) Bielska, S.; Sibinski, M.; Lukasik, A. Polymer Temperature Sensor for Textronic Applications. Mater. Sci. Eng. B 2009, 165 (1), 50–52. https://doi.org/10.1016/j.mseb.2009.07.014.

(45) Enzo Pasquale Scilingo; Lorussi, F.; Mazzoldi, A.; De Rossi, D. Strain-Sensing Fabrics for Wearable Kinaesthetic-like Systems. IEEE Sens. J. 2003, 3 (4), 460–467. https://doi.org/10.1109/JSEN.2003.815771.
(46) He, Y.; Gui, Q.; Liao, S.; Jia, H.; Wang, Y. Coiled Fiber-Shaped Stretchable Thermal Sensors for Wearable Electronics. Adv. Mater. Technol. 2016, 1 (8), 1600170. https://doi.org/10.1002/admt.201600170.
(47) Kim, J.; Cho, G. Thermal Storage/Release, Durability, and Temperature Sensing Properties of Thermostatic Fabrics Treated with Octadecane-Containing Microcapsules. Text. Res. J. 2002, 72 (12), 1093–1098. https://doi.org/10.1177/004051750207201209.
(48) Lim, Z. H.; Chia, Z. X.; Kevin, M.; Wong, A. S. W.; Ho, G. W. A Facile Approach towards ZnO Nanorods Conductive Textile for Room Temperature Multifunctional Sensors. Sens. Actuators B Chem. 2010, 151 (1), 121–126. https://doi.org/10.1016/j.snb.2010.09.037.
(49) Sibinski, M.; Jakubowska, M.; Sloma, M. Flexible Temperature Sensors on Fibers. Sensors 2010, 10 (9), 7934–7946. https://doi.org/10.3390/s100907934.
(50) Ramachandran, T.; Vigneswaran, C. Design and Development of Copper Core Conductive Fabrics for Smart Textiles. J. Ind. Text. 2009, 39 (1), 81–93. https://doi.org/10.1177/1528083709103317.
(51) Hughes-Riley, T.; Lugoda, P.; Dias, T.; Trabi, C. L.; Morris, R. H. A Study of Thermistor Performance within a Textile Structure. Sensors 2017, 17 (8). https://doi.org/10.3390/s17081804.
(52) Agcayazi, T.; Chatterjee, K.; Bozkurt, A.; Ghosh, T. K. Flexible Interconnects for Electronic Textiles. Adv. Mater. Technol. 2018, 3 (10), 1700277. https://doi.org/10.1002/admt.201700277.
(53) Yang, J.-H.; Cho, H.-S.; Kwak, H.; Chae, J.-W.; Lee, H.-J.; Lee, J.-W.; Oh, S.; Lee, J.-H. Sensing Efficiency of Three-Dimensional Textile Sensors with an Open-and-Close Structure for Respiration Rate Detection. Text. Res. J. 2020, 90 (19–20), 2258–2274. https://doi.org/10.1177/0040517520915846.
(54) Catarino, A.; Carvalho, H.; Dias, M. J.; Pereira, T.; Postolache, O.; Girão, P. S. Continuous Health Monitoring Using E-Textile Integrated Biosensors. In 2012 International Conference and Exposition on Electrical and Power Engineering; 2012; pp 605–609. https://doi.org/10.1109/ICEPE.2012.6463867.
(55) Carvalho, H.; Catarino, A. P.; Rocha, A.; Postolache, O. Health Monitoring Using Textile Sensors and Electrodes: An Overview and Integration of Technologies. In 2014 IEEE International Symposium on Medical Measurements and Applications (MeMeA); 2014; pp 1–6. https://doi.org/10.1109/MeMeA.2014.6860033.
(56) Rai, P.; Kumar, P. S.; Oh, S.; Kwon, H.; Mathur, G. N.; Varadan, V. K.; Agarwal, M. P. Smart Healthcare Textile Sensor System for Unhindered-Pervasive Health Monitoring. In Nanosensors, Biosensors, and Info-Tech Sensors and Systems 2012; International Society for Optics and Photonics, 2012; Vol. 8344, p 83440E. https://doi.org/10.1117/12.921253.
(57) Rai, P.; Oh, S.; Shyamkumar, P.; Ramasamy, M.; Harbaugh, R. E.; Varadan, V. K. Nano- Bio- Textile Sensors with Mobile Wireless Platform for Wearable Health Monitoring of Neurological and Cardiovascular Disorders. J. Electrochem. Soc. 2013, 161 (2), B3116. https://doi.org/10.1149/2.012402jes.

(58) Kiaghadi, A.; Homayounfar, S. Z.; Gummeson, J.; Andrew, T.; Ganesan, D. Phyjama: Physiological Sensing via Fiber-Enhanced Pyjamas. Proc. ACM Interact. Mob. Wearable Ubiquitous Technol. 2019, 3 (3), 89:1-89:29. https://doi.org/10.1145/3351247.
(59) Lund, A.; Tian, Y.; Darabi, S.; Müller, C. A Polymer-Based Textile Thermoelectric Generator for Wearable Energy Harvesting. J. Power Sources 2020, 480, 228836. https://doi.org/10.1016/j.jpowsour.2020.228836.
(60) Elmoughni, H. M.; Menon, A. K.; Wolfe, R. M. W.; Yee, S. K. A Textile-Integrated Polymer Thermoelectric Generator for Body Heat Harvesting. Adv. Mater. Technol. 2019, 4 (7), 1800708. https://doi.org/10.1002/admt.201800708.
(61) Komatsu, N.; Ichinose, Y.; Dewey, O. S.; Taylor, L. W.; Trafford, M. A.; Yomogida, Y.; Wehmeyer, G.; Pasquali, M.; Yanagi, K.; Kono, J. Macroscopic Weavable Fibers of Carbon Nanotubes with Giant Thermoelectric Power Factor. Nat. Commun. 2021, 12 (1), 4931. https://doi.org/10.1038/s41467-021-25208-z.
(62) Carbon Nanotubes.
(63) Gordon, M. P.; Zaia, E. W.; Zhou, P.; Russ, B.; Coates, N. E.; Sahu, A.; Urban, J. J. Soft PEDOT:PSS Aerogel Architectures for Thermoelectric Applications. J. Appl. Polym. Sci. 2017, 134 (3). https://doi.org/10.1002/app.44070.
(64) Elschner, A.; Kirchmeyer, S.; Lovenich, W.; Merker, U.; Reuter, K. PEDOT: Principles and Applications of an Intrinsically Conductive Polymer; CRC Press, 2010.
(65) Åkerfeldt, M.; Strååt, M.; Walkenström, P. Influence of Coating Parameters on Textile and Electrical Properties of a Poly(3,4-Ethylene Dioxythiophene):Poly(Styrene Sulfonate)/Polyurethane-Coated Textile. Text. Res. J. 2013, 83 (20), 2164–2176. https://doi.org/10.1177/0040517513487786.
(66) Luo, J.; Billep, D.; Waechtler, T.; Otto, T.; Toader, M.; Gordan, O.; Sheremet, E.; Martin, J.; Hietschold, M.; Zahn, D. R. T.; Gessner, T. Enhancement of the Thermoelectric Properties of PEDOT:PSS Thin Films by Post-Treatment. J. Mater. Chem. A 2013, 1 (26), 7576–7583. https://doi.org/10.1039/C3TA11209H.
(67) Zhu, Z.; Liu, C.; Jiang, F.; Xu, J.; Liu, E. Effective Treatment Methods on PEDOT:PSS to Enhance Its Thermoelectric Performance. Synth. Met. 2017, 225, 31–40. https://doi.org/10.1016/j.synthmet.2016.11.011.
(68) Bubnova, O.; Crispin, X. Towards Polymer-Based Organic Thermoelectric Generators. Energy Environ. Sci. 2012, 5 (11), 9345–9362. https://doi.org/10.1039/C2EE22777K.
(69) Ail, U.; Jafari, M. J.; Wang, H.; Ederth, T.; Berggren, M.; Crispin, X. Thermoelectric Properties of Polymeric Mixed Conductors. Adv. Funct. Mater. 2016, 26 (34), 6288–6296. https://doi.org/10.1002/adfm.201601106.
(70) Daoud, W. A.; Xin, J. H.; Szeto, Y. S. Polyethylenedioxythiophene Coatings for Humidity, Temperature and Strain Sensing Polyamide Fibers. Sens. Actuators B Chem. 2005, 109 (2), 329–333. https://doi.org/10.1016/j.snb.2004.12.067.
(71) Wang, H.; Ail, U.; Gabrielsson, R.; Berggren, M.; Crispin, X. Ionic Seebeck Effect in Conducting Polymers. Adv. Energy Mater. 2015, 5 (11), 1500044. https://doi.org/10.1002/aenm.201500044.
(72) Verma, A. K.; Dash, R. R.; Bhunia, P. A Review on Chemical Coagulation/Flocculation Technologies for Removal of Colour from Textile

Wastewaters. J. Environ. Manage. 2012, 93 (1), 154–168. https://doi.org/10.1016/j.jenvman.2011.09.012.
(73) Kant, R. Textile Dyeing Industry an Environmental Hazard. Nat. Sci. 2011, 04 (01), 22. https://doi.org/10.4236/ns.2012.41004.
(74) Chelawat, H.; Vaddiraju, S.; Gleason, K. Conformal, Conducting Poly(3,4-Ethylenedioxythiophene) Thin Films Deposited Using Bromine as the Oxidant in a Completely Dry Oxidative Chemical Vapor Deposition Process. Chem. Mater. 2010, 22 (9), 2864–2868. https://doi.org/10.1021/cm100092c.
(75) Goktas, H.; Wang, X.; Boscher, N. D.; Torosian, S.; Gleason, K. K. Functionalizable and Electrically Conductive Thin Films Formed by Oxidative Chemical Vapor Deposition (OCVD) from Mixtures of 3-Thiopheneethanol (3TE) and Ethylene Dioxythiophene (EDOT). J. Mater. Chem. C 2016, 4 (16), 3403–3414. https://doi.org/10.1039/C6TC00567E.
(76) Goktas, H.; Wang, X.; Ugur, A.; Gleason, K. K. Water-Assisted Vapor Deposition of PEDOT Thin Film. Macromol. Rapid Commun. 2015, 36 (13), 1283–1289. https://doi.org/10.1002/marc.201500069.
(77) Chen, N.; Kim, D. H.; Kovacik, P.; Sojoudi, H.; Wang, M.; Gleason, K. K. Polymer Thin Films and Surface Modification by Chemical Vapor Deposition: Recent Progress. Annu. Rev. Chem. Biomol. Eng. 2016, 7 (1), 373–393. https://doi.org/10.1146/annurev-chembioeng-080615-033524.
(78) Chen, N.; Wang, X.; Gleason, K. K. Conformal Single-Layer Encapsulation of PEDOT at Low Substrate Temperature. Appl. Surf. Sci. 2014, 323, 2–6. https://doi.org/10.1016/j.apsusc.2014.06.123.
(79) Tenhaeff Wyatt E.; Gleason Karen K. Initiated and Oxidative Chemical Vapor Deposition of Polymeric Thin Films: ICVD and OCVD. Adv. Funct. Mater. 2008, 18 (7), 979–992. https://doi.org/10.1002/adfm.200701479.
(80) Wang, X.; Zhang, X.; Sun, L.; Lee, D.; Lee, S.; Wang, M.; Zhao, J.; Shao-Horn, Y.; Dincă, M.; Palacios, T.; Gleason, K. K. High Electrical Conductivity and Carrier Mobility in OCVD PEDOT Thin Films by Engineered Crystallization and Acid Treatment. Sci. Adv. 2018, 4 (9), eaat5780. https://doi.org/10.1126/sciadv.aat5780.
(81) Gueye, M. N.; Carella, A.; Faure-Vincent, J.; Demadrille, R.; Simonato, J.-P. Progress in Understanding Structure and Transport Properties of PEDOT-Based Materials: A Critical Review. Prog. Mater. Sci. 2020, 108, 100616. https://doi.org/10.1016/j.pmatsci.2019.100616.
(82) Stepien, L.; Roch, A.; Tkachov, R.; Gedrange, T. Progress in Polymer Thermoelectrics. 2016. https://doi.org/10.5772/66196.
(83) Wang, J.; Cai, K.; Shen, S. A Facile Chemical Reduction Approach for Effectively Tuning Thermoelectric Properties of PEDOT Films. Org. Electron. 2015, 17 (Supplement C), 151–158. https://doi.org/10.1016/j.orgel.2014.12.007.
(84) Snyder, G. J.; Toberer, E. S. Complex Thermoelectric Materials. Nat. Mater. 2008, 7 (2), 105–114. https://doi.org/10.1038/nmat2090.
(85) Zhu, T.; Liu, Y.; Fu, C.; Heremans, J. P.; Snyder, J. G.; Zhao, X. Compromise and Synergy in High-Efficiency Thermoelectric Materials. Adv. Mater. 2017, 29 (14), n/a-n/a. https://doi.org/10.1002/adma.201605884.

(86) Bell, L. E. Cooling, Heating, Generating Power, and Recovering Waste Heat with Thermoelectric Systems. Science 2008, 321 (5895), 1457–1461. https://doi.org/10.1126/science.1158899.
(87) Petsagkourakis, I.; Pavlopoulou, E.; Cloutet, E.; Chen, Y. F.; Liu, X.; Fahlman, M.; Berggren, M.; Crispin, X.; Dilhaire, S.; Fleury, G.; Hadziioannou, G. Correlating the Seebeck Coefficient of Thermoelectric Polymer Thin Films to Their Charge Transport Mechanism. Org. Electron. 2018, 52 (Supplement C), 335–341. https://doi.org/10.1016/j.orgel.2017.11.018.
(88) Menon, A. K.; Yee, S. K. Design of a Polymer Thermoelectric Generator Using Radial Architecture. J. Appl. Phys. 2016, 119 (5), 055501. https://doi.org/10.1063/1.4941101.
(89) Rowe, D. M.; Min, G. Design Theory of Thermoelectric Modules for Electrical Power Generation. IEE Proc. - Sci. Meas. Technol. 1996, 143 (6), 351–356. https://doi.org/10.1049/ip-smt:19960714.
(90) Chang, W. B.; Fang, H.; Liu, J.; Evans, C. M.; Russ, B.; Popere, B. C.; Patel, S. N.; Chabinyc, M. L.; Segalman, R. A. Electrochemical Effects in Thermoelectric Polymers. ACS Macro Lett. 2016, 5 (4), 455–459. https://doi.org/10.1021/acsmacrolett.6b00054.
(91) Patel, S. N.; Glaudell, A. M.; Kiefer, D.; Chabinyc, M. L. Increasing the Thermoelectric Power Factor of a Semiconducting Polymer by Doping from the Vapor Phase. ACS Macro Lett. 2016, 5 (3), 268–272. https://doi.org/10.1021/acsmacrolett.5b00887.
(92) Dresselhaus, M. S.; Chen, G.; Tang, M. Y.; Yang, R. G.; Lee, H.; Wang, D. Z.; Ren, Z. F.; Fleurial, J.-P.; Gogna, P. New Directions for Low-Dimensional Thermoelectric Materials. Adv. Mater. 2007, 19 (8), 1043–1053. https://doi.org/10.1002/adma.200600527.
(93) Yao, H.; Fan, Z.; Cheng, H.; Guan, X.; Wang, C.; Sun, K.; Ouyang, J. Recent Development of Thermoelectric Polymers and Composites. Macromol. Rapid Commun. 2018, 39 (6), 1700727. https://doi.org/10.1002/marc.201700727.
(94) Chen, Y.; Zhao, Y.; Liang, Z. Solution Processed Organic Thermoelectrics: Towards Flexible Thermoelectric Modules. Energy Environ. Sci. 2015, 8 (2), 401–422. https://doi.org/10.1039/C4EE03297G.
(95) Faleev, S. V. Theory of Enhancement of Thermoelectric Properties of Materials with Nanoinclusions. Phys. Rev. B 2008, 77 (21). https://doi.org/10.1103/PhysRevB.77.214304.
(96) Moriarty Gregory P.; De Sukanta; King Paul J.; Khan Umar; Via Michael; King Julia A.; Coleman Jonathan N.; Grunlan Jaime C. Thermoelectric Behavior of Organic Thin Film Nanocomposites. J. Polym. Sci. Part B Polym. Phys. 2012, 51 (2), 119–123. https://doi.org/10.1002/polb.23186.
(97) Chabinyc, M. Thermoelectric Polymers: Behind Organics' Thermopower. Nat. Mater. 2014, 13 (2), 119–121. https://doi.org/10.1038/nmat3859.
(98) Reddy, P.; Jang, S.-Y.; Segalman, R. A.; Majumdar, A. Thermoelectricity in Molecular Junctions. Science 2007, 315 (5818), 1568–1571. https://doi.org/10.1126/science.1137149.

Chapter 2

A REVIEW OF ELECTRONIC TEXTILE COATINGS AND FUNCTIONALIZING TEXTILES WITH PEDOT-Cl COATINGS USING VAPOR PRINTING

2.1 Introduction

Wearable electronics constitute the frontier of human interface devices that are making possible advanced performance monitoring, physiochemical sensing, new haptic interfaces, and portable energy harvesting and energy storage, to name a few innovations.[1–5] Most recently reported devices can be considered as non-natural approximations of traditional textiles or threads. Many wearable devices are built on thin or ultrathin plastic substrates that display sufficient flexibility to be skin- or body-mounted, or incorporated into garments and accessories via patching. [6–9] Selected other devices are created using specialty or designer threads/fibers, which are sometimes yarned together then coated with a protective polymer cladding to yield a fiber-based electronic device.[10–15] To date, these devices demonstrate acceptable device metrics, but their performance and longevity is far from matching those of devices built on rigid substrates, such as glass and silicon.[5,16]

For nascent wearable technology, in particular, aesthetics and haptic perception can uniquely determine the difference between success (i.e., widespread

adoption) and failure, irrespective of device metrics. There is strong motivation for using substrates and scaffolds that are already familiar, such as cotton/silk thread, fabrics and clothes, and imperceptibly adapting them to a new technological application. The pliability, breathability, wearability and feel of fabrics is unmatched. Especially for skin-mountable devices and smart garments, the intrinsic breathability and feel of fabrics cannot be replicated by devices built on plastic substrates or designer fibers, no matter how thin or flexible these devices can be made. Moreover, using traditional textile materials means that prototypes of promising new technologies can be easily produced using existing manufacturing routines.

A number of research groups are endeavoring to transform familiar fibers and/or fabrics into fiber- or textile-based electrodes for electronic devices. This is usually achieved by coating or soaking (i.e., dyeing) mass-produced threads or fabrics with electronically- or optoelectronically-active materials.[17,18] Intrinsically conducting polymers (ICPs) are typically used as the active layer materials for many fiber-and textile-based devices due to their advantageous mechanical properties and processing ease. The elasticity and plasticity of ICPs are similar to those of common, mass-produced threads, which should prevent delamination and microfissure formation within the active layer upon bending or twisting the coated/dyed threads. Nonetheless, fabrics and threads/yarns are demanding substrates onto which to deposit a conjugated polymer film because their surfaces are densely textured and display roughness over a wide range of length scales—micron length scales for fibers, micron to millimeter length scales for threads/yarns and millimeter to

centimeter length scales for woven and knitted fabrics. Indeed, tremendous variation in the surface morphology of conjugated polymer-coated fibers can be observed with different coating or processing conditions.

Importantly, the morphology of the conjugated polymer active layer determines electrical performance and device ruggedness. For fiber-based devices, in particular, the stability of a particular coating against high friction forces, extreme bending radii and other large, cyclic mechanical stresses is paramount. Typical textile manufacturing processes, such as weaving, knitting, and sewing, subject threads/yarns to astonishingly high mechanical strain.[19] Further, any textiles thus produced are subjected to significant strain, friction forces and chemical exfoliation during wear, laundering, and/or ironing. To survive these stresses, electronically active coatings must be smooth, uniform, conformal and, ideally but not necessarily, covalently tethered to the surface of a fiber to limit exfoliation and de-adhesion events.

Here we summarize selected recent approaches to coat familiar, mass-produced threads, yarns, or fabrics with electronically active conjugated polymers to produce textile-based electronic devices. Previous reviews have described recent advances in fiber-based photovoltaic devices and textile energy storage, with particular emphasis on device performance.[5,16] Therefore, in this article, we place emphasis on the fabrication method used to create various fiber- and textile-based devices and attempt to highlight the influence of the coating method on active layer morphology and device stability.

2.2 Dipcoating Film Morphology and Stability

Dip coating or, effectively, dyeing fibers and textiles with pre-synthesized conducting polymers is the most prevalent approach for creating electronically active textiles. This method is relatively simple and does not require specialized or expensive equipment. Dip coating only requires that the conjugated polymer be soluble in a solvent that does not degrade the fiber or textile substrate. This allows for the fiber/textile to be simply soaked in a solution of the solubilized polymer then dried, leaving behind a conductive coating. The dipping-drying cycle can also be repeated multiple times to either systematically increase the thickness of a polymer coating or add multiple layers of different conjugated polymers. However, caution must be exercised to ensure that the fibers/fabrics are completely dry before undertaking a subsequent dipping cycle to prevent dissolution of the already-formed coating.

For example, Sonkusale and Khademhosseini *et al.* used sequential dipcoating to create a fully-integrated thread-based diagnostic device platform that contained both a thread-based microfluidic network and an array of thread-based physical and chemical sensors capable of monitoring physiochemical tissue properties in vitro and in vivo (Figure 2.1).[2] The thread-based chemical sensors were fabricated by sequentially passing raw cotton yarns through multiple wells containing acidic poly(aniline) (PANI) and isopropanol-solubilized conductive carbon inks. A dryer was utilized to cure each coating in between each dipping event. Meters of functionalized threads were thus fabricated and collected on rotating spools.

A similar assembly line approach was used by Gaudiana *et al.* to fabricate fiber-based organic photovoltaic devices.[11] The authors drew specially-extruded stainless steel threads through a sequence of vertically-aligned coating cups containing, first, an isopropanol solution of tetrabutyl titanate, second, a semiconducting polymer-fullerene mixture in an organic solvent and, third, an aqueous solution of the highly-conductive composite material, poly(3,4-ethylenedioxythiophene)-co-poly(styrene sulfonic acid) (PEDOT:PSS). Here, too, a dryer was utilized to cure each coating in between each dipping event. These multiple coated threads were then yarned together with a second, silver-coated stainless-steel thread and the yarns dipcoated with a transparent protective cladding to produce fiber solar cells displaying power conversion efficiencies between 2.79% to 3.27%.

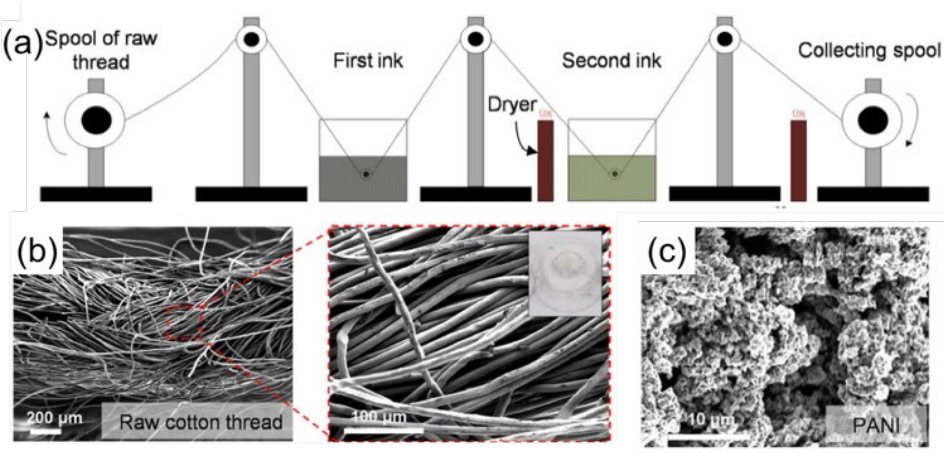

Figure 2.1 a) Sequential dipcoating process reported by Sonkusale and Khademhosseini et al. b) SEMs of raw cotton thread before dipcoating. c) SEM of poly(aniline) coated cotton thread.[2]

The primary disadvantage with dipcoating is the large observed variance in smoothness and uniformity of the conducting polymer coating. Often, rough, textured coatings resulting from incomplete wetting and/or agglomerated

conjugated polymer chains are obtained. For instance, scanning electron micrographs (SEMs) of Sonkusale and Khademhosseini's aforementioned PANI-coated cotton threads reveal that the PANI coat is non-uniformly bulbous, microporous and rough on the micron length scale (Figure 2.2c). In the long term, these bulbous regions are undesirable as they can potentially serve as points of de-adhesion and exfoliation during subsequent textile processing and body-mounting. Along the same lines, Gaudiana *et al.* explain in their report that diamond tip-extruded stainless steel thread needed to be used as the substrate onto which a solar cell was elaborated because these specialty threads displayed a particularly smooth, protrusion-free surface that allowed for smooth active layer coatings, which, in turn, lead to solar cells with functional rectification ratios. The presence of even a small number of rough surface features or active layer agglomerates on the fiber surface would lead to insurmountable shunting pathways that can significantly deteriorate device performance, even to the point of rendering it unfunctional.

Despite a large variation in observed coating morphology, dipcoating remains the most popular method of fiber/fabric functionalization to date. This is due, in part, to a selected number of conducting polymer formulations that yield smooth, functional coatings or composites with various natural and synthetic fibers and fabrics.

Fibers and fabrics dipcoated with aqueous solutions of PEDOT:PSS are the most common components of electronic textiles. Sotzing *et al.* created highly conductive fabrics by soaking a selection of fabrics in a commercially-available aqueous solution of PEDOT:PSS.[20] Fabrics investigated included: Spandex (50%

nylon / 50% polyurethane); cotton; polyester, 60% cotton / 40% polyester; 95% cotton / 5% Lycra; 60% polyester / 40% rayon; and 80% nylon / 20% Spandex. The conductive Spandex fabric thus obtained (see Figure 2.2b) had an average conductivity of 0.1 S/cm (for reference, the conductivity of a 100 nm-thick "conductive-grade" PEDOT:PSS film on glass is 1 S/cm). Subjecting the fabric to more than one soaking step increased its conductivity up to ca. 2.0 S/cm by increasing the weight fraction of the conducting polymer component.

It must be noted that fibers and fabrics can be swelled, i.e., impregnated, by the electronically active materials during dip coating, depending on the soaking time and solvent used. Such swelling and impregnation events can change the mechanical properties of the starting fiber/fabric. Different fibers and fabrics display different degrees of uptake of various soaking solvents and conjugated polymers, approximately obeying a "like swells like" pattern of behavior. For instance, in the aforementioned work by Sotzing *et al.*, it was concluded that the PEDOT:PSS was not a continuous smooth film on a fabric surface but, rather, a homogeneously dispersed network of PEDOT:PSS nanoparticles impregnated within a fabric matrix, which formed a percolation pathway past a particular weight fraction (Figure 2.2b). Further, the authors found that those fabrics with higher water uptake resulted in higher conductivities because they soaked up higher amounts of PEDOT:PSS from the aqueous dipcoating solution compared to more hydrophobic fabrics.[20]

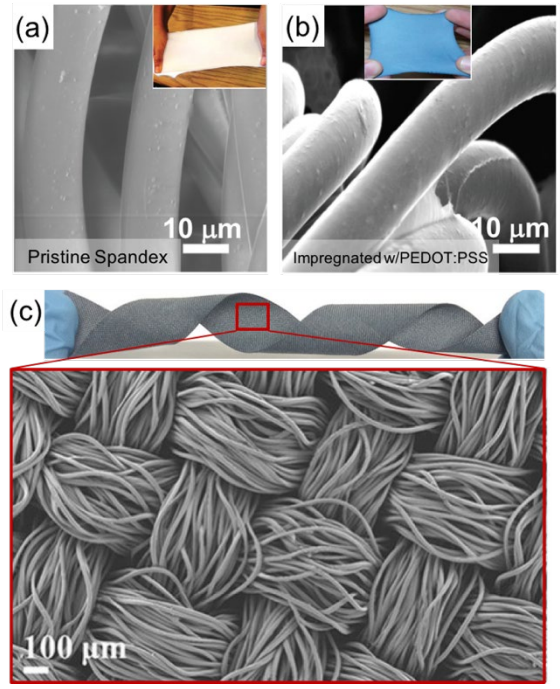

Figure 2.2 a) SEM of Spandex fabric used by Sotzing et al. The inset shows a photograph of this fabric. b) SEM of Spandex dipcoated with PEDOT:PSS. The inset shows a photograph of this fabric. Adapted from Ref. 11. c) Photograph (top) and SEM (bottom) of a PEDOT:PSS coated polyester fabric reported by Lin et al. Adapted from Ref 18.

The presence of various additives, both insulating polymer and small-molecule additives, in the dipcoating solution has been found to significantly affect the conductivities and/or sheet resistances of PEDOT:PSS coated fibers and fabrics by increasing the long-range order in the PEDOT domains of PEDOT:PSS. Changing the dipcoating solvent similarly affects sheet resistance and conductivity. Post-deposition treatments, such as thermal annealing and post-deposition exposure to small-molecule detergents or plasticizers vastly increases the observed conductivity of PEDOT:PSS coated fabrics. Mohanta *et al.* reported that the resistance of a PEDOT:PSS coated cotton yarn can be decreased from 2.32 MΩ/cm to 77 Ω/cm if the cotton yarn is first dipcoated in DMSO instead of water then

washed with ethylene glycol before drying.[21] Similarly, Yun *et al.* reported that cotton and polyurethane fabrics dipcoated with PEDOT:PSS solutions containing a sodium dodecylsulfate (SDS) detergent displayed sheet resistances of 24 and 48 Ω/square, respectively, with the cotton fabrics displaying lower sheet resistances because of a higher amount of impregnated PEDOT:PSS in these fabrics. Using these fabrics, the authors then created metal-free textile heaters by taking advantage of efficient Joule heating in these conductive fabrics.[22]

Hu *et al.* dipcoated both cotton and polyester yarns in an aqueous solution containing a mixture of PEDOT:PSS, multiwalled carbon nanotubes (MWCNTs) and a polyurethane binder in various ratios to create fabrics displaying thermoelectric properties.[23] In this report, the polyurethane functions as an insulating, hydrophobic polymer matrix that binds together the two conductive components (PEDOT:PSS and MWCNTs) in the dried coating. Synthetic polyester yarns were completely coated after five dipping-drying cycles. However, cotton yarns, which are more geometrically unorganized, remained non-uniformly coated, even after five dipping cycles. Accordingly, the non-uniformly coated cotton yarn displayed a resistance of 200 Ω/cm, whereas the uniformly coated polyester yarns displayed a lower resistance of 50 Ω/cm.

Åkerfeldt *et al.* created conductive synthetic fabrics by dipcoating poly(ethylene terephthalate) (PET) fabrics into a mixture of aqueous PEDOT:PSS, Performax (a commercially-available aqueous solution of polyurethane and hydroxyethylcellulose that acted as a binder), ethylene glycol (a small-molecule surfactant), and an ethoxylated urethane (a rheology modifier).[24] Similar to previous

reports, PEDOT:PSS was observed to impregnate into the PET substrates to produce conductive fabrics with smooth surfaces (Figure 2.3). Dipcoating solutions containing the highest weight percent of the PEDOT:PSS component were, unsurprisingly, found to yield the most conductive fabrics after dipcoating/drying sheet resistances as low as 12.7 Ω/square were observed. Slow drying and post-deposition thermal annealing were also found to contribute to the low observed sheet resistance of these conductive fabrics. This work is notable because the authors perform extensive and systematic mechanical and abrasion testing on their conductive fabrics. A high PEDOT:PSS weight fraction (80 wt%) and the presence of an ethylene glycol surfactant in the dipcoating solution was found to produce conductive textiles with high tear strength. However, these same samples demonstrated the greatest degree of coating degradation with abrasion (it was even visually apparent that the coatings were smeared and faded after abrasion, see Figure 2.3b). Increasing the weight fraction of the polyurethane binder to 28% in the dipcoating solution afforded admirably abrasion-resistant coatings; however, an increased binder concentration also increased the sample's sheet resistance to 78.3 Ω/square.[24]

Müller *et al.* used a dipcoating solution containing PEDOT:PSS, Zonyl FS-300 (binder), and either DMSO or ethylene glycol (surfactant) to impregnate/coat silk and cotton yarns.[25] The notable component here is the Zonyl FS-300 binder, which is a commercially available fluoroalkyl-containing oligo(ethylene glycol) surfactant. After two dipcoating-drying-thermal annealing cycles, silk yarns with conductivities between 14 and 15 S/cm were obtained. Notably, these conductive

yarns were found to be resistant to mechanical stress and laundering. The PEDOT:PSS dyed silk yarns maintained their bulk electrical conductivity after being subjected to repeated bending stresses and mechanical wear during sewing. No change in conductivity could be detected after four washing cycles in a household washing machine; however, the conductivity of the yarns decreased by a factor of 2 after five dry cleaning cycles.[25] Such varying responses to different laundering actions can be easily correlated to the Zonyl FS-300 binder: fluoroalkyl chains do not interact with the long alkyl chains of the surfactants found in most household laundry detergents (such as SDS) but are easily solvated by the halogenated solvents used in dry cleaning. Therefore, dry cleaning likely dissolves away some of the conductive coating, leading to higher observed resistances.

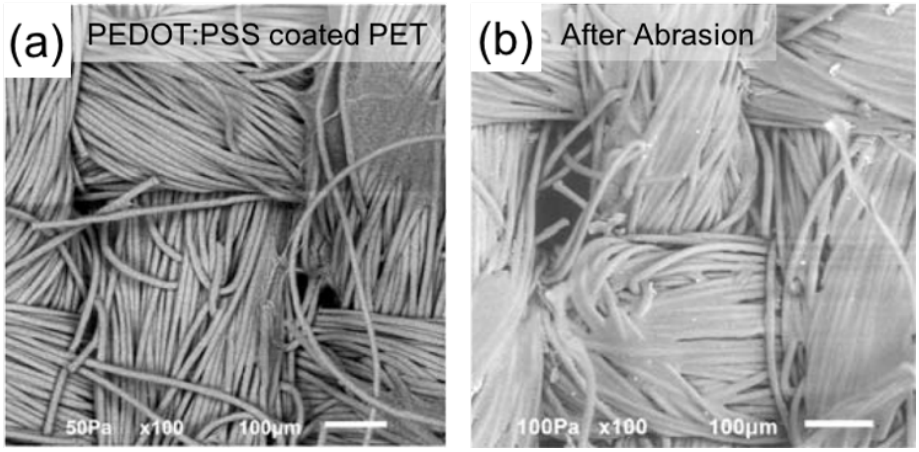

Figure 2.3 a) SEM of the most-conductive PEDOT:PSS coated fabric reported by Åkerfeldt et al. This sample had a sheet resistance of 12.7 Ω/square. (b) SEM of this fabric after surface abrasion, revealing smearing of the conductive coating. Adapted from Ref. 15.

A few patterns can be gleaned from a survey of the literature reports highlighted thus far. First, certain conjugated polymers and their composites afford smooth coatings compared to others. In particular, PEDOT:PSS likely swells and

impregnates most hydrophilic fibers, as opposed to forming a strictly surface coating, leading to highly conductive fibers and fabrics due to high polymer loading. In contrast, poly(aniline) accumulates primarily on the surface of most fibers, which leads to rough, textured surfaces and low polymer loadings in the final fiber/fabric composite. Second, when using polymers that do not impregnate fibers/fabrics, threads/fibers with longer and monodisperse staple lengths, such as nylon, silk and synthetic threads, display smoother surface coatings in comparison to threads/fibers with short and/or polydisperse staple lengths, such as cotton threads and yarns. Third, the wash and wear resistance of conducting coatings obtained via dipcoating is controlled by the presence of carefully chosen binders and/or surfactants in the dipcoating solution.

2.3 Dipcoating Devices

In addition to the few cases highlighted above, many other types of electronic devices are enabled by conductive fibers and textiles created using dipcoating. Ishida *et al.* constructed a single-type (*p*-type only) thermoelectric generator using square patches of a PEDOT:PSS coated cotton fabric sewn together with nickel foil, which yielded a thermoelectric power density of 4.5 μW cm^{-2} mg^{-1}.[26] Lin *et al.* fabricated thermoelectric fabrics by dipcoating pre-woven polyester fabrics with PEDOT:PSS dispersed in DMSO.[27] The coating process was repeated twice to afford fabrics with a smooth surface (Figure 2c), conductivities of 1.5 S/cm and a maximum power factor of 0.045 μW m^{-1} K^{-2} at 390 K. Single-type fabric thermoelectric generators were then created by stitching strips of this conductive fabric onto a raw polyester

fabric backing and electrically connecting these strips with silver-coated nylon thread.

Inganäs *et al.* demonstrated that a conductive silk fiber could be utilized as the source-drain channel in an organic electrochemical transistor (OECT) by dip coating either natural or recombinant silk fibers with poly(2,3-dihydrothieno[3,4-b]-[1,4]dioxin-2-yl-methoxy)-1-butanesulfonic acid (PEDOT:S). These dipcoated fibers exhibited conductivities as high as 0.044 S/cm.[28,29] In a different report, Inganäs *et al.* demonstrated a novel fiber-based OECT device architecture comprised of two PEDOT:PSS coated cotton yarns arranged in a cross geometry. One yarn comprised the source-drain channel and the second yarn acted as a gate electrode. A droplet of a polymer gel electrolyte placed at the intersection between the two yarns completed the gate-source conduction pathway.[9] Coppedè *et al.* also created several fiber-based OECTs using a PEDOT:PSS coated cotton yarn sewn onto an insulating substrate. Notably, human sweat was needed to complete a conductive channel between the gate and source electrodes in this device, allowing these OECTs to function as skin-mountable sensors to monitor the concentrations of varying analytes in human sweat.[30,31]

Andrew *et al.* used dipcoating to create all-textile triboelectric generators that generated power due to the creation of surface charge upon the physical contact of two fabric surfaces of opposite polarity (Figure 2.4).[32] Cotton fabrics were dipcoated with a fluoroalkyl alkoxysiloxane compound, which formed a rugged, polymeric fluoroalkylsiloxane surface coating on the cotton fabrics upon drying. This dipcoated cotton fabric was then sewn onto a conductive fabric electrode and

subsequently placed atop a complementary electrode (comprised of a nylon fabric sewn onto a conductive fabric) to create an all-textile triboelectric generator. This device yielded an average power output of 13 □W cm^{-2} when the stacked electrodes were connected to a 50 MΩ load and lightly patted together. This work is interesting because the densely microstructured surface of cotton textiles was integral in creating useable surface charge density upon physical contact (typically, planar surfaces do not produce notable triboelectric power).

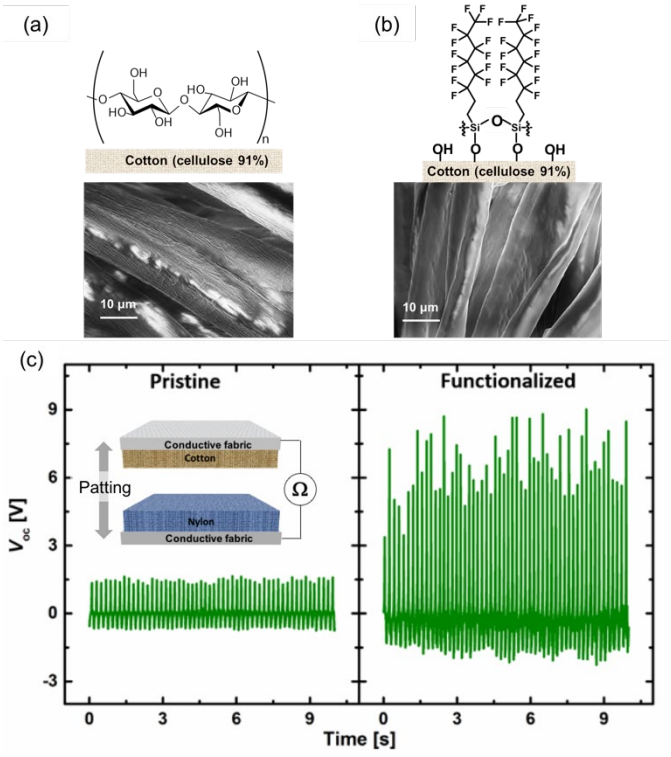

Figure 2.4 a) SEM of pristine cotton fabric. b) SEM of cotton cloth dipcoated with a fluoroalkylsiloxane. c) Voltage outputs obtained upon light patting of two textile triboelectric generators constructed using either pristine cotton cloth (left) or fluoroalkylsiloxane coated cotton cloth (right). A cartoon of the device is provided as an inset. Adapted from Ref. 24.

2.4 Electrochemical Coating

Electrochemical polymerization is another coating method that combines polymer synthesis and deposition into one step. A monomer is dissolved in an appropriate solvent along with an electrolyte salt and a linearly varying (triangle-wave) potential is applied using a voltage source and, typically, a three-electrode setup (working, counter and reference electrodes). Monomer oxidation occurs when sufficient positive bias is applied, which initiates polymerization at the working electrode.[33] Several textiles have been coated with conducting polymers via electropolymerization.[34]

The main requirement for electrochemical deposition of conjugated polymers is a conductive working electrode. Since standard fiber or fabric substrates are normally insulating, they cannot be directly used as an electrode onto which a polymer coating is deposited via electrochemical means. One creative approach for depositing polymers onto an insulating fiber substrate is to simply wrap a metal working electrode with the fiber, allowing the polymers formed in the vicinity of the working electrode to passively coat the fiber. Gupta *et al.* coated natural fibers, such as silk, cotton, and wool, with poly(pyrrole) in this fashion, using a platinum wire working electrode.[35]

Most reports that use electrochemical polymerization to form conjugated polymer coatings first create a thin conductive base coat, or seed layer, on the fiber/fabric using dipcoating, VPP or solution polymerization, which then allows the fiber/fabric to directly act as the working electrode. In this sense, electrochemical polymerization can be best considered as a method with which to increase the

thickness of a conductive coating on fibers/fabrics. Under optimized conditions, the morphology of the electrodeposited polymer coating is largely determined by the morphology of the underlying seed layer.

Cases *et al.* used this approach to make conductive polyester textiles. Textiles were first coated with a seed layer of poly(pyrrole) via in situ solution polymerization (see Section 4), and this coated textile was subsequently used as the working electrode for an electrochemical polymerization of pyrrole or aniline. The conductivities of the resulting textiles were approximately 20 Ω/square for both poly(pyrrole) and poly(aniline) coated textiles.[36,37] Murphy *et al.* also prepared poly(pyrrole)-coated textiles using this technique, however the textile substrate was silk instead of polyester. The authors demonstrated that these poly(pyrrole) coated conducting silks are uniquely-biocompatible biosensors.[38] Similarly, Jager *et al.* created metal-free textile actuators that act as artificial muscles using poly(pyrrole)-coated conductive yarns obtained via electrochemical polymerization.[39] Single- and two-ply twisted Lyocell cellulose staple yarns were first coated with a seed layer of PEDOT using vapor phase polymerization (see section 2). Next, these conductive yarns were used as the working electrode to effect electrochemical polymerization of poly(pyrrole). These textile actuators showed a 27% decrease in actuation force when cycled between -1 and 0.5 V at 0.05 Hz for 8000 cycles. Notably, uniform polymer coatings were found to be integral to enabling macroscale actuation and the observed uniformity of the PPy coat was mostly ascribed the use of vapor phase polymerization to create a smooth PEDOT seed layer. Krishnamoorthy *et al.* transformed various naturally occurring fibers/threads into fiber supercapacitors

using, first, a novel redox reaction to deposit a gold coating onto these natural fibers and subsequently creating a PEDOT layer on the gold-coated fibers using electrochemical polymerization. These gold/PEDOT coated fibers displayed capacitances as high as 254 F/g.[40]

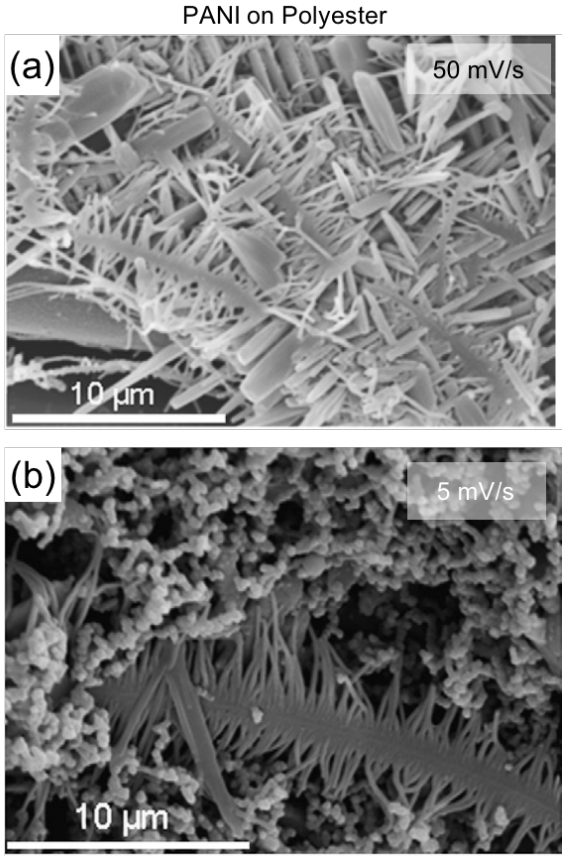

Figure 2.5 SEMs of poly(aniline) films deposited on conductive polyester fabrics via electrodeposition at a scan rate of (a) 50 mV/s or (b) 5 mV/s. Adapted from Ref. 49.

The morphology of electrodeposited conjugated polymer films on fibers/fabrics is also influenced by the rate at which the applied potential is varied (i.e, the scan rate). Cases *et al.* investigated scan rate effects on the morphology of poly(aniline) films deposited onto polyester fabrics via electrochemical

polymerization.[41] Notably, the poly(aniline) coatings displayed "centipede-like" features—i.e., two rows of fuzzy polymer nanofibers branching from a common core—at low scan rates (Figure 2.5), which is a highly-unusual and unmatched solid-state structure. The surface resistivity of the poly(aniline) coated fabrics was as low as 3 Ω/square for samples synthesized at a scan rate of 1 mV/s.

2.5 In Situ Solution Polymerization

Certain conducting polymers are not readily available as stable, pre-formulated conducting inks—for example, poly(pyrrole) (PPy) and poly(aniline) (PANI). In these cases, the polymer can be chemically synthesized in the presence of a desired substrate to simultaneously effect polymerization and deposition. We label this method as *in situ* solution polymerization. In this method, a substrate is placed into a solution containing the desired monomer and, if appropriate, other reagents, after which an oxidant is added to solution to initiate polymerization. A certain fraction of the polymers formed in the reaction solution will passively adhere to the surface of the substrate. Depending on the surface chemistry of the substrate and the presence/absence of reactive functional groups, reactive monomers or growing polymer chains can also become covalently attached to the substrate during the reaction.

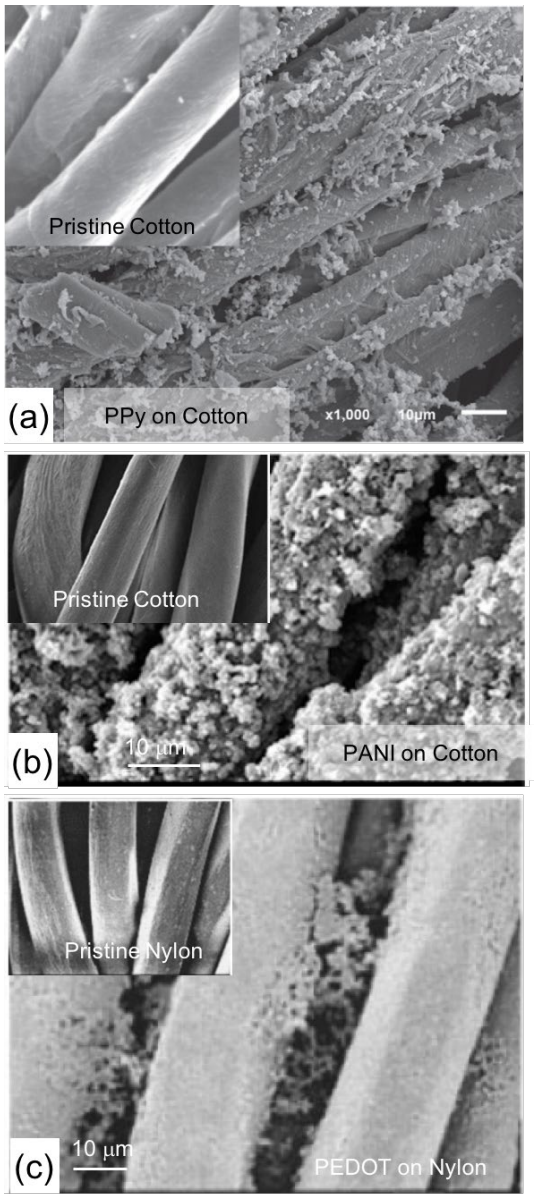

Figure 2.6 SEMs of conducting polymer films on fabrics deposited via in situ solution polymerization. (a) Poly(pyrrole) on cotton. Adapted from Ref. 52. (b) Poly(aniline) on cotton. Adapted from Ref. 53. (c) PEDOT on nylon showing nylon degradation. Adapted from Ref. 50.

Though seemingly straight-forward, *in situ* solution polymerization is hard to control in real time. Ways to control mass transport during polymerization/deposition are minimal and strategies to direct film growth kinetics

are hard to enforce. The conjugated polymer coatings obtained via *in situ* solution polymerization display the highest degree of nonuniformity, surface roughness and batch-to-batch variance among all the fabrication methods summarized in this article (Figure 2.6). Small changes in reaction conditions (such as stirring/no stirring), monomer/oxidant concentrations and reagent addition order can lead to significant differences in film crystallinity/morphology, coating uniformity and correlated electronic properties. Moreover, some fabrics have been observed to degrade under the acidic reaction conditions necessary to effect pyrrole and aniline polymerization in solution. Therefore, this technique is best used with caution.

Kang *et al.* explored various *in situ* solution polymerization procedures to create PEDOT-coated nylon, PET and PTT fabrics, with the aim of optimizing their conductivities.[42] The authors found that most solution polymerization conditions degraded and/or partially dissolved nylon fibers, leading to products with inferior mechanical properties. Varesano *et al.* created conductive PPy-cotton fabrics with sheet resistances as low as 2.18 Ω/sq.[43] Xu and Xu *et al.* also used *in situ* solution polymerization to create PPy-coated cotton fabrics that served as supercapacitors with a specific capacitance of up to 325 F/g and energy densities up to 24.7 Wh/kg.[44] Akşit *et al.* coated cotton fibers with PANI and subsequently doped these films with barium ferrite, achieving sheet resistances as low as 350 Ω/cm.[45] Stejskal *et al.* used the reducing ability of PPy and PANI coatings on cotton fabrics to deposit silver nanoparticles from silver nitrate solutions onto the surface of the fabrics. These silver/PANI and silver/PPy coated cotton fabrics displayed notable antimicrobial activity and cytotoxicity.[46]

2.6 Miscellaneous Coating Methods

Due to the popularity and utility of PEDOT:PSS coated textiles, there exist isolated reports in which creative or unusual fabrication methods are used to access electronically active textiles. One such example comes from Kim *et al.* who used blade coating to coat PEDOT:PSS onto the surface of a specially formulated synthetic fabric comprised of polyester/silver nanowires/graphene.[47] The bladecoated PEDOT:PSS film served as a hole-transport / electron-blocking layer for a semiconducting polymer-fullerene bulk heterojunction solar cell that was subsequently elaborated onto the fabric surface. The solar textile thus obtained demonstrated a power conversion efficiency of 2.27% and a specific power of 0.45 W/g.

Sotzing *et al.* created patterned circuits on the surface of PET fabrics by inkjet printing a specially formulated PEDOT:PSS ink containing commercially available "high conductivity grade" PEDOT:PSS, ethanol, and diethylene glycol.[48] The ratios of these three components were optimized to obtain an appropriate ink viscosity. The sheet resistance of these inkjet printed wires was high (3185.7 Ω/sq), which the authors ascribed to a low concentration of PEDOT:PSS in the deposited film: a 125 mm^2 area was found to contain only 0.15 mg of PEDOT:PSS, even after 10 printing passes. The authors then created patterned circuit pathways on the surface of PET fabrics using a stenciling method.[49] A plastic stencil was fashioned and placed atop the PET fabric, after which a concentrated PEDOT:PSS solution was stippled onto the PET fabric through the stencil using a sponge. The sheet resistance of the wires thus fabricated was 2.7 Ω/sq, which was attributed to an increased amount of

deposited PEDOT:PSS: the sponge stencil method deposited 1.59 mg of PEDOT:PSS over a 125 mm^2 area. The current carrying capacity (CCC) for these PEDOT:PSS wires were measured and compared against silver-coated conductive fabrics and carbon nanotube-impregnated paper (buckypaper). The CCC of the PEDOT:PSS circuit on PET fabrics was measured to be 1000 A/cm2, comparable to that of buckypaper but lower than that of silver-coated bamboo cloths.

2.7 Vapor Coating

Vapor phase polymerization of conducting polymers is a nascent technique that combines polymer synthesis and deposition into one step.[50–52] This method allows for any textile or fiber to be coated with conducting polymers without the use of solvents, detergents, fixing agents or surface pretreatments, making it an environmentally friendly way to create electronically active fabrics. Vapor deposition is an attractive technique that allows for uniform and conformal coating of arbitrary substrates of any surface topography/roughness and produces conductive materials without any insulating moieties.[53] Vapor deposited coatings are often thin enough such that the original mechanical properties of the substrate (and not that of the coating) will be the dominant observable.[54]

Two main components are required for vapor deposition: a conjugated monomer and oxidant. Monomers include 3,4-ethylenedioxythiophene (EDOT), aniline (ANI) and pyrrole (Py). A variety of iron(III) salts are used as the oxidant, including iron (III) chloride and iron (III) p-toluenesulfonate. Two major subclasses of vapor deposition methods exist, both of which have been used to coat textiles and

yarns with conducting polymers. The first technique is called vapor phase polymerization (VPP) and involves impregnating the iron oxidant into a fiber/fabric via dipcoating or dropcasting and then exposing this iron-impregnated fiber/fabric to vapors of the desired monomer in a closed chamber. The second vapor deposition technique is called oxidative chemical vapor deposition (oCVD) and is distinct from VPP in that both the oxidant and monomer are introduced simultaneously in the vapor phase to create a conjugated polymer film. oCVD is typically conducted in a reactive vapor deposition chamber, although the requirements for this chamber are not exact, and a variety of widely-available reaction glassware can be adapted to effect polymer deposition. The basic requirements for a deposition chamber include a controlled inlet for the gaseous monomer, a heated crucible to generate oxidant vapor, a heated surface to hold the fabric/fiber substrate in the vicinity of the oxidant vapor plume, and a vacuum pump.[55]

In both vapor deposition methods, the gaseous monomer reacts with an oxidant at or near a heated substrate to form oligomers and polymers that will be deposited onto the substrate.[56] Exposed oxidants on the surface of the fiber/fabric create reactive radical cations of the monomer at or near the surface of the substrate, which then react with other monomers to produce a growing polymer chain. Depending on the chemical composition of the fiber/fabric substrate, the monomer radical cations can also react with functional groups on the fiber/fabric surface to afford mechanically stable surface-grafted conjugated polymer films on fibers/fabrics. Notably, whereas the degradation and swelling of a fiber/fabric in

certain solvents needs to be considered when using solution-based polymerization and/or deposition methods, this is not a concern with vapor deposition methods.[52]

All vapor deposition procedures are followed by necessary rinsing steps to remove residual oxidant and other small-molecule reaction byproducts from the deposited polymer film. Rinsing in methanol or sulfuric acid/methanol mixtures effectively removes residual iron salts from the films and also improves the conductivity of the isolated conjugated polymer films.[52]

Dall'Acqua and Tonin *et al.* created poly(pyrrole) (PPy) coated cellulose textiles using VPP for eventual use as an electroactive membrane in fuel cells. Fabrics were first soaked in ferric chloride hexahydrate and then exposed to vaporized pyrrole to afford PPy coatings. Coating uniformity was affected by the weight loading and degree of impregnation of the iron oxidant—higher oxidant loadings lead to greater oxidant impregnation in the cellulose textiles, which, in turn, yielded smoother and more-uniform PPy coatings upon exposure to pyrrole vapor.[57] Shang *et al.* investigated the influence of reaction conditions, such as oxidant loading, reaction time and reaction temperature, on the structure and electronic properties of PPy coatings created on PET fabrics using VPP. The authors concluded that oxidant loading did not have a notable effect on the conductivity of the PPy coating obtained by VPP and that intermediate reaction times (4-5 hours) at low temperatures (4 °C) afforded the smoothest, most uniform PPy coating with the lowest sheet resistance (250 Ω / square).[58]

Skrifvars *et al.* used VPP to deposit PEDOT onto textiles.[59] Contrary to observations made for dipcoated samples, the authors determined that pre-treating

textiles with organic solvents reduced the electrical conductivity of PEDOT coatings obtained via VPP. Further, brittle, flaky PEDOT coatings were obtained on solvent-treated textiles. Different types of oxidants were explored for the VPP of PEDOT. PEDOT coatings obtained using $FeCl_3$ as the oxidant displayed high electrical conductivity, whereas samples obtained using iron (III) p-toluenesulfonate as the oxidant resulted in strong mechanical properties. Non-natural, designer fibers have also been used as substrates for VPP. Laforgue *et al.* exposed electrospun fiber mats comprised of the oxidant, iron(III) p-toluenesulfonate, dispersed in an insulating polymer matrix to EDOT vapor in order to create quasi-pure PEDOT nanofibers with a measured electrical conductivity of 60 S/cm.[60,61]

Vapor deposition methods afford highly conformal conjugated polymer coatings that preserve the topography and texture of the underlying substrate with high fidelity. This feature can be advantageous when working with certain morphologically distinct substrates. Bashir *et al.* proved this point by coating porous poly(tetrafluoroethylene) (PTFE) membranes with PEDOT via oCVD and demonstrating that the vapor deposited PEDOT coating did not clog the membrane pores.[62] Figure 2.7 shows the PTFE membrane pores before and after coating with PEDOT. Additionally, the necessary post-deposition sulfuric acid rinse to remove residual iron oxidant was also found to lower the sheet resistance of the PEDOT-coated membranes to a final value of 0.8 kΩ after 72 hours.

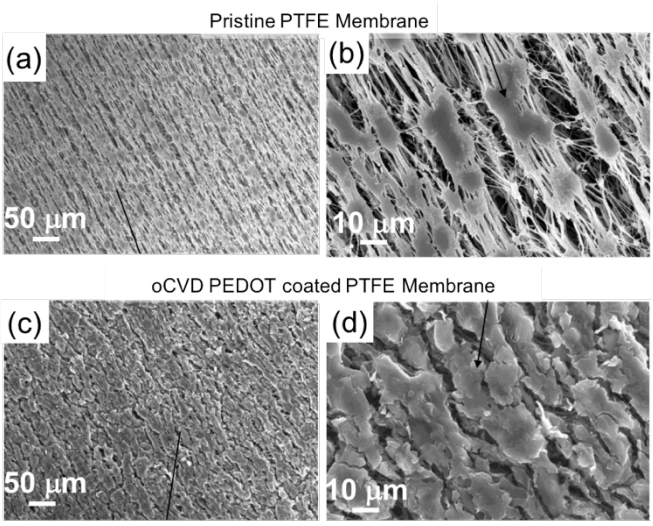

Figure 2.7 (a-b) SEMs of a porous PTFE membrane at two different magnifications. (c-d) SEM of these membranes after PEDOT coating using ocVD. Adapted from Ref. 39.

Textile scientists have traditionally shied away from using vapor deposition methods to create various textile-based electronics because of the perceived difficulty and high cost of scaling up vapor coating chambers to satisfy the high-volume demand of the textile industry. However, as described by Gleason *et al.*, advancements made over the past decade have resulted in the use of vapor deposition methods to stain-guard carpets, lubricate large area mechanical components and protect microelectronic devices, demonstrating that vapor coating methods are indeed conducive to large-scale, high-throughput manufacturability.[63] Moreover, the tremendous wash and wear resistance of vapor deposited films is an intrinsic property, as opposed to a feature imparted by the addition of a carefully-chosen binder, as in the case of conductive fibers/fabrics created via dipcoating. The electrical properties of the conjugated polymer films created by vapor deposition are also superior to those created from commercial conducting polymer inks: vapor-

deposited conducting polymer films lack an insulating component (such as PSS or solubilizing side chains on each repeat unit) and can therefore support much higher current densities per unit volume than their solution-processed counterparts.

2.8 Chemical Vapor Deposition of PEDOT

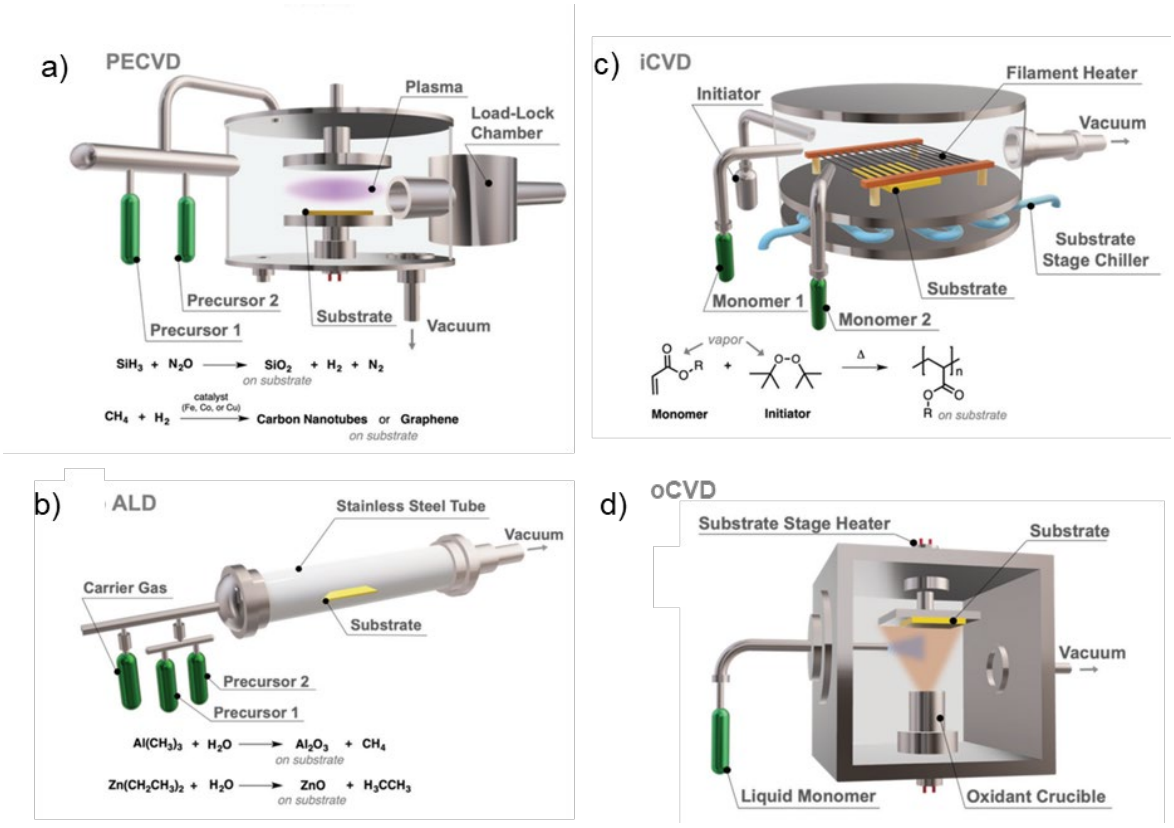

Figure 2.8 Reaction chamber designs for a)PECVD, b) ALD, c) iCVD, and d) oCVD adapted from Ref [83].

Chemical Vapor Deposition (CVD) is a technique used to apply coatings or create films on the surface of a substrate through vaporized precursors.[67–85] It is a very versatile technique and has been used on industrial levels for several decades. Vapor deposition has been performed in a variety of chamber reactors; some examples are shown in Figure 2.8.

Plasma-enhanced chemical vapor deposition (PECVD) requires a "pancake" style chamber and is commonly used to deposit films of Si, Si_3N_4, and SiO_2, as well as free-standing carbon nanostructures (Figure 2.8a). These chambers include a cylindrical, flat body with an inlet for the precursors, a vacuum inlet, and a load-lock chamber. Inside of the body there are two parallel-plate electrodes which are used to apply direct or alternating current. A carrier gas used in the deposition reacts with the current to generate a plasma, which is then used to create the reactive species used in the chemical reaction.[83]

Atomic layer deposition (ALD) is a technique designed to produce multilayer optical coatings and for the controlled growth of metal oxides (Figure 2.8b). This chamber design consists of a horizontal, stainless-steel tube. Under an applied vacuum, the precursors and carrier gas are introduced into the chamber body via sequential pulse-purge-pulse cycles. This allows for the reaction of species at predetermined active sites on the substrate. Through this technique atomic level control over film growth is achieved, although this process is time consuming as the deposition rate is so slow.[83]

Initiated chemical vapor deposition (iCVD) is a technique that uses a modified PECVD chamber for controlled depositions of polymer films on numerous textured surfaces with different surface energies (Figure 2.8c). Plasma coupled with an initiator precursor is used to create reactive species that react and form polymer films on the cool surface at the base of the chamber.

Oxidative chemical vapor deposition (oCVD) is also a technique used to deposit polymer, specifically conductive polymer, films. The chamber design allows for a vaporized monomer to react with a vaporized oxidant on the substrate which is placed on a heated surface. The chamber design show in Figure 2.8d shows a cube-shaped chamber

body with monomer inlets and a vacuum inlet. In this chamber, the oxidant crucible creates a cone of vaporized oxidant which the monomer vapors intersect with perpendicularly, directly on the surface of the substrate.[83]

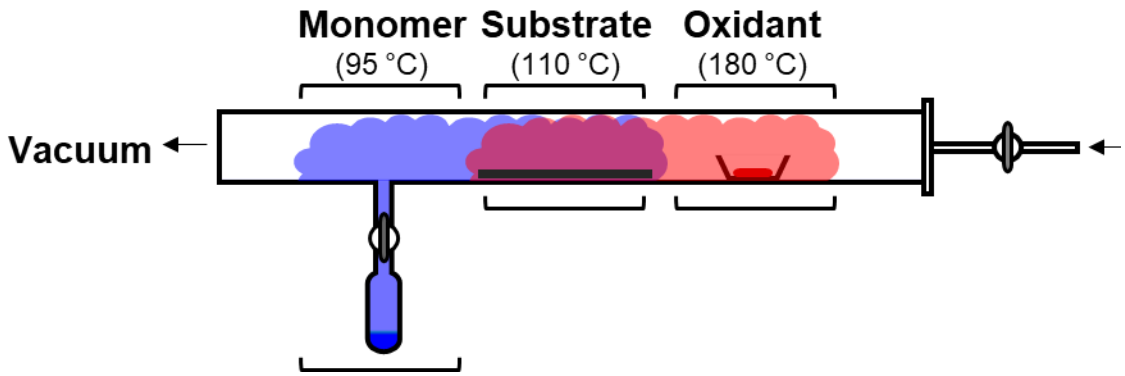

Figure 2.9 Custom built reaction chamber with three independent heating zones and adjustable gas/monomer flow. The blue indicates monomer vapors, the red for oxidant vapors, and the purple indicates the polymerization zone.

In this work, the polymerization reaction occurs in a custom-built tube-shaped reaction chamber, as pictured in Figure 2.9. The chamber is made from a customized quartz tube and functionalized with adjustable valves to control the monomer flow rate. The reaction occurs under an applied vacuum (100-200 mTorr), which is pulled from the left side of the chamber. There are three adjustable, independent heating zones for the monomer, substrate, and oxidant. The monomer is added to a vial which is attached to the inlet on left side of the chamber, closest to the vacuum. The oxidant is held in a boat and placed so there is 2.5-5 inches of space between the monomer inlet and the left edge of the boat. This distance can be adjusted to increase/decrease reaction times and the uniformity of the polymer films. The substrates are placed in the space between the monomer inlet and the oxidant boat. The monomer, substrate, and oxidant zones are heated at 95 °C, 110

°C, and 180 °C, respectively. The oxidant is vaporized first and allowed to fully fill the tube. Then the monomer vapors are introduced and the polymer forms on the surface of the substrate and the heated chamber walls.

The tube chamber used herein and the cube chamber (shown in Figure 2.8d) are similar in that they can both be used to deposit conductive polymers using oCVD. The cube chamber includes a metal "flap" that is used to protect the substrate from the oxidant while the crucible is ramping up to the desired temperature. This flap is mechanically adjusted when the monomer is introduced to the chamber so the reaction can occur on the surface of the substrate. This allows for the polymer to better adsorb onto smooth surfaces, such as glass. If there is a thick layer of oxidant on the surface of a smooth substrate, the polymer is more likely to delaminate during the rinsing process. Additionally, this chamber uses a quartz crystal microbalance (QCM) to give real-time thickness measurements of the film during the polymerization, providing a more fine-tuned control of the film thickness. The cube-shape design of this chamber means that it is larger than the tube chamber, as such, more time is required for a deposition.

The tube-shaped reaction chamber is a faster method to obtain conductive polymers coatings. In this chamber, the distance between the oxidant, substrate, and monomer are all highly adjustable, as are the heating zones. This gives more flexibility in terms of adjusting reaction times, but also allows for the adaption of more complex polymerization setups. For example, our lab has shown that conductive polymers can be deposited on plants in this chamber because the substrate could be arranged in such a way that the moisture from the plant did not react with the oxidant before it is able to vaporize.[84] Although this chamber cannot prevent oxidant from depositing on the surface of the substrate before the monomer

is introduced, if a rough or textured substrate is used the polymer does not delaminate during the rinsing stage. The thickness of the films deposited in this chamber are able to be controlled by standardizing the deposition conditions such as the chamber pressure, distance between the oxidant, monomer, and substrate, and reaction time. The thickness is not able to be measured during the deposition, so it is measured using profilometry measurements of a polymer-coated glass slide post deposition. Because this work focuses mostly on fabric substrates, the tube chamber was chosen for this work over the cube chamber.

The work described within this dissertation will focus on oCVD as a method for coating substrates with Poly(3,4-ethylenedioxythiophene) (PEDOT-Cl). PEDOT films on glass displaying conductivities as high as 2500 S/cm and 1500 S/cm have been obtained via VPP and oCVD, respectively.[85]

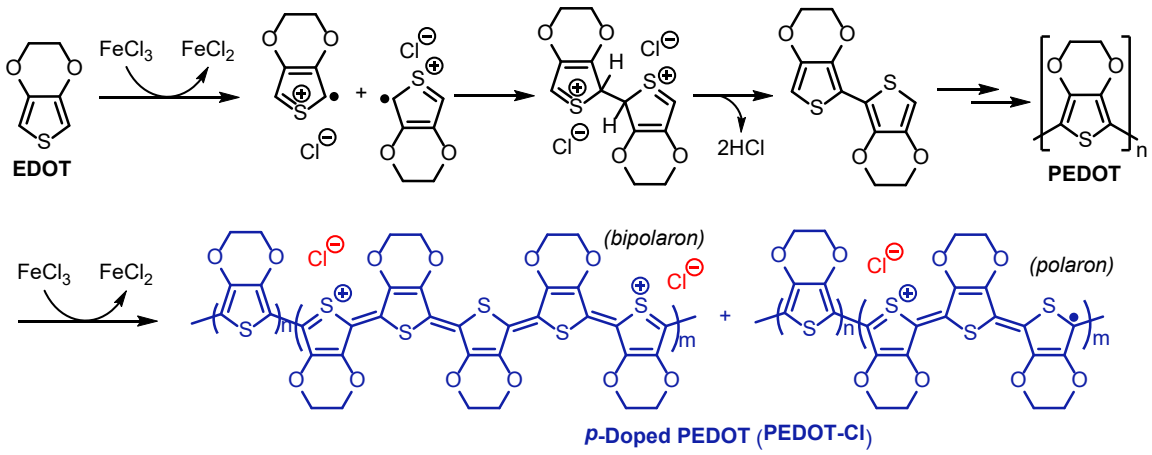

Figure 2.10 Reaction scheme for vapor deposited PEDOT-Cl

Gleason et.al. first reported the mechanism of PEDOT-Cl synthesized by using oCVD in 2006.[86] Our proposed reaction scheme for the oxidative polymerization of

persistently doped PEDOT-Cl can be found in Figure 2.10. First, the vaporized monomer, 3,4-ethylenedioxythiophene (EDOT), reacts with the vaporized oxidant (Iron (III) chloride) on a heated surface to form a radical cation. The radical cations will then combine with another oxidized monomer to create a neutral dimer. The neutral dimers are further oxidized and join with other dimers or oligomeric chains to produce the polymer PEDOT. The oligomer has a lowered oxidation potential due to alternating single and double bonds making them π-conjugated which delocalizes the electrons. During polymerization a counter ion, in this case chloride (Cl^-) which is introduced from the oxidant, binds to the polymer to balance the positive charges which form along the backbone every three or four chain segments.[86]

2.9 PEDOT-Cl Coated Textiles (Tube Reactor)

We have shown that PEDOT-Cl is able to be deposited onto a variety of substrates from glass to textiles and even directly onto plants regardless of surface roughness.[55,84,87,88] Due to oCVD being a multidirectional coating technique we observe conformal and uniform polymer films. Additionally, the oCVD technique is a strictly surface coating technique, as such we do not see penetration of the polymers into the substrate, which has been confirmed through cross-sectional EDX measurements and published in previous work from our lab (Figure 2.11 a-c).[89] Therefor, complex patterns of PEDOT-Cl can be produced on the surface of the substrate through a facile shadow masking technique using Kapton tape. Figure 2.11d-e shows a sample of pristine cotton masked with Kapton Tape and the same sample after PEDOT-Cl has been deposited. We see no bleeding of the polymer to the areas masked by the tape post-deposition, instead we see clean lines where

the mask was applied. Figure 2.11f shows SEM images taken at the boundary between the cotton under the Kapton tape and the cotton exposed to the PEDOT-Cl polymerization. It is clear that there was no polymer bleed even on the microscale. We also see that each individual fiber is coated uniformly and conformally with PEDOT-Cl and there are no areas of polymer aggregation.

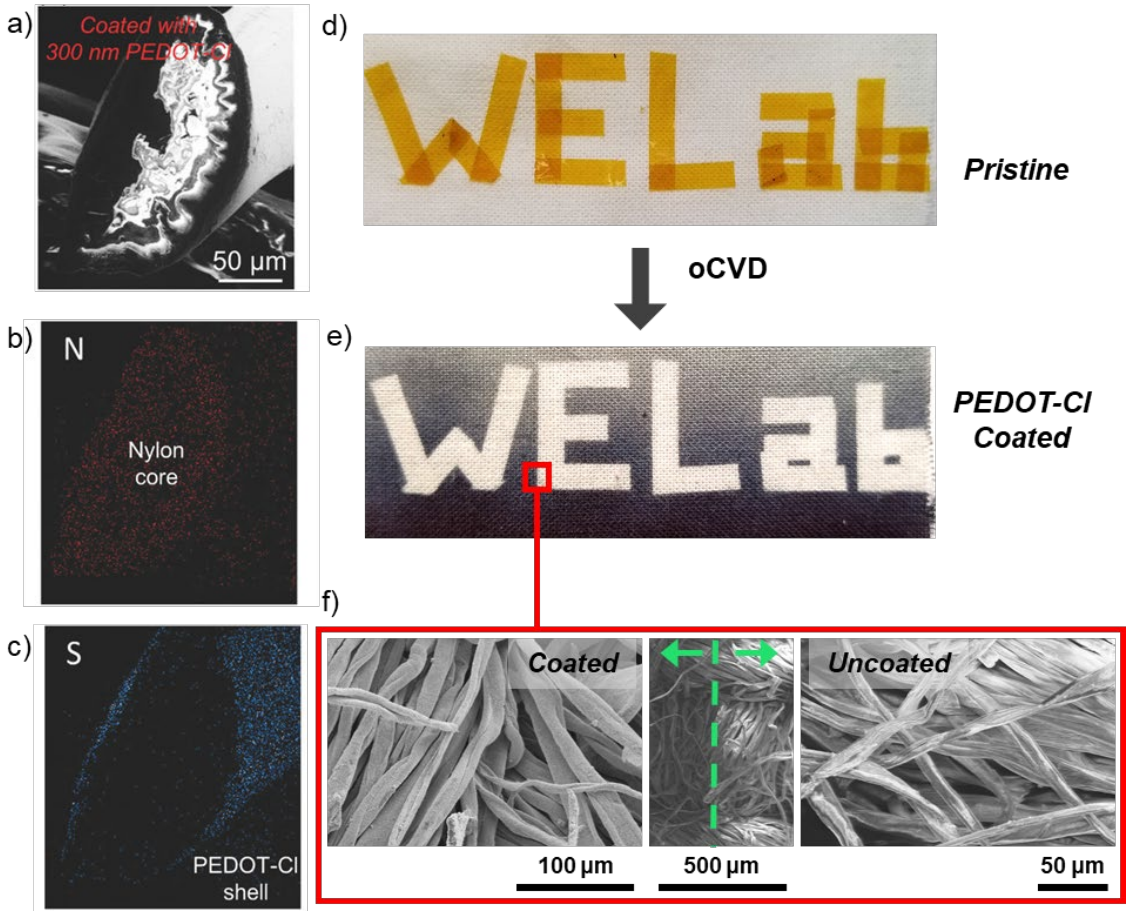

Figure 2.11 a) Cross-section SEM image of a nylon fiber with a 300 nm-thick PEDOT-Cl coating. b) EDX mapping of element N and c) element S of the SEM image in (a) [Ref 8], Cotton templated with Kapton Tape d) before and e) after coating with PEDOT-Cl, f) SEM images of the boundary between the pristine fabric from the shadow mask and the PEDOT-Cl fabric.

The work herein explores the use of different types of fabrics when producing PEDOT-Cl coated textiles. All of the textiles used for coating have not gone through chemical treatment, known as raw textiles, and do not have a coating on the surface that might interfere with adsorption of the polymer. SEM images, Figure 2.12, shows the conformality of the polymer coating on a wool felt and a polyester knit. The polyester knit is a synthetically made textile and as a result the surface of the fibers are smooth.

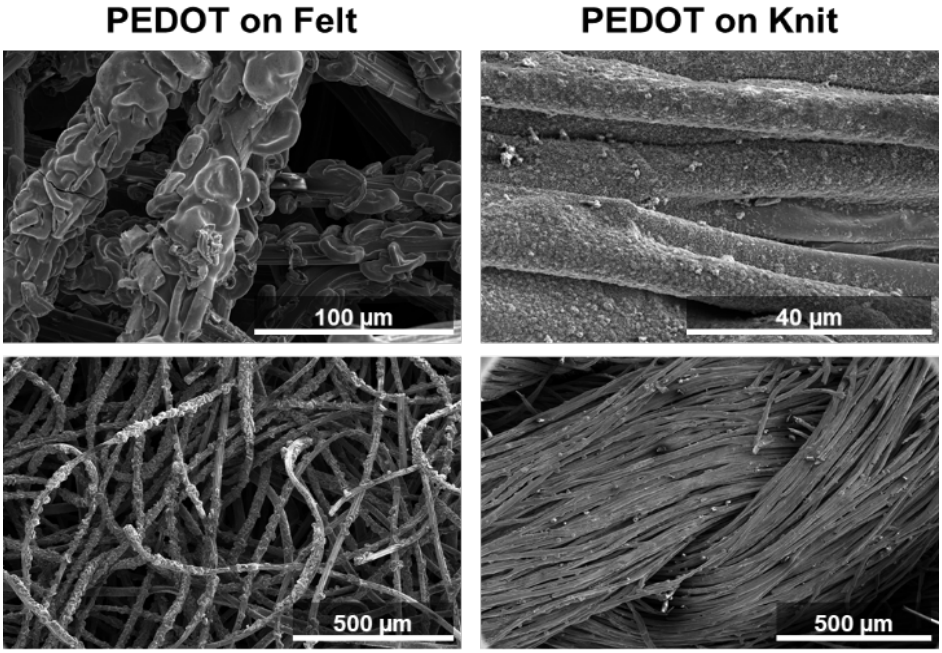

Figure 2.12 SEM images of PEDOT-Cl coated wool felt and polyester knit.

Wool fibers, on the other hand, have cuticle cells covering the exterior of the fiber that look like overlapping plates, giving the fiber a lot of texture (Figure 2.13a). The PEDOT-Cl coatings in the SEM images shown in Figure 2.13b, previously obtained from our lab, reflect the microstructures of these fibers respectively. Additionally, the wool fibers, which naturally have a waxy coating made of fat, demonstrated hydrophobicity after

the PEDOT-Cl coating was deposited. In order for these polymer-coated textiles to be functional in wearable applications, they must show durability under conditions that normal clothing is regularly exposed to. We simulated this by washing a sample of PEDOT-Cl coated cotton in Gain detergent for 5 cycles, as well as folding a sample in half and rubbing it against itself for 100 cycles. The conductivities of these samples as well as a pristine sample of PEDOT-Cl cotton were taken using a 4-point probe and show little to no change (Figure 2.14a).

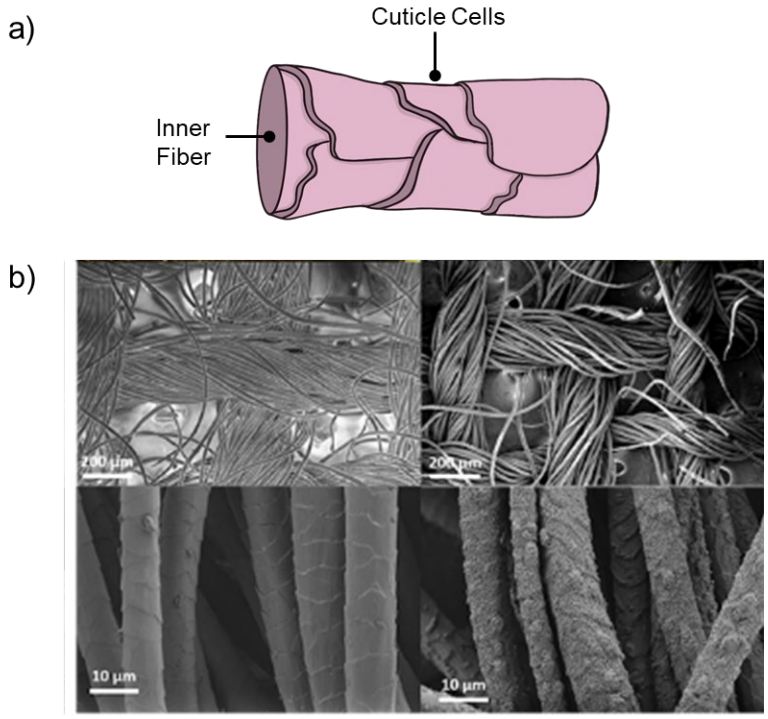

Figure 2.13 a) Diagram of a wool fiber and texture caused by cuticle cells, b) SEM images of PEDOT-Cl coated wool fibers.

We also show that the polymer does not delaminate from the surface of the textile after these conditions are applied. The samples show no visual change after washing and rubbing as analyzed through SEM images (Figure 2.14b-d). We also evaluated the

biocompatibility of PEDOT-Cl through a skin reactivity test. PEDOT-Cl was found to rank alongside polystyrene, which is considered a non-irritant and thus safe for use as a wearable.[55,87,88,90]

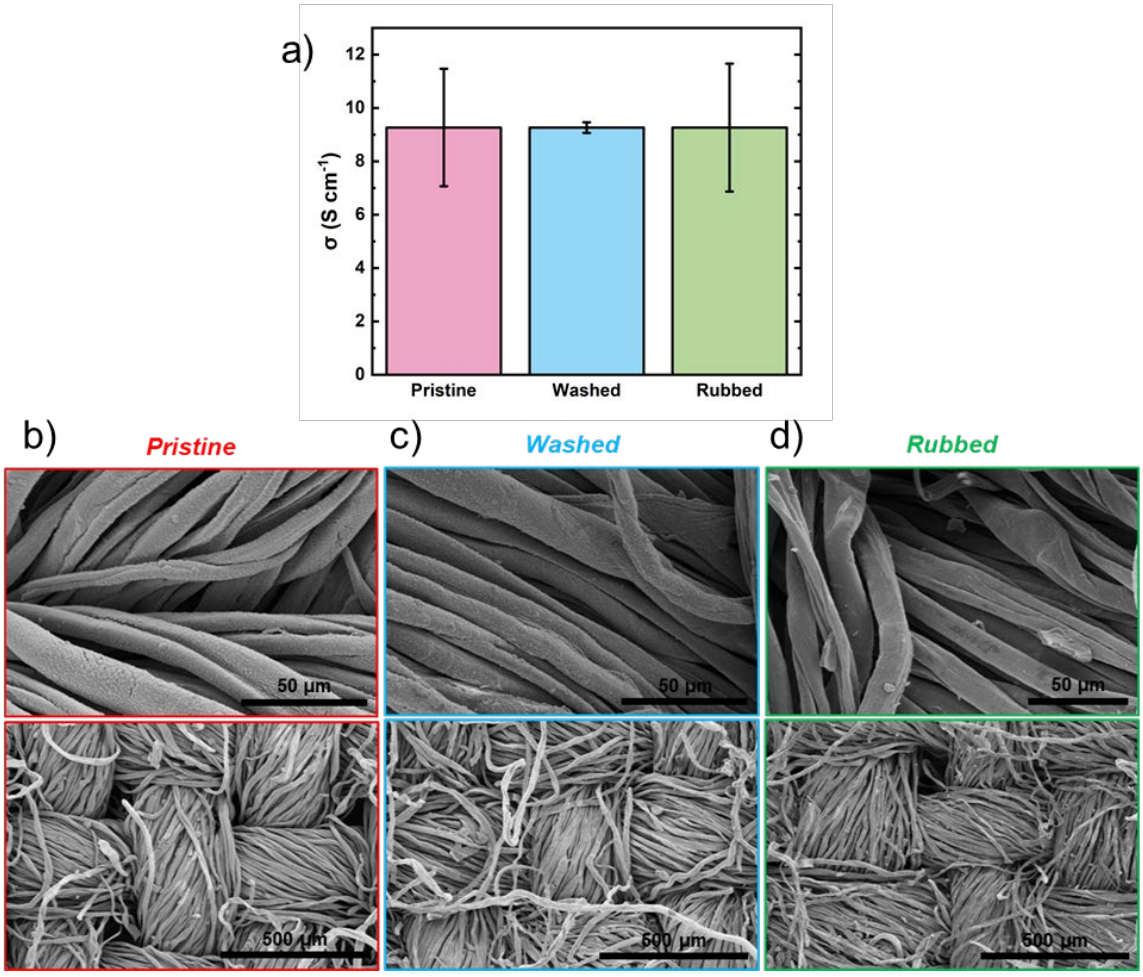

Figure 2.14 a) Conductivity of PEDOT-Cl coated cotton that has been washed and rubbed, b-d) SEM images of PEDOT-Cl cotton pristine, washed, and rubbed, respectively.

2.10 Summary

Chapter 2 explained the oCVD technique of synthesizing PEDOT-Cl. Using this method, PEDOT-Cl coated textiles were produced. The textiles demonstrated uniform and conformal coatings of the fibers and maintained their natural feel. The coatings textiles

were able to maintain their natural properties after coating, as demonstrated by the PEDOT-Cl wool samples' hydrophobicity. These textiles showed durability under washing and rubbing conditions making them a viable option for wearable applications. In Chapter 3, the applications of PEDOT-Cl textiles will be explored.

2.11 References

(1) Kim, D.-H.; Lu, N.; Ma, R.; Kim, Y.-S.; Kim, R.-H.; Wang, S.; Wu, J.; Won, S. M.; Tao, H.; Islam, A.; Yu, K. J.; Kim, T.; Chowdhury, R.; Ying, M.; Xu, L.; Li, M.; Chung, H.-J.; Keum, H.; McCormick, M.; Liu, P.; Zhang, Y.-W.; Omenetto, F. G.; Huang, Y.; Coleman, T.; Rogers, J. A. Epidermal Electronics. Science 2011, 333 (6044), 838–843. https://doi.org/10.1126/science.1206157.

(2) Mostafalu, P.; Akbari, M.; Alberti, K. A.; Xu, Q.; Khademhosseini, A.; Sonkusale, S. R. A Toolkit of Thread-Based Microfluidics, Sensors, and Electronics for 3D Tissue Embedding for Medical Diagnostics. Microsyst. Nanoeng. 2016, 2 (1), 1–10. https://doi.org/10.1038/micronano.2016.39.

(3) Schwartz, G.; Tee, B. C.-K.; Mei, J.; Appleton, A. L.; Kim, D. H.; Wang, H.; Bao, Z. Flexible Polymer Transistors with High Pressure Sensitivity for Application in Electronic Skin and Health Monitoring. Nat. Commun. 2013, 4 (1), 1859. https://doi.org/10.1038/ncomms2832.

(4) O'Connor, T. F.; Zaretski, A. V.; Savagatrup, S.; Printz, A. D.; Wilkes, C. D.; Diaz, M. I.; Sawyer, E. J.; Lipomi, D. J. Wearable Organic Solar Cells with High Cyclic Bending Stability: Materials Selection Criteria. Sol. Energy Mater. Sol. Cells 2016, 144, 438–444. https://doi.org/10.1016/j.solmat.2015.09.049.

(5) Jost, K.; Dion, G.; Gogotsi, Y. Textile Energy Storage in Perspective. J. Mater. Chem. A 2014, 2 (28), 10776–10787. https://doi.org/10.1039/C4TA00203B.

(6) Kaltenbrunner, M.; White, M. S.; Głowacki, E. D.; Sekitani, T.; Someya, T.; Sariciftci, N. S.; Bauer, S. Ultrathin and Lightweight Organic Solar Cells with High Flexibility. Nat. Commun. 2012, 3, 770. https://doi.org/10.1038/ncomms1772.

(7) Kaltenbrunner, M.; Sekitani, T.; Reeder, J.; Yokota, T.; Kuribara, K.; Tokuhara, T.; Drack, M.; Schwödiauer, R.; Graz, I.; Bauer-Gogonea, S.; Bauer, S.; Someya, T. An Ultra-Lightweight Design for Imperceptible Plastic Electronics. Nature 2013, 499 (7459), 458–463. https://doi.org/10.1038/nature12314.

(8) White, M. S.; Kaltenbrunner, M.; Głowacki, E. D.; Gutnichenko, K.; Kettlgruber, G.; Graz, I.; Aazou, S.; Ulbricht, C.; Egbe, D. A. M.; Miron, M. C.; Major, Z.; Scharber, M. C.; Sekitani, T.; Someya, T.; Bauer, S.; Sariciftci, N. S. Ultrathin,

Highly Flexible and Stretchable PLEDs. Nat. Photonics 2013, 7 (10), 811–816. https://doi.org/10.1038/nphoton.2013.188.
(9) Hamedi, M.; Forchheimer, R.; Inganäs, O. Towards Woven Logic from Organic Electronic Fibres. Nat. Mater. 2007, 6 (5), 357–362. https://doi.org/10.1038/nmat1884.
(10) Yang, Z.; Deng, J.; Chen, X.; Ren, J.; Peng, H. A Highly Stretchable, Fiber-Shaped Supercapacitor. Angew. Chem. 2013, 125 (50), 13695–13699. https://doi.org/10.1002/ange.201307619.
(11) Lee, M. R.; Eckert, R. D.; Forberich, K.; Dennler, G.; Brabec, C. J.; Gaudiana, R. A. Solar Power Wires Based on Organic Photovoltaic Materials. Science 2009, 324 (5924), 232–235. https://doi.org/10.1126/science.1168539.
(12) Cai, Z.; Li, L.; Ren, J.; Qiu, L.; Lin, H.; Peng, H. Flexible, Weavable and Efficient Microsupercapacitor Wires Based on Polyaniline Composite Fibers Incorporated with Aligned Carbon Nanotubes. J. Mater. Chem. A 2012, 1 (2), 258–261. https://doi.org/10.1039/C2TA00274D.
(13) Zheng, L.; Zhang, X.; Li, Q.; Chikkannanavar, S. B.; Li, Y.; Zhao, Y.; Liao, X.; Jia, Q.; Doorn, S. K.; Peterson, D. E.; Zhu, Y. Carbon-Nanotube Cotton for Large-Scale Fibers. Adv. Mater. 2007, 19 (18), 2567–2570. https://doi.org/10.1002/adma.200602648.
(14) Ma, R.; Lee, J.; Choi, D.; Moon, H.; Baik, S. Knitted Fabrics Made from Highly Conductive Stretchable Fibers. Nano Lett. 2014, 14 (4), 1944–1951. https://doi.org/10.1021/nl404801t.
(15) Lee, J. A.; Shin, M. K.; Kim, S. H.; Cho, H. U.; Spinks, G. M.; Wallace, G. G.; Lima, M. D.; Lepró, X.; Kozlov, M. E.; Baughman, R. H.; Kim, S. J. Ultrafast Charge and Discharge Biscrolled Yarn Supercapacitors for Textiles and Microdevices. Nat. Commun. 2013, 4 (1), 1970. https://doi.org/10.1038/ncomms2970.
(16) Peng, M.; Zou, D. Flexible Fiber/Wire-Shaped Solar Cells in Progress: Properties, Materials, and Designs. J. Mater. Chem. A 2015, 3 (41), 20435–20458. https://doi.org/10.1039/C5TA03731J.
(17) Jost, K.; R. Perez, C.; K. McDonough, J.; Presser, V.; Heon, M.; Dion, G.; Gogotsi, Y. Carbon Coated Textiles for Flexible Energy Storage. Energy Environ. Sci. 2011, 4 (12), 5060–5067. https://doi.org/10.1039/C1EE02421C.
(18) Hu, L.; Pasta, M.; La Mantia, F.; Cui, L.; Jeong, S.; Deshazer, H. D.; Choi, J. W.; Han, S. M.; Cui, Y. Stretchable, Porous, and Conductive Energy Textiles. Nano Lett. 2010, 10 (2), 708–714. https://doi.org/10.1021/nl903949m.
(19) Koncar, V. Smart Textiles and Their Applications; Woodhead Publishing, 2016.
(20) Ding, Y.; Invernale, M. A.; Sotzing, G. A. Conductivity Trends of PEDOT-PSS Impregnated Fabric and the Effect of Conductivity on Electrochromic Textile. ACS Appl. Mater. Interfaces 2010, 2 (6), 1588–1593. https://doi.org/10.1021/am100036n.
(21) Amba Sankar K., N.; Mohanta, K. Dwindling the Resistance Value of PEDOT:PSS - Coated on Fabric Yarns. 2016, 1731, 120019. https://doi.org/10.1063/1.4948091.

(22) Yeon, C.; Kim, G.; W. Lim, J.; J. Yun, S. Highly Conductive PEDOT:PSS Treated by Sodium Dodecyl Sulfate for Stretchable Fabric Heaters. RSC Adv. 2017, 7 (10), 5888–5897. https://doi.org/10.1039/C6RA24749K.

(23) Wu, Q.; Hu, J. Waterborne Polyurethane Based Thermoelectric Composites and Their Application Potential in Wearable Thermoelectric Textiles. Compos. Part B Eng. 2016, 107, 59–66. https://doi.org/10.1016/j.compositesb.2016.09.068.

(24) Åkerfeldt, M.; Strååt, M.; Walkenström, P. Influence of Coating Parameters on Textile and Electrical Properties of a Poly(3,4-Ethylene Dioxythiophene):Poly(Styrene Sulfonate)/Polyurethane-Coated Textile. Text. Res. J. 2013, 83 (20), 2164–2176. https://doi.org/10.1177/0040517513487786.

(25) Ryan, J. D.; Mengistie, D. A.; Gabrielsson, R.; Lund, A.; Müller, C. Machine-Washable PEDOT:PSS Dyed Silk Yarns for Electronic Textiles. ACS Appl. Mater. Interfaces 2017, 9 (10), 9045–9050. https://doi.org/10.1021/acsami.7b00530.

(26) Kirihara, K.; Wei, Q.; Mukaida, M.; Ishida, T. Thermoelectric Power Generation Using Nonwoven Fabric Module Impregnated with Conducting Polymer PEDOT:PSS. Synth. Met. https://doi.org/10.1016/j.synthmet.2017.01.001.

(27) Du, Y.; Cai, K.; Chen, S.; Wang, H.; Shen, S. Z.; Donelson, R.; Lin, T. Thermoelectric Fabrics: Toward Power Generating Clothing. Sci. Rep. 2015, 5, 6411. https://doi.org/10.1038/srep06411.

(28) Müller, C.; Jansson, R.; Elfwing, A.; Askarieh, G.; Karlsson, R.; Hamedi, M.; Rising, A.; Johansson, J.; Inganäs, O.; Hedhammar, M. Functionalisation of Recombinant Spider Silk with Conjugated Polyelectrolytes. J. Mater. Chem. 2011, 21 (9), 2909–2915. https://doi.org/10.1039/C0JM03270K.

(29) Müller, C.; Hamedi, M.; Karlsson, R.; Jansson, R.; Marcilla, R.; Hedhammar, M.; Inganäs, O. Woven Electrochemical Transistors on Silk Fibers. Adv. Mater. 2011, 23 (7), 898–901. https://doi.org/10.1002/adma.201003601.

(30) Tarabella, G.; Villani, M.; Calestani, D.; Mosca, R.; Iannotta, S.; Zappettini, A.; Coppedè, N. A Single Cotton Fiber Organic Electrochemical Transistor for Liquid Electrolyte Saline Sensing. J. Mater. Chem. 2012, 22 (45), 23830–23834. https://doi.org/10.1039/C2JM34898E.

(31) Coppedè, N.; Tarabella, G.; Villani, M.; Calestani, D.; Iannotta, S.; Zappettini, A. Human Stress Monitoring through an Organic Cotton-Fiber Biosensor. J. Mater. Chem. B 2014, 2 (34), 5620–5626. https://doi.org/10.1039/C4TB00317A.

(32) Zhang, L.; Yu, Y.; Eyer, G. P.; Suo, G.; Kozik, L. A.; Fairbanks, M.; Wang, X.; Andrew, T. L. All-Textile Triboelectric Generator Compatible with Traditional Textile Process. Adv. Mater. Technol. 2016, 1 (9), 1600147. https://doi.org/10.1002/admt.201600147.

(33) Sadki, S.; Schottland, P.; Brodie, N.; Sabouraud, G. The Mechanisms of Pyrrole Electropolymerization. Chem. Soc. Rev. 2000, 29 (5), 283–293. https://doi.org/10.1039/A807124A.

(34) Subianto, S.; Will, GeoffreyD.; Kokot, S. Electropolymerization of Pyrrole on Cotton Fabrics. Int. J. Polym. Mater. 2005, 54 (2), 141–150. https://doi.org/10.1080/00914030390246252.

(35) Bhadani, S. N.; Kumari, M.; Gupta, S. K. S.; Sahu, G. C. Preparation of Conducting Fibers via the Electrochemical Polymerization of Pyrrole. J. Appl. Polym. Sci. 1997, 64 (6), 1073–1077. https://doi.org/10.1002/(SICI)1097-4628(19970509)64:6<1073::AID-APP6>3.0.CO;2-I.
(36) Molina, J.; del Río, A. I.; Bonastre, J.; Cases, F. Electrochemical Polymerisation of Aniline on Conducting Textiles of Polyester Covered with Polypyrrole/AQSA. Eur. Polym. J. 2009, 45 (4), 1302–1315. https://doi.org/10.1016/j.eurpolymj.2008.11.003.
(37) Molina, J.; del Río, A. I.; Bonastre, J.; Cases, F. Chemical and Electrochemical Polymerisation of Pyrrole on Polyester Textiles in Presence of Phosphotungstic Acid. Eur. Polym. J. 2008, 44 (7), 2087–2098. https://doi.org/10.1016/j.eurpolymj.2008.04.007.
(38) Severt, S. Y.; Ostrovsky-Snider, N. A.; Leger, J. M.; Murphy, A. R. Versatile Method for Producing 2D and 3D Conductive Biomaterial Composites Using Sequential Chemical and Electrochemical Polymerization. ACS Appl. Mater. Interfaces 2015, 7 (45), 25281–25288. https://doi.org/10.1021/acsami.5b07332.
(39) Maziz, A.; Concas, A.; Khaldi, A.; Stålhand, J.; Persson, N.-K.; Jager, E. W. H. Knitting and Weaving Artificial Muscles. Sci. Adv. 3 (1), e1600327. https://doi.org/10.1126/sciadv.1600327.
(40) Das, C.; Jain, B.; Krishnamoorthy, K. Phenols from Green Tea as a Dual Functional Coating to Prepare Devices for Energy Storage and Molecular Separation. Chem. Commun. 2015, 51 (58), 11662–11664. https://doi.org/10.1039/C5CC03108G.
(41) Molina, J.; del Río, A. I.; Bonastre, J.; Cases, F. Influence of the Scan Rate on the Morphology of Polyaniline Grown on Conducting Fabrics. Centipede-like Morphology. Synth. Met. 2010, 160 (1), 99–107. https://doi.org/10.1016/j.synthmet.2009.10.012.
(42) Hong, K. H.; Oh, K. W.; Kang, T. J. Preparation and Properties of Electrically Conducting Textiles by in Situ Polymerization of Poly(3,4-Ethylenedioxythiophene). J. Appl. Polym. Sci. 2005, 97 (3), 1326–1332. https://doi.org/10.1002/app.21835.
(43) Varesano, A.; Aluigi, A.; Florio, L.; Fabris, R. Multifunctional Cotton Fabrics. Synth. Met. 2009, 159 (11), 1082–1089. https://doi.org/10.1016/j.synthmet.2009.01.036.
(44) Xu, J.; Wang, D.; Fan, L.; Yuan, Y.; Wei, W.; Liu, R.; Gu, S.; Xu, W. Fabric Electrodes Coated with Polypyrrole Nanorods for Flexible Supercapacitor Application Prepared via a Reactive Self-Degraded Template. Org. Electron. 2015, 26, 292–299. https://doi.org/10.1016/j.orgel.2015.07.054.
(45) Akşit, A. C.; Onar, N.; Ebeoglugil, M. F.; Birlik, I.; Celik, E.; Ozdemir, I. Electromagnetic and Electrical Properties of Coated Cotton Fabric with Barium Ferrite Doped Polyaniline Film. J. Appl. Polym. Sci. 2009, 113 (1), 358–366. https://doi.org/10.1002/app.29856.
(46) Maráková, N.; Humpolíček, P.; Kašpárková, V.; Capáková, Z.; Martinková, L.; Bober, P.; Trchová, M.; Stejskal, J. Antimicrobial Activity and Cytotoxicity of

Cotton Fabric Coated with Conducting Polymers, Polyaniline or Polypyrrole, and with Deposited Silver Nanoparticles. Appl. Surf. Sci. 2017, 396, 169–176. https://doi.org/10.1016/j.apsusc.2016.11.024.

(47) Sarvi, A.; Silva, A. B.; Bretas, R. E.; Sundararaj, U. A New Approach for Conductive Network Formation in Electrospun Poly(Vinylidene Fluoride) Nanofibers. Polym. Int. 2015, 64 (9), 1262–1267. https://doi.org/10.1002/pi.4915.

(48) Ding, B.; Wang, M.; Wang, X.; Yu, J.; Sun, G. Electrospun Nanomaterials for Ultrasensitive Sensors. Mater. Today 2010, 13 (11), 16–27. https://doi.org/10.1016/S1369-7021(10)70200-5.

(49) Ye, W.; Zhu, J.; Liao, X.; Jiang, S.; Li, Y.; Fang, H.; Hou, H. Hierarchical Three-Dimensional Micro/Nano-Architecture of Polyaniline Nanowires Wrapped-on Polyimide Nanofibers for High Performance Lithium-Ion Battery Separators. J. Power Sources 2015, 299, 417–424. https://doi.org/10.1016/j.jpowsour.2015.09.037.

(50) Alf, M. E.; Asatekin, A.; Barr, M. C.; Baxamusa, S. H.; Chelawat, H.; Ozaydin-Ince, G.; Petruczok, C. D.; Sreenivasan, R.; Tenhaeff, W. E.; Trujillo, N. J.; Vaddiraju, S.; Xu, J.; Gleason, K. K. Chemical Vapor Deposition of Conformal, Functional, and Responsive Polymer Films. Adv. Mater. 2010, 22 (18), 1993–2027. https://doi.org/10.1002/adma.200902765.

(51) Bhattacharyya, D.; Howden, R. M.; Borrelli, D. C.; Gleason, K. K. Vapor Phase Oxidative Synthesis of Conjugated Polymers and Applications. J. Polym. Sci. Part B Polym. Phys. 2012, 50 (19), 1329–1351. https://doi.org/10.1002/polb.23138.

(52) Tenhaeff Wyatt E.; Gleason Karen K. Initiated and Oxidative Chemical Vapor Deposition of Polymeric Thin Films: ICVD and OCVD. Adv. Funct. Mater. 2008, 18 (7), 979–992. https://doi.org/10.1002/adfm.200701479.

(53) Vaeth, K. M.; Jensen, K. F. Selective Growth of Poly(p-Phenylene Vinylene) Prepared by Chemical Vapor Deposition. Adv. Mater. 1999, 11 (10), 814–820. https://doi.org/10.1002/(SICI)1521-4095(199907)11:10<814::AID-ADMA814>3.0.CO;2-Z.

(54) Lau, K. K. S.; Gleason, K. K. Initiated Chemical Vapor Deposition (ICVD) of Poly(Alkyl Acrylates): An Experimental Study. Macromolecules 2006, 39 (10), 3688–3694. https://doi.org/10.1021/ma0601619.

(55) Allison, L. K.; Andrew, T. L. A Wearable All-Fabric Thermoelectric Generator. Adv. Mater. Technol. 2019, 4 (5), 1800615. https://doi.org/10.1002/admt.201800615.

(56) Choy, K. L. Chemical Vapour Deposition of Coatings. Prog. Mater. Sci. 2003, 48 (2), 57–170. https://doi.org/10.1016/S0079-6425(01)00009-3.

(57) Dall'Acqua, L.; Tonin, C.; Varesano, A.; Canetti, M.; Porzio, W.; Catellani, M. Vapour Phase Polymerisation of Pyrrole on Cellulose-Based Textile Substrates. Synth. Met. 2006, 156 (5), 379–386. https://doi.org/10.1016/j.synthmet.2005.12.021.

(58) Shang, S.; Yang, X.; Tao, X.; Lam, S. S. Vapor-Phase Polymerization of Pyrrole on Flexible Substrate at Low Temperature and Its Application in Heat Generation. Polym. Int. 2010, 59 (2), 204–211. https://doi.org/10.1002/pi.2709.
(59) Bashir, T.; Ali, M.; Cho, S.-W.; Persson, N.-K.; Skrifvars, M. OCVD Polymerization of PEDOT: Effect of Pre-Treatment Steps on PEDOT-Coated Conductive Fibers and a Morphological Study of PEDOT Distribution on Textile Yarns. Polym. Adv. Technol. 2013, 24 (2), 210–219. https://doi.org/10.1002/pat.3073.
(60) Laforgue, A.; Robitaille, L. Production of Conductive PEDOT Nanofibers by the Combination of Electrospinning and Vapor-Phase Polymerization. Macromolecules 2010, 43 (9), 4194–4200. https://doi.org/10.1021/ma9027678.
(61) Laforgue, A. Electrically Controlled Colour-Changing Textiles Using the Resistive Heating Properties of PEDOT Nanofibers. J. Mater. Chem. 2010, 20 (38), 8233–8235. https://doi.org/10.1039/C0JM02307H.
(62) Bashir, T.; Naeem, J.; Skrifvars, M.; Persson, N.-K. Synthesis of Electro-Active Membranes by Chemical Vapor Deposition (CVD) Process. Polym. Adv. Technol. 2014, 25 (12), 1501–1508. https://doi.org/10.1002/pat.3392.
(63) Kovacik, P.; Hierro, G. del; Livernois, W.; Gleason, K. K. Scale-up of OCVD: Large-Area Conductive Polymer Thin Films for next-Generation Electronics. Mater. Horiz. 2015, 2 (2), 221–227. https://doi.org/10.1039/C4MH00222A.
(64) Park, J.-H.; Sudarshan, T. S. Chemical Vapor Deposition; ASM International, 2001.
(65) Rajendran, S.; Nguyen, T. A.; Kakooei, S.; Li, Y.; Yeganeh, M. Corrosion Protection at the Nanoscale; Elsevier, 2020.
(66) Im, S. G.; Kusters, D.; Choi, W.; Baxamusa, S. H.; van de Sanden, M. C. M.; Gleason, K. K. Conformal Coverage of Poly(3,4-Ethylenedioxythiophene) Films with Tunable Nanoporosity via Oxidative Chemical Vapor Deposition. ACS Nano 2008, 2 (9), 1959–1967. https://doi.org/10.1021/nn800380e.
(67) Chen, N.; Wang, X.; Gleason, K. K. Conformal Single-Layer Encapsulation of PEDOT at Low Substrate Temperature. Appl. Surf. Sci. 2014, 323, 2–6. https://doi.org/10.1016/j.apsusc.2014.06.123.
(68) Chelawat, H.; Vaddiraju, S.; Gleason, K. Conformal, Conducting Poly(3,4-Ethylenedioxythiophene) Thin Films Deposited Using Bromine as the Oxidant in a Completely Dry Oxidative Chemical Vapor Deposition Process. Chem. Mater. 2010, 22 (9), 2864–2868. https://doi.org/10.1021/cm100092c.
(69) Barr Miles C.; Rowehl Jill A.; Lunt Richard R.; Xu Jingjing; Wang Annie; Boyce Christopher M.; Im Sung Gap; Bulović Vladimir; Gleason Karen K. Direct Monolithic Integration of Organic Photovoltaic Circuits on Unmodified Paper. Adv. Mater. 2011, 23 (31), 3500–3505. https://doi.org/10.1002/adma.201101263.
(70) Goktas, H.; Wang, X.; Boscher, N. D.; Torosian, S.; Gleason, K. K. Functionalizable and Electrically Conductive Thin Films Formed by Oxidative Chemical Vapor Deposition (OCVD) from Mixtures of 3-Thiopheneethanol (3TE)

and Ethylene Dioxythiophene (EDOT). J. Mater. Chem. C 2016, 4 (16), 3403–3414. https://doi.org/10.1039/C6TC00567E.

(71) Howden, R. M.; McVay, E. D.; Gleason, K. K. OCVD Poly(3,4-Ethylenedioxythiophene) Conductivity and Lifetime Enhancement via Acid Rinse Dopant Exchange. J. Mater. Chem. A 2012, 1 (4), 1334–1340. https://doi.org/10.1039/C2TA00321J.

(72) Chen, N.; Kim, D. H.; Kovacik, P.; Sojoudi, H.; Wang, M.; Gleason, K. K. Polymer Thin Films and Surface Modification by Chemical Vapor Deposition: Recent Progress. Annu. Rev. Chem. Biomol. Eng. 2016, 7 (1), 373–393. https://doi.org/10.1146/annurev-chembioeng-080615-033524.

(73) Im, S. G.; Gleason, K. K. Systematic Control of the Electrical Conductivity of Poly(3,4-Ethylenedioxythiophene) via Oxidative Chemical Vapor Deposition. Macromolecules 2007, 40 (18), 6552–6556. https://doi.org/10.1021/ma0628477.

(74) Goktas, H.; Wang, X.; Ugur, A.; Gleason, K. K. Water-Assisted Vapor Deposition of PEDOT Thin Film. Macromol. Rapid Commun. 2015, 36 (13), 1283–1289. https://doi.org/10.1002/marc.201500069.

(75) Li, Y.; Cheng, X. Y.; Leung, M. Y.; Tsang, J.; Tao, X. M.; Yuen, M. C. W. A Flexible Strain Sensor from Polypyrrole-Coated Fabrics. Synth. Met. 2005, 155 (1), 89–94. https://doi.org/10.1016/j.synthmet.2005.06.008.

(76) Hilt, F.; Boscher, N. D.; Duday, D.; Desbenoit, N.; Levalois-Grützmacher, J.; Choquet, P. Atmospheric Pressure Plasma-Initiated Chemical Vapor Deposition (AP-PiCVD) of Poly(Diethylallylphosphate) Coating: A Char-Forming Protective Coating for Cellulosic Textile. ACS Appl. Mater. Interfaces 2014, 6 (21), 18418–18422. https://doi.org/10.1021/am504892q.

(77) Abessolo Ondo, D.; Loyer, F.; Werner, F.; Leturcq, R.; Dale, P. J.; Boscher, N. D. Atmospheric-Pressure Synthesis of Atomically Smooth, Conformal, and Ultrathin Low-k Polymer Insulating Layers by Plasma-Initiated Chemical Vapor Deposition. ACS Appl. Polym. Mater. 2019, 1 (12), 3304–3312. https://doi.org/10.1021/acsapm.9b00759.

(78) Mohammadi, A.; Hasan, M.-A.; Liedberg, B.; Lundström, I.; Salaneck, W. R. Chemical Vapour Deposition (CVD) of Conducting Polymers: Polypyrrole. Synth. Met. 1986, 14 (3), 189–197. https://doi.org/10.1016/0379-6779(86)90183-9.

(79) Zhang, L.; Andrew, T. L. Deposition Dependent Ion Transport in Doped Conjugated Polymer Films: Insights for Creating High-Performance Electrochemical Devices. Adv. Mater. Interfaces 2017, 4 (23), n/a-n/a. https://doi.org/10.1002/admi.201700873.

(80) Wang, X.; Zhang, X.; Sun, L.; Lee, D.; Lee, S.; Wang, M.; Zhao, J.; Shao-Horn, Y.; Dincă, M.; Palacios, T.; Gleason, K. K. High Electrical Conductivity and Carrier Mobility in OCVD PEDOT Thin Films by Engineered Crystallization and Acid Treatment. Sci. Adv. 2018, 4 (9), eaat5780. https://doi.org/10.1126/sciadv.aat5780.

(81) Smolin, Yuriy. Y.; Soroush, M.; Lau, K. K. S. Influence of OCVD Polyaniline Film Chemistry in Carbon-Based Supercapacitors. Ind. Eng. Chem. Res. 2017, 56 (21), 6221–6228. https://doi.org/10.1021/acs.iecr.7b00441.
(82) Bhattacharya, S.; Datta, A.; Berg, J. M.; Gangopadhyay, S. Studies on Surface Wettability of Poly(Dimethyl) Siloxane (PDMS) and Glass under Oxygen-Plasma Treatment and Correlation with Bond Strength. J. Microelectromechanical Syst. 2005, 14 (3), 590–597. https://doi.org/10.1109/JMEMS.2005.844746.
(83) Bilger, D.; Homayounfar, S. Z.; Andrew, T. L. A Critical Review of Reactive Vapor Deposition for Conjugated Polymer Synthesis. J. Mater. Chem. C 2019, 7 (24), 7159–7174. https://doi.org/10.1039/C9TC01388A.
(84) Kim, J. J.; Allison, L. K.; Andrew, T. L. Vapor-Printed Polymer Electrodes for Long-Term, on-Demand Health Monitoring. Sci. Adv. 2019, 5 (3), eaaw0463. https://doi.org/10.1126/sciadv.aaw0463.
(85) Atanasov, S. E.; Losego, M. D.; Gong, B.; Sachet, E.; Maria, J.-P.; Williams, P. S.; Parsons, G. N. Highly Conductive and Conformal Poly(3,4-Ethylenedioxythiophene) (PEDOT) Thin Films via Oxidative Molecular Layer Deposition. Chem. Mater. 2014, 26 (11), 3471–3478. https://doi.org/10.1021/cm500825b.
(86) Lock, J. P.; Im, S. G.; Gleason, K. K. Oxidative Chemical Vapor Deposition of Electrically Conducting Poly(3,4-Ethylenedioxythiophene) Films. Macromolecules 2006, 39 (16), 5326–5329. https://doi.org/10.1021/ma060113o.
(87) Zhang, L.; Baima, M.; Andrew, T. L. Transforming Commercial Textiles and Threads into Sewable and Weavable Electric Heaters. ACS Appl. Mater. Interfaces 2017, 9 (37), 32299–32307. https://doi.org/10.1021/acsami.7b10514.
(88) Zhang Lushuai; Fairbanks Marianne; Andrew Trisha L. Rugged Textile Electrodes for Wearable Devices Obtained by Vapor Coating Off-the-Shelf, Plain-Woven Fabrics. Adv. Funct. Mater. 2017, 27 (24), 1700415. https://doi.org/10.1002/adfm.201700415.
(89) Zhang, L.; Andrew, T. Vapor-Coated Monofilament Fibers for Embroidered Electrochemical Transistor Arrays on Fabrics. Adv. Electron. Mater. 2018, 4 (9), 1800271. https://doi.org/10.1002/aelm.201800271.
(90) Allison, L.; Hoxie, S.; Andrew, T. L. Towards Seamlessly-Integrated Textile Electronics: Methods to Coat Fabrics and Fibers with Conducting Polymers for Electronic Applications. Chem. Commun. 2017, 53 (53), 7182–7193. https://doi.org/10.1039/C7CC02592K.

Chapter 3

EXPLORING THE HYGRO-RESISTIVE PROPERTIES OF VAPOR-DEPOSITED PEDOT-CL AND ITS USE IN WEARABLE RESPIRATION MONITORING

3.1 Introduction

In Chapter 2 the process of creating PEDOT-Cl coated textiles using the CVD method was explained. Chapter 3 explores the innate properties of PEDOT-Cl in relation to moisture. The change of a material's electrical resistance when exposed to moisture is known as the hygroresistivity. This is an inherent property of mixed ionic-electronic conductors, such as PEDOT-Cl.

In recent years there has been a rise in demand for wearable health sensors. By integrating sensors with garments, we are able to create a means of non-invasive and long-term health monitoring, which is more accessible to patients and lay consumers. More recently, wearable respiration sensors have received a lot of attention and can be used for detecting and monitoring respiratory diseases such as asthma, and respiratory viruses such as pneumonia.[1–16] Techniques that are used to accurately assess respiration involve tracking the rise and fall of breaths using a pressure sensor, which can be subject to motion artifacts,

as well as techniques such as nasal cannula where pipes are inserted into the nose, which are much more invasive, however these techniques are not practical for large-scale or long-term monitoring.[17–20] Respiration allows for physiological signals, such as humidity and temperature, to be released from the mouth and nose through an air flow. By using a material that can sense these physiological signals, we can develop a functional and practical way of monitoring respiration as well as other health indicators.[21]

One way of sensing respiration is by using a resistive humidity sensor, which converts humidity changes into electrical signals. Borini et. al. reported an ultrafast graphene oxide humidity sensor with a 30 ms response and recovery time on a polyethylene naphthalate substrate.[22] These devices were able to distinguish between breathing and speaking based on the electrical response pattern of the device. Pang et. al. and Chen et. al. have reported success with monitoring respiration using a graphene and graphene oxide humidity sensor, respectively, mounted into face masks.[23,24] Both of these reports, however, involve a complex synthetic process that mixes vapor phase synthesis and solution synthesis, which would be difficult to scale up for commercial production.

Herein we report a resistive humidity sensor composed of a fabric vapor coated with poly(3,4-ethylenedioxythiophene): chloride (PEDOT-Cl). We integrate the device into a heat-molded mask as well as a cotton mask and analyze the electrical response of the sensor to monitor a person's respiration. We show that these devices can be used longitudinally to differentiate between shallow breathing and deep breaths, as well as differentiating between breathing and talking, in both indoor and outdoor environments.

These functions will allow our wearable sensor to alert wearers to potential respiratory distress as they go about their lives.

3.2 Results and Discussion

3.2.1 Humidity Sensors and Mask Design

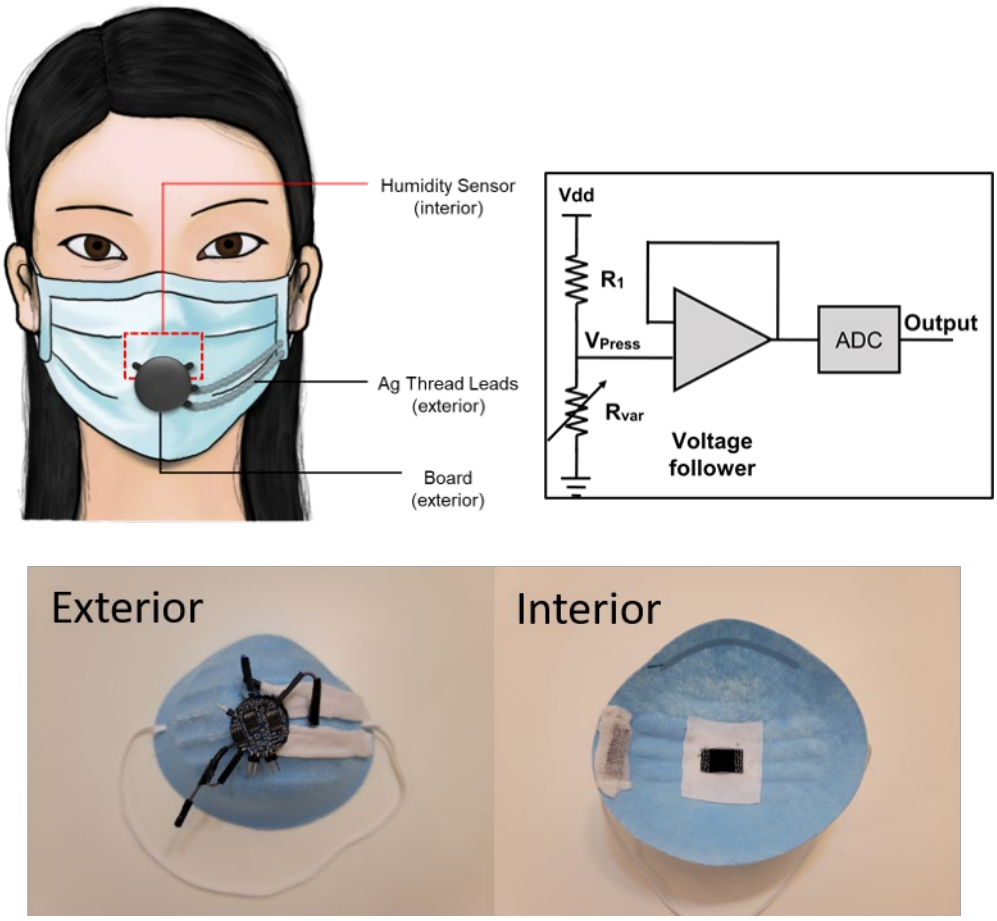

Figure 3.1 a) Illustration of a smart mask for respiration monitoring. b) Circuit diagram of the control board. c) Pictures of the exterior and interior of the mask.

The humidity sensors, also known as hygristors, were made out of a standard cotton coated with poly(3,4-ethylenedioxythiophene) (PEDOT-Cl), using a reactive vapor deposition (RVD) process. This procedure has been previously reported by our group.[25] The resulting fabrics have a conformal and uniform coating of the polymer, which makes them very robust. The fabrics were subjected to 10 wash cycles to assess the robustness, the resulting resistance being 1.16 ± 0.09 kΩ, which indicates excellent adsorption of the polymer to the textile fibers.[26]

The hygristor devices were constructed by sewing silver thread to each end of a 2 cm x 2 cm rectangle of PEDOT-Cl coated cotton with a hydrophobic fabric backing. The hygristor was then mounted in the mask in a location that sits between the nose and the mouth in order to sense respiration coming from both (Figure 3.1 a). The silver thread leads were yarned and threaded through the mask to connect to the electrical board which is mounted on the exterior of the mask. The electrical board measures the voltage changes of the hygristor, the circuit diagram can be found in Figure 3.1 c. Motion artifacts are able to be reduced through the use of cotton tubing.

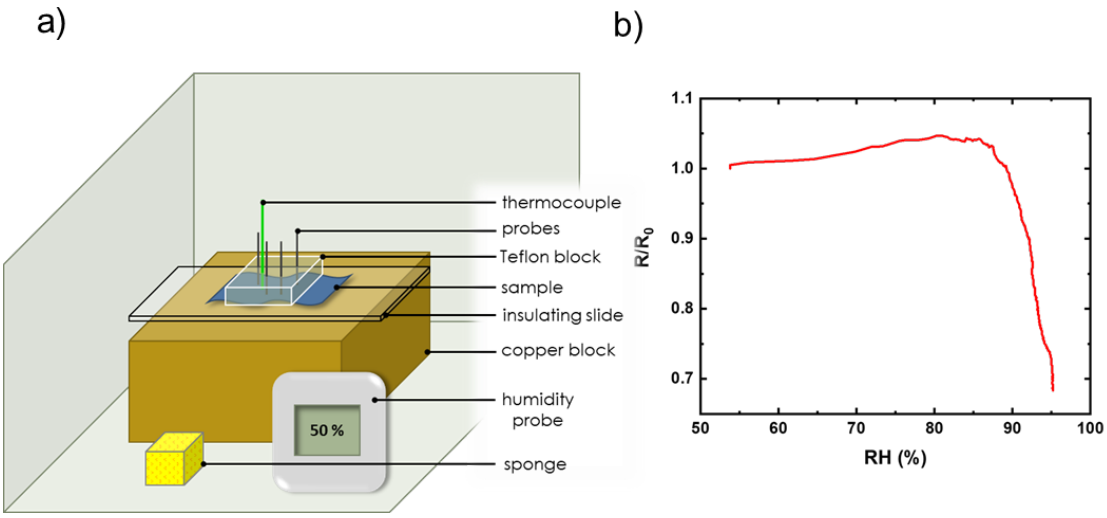

Figure 3.2 a) The measurement setup for evaluating the humidity dependent resistance of the sensors, b) the normalized resistance response of the PEDOT-Cl sensor to an increase in humidity.

Because the PEDOT-Cl samples demonstrate a moisture dependent conductivity, we can conclusively categorize this polymer as a mixed ionic-electronic conductor. This means that when moisture is introduced, ions within the polymer become mobile and are able to increase the ionic conductivity. In PEDOT-Cl the mobile ions are Cl^- ions that are introduced during the deposition process (Figure 3.3a). Comparatively, PEDOT:PSS, which is also a mixed ionic-electronic conductor, can have several mobile ions in the form of free SO_3 anions, $Na^+SO_3^-$, or SO_3H ions (Figure 3.3b). These ions are introduced during the synthesis of PEDOT:PSS and can be present in the final product.

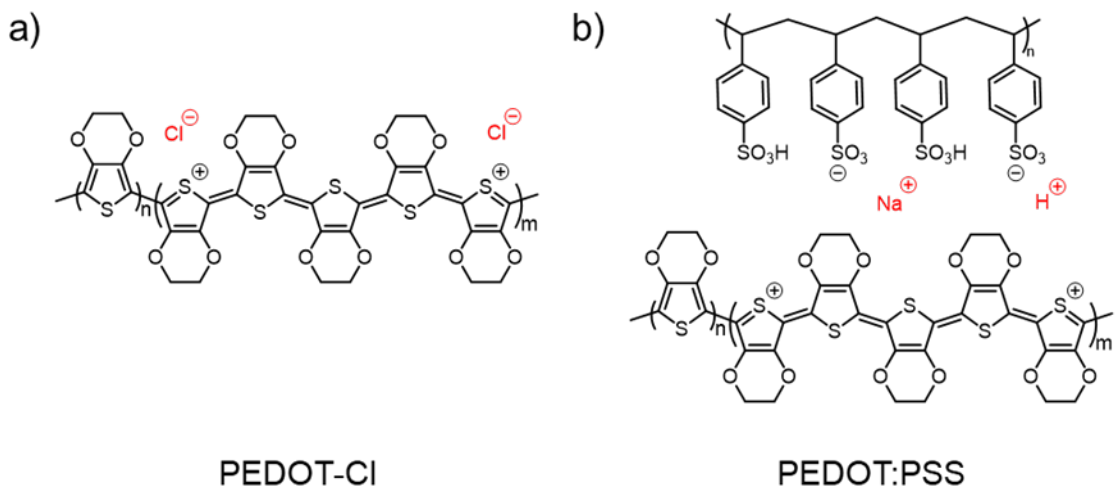

Figure 3.3 a) Chemical structure of PEDOT-Cl with mobile ions (Cl^-) labeled in red, b) Chemical structure of PEDOT:PSS with possible mobile ions labeled in red.

The post-deposition rinse that we perform on our PEDOT-Cl samples insures that residual salts are removed before samples are measured. The polymer reported herein has Chloride as a counter ion, however it is possible to perform an ion exchange by rinsing the samples with an acid. Previously, we have shown that we can perform an ion exchange by rinsing with sulfuric acid. Figure 3.4 depicts the XPS measurements of samples unrinsed, rinsed with methanol, and rinsed with methanol/sulfuric acid. These results show that the Fe peak disappears after the rinses, and the only ions present are the counterions of the polymer.[26]

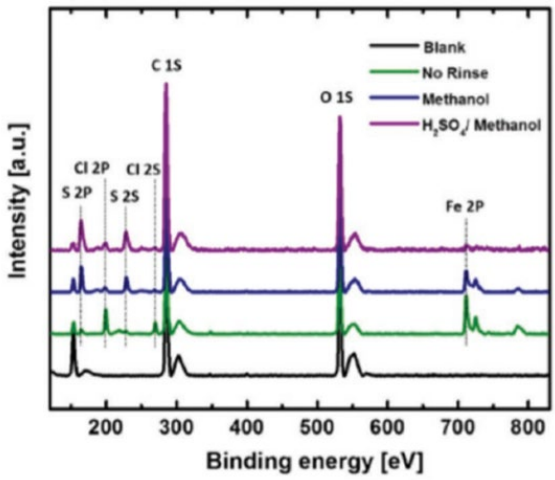

Figure 3.4 XPS measurements of PEDOT, where green is unrinsed, blue is rinsed with only methanol, and purple is rinsed with sulfuric acid and methanol.[26]

3.2.2 Respiration Monitoring

Real time outputs from the mask were recorded for two separate participants in various settings. In order to assess the accuracy of the humidity sensor, a ground-truth respiration belt was also worn, which senses respiration from expansion and deflation of the diaphragm. We show that the humidity sensor is able to accurately sense the moisture in a breath and recover quickly enough in order to sense the next breath. We also show that the humidity sensor can distinguish between deep and shallow breaths taken by the wearer (Figure 3.5 a-b). The signal quality remains constant even when the breaths were measured outdoors (Figure 3.5 c-d).

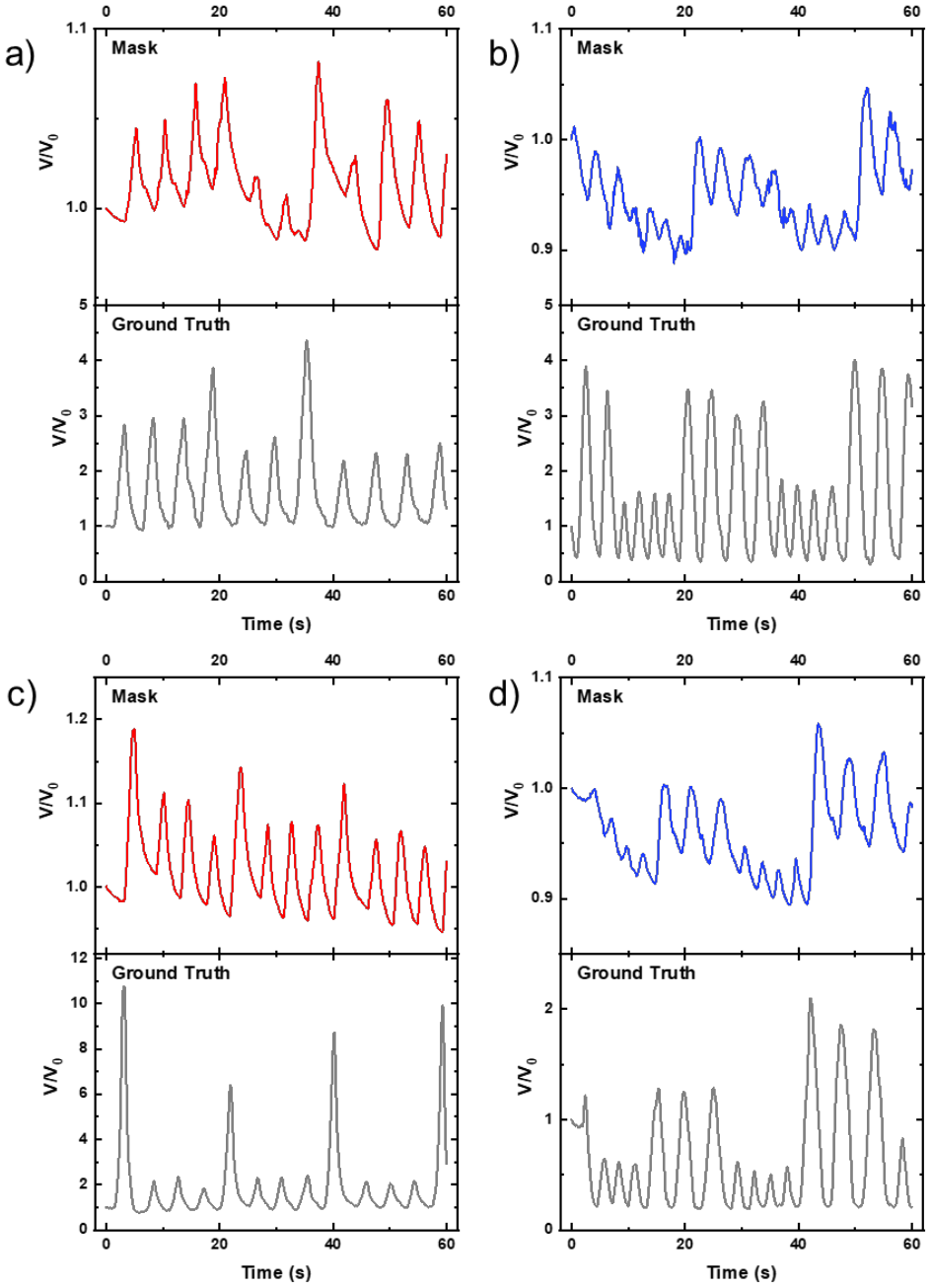

Figure 3.5 Shallow vs deep breaths sensed by the mask and compared to the ground truth belt a) indoors User 1, b) indoors User 2, c) outdoors User 1, and d) outdoors User 2.

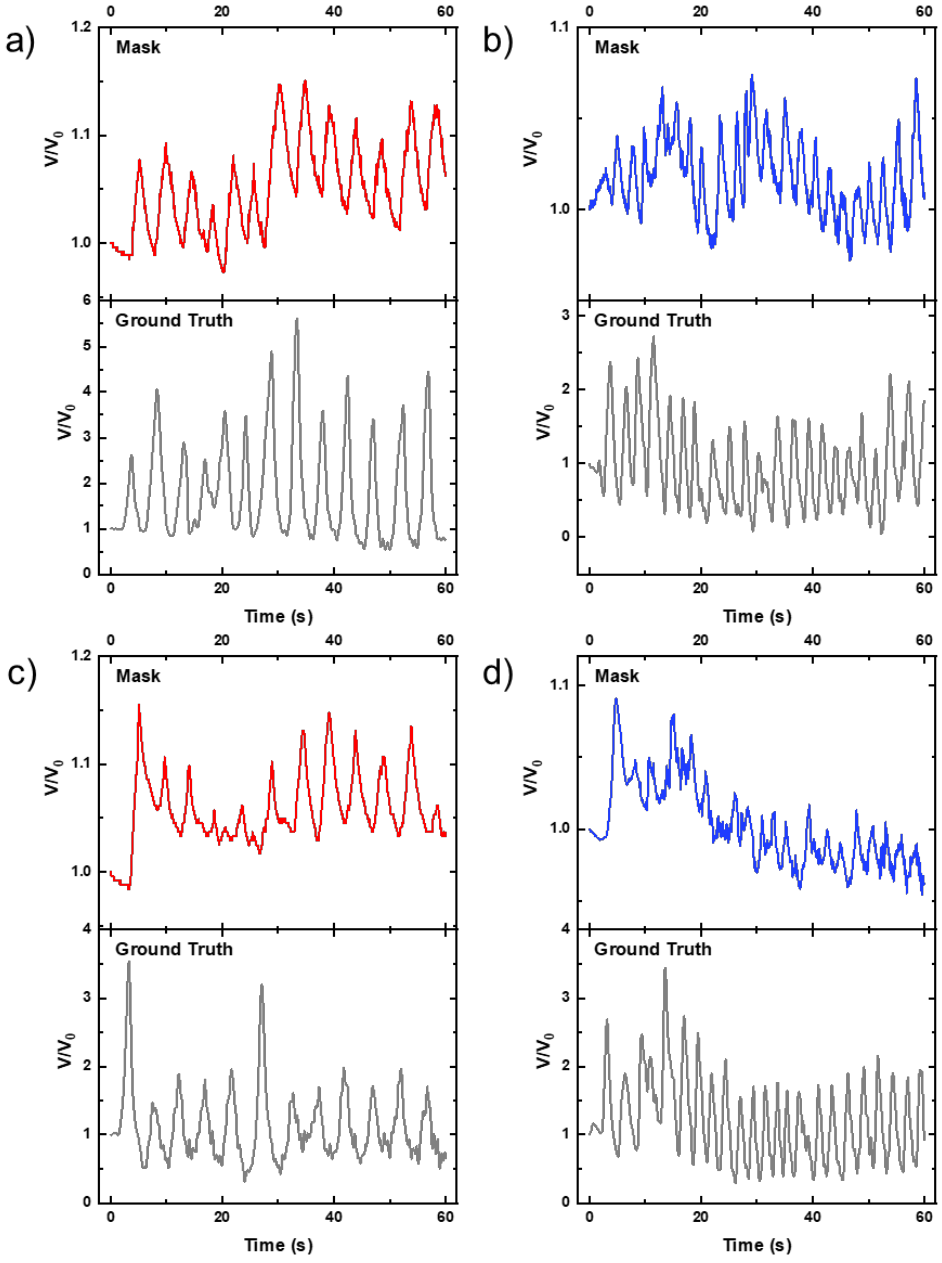

Figure 3.6 Sensing respiration while the user is walking a) indoors User 1, b) indoors User 2 c) outdoors User 1 and d) outdoors User 2.

The sensor was also tested by measuring respiration while the wearer was walking, and the results show that there are very little motion artifacts (Figure 3.6 a-b). We believe that these artifacts can be effectively eliminated or significantly reduced by using a Bluetooth connection between the board and the software. The outdoor walking results show a small amount of motion artifacts, but the overall respiration is still distinct (Figure 3.6 c-d).

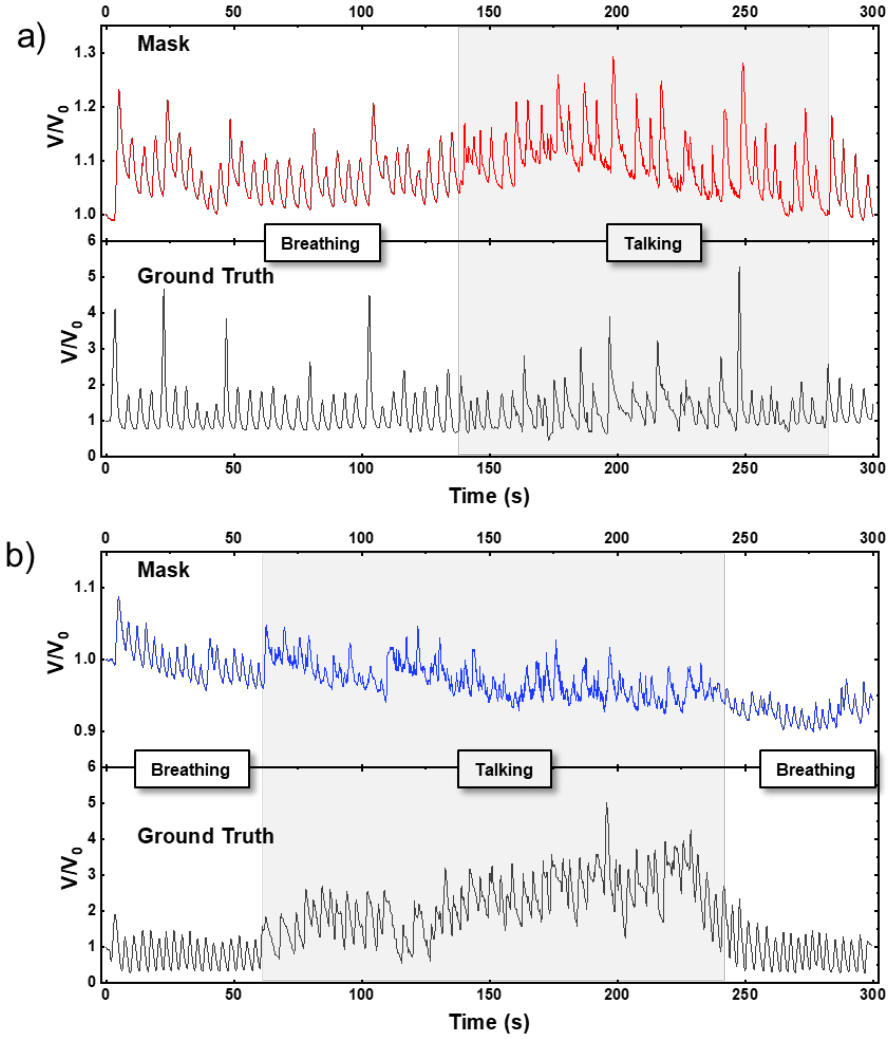

Figure 3.7 Respiration pattern of breathing vs talking for a) User 1 and b) User 2.

We found that the humidity sensor is sensitive enough to be able to differentiate breathing from talking (Figure 3.7). The signal from speaking is less systematic than the breathing, which is representative of the variations in breath that are released from a person's mouth while they are talking. This is an important difference to note, because

during remote or long-term monitoring using this mask, any changes in respiration need to be easily distinguishable in order to come to medical conclusions.

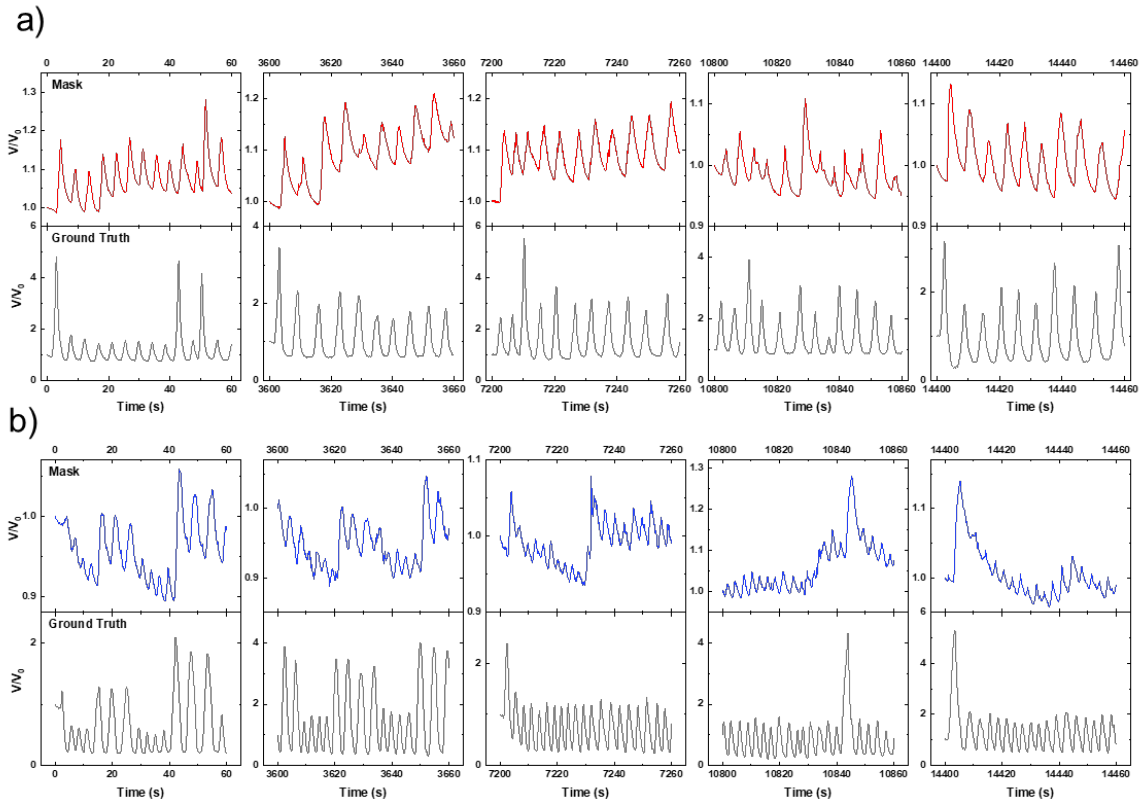

Figure 3.8 Longitudinal data of the user where measurements were taken every hour from 0- 4 hours, a) User 1 and b) User 2.

To show that the mask can be used for long-term health monitoring, we performed longitudinal respiration monitoring (Figure 3.8). The participant wore the mask for 4.5 hours, and the respiration was recorded every 30 minutes. We see that long term use of the sensors does not result in saturation of the signal. Furthermore, to show the versatility of this sensor design, we mounted the humidity sensor in a fabric mask and recorded a

participant taking deep and shallow breaths, the results of which can be found in the supporting information (Figure 3.9).

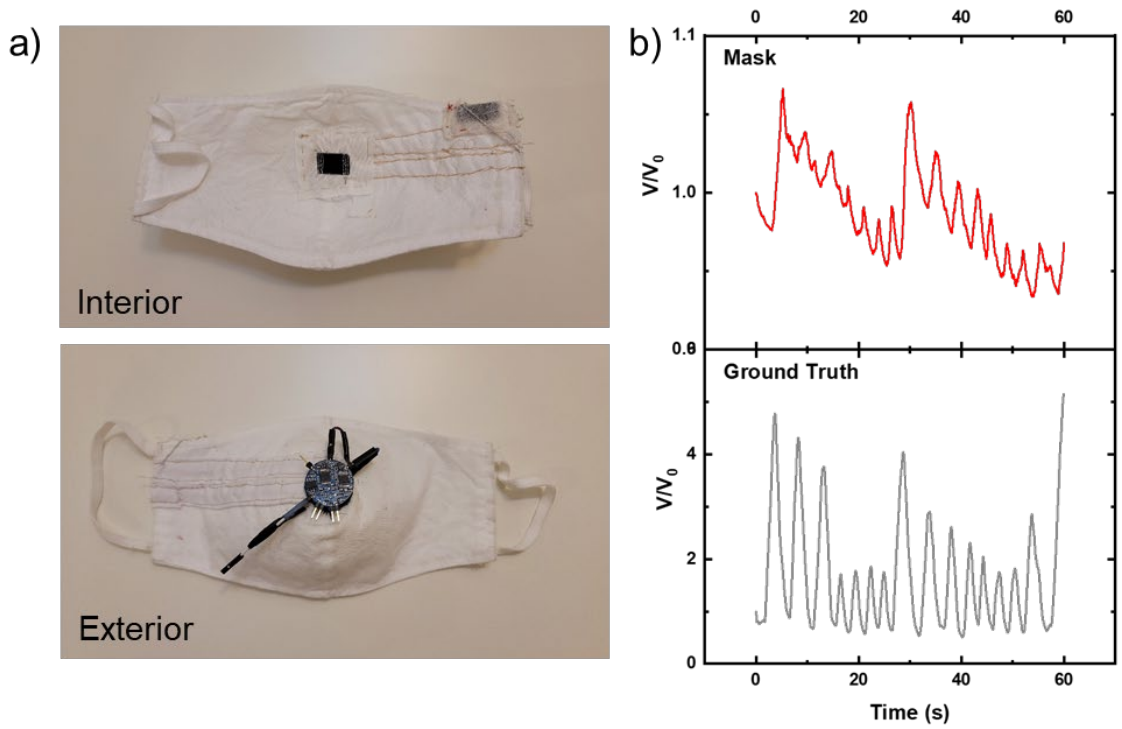

Figure 3.9 a) Interior (upper) and exterior (lower) of humidity sensor mounted in a fabric mask, and b) breathing response of User 2 taking deep and shallow breaths with sensor mounted in a fabric mask.

We tested a sample of PEDOT:PSS coated on the same cotton as the PEDOT-Cl sensor in order to compare the sensitivities (Figure 3.10). We found that the PEDOT:PSS sensors were much more conductive than the PEDOT-Cl sensors, and the coating procedure to be significantly longer and produced more waste. The PEDOT:PSS sensors showed a respiration signal, but were unable to differentiate between deep and shallow breaths. After 2-3 minutes of breathing on the sensor we saw the signal decay into noise

suggesting that the sensor had fully saturated. This leads us to believe that the PEDOT-Cl sensors were more sensitive and robust and therefor better for use in this application than the PEDOT:PSS sensors.

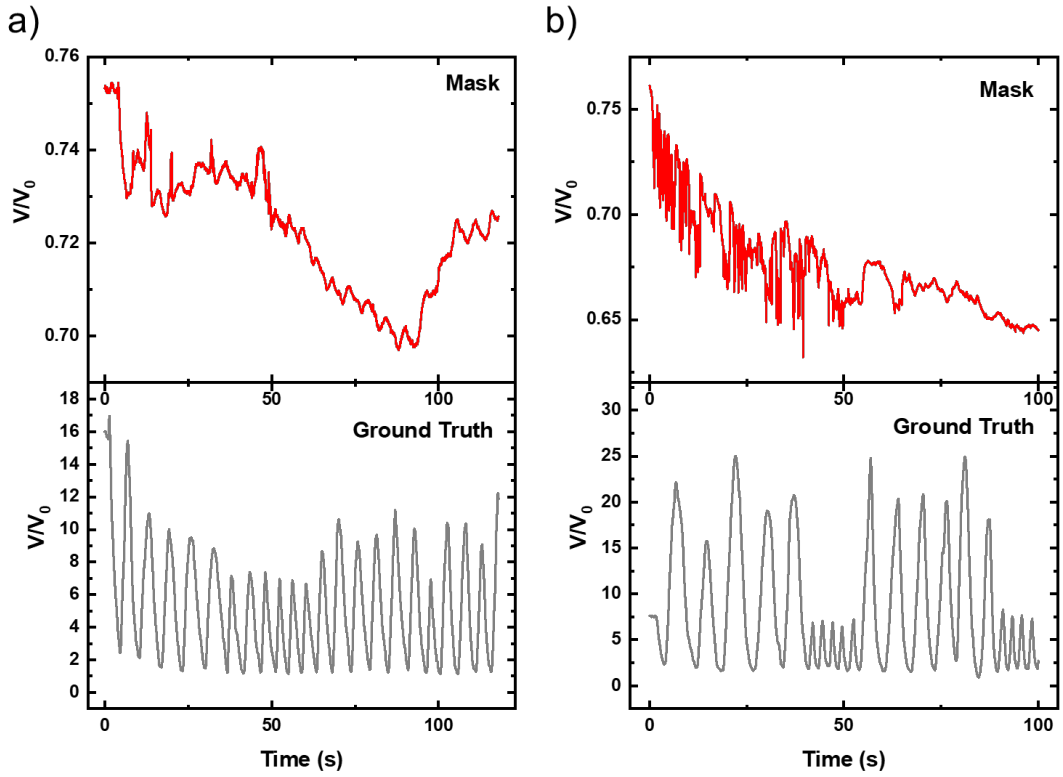

Figure 3.10 Respiration measured using the PEDOT:PSS sensor mounted in the mask for a) minute 1-2, and b) minute 3-4.

3.3 Summary

We demonstrated a PEDOT-Cl coated cotton humidity sensor mounted in a face mask for use in respiration monitoring. Through experiments on two different participants, the sensor proved to be sensitive enough to distinguish between deep and shallow breathing, as well as being able to discern talking from breathing. The signal quality of

measurements taken outdoors was comparable to those taken indoors. We also demonstrated that the breathing signal of a participant taken while walking was insensitive to motion artifacts. The mask proved to be capable of measuring respiration for four consecutive hours without indication of signal saturation. We additionally demonstrated that the sensor can be integrated and functional within different types of masks by measuring respiration of a participant using a sensor mounted in a fabric mask. We believe that these findings can lead to a comfortable, functional, and long-term form of respiration monitoring.

3.4 Materials and Methods

3.4.1 Sensor Fabrication.

The humidity sensors were made from PEDOT-Cl coated cotton using reactive vapor deposition (RVD). The deposition conditions can be found in our previous work.[25] The devices were constructed using the coated fabric and Silver Thread (LessEMF, 66 Yarn 22+3ply 110 PET).

3.4.2 Sensor Characterization.

The sensors function by translating changes in humidity into changes in resistance of the device. In order to convert resistance changes into voltage, we designed an electronic board with a voltage divider by placing a constant resistance (R_1 in Figure 1(b)) in series

with the sensor and capturing the output voltage (V_{press}). A voltage follower is placed to minimize the effect of load on the sensor and to provide a low-impedance output for Analog to Digital Converter (ADC).

3.5 References

(1) Chu, M.; Nguyen, T.; Pandey, V.; Zhou, Y.; Pham, H. N.; Bar-Yoseph, R.; Radom-Aizik, S.; Jain, R.; Cooper, D. M.; Khine, M. Respiration Rate and Volume Measurements Using Wearable Strain Sensors. Npj Digit. Med. 2019, 2 (1), 1–9. https://doi.org/10.1038/s41746-019-0083-3.

(2) Jortberg, E.; Silva, I.; Bhatkar, V.; McGinnis, R. S.; Sen-Gupta, E.; Morey, B.; Wright, J. A.; Pindado, J.; Bianchi, M. T. A Novel Adhesive Biosensor System for Detecting Respiration, Cardiac, and Limb Movement Signals during Sleep: Validation with Polysomnography. Nat. Sci. Sleep 2018, 10, 397–408. https://doi.org/10.2147/NSS.S179588.

(3) Raziq, A.; Kidakova, A.; Boroznjak, R.; Reut, J.; Öpik, A.; Syritski, V. Development of a Portable MIP-Based Electrochemical Sensor for Detection of SARS-CoV-2 Antigen. Biosens. Bioelectron. 2021, 178, 113029. https://doi.org/10.1016/j.bios.2021.113029.

(4) Jayarathna, T.; Gargiulo, G. D.; Breen, P. P. Continuous Vital Monitoring During Sleep and Light Activity Using Carbon-Black Elastomer Sensors. Sensors 2020, 20 (6). https://doi.org/10.3390/s20061583.

(5) Zhou, C.; Zhang, X.; Tang, N.; Fang, Y.; Zhang, H.; Duan, X. Rapid Response Flexible Humidity Sensor for Respiration Monitoring Using Nano-Confined Strategy. Nanotechnology 2020, 31 (12), 125302. https://doi.org/10.1088/1361-6528/ab5cda.

(6) Dai, J.; Zhao, H.; Lin, X.; Liu, S.; Fei, T.; Zhang, T. Design Strategy for Ultrafast-Response Humidity Sensors Based on Gel Polymer Electrolytes and Application for Detecting Respiration. Sens. Actuators B Chem. 2020, 304, 127270. https://doi.org/10.1016/j.snb.2019.127270.

(7) Dai, J.; Zhao, H.; Lin, X.; Liu, S.; Liu, Y.; Liu, X.; Fei, T.; Zhang, T. Ultrafast Response Polyelectrolyte Humidity Sensor for Respiration Monitoring. ACS Appl. Mater. Interfaces 2019, 11 (6), 6483–6490. https://doi.org/10.1021/acsami.8b18904.

(8) Wu, Z.; Yang, J.; Sun, X.; Wu, Y.; Wang, L.; Meng, G.; Kuang, D.; Guo, X.; Qu, W.; Du, B.; Liang, C.; Fang, X.; Tang, X.; He, Y. An Excellent Impedance-Type Humidity Sensor Based on Halide Perovskite CsPbBr3 Nanoparticles for Human

Respiration Monitoring. Sens. Actuators B Chem. 2021, 337, 129772. https://doi.org/10.1016/j.snb.2021.129772.

(9) Guan, Y.; Le, X.; Hu, M.; Liu, W.; Xie, J. A Noninvasive Method for Monitoring Respiratory Rate of Rats Based on a Microcantilever Resonant Humidity Sensor. J. Micromechanics Microengineering 2019, 29 (12), 125001. https://doi.org/10.1088/1361-6439/ab43e8.

(10) Güder, F.; Ainla, A.; Redston, J.; Mosadegh, B.; Glavan, A.; Martin, T. J.; Whitesides, G. M. Paper-Based Electrical Respiration Sensor. Angew. Chem. Int. Ed. 2016, 55 (19), 5727–5732. https://doi.org/10.1002/anie.201511805.

(11) Wang, S.; Jiang, Y.; Tai, H.; Liu, B.; Duan, Z.; Yuan, Z.; Pan, H.; Xie, G.; Du, X.; Su, Y. An Integrated Flexible Self-Powered Wearable Respiration Sensor. Nano Energy 2019, 63, 103829. https://doi.org/10.1016/j.nanoen.2019.06.025.

(12) Min, S. D.; Yun, Y.; Shin, H. Simplified Structural Textile Respiration Sensor Based on Capacitive Pressure Sensing Method. IEEE Sens. J. 2014, 14 (9), 3245–3251. https://doi.org/10.1109/JSEN.2014.2327991.

(13) Guay, P.; Gorgutsa, S.; LaRochelle, S.; Messaddeq, Y. Wearable Contactless Respiration Sensor Based on Multi-Material Fibers Integrated into Textile. Sensors 2017, 17 (5), 1050. https://doi.org/10.3390/s17051050.

(14) Kano, S.; Dobashi, Y.; Fujii, M. Silica Nanoparticle-Based Portable Respiration Sensor for Analysis of Respiration Rate, Pattern, and Phase During Exercise. IEEE Sens. Lett. 2018, 2 (1), 1–4. https://doi.org/10.1109/LSENS.2017.2787099.

(15) Kano, S.; Fujii, M. All-Painting Process To Produce Respiration Sensor Using Humidity-Sensitive Nanoparticle Film and Graphite Trace. ACS Sustain. Chem. Eng. 2018, 6 (9), 12217–12223. https://doi.org/10.1021/acssuschemeng.8b02550.

(16) Jin, H.; Tao, X.; Dong, S.; Qin, Y.; Yu, L.; Luo, J.; Deen, M. J. Flexible Surface Acoustic Wave Respiration Sensor for Monitoring Obstructive Sleep Apnea Syndrome. J. Micromechanics Microengineering 2017, 27 (11), 115006. https://doi.org/10.1088/1361-6439/aa8ae0.

(17) Improving the Accuracy and Efficiency of Respiratory Rate Measurements in Children Using Mobile Devices https://journals.plos.org/plosone/article?id=10.1371/journal.pone.0099266 (accessed 2020 -09 -22).

(18) Mauri, T.; Turrini, C.; Eronia, N.; Grasselli, G.; Volta, C. A.; Bellani, G.; Pesenti, A. Physiologic Effects of High-Flow Nasal Cannula in Acute Hypoxemic Respiratory Failure. Am. J. Respir. Crit. Care Med. 2016, 195 (9), 1207–1215. https://doi.org/10.1164/rccm.201605-0916OC.

(19) Current evidence for the effectiveness of heated and humidified high flow nasal cannula supportive therapy in adult patients with respiratory failure | SpringerLink https://link.springer.com/article/10.1186/s13054-016-1263-z (accessed 2020 -09 -22).

(20) Zhang, H.; Zhang, J.; Hu, Z.; Quan, L.; Shi, L.; Chen, J.; Xuan, W.; Zhang, Z.; Dong, S.; Luo, J. Waist-Wearable Wireless Respiration Sensor Based on Triboelectric Effect. Nano Energy 2019, 59, 75–83. https://doi.org/10.1016/j.nanoen.2019.01.063.

(21) Dinh, T.; Nguyen, T.; Phan, H.-P.; Nguyen, N.-T.; Dao, D. V.; Bell, J. Stretchable Respiration Sensors: Advanced Designs and Multifunctional Platforms for Wearable Physiological Monitoring. Biosens. Bioelectron. 2020, 166, 112460. https://doi.org/10.1016/j.bios.2020.112460.

(22) Borini, S.; White, R.; Wei, D.; Astley, M.; Haque, S.; Spigone, E.; Harris, N.; Kivioja, J.; Ryhänen, T. Ultrafast Graphene Oxide Humidity Sensors. ACS Nano 2013, 7 (12), 11166–11173. https://doi.org/10.1021/nn404889b.

(23) Wang, Y.; Zhang, L.; Zhang, Z.; Sun, P.; Chen, H. High-Sensitivity Wearable and Flexible Humidity Sensor Based on Graphene Oxide/Non-Woven Fabric for Respiration Monitoring. Langmuir 2020, 36 (32), 9443–9448. https://doi.org/10.1021/acs.langmuir.0c01315.

(24) Pang, Y.; Jian, J.; Tu, T.; Yang, Z.; Ling, J.; Li, Y.; Wang, X.; Qiao, Y.; Tian, H.; Yang, Y.; Ren, T.-L. Wearable Humidity Sensor Based on Porous Graphene Network for Respiration Monitoring. Biosens. Bioelectron. 2018, 116, 123–129. https://doi.org/10.1016/j.bios.2018.05.038.

(25) Allison, L. K.; Andrew, T. L. A Wearable All-Fabric Thermoelectric Generator. Adv. Mater. Technol. 0 (0), 1800615. https://doi.org/10.1002/admt.201800615.

(26) Zhang Lushuai; Fairbanks Marianne; Andrew Trisha L. Rugged Textile Electrodes for Wearable Devices Obtained by Vapor Coating Off-the-Shelf, Plain-Woven Fabrics. Adv. Funct. Mater. 2017, 27 (24), 1700415. https://doi.org/10.1002/adfm.201700415.

(27) Wang, H.; Ail, U.; Gabrielsson, R.; Berggren, M.; Crispin, X. Ionic Seebeck Effect in Conducting Polymers. Adv. Energy Mater. 2015, 5 (11), 1500044. https://doi.org/10.1002/aenm.201500044.

Chapter 4

THE THERMORESISTIVE PROPERTIES OF VAPOR PRINTED PEDOT-Cl

4.1 Introduction to thermoresistive textiles

In Chapter 2 the process of creating PEDOT-Cl coated textiles using the CVD method was explained. Much like PEDOT:PSS, PEDOT-Cl has a variety of applications. One property of PEDOT-Cl that makes it attractive is its thermoresistive property, which is the temperature dependent resistance.

Thermistors are materials categorized as variable resistors, meaning the resistance of the material is not fixed and can be increased or decreased by environmental conditions, such as temperature changes. Metals, metal oxides, and inorganic semiconductors are thermosensitive materials commonly used in rigid temperature sensors. However, carbon nanomaterials and polymer semiconductors have become excellent candidates for wearable temperature sensors as they can be made into flexible films. Additionally, these materials show biocompatibility, fast response, and high sensitivity making them practical for applications in the wearable field.[1–4]

Semiconducting polymers conduct electricity in the form of charge carriers. The electrical conductivity of PEDOT-Cl, described in Chapter 2, comes from the conducting of holes through the polymer material. As the temperature of the polymer increases, the number of charge carriers is also increased. As a result the material has an increase of

conductivity with increasing temperature.[5] Due to this thermosensitivity, PEDOT-Cl can be used to make thermistors which are circuit components used to sense temperature.

In recent years, there has been a push towards the development of fabric-based circuits and circuit components.[6–10] These circuits will allow for the development of textile health monitoring systems, which can bring about a more comfortable and functional device design.[11–17] Among these circuit components, thermistors have proven to be a difficult element to effectively transfer to textiles. Developing a successful textile-based thermistor requires a material that is an accurate temperature sensor, has a sensitivity in the temperature range of the body, and is not subject to mechanical failure from the stress of regular wear.[18–35]

The utilization of a textile is important for the overall comfort of the sensing garment. Several reports have demonstrated the incorporation of rigid temperature sensing elements by embedding them into a yarn or fabric or by mimicking textiles or fibers (Figure 4.1).[36–41] Kennon and Dias et.al. reported the fabrication of a temperature sensing fabric. In this work, temperature sensing elements made from copper, nickel, and tungsten wires were woven into a fabric with a spacer yarn (Figure 4.1a). This was able to be done through industrial weaving equipment that can handle the metal materials without it being damaging to the equipment as it would normally be for an average sewing machine. Although the mechanical stability under normal wear should be explored before this design is made into a wearable garment.[27]

Dias et.al. described the design of a textile thermograph made from temperature sensing yarns (Figure 4.1b). The yarns were made by encapsulating an off-the-shelf

thermistor using a polymer resin “micro-pod,” which was then embedded into the center of the yarns. Using this technique, they produced a fabric consisting of multiple temperature sensors. This allowed for the temperature of a larger area to be measured instead of just the single contact point of a thermistor to the body. They were even able to use this thermograph to measure the temperature of Ionised water, because of the polymer encapsulation. However, the thermistors used were rigid and could create discomfort for the wearer.[37]

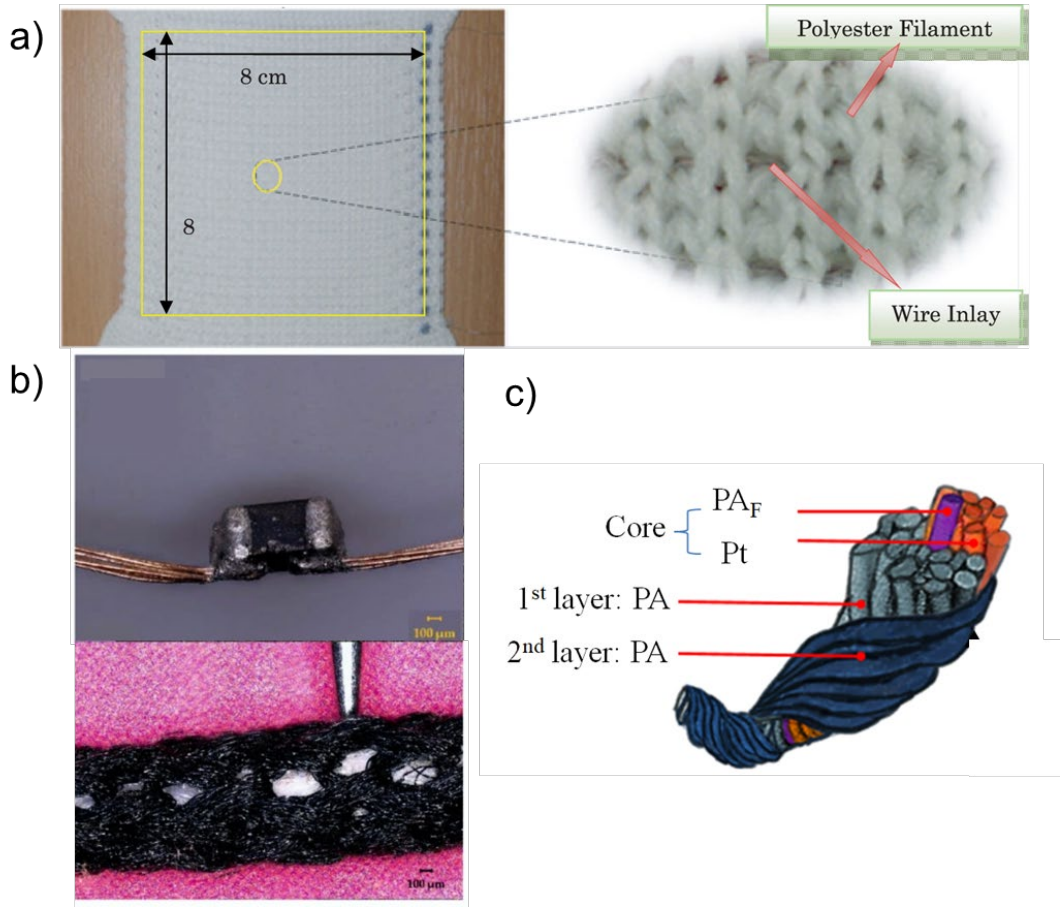

Figure 4.1 Fabric based temperature sensors, a) copper, nickel, and tungsten thermosensitive wires woven with a spacer yarn to create a textile, b) off-the-shelf thermistors embedded into yarns as a temperature sensing yarn, and c) Pt wires yarned with a protective layer of polyamide fibers.

Li et.al. reported a yarn composed of wrapped platinum (Pt) and polyamide fibers, where the Pt wires served as the temperature sensing element (Figure 4.1c). These yarns were designed so the polyamide fibers worked as a protective layer around the Pt wires. The results showed that the yarns were able to sense temperature through resistance measurements. Although, the difference between the resistance at each temperature was minimal, and thus may be difficult to use as an accurate temperature sensor.[4]

These non-flexible elements can result in discomfort for a patient, and occasionally poor contact with the skin. In order to alleviate this discomfort, the utilization of an all-textile temperature sensor is needed. For this, the field has been expanding into coating textiles with conducting polymers, which faces unique challenges such as delamination of the polymer from the substrate, mechanical failure, and biocompatibility.[42,43] Herein, we discuss using PEDOT-Cl coatings on fabrics to create flexible and durable thermoresistive textiles.

Chapter 4 discusses the use of various fabrics coated in PEDOT-Cl to explore the thermoresistive properties. We show that taking advantage of different fabrics as substrates can allow for a highly tunable product. Additionally, we explore the impacts of humidity on the PEDOT-Cl coated textiles under different temperature conditions and show that the sign of the temperature coefficient can be flipped by exposing the sample to a humid environment.

4.2 Results and Discussion

4.2.1 PEDOT-Cl Coated Fabrics

For this work, we coated five types of commercial fabric with PEDOT-Cl, using the procedure outlined in Chapter 2. We wanted to explore fabrics of different compositions, thicknesses, and weave porosities. Therefore, we chose a medium weight cotton with a low weave porosity, a tobacco cotton with a high weave porosity, a tick polyester knit, a lightweight spandex/rayon blend, and a thick wool felt. We deposited PEDOT-Cl on each of these fabrics, shown in Figure 4.2, and each fabric maintained the feel and look (other than color) of the pristine textile. We observed no delamination of the PEDOT-Cl film from any of the textiles.

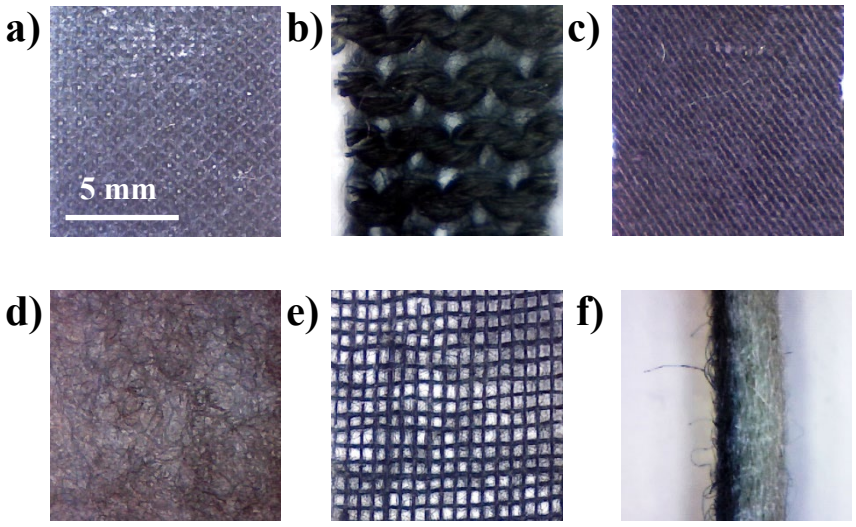

Figure 4.2 Microscope images of PEDOT-Cl coated a) cotton, b) polyester knit, c) rayon/spandex blend, d) wool felt, and e) tobacco cotton. f) Cross-section image of PEDOT-Cl coated wool felt.

It is important to consider how the properties of the textile impact the PEDOT-Cl coating. Since the oxidative chemical vapor deposition (oCVD) technique creates coatings on the surface of the substrate and does not penetrate into the fibers of the fabric, wherever fibers are overlapping each other, such as at the weave intersects, there will be a break in the polymer coating.

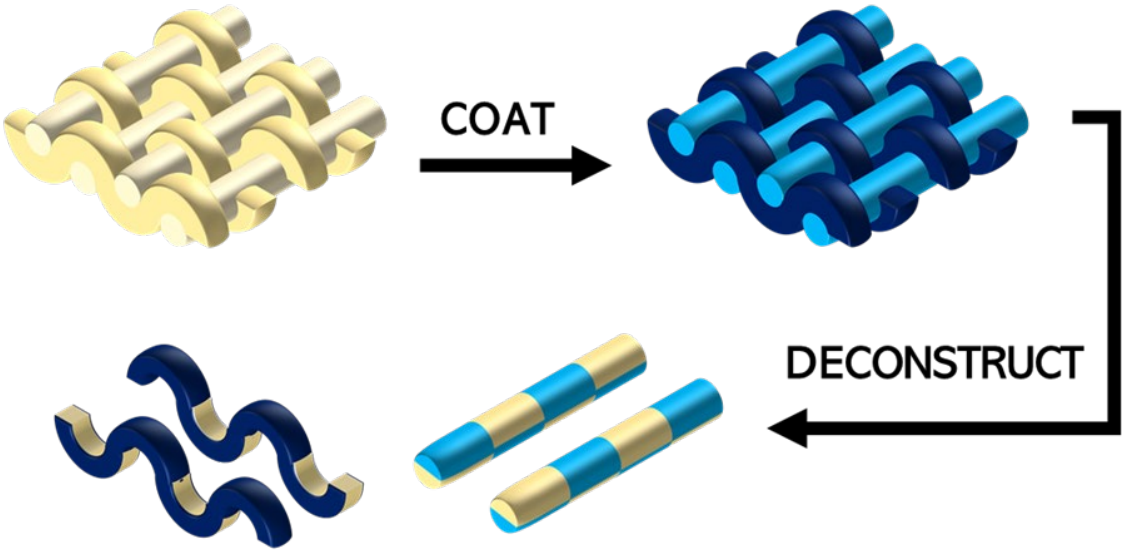

Figure 4.3 Polymer coated textiles deconstructed to show breaks in the polymer film from fiber overlap.

Figure 4.3 shows how the fibers of the polymer coated textile look when the fabric is deconstructed. Due to this, we can draw some conclusions about the textiles we explore in this work. Textiles with tighter weave, such as the standard cotton and the spandex/rayon blend, will have more surface area for the polymer to coat, however they will also have

frequent breaks in the polymer film due to a higher amount of fiber overlap. Textiles with a loose weave, such as the tobacco cotton, will have fewer breaks in the polymer film, but resultantly will also have fewer fibers per square inch to be coated with the polymer. Wool felt is a non-woven textile, which means the geometry of the fibers is randomized, but also means that there are fewer fibers overlapping.

Each of these textiles has its own material properties that makes it interesting for possible wearable applications. The cottons tend to have a more textured surface which provides more surface area for the polymer to coat. The spandex/rayon blend and the polyester fibers are refined and synthetic respectively and have a smoother surface and more stretchability. The wool felt is a nonwoven material, so there aren't as many fiber overlaps compared to a woven material. The felt is also a thick, porous textile that allows for the polymer film to partially penetrate the bulk of the fabric and results in higher polymer mass loading.

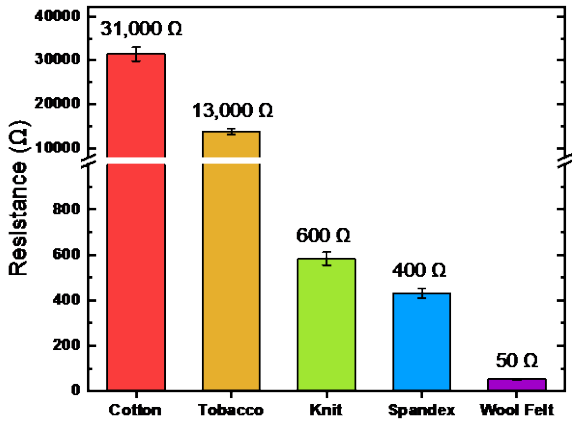

Figure 4.4 The electrical resistances of PEDOT-Cl coated textiles measured at room temperature

All of these textile properties contribute to the resistance of the PEDOT-Cl coatings on the textiles as shown in Figure 4.4. The cotton has a high resistance because of the frequent breaks in the polymer film. The tobacco cotton has a high resistance as well because of the low surface area. The knit and spandex/rayon blend have higher conductivities due to the smooth texture of the fibers. Finally, the wool felt has the highest conductivity because of the low rate of fiber overlap and the increased mass loading of the polymer.

4.2.2 Thermo-resistive Characterization

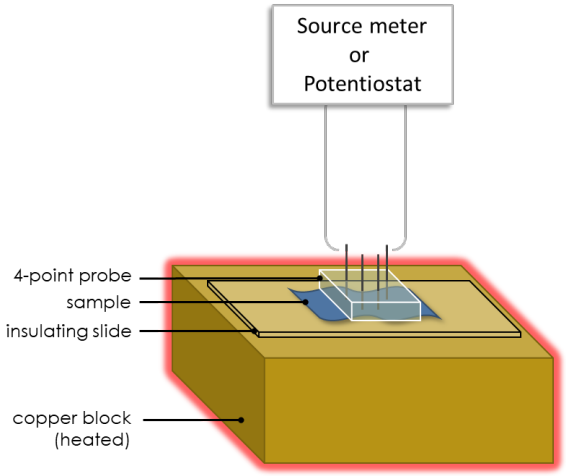

Figure 4.5 The experimental setup for measuring the thermoresistive properties.

The thermoresistive properties were measured on the setup shown in Figure 4.5. The samples were heated on a temperature-controlled copper block while the resistances

were measured using a custom built 4-point probe. The measurements were taken over the course of several hours, allowing the samples to equilibrate to the measured temperature before the conductivity was measured.

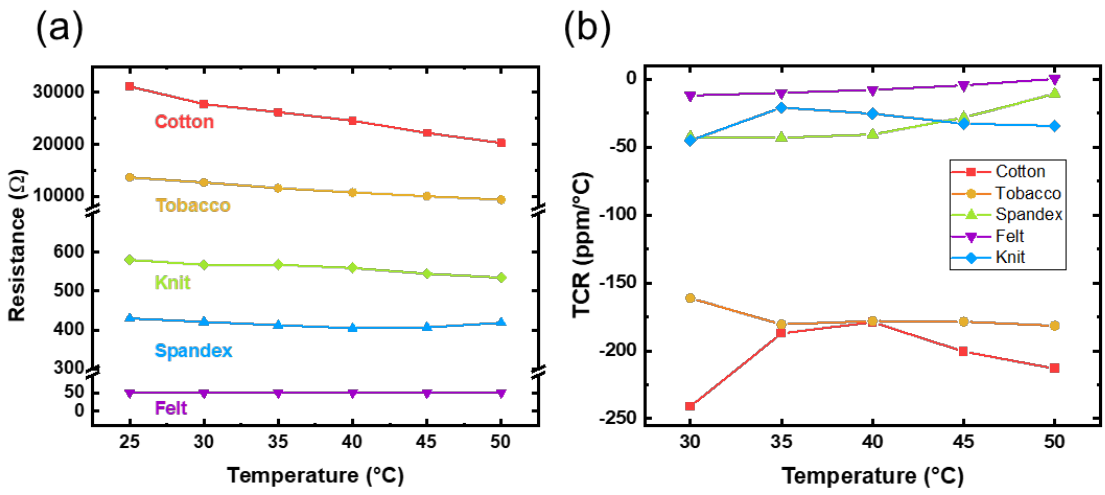

Figure 4.6 The results of the thermoresistive measurements of PEDOT-Cl fabrics a) the resistances and b) TCR values plotted with increasing temperature.

The results of the thermoresistive measurements of the PEDOT-Cl coatings demonstrated a decrease in resistance with increasing temperature for all of the fabrics tested (Figure 4.6a). This categorizes PEDOT-Cl as a negative temperature coefficient (NTC) thermistor. The PEDOT-Cl coated fabrics that measured a high resistance at room temperature show the greatest change in resistance between temperature values. The fabrics with low resistances at room temperature have a comparatively smaller difference between temperature values. For a temperature sensing application, it is best to have a thermosensitive material with a higher resistance because the large resistance fluctuations

with temperature can easily be assigned to the thermoresistive properties. With a lower resistance the change between temperature values is much smaller and is harder to definitively associate with thermoresistive characteristics. So, for a fabric temperature sensor, it is better to chose cotton or tobacco cotton as the substrate for the sensor.

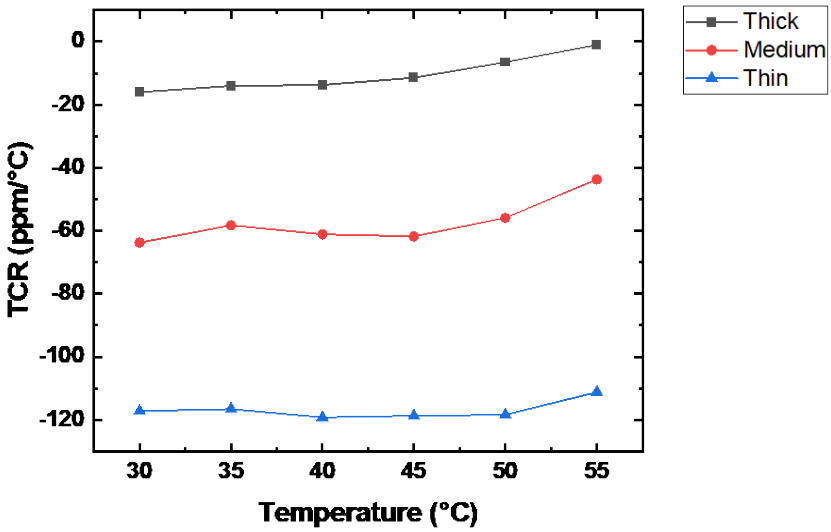

Figure 4.7 TCR of various thicknesses of PEDOT-Cl coated on cotton

Figure 4.6b shows the temperature coefficient of resistance (TCR), which was calculated using Equation 1.

Equation 2

$$TCR = \frac{1}{R}\frac{(R_2 - R_1)}{(T_2 - T_1)}$$

Where R_1 is the resistance of the sample at 25 °C (T_1). The TCR represents the temperature where the sample is most sensitive, i.e., has the largest resistance change. For a wearable application we are targeting the temperature range where body temperatures can be measured, so 35-37 °C. The cotton and tobacco cotton samples demonstrated the most sensitivity in this range, making them ideal candidates for a wearable temperature sensor. All of the fabrics tested showed a negative TCR, or a trend of decreasing resistances in relationship with increasing temperatures. The temperature range where the sample demonstrated the highest sensitivity was able to be shifted by merely changing the type of fabric.

We also found that the amplitude of the TCR can be altered by changing the thickness of the polymer coating. We tested the thermoresistive properties of cotton coated with 1 μm, 3 μm, and 5 μm respectively and plotted the TCR values, shown in Figure 4.7. When measured at room temperature the resistance of these samples decreased as the thickness increased, with the thin coating being the highest base resistance. These samples showed very similar trends with increasing temperature, however the magnitude of the TCR values differed. The sample with the highest resistance, the thin sample, showed the lowest TCR values, making it the most sensitive of the samples tested. This high tunability of the TCR values by making a minor adjustment. such as film thickness, makes this a versatile method for creating temperature sensors.

4.2.3 Device Characterization and Humidity Effects

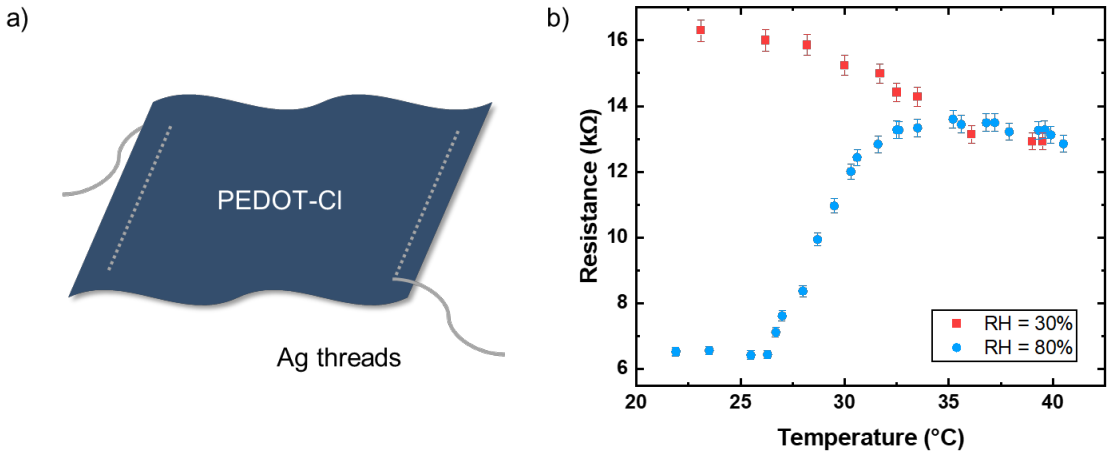

The fabrics were made into devices using silver threads as electrodes (Figure 4.8a). The devices were tested using chronoamperometry to measure the resistance change in response to the change in temperature. It has previously been shown that conducting polymers, particularly PEDOT derivatives, are sensitive to humidity changes.[44] In order to determine the extent of the humidity effects on the thermistors, the thermoresistive properties of the samples were taken at ambient humidity, then the relative humidity (RH) of the testing environment was increased, and the samples were measured again at high humidity. We show that the relative humidity of the testing environment affects the samples response to temperature (Figure 4.8b). For PEDOT-Cl coated cotton we see that at 30% RH the thermistor demonstrates a NTC trend. However, when the RH is increased to 80% the same thermistor exhibits a positive temperature coefficient (PTC) trend. It is

important to note that during these measurements, the sample was allowed to fully equilibrate to each temperature for several minutes. Thus, a real-time curve is not able to be provided.

The hygroresistive properties make measuring the thermoresistive properties of the polymer fabrics complicated. It is difficult to assign a resistance change in the device to either the temperature or humidity if both variables are changing, as they would be when used in a wearable. In order to isolate the thermoresistive changes, an encapsulation of the polymer fabric is needed. By introducing a hydrophobic layer, the moisture will not be able to impact the resistance values of the polymer. This work still needs to be done in order for these PEDOT-Cl coated fabrics to be viable as temperature sensors.

4.3 Summary

Thermistors have proven to be a challenging textile circuit component to produce, due to the demands for efficiency, flexibility, biocompatibility, and mechanical stability. The thermo-resistive material must also be sensitive in the temperature range of the human body.

Herein we produced a textile thermistor by using the RVD technique to conformally and uniformly coat PEDOT-Cl on commercially available fabric. We showed that these PEDOT-Cl coated textiles have thermo-resistive properties and can operate in the optimal temperature range for measuring body temperature. We demonstrated that the sensitivity can be tuned using different fabrics, making them a viable choice for a larger range of

applications. When exploring the TCR values for the thermistors, they exhibited different ranges of sensitivity which can be tuned by the fabric choice.

Additionally, we created textile thermistor devices that show equivalent sensitivities to the thermo-resistive fabrics. Through further investigation we also found that the relative humidity can be used to tune the thermo-resistive properties, to the point of entirely changing the type of thermo-resistive behavior.

4.4 Experimental

4.4.1 Reactive Vapor Deposition

Samples were prepared in a custom quartz tube reaction chamber. Polymerizations took place at pressures <200 mTorr. The monomer zone (95 °C), substrate zone (110 °C), and oxidant zone (180 °C) were heated individually to their respective temperatures. Coating thicknesses range from 3-10 μm depending on the sample positioning in the chamber. Samples were rinsed thoroughly with methanol and hydrochloric acid (1 M) and dried/stored under ambient conditions.

4.4.2 Thermoresistive and Hygro-resistive Measurements

Thermoresistive measurements were taken using a custom-built setup using a LabVIEW program. Samples were heated using a copper block powered by a VARIAC transformer. The resistance was measured using a custom 4-point probe, a Keithley, and

thermocouples to measure the temperature on the surface of the sample. The hygro-resistive properties were measure either on this setup or using an Autolab Potentiostat to run chronoamperometry. The relative humidity of the testing environment was increased by introducing water-soaked sponges and sealing the setup. RH was measured by a Temtop temperature and humidity logger.

4.5 References

(1) Chen, Z.; Zhao, D.; Ma, R.; Zhang, X.; Rao, J.; Yin, Y.; Wang, X.; Yi, F. Flexible Temperature Sensors Based on Carbon Nanomaterials. J. Mater. Chem. B 2021, 9 (8), 1941–1964. https://doi.org/10.1039/D0TB02451A.

(2) Koo, J.; Lee, C.; Chu, C. R.; Kang, S.-K.; Lee, H. M. Integration of Ultrathin Silicon and Metal Nanowires for High-Performance Transparent Electronics. Adv. Mater. Technol. 2020, 5 (4), 1900962. https://doi.org/10.1002/admt.201900962.

(3) Shin, J.; Jeong, B.; Kim, J.; Nam, V. B.; Yoon, Y.; Jung, J.; Hong, S.; Lee, H.; Eom, H.; Yeo, J.; Choi, J.; Lee, D.; Ko, S. H. Sensitive Wearable Temperature Sensor with Seamless Monolithic Integration. Adv. Mater. 2020, 32 (2), 1905527. https://doi.org/10.1002/adma.201905527.

(4) Yang, Q.; Wang, X.; Ding, X.; Li, Q. Fabrication and Characterization of Wrapped Metal Yarns-Based Fabric Temperature Sensors. Polymers 2019, 11 (10), 1549. https://doi.org/10.3390/polym11101549.

(5) Yan, C.; Wang, J.; Lee, P. S. Stretchable Graphene Thermistor with Tunable Thermal Index. ACS Nano 2015, 9 (2), 2130–2137. https://doi.org/10.1021/nn507441c.

(6) Agcayazi, T.; Chatterjee, K.; Bozkurt, A.; Ghosh, T. K. Flexible Interconnects for Electronic Textiles. Adv. Mater. Technol. 2018, 3 (10), 1700277. https://doi.org/10.1002/admt.201700277.

(7) Castano, L. M.; Flatau, A. B. Smart Fabric Sensors and E-Textile Technologies: A Review. Smart Mater. Struct. 2014, 23 (5), 053001. https://doi.org/10.1088/0964-1726/23/5/053001.

(8) Chen, N.; Kim, D. H.; Kovacik, P.; Sojoudi, H.; Wang, M.; Gleason, K. K. Polymer Thin Films and Surface Modification by Chemical Vapor Deposition: Recent Progress. Annu. Rev. Chem. Biomol. Eng. 2016, 7 (1), 373–393. https://doi.org/10.1146/annurev-chembioeng-080615-033524.

(9) Menon, A. K.; Meek, O.; Eng, A. J.; Yee, S. K. Radial Thermoelectric Generator Fabricated from N- and p-Type Conducting Polymers. J. Appl. Polym. Sci. 2017, 134 (3), n/a-n/a. https://doi.org/10.1002/app.44060.

(10) Kim, J.; Cho, G. Thermal Storage/Release, Durability, and Temperature Sensing Properties of Thermostatic Fabrics Treated with Octadecane-Containing Microcapsules. Text. Res. J. 2002, 72 (12), 1093–1098. https://doi.org/10.1177/004051750207201209.

(11) Catarino, A.; Carvalho, H.; Dias, M. J.; Pereira, T.; Postolache, O.; Girão, P. S. Continuous Health Monitoring Using E-Textile Integrated Biosensors. In 2012 International Conference and Exposition on Electrical and Power Engineering; 2012; pp 605–609. https://doi.org/10.1109/ICEPE.2012.6463867.

(12) Carvalho, H.; Catarino, A. P.; Rocha, A.; Postolache, O. Health Monitoring Using Textile Sensors and Electrodes: An Overview and Integration of Technologies. In 2014 IEEE International Symposium on Medical Measurements and Applications (MeMeA); 2014; pp 1–6. https://doi.org/10.1109/MeMeA.2014.6860033.

(13) Rai, P.; Kumar, P. S.; Oh, S.; Kwon, H.; Mathur, G. N.; Varadan, V. K.; Agarwal, M. P. Smart Healthcare Textile Sensor System for Unhindered-Pervasive Health Monitoring. In Nanosensors, Biosensors, and Info-Tech Sensors and Systems 2012; International Society for Optics and Photonics, 2012; Vol. 8344, p 83440E. https://doi.org/10.1117/12.921253.

(14) Rai, P.; Oh, S.; Shyamkumar, P.; Ramasamy, M.; Harbaugh, R. E.; Varadan, V. K. Nano- Bio- Textile Sensors with Mobile Wireless Platform for Wearable Health Monitoring of Neurological and Cardiovascular Disorders. J. Electrochem. Soc. 2013, 161 (2), B3116. https://doi.org/10.1149/2.012402jes.

(15) Merritt, C. R.; Troy Nagle, H.; Grant, E. Fabric-Based Active Electrode Design and Fabrication for Health Monitoring Clothing. IEEE Trans. Inf. Technol. Biomed. 2009, 13 (2), 274–280. https://doi.org/10.1109/TITB.2009.2012408.

(16) Kiaghadi, A.; Homayounfar, S. Z.; Gummeson, J.; Andrew, T.; Ganesan, D. Phyjama: Physiological Sensing via Fiber-Enhanced Pyjamas. Proc. ACM Interact. Mob. Wearable Ubiquitous Technol. 2019, 3 (3), 89:1-89:29. https://doi.org/10.1145/3351247.

(17) High Energy Density, Super-Deformable, Garment-Integrated Microsupercapacitors for Powering Wearable Electronics | ACS Applied Materials & Interfaces https://pubs.acs.org/doi/full/10.1021/acsami.8b08408 (accessed 2020 -10 -15).

(18) Heikenfeld, J.; Jajack, A.; Rogers, J.; Gutruf, P.; Tian, L.; Pan, T.; Li, R.; Khine, M.; Kim, J.; Wang, J.; Kim, J. Wearable Sensors: Modalities, Challenges, and Prospects. Lab. Chip 2018, 18 (2), 217–248. https://doi.org/10.1039/C7LC00914C.

(19) Lim, Z. H.; Chia, Z. X.; Kevin, M.; Wong, A. S. W.; Ho, G. W. A Facile Approach towards ZnO Nanorods Conductive Textile for Room Temperature Multifunctional

Sensors. Sens. Actuators B Chem. 2010, 151 (1), 121–126. https://doi.org/10.1016/j.snb.2010.09.037.
(20) Li, Y.; Cheng, X. Y.; Leung, M. Y.; Tsang, J.; Tao, X. M.; Yuen, M. C. W. A Flexible Strain Sensor from Polypyrrole-Coated Fabrics. Synth. Met. 2005, 155 (1), 89–94. https://doi.org/10.1016/j.synthmet.2005.06.008.
(21) Kano, S.; Fujii, M. All-Painting Process To Produce Respiration Sensor Using Humidity-Sensitive Nanoparticle Film and Graphite Trace. ACS Sustain. Chem. Eng. 2018, 6 (9), 12217–12223. https://doi.org/10.1021/acssuschemeng.8b02550.
(22) Wu, Z.; Yang, J.; Sun, X.; Wu, Y.; Wang, L.; Meng, G.; Kuang, D.; Guo, X.; Qu, W.; Du, B.; Liang, C.; Fang, X.; Tang, X.; He, Y. An Excellent Impedance-Type Humidity Sensor Based on Halide Perovskite CsPbBr3 Nanoparticles for Human Respiration Monitoring. Sens. Actuators B Chem. 2021, 337, 129772. https://doi.org/10.1016/j.snb.2021.129772.
(23) Krucińska, I.; Surma, B.; Chrzanowski, M.; Skrzetuska, E.; Puchalski, M. Application of Melt-Blown Technology for the Manufacture of Temperature-Sensitive Nonwoven Fabrics Composed of Polymer Blends PP/PCL Loaded with Multiwall Carbon Nanotubes. J. Appl. Polym. Sci. 2013, 127 (2), 869–878. https://doi.org/10.1002/app.37834.
(24) Huynh, T.-P.; Haick, H. Autonomous Flexible Sensors for Health Monitoring. Adv. Mater. 0 (0), 1802337. https://doi.org/10.1002/adma.201802337.
(25) Chen, Y.; Lu, B.; Chen, Y.; Feng, X. Breathable and Stretchable Temperature Sensors Inspired by Skin. Sci. Rep. 2015, 5 (1), 11505. https://doi.org/10.1038/srep11505.
(26) Im, S. G.; Kusters, D.; Choi, W.; Baxamusa, S. H.; van de Sanden, M. C. M.; Gleason, K. K. Conformal Coverage of Poly(3,4-Ethylenedioxythiophene) Films with Tunable Nanoporosity via Oxidative Chemical Vapor Deposition. ACS Nano 2008, 2 (9), 1959–1967. https://doi.org/10.1021/nn800380e.
(27) Husain, M. D.; Kennon, R.; Dias, T. Design and Fabrication of Temperature Sensing Fabric. J. Ind. Text. 2014, 44 (3), 398–417. https://doi.org/10.1177/1528083713495249.
(28) Bhat, N. V.; Seshadri, D. T.; Nate, M. M.; Gore, A. V. Development of Conductive Cotton Fabrics for Heating Devices. J. Appl. Polym. Sci. 2006, 102 (5), 4690–4695. https://doi.org/10.1002/app.24708.
(29) Tang, K.-P. M.; Kan, C.-W.; Fan, J. Evaluation of Water Absorption and Transport Property of Fabrics. Text. Prog. 2014, 46 (1), 1–132. https://doi.org/10.1080/00405167.2014.942582.
(30) Zhong, J.; Zhang, Y.; Zhong, Q.; Hu, Q.; Hu, B.; Wang, Z. L.; Zhou, J. Fiber-Based Generator for Wearable Electronics and Mobile Medication. ACS Nano 2014, 8 (6), 6273–6280. https://doi.org/10.1021/nn501732z.
(31) Zhang, F.; Zang, Y.; Huang, D.; Di, C.; Zhu, D. Flexible and Self-Powered Temperature–Pressure Dual-Parameter Sensors Using Microstructure-Frame-

Supported Organic Thermoelectric Materials. Nat. Commun. 2015, 6, 8356. https://doi.org/10.1038/ncomms9356.

(32) Khan, Y.; Garg, M.; Gui, Q.; Schadt, M.; Gaikwad, A.; Han, D.; Yamamoto, N. A. D.; Hart, P.; Welte, R.; Wilson, W.; Czarnecki, S.; Poliks, M.; Jin, Z.; Ghose, K.; Egitto, F.; Turner, J.; Arias, A. C. Flexible Hybrid Electronics: Direct Interfacing of Soft and Hard Electronics for Wearable Health Monitoring. Adv. Funct. Mater. 2016, 26 (47), 8764–8775. https://doi.org/10.1002/adfm.201603763.

(33) Kim, S. L.; Choi, K.; Tazebay, A.; Yu, C. Flexible Power Fabrics Made of Carbon Nanotubes for Harvesting Thermoelectricity. ACS Nano 2014, 8 (3), 2377–2386. https://doi.org/10.1021/nn405893t.

(34) Lee, J.-W.; Han, D.-C.; Shin, H.-J.; Yeom, S.-H.; Ju, B.-K.; Lee, W. PEDOT:PSS-Based Temperature-Detection Thread for Wearable Devices. Sensors 2018, 18 (9). https://doi.org/10.3390/s18092996.

(35) Strümpler, R. Polymer Composite Thermistors for Temperature and Current Sensors. J. Appl. Phys. 1996, 80 (11), 6091–6096. https://doi.org/10.1063/1.363682.

(36) Hughes-Riley, T.; Lugoda, P.; Dias, T.; Trabi, C. L.; Morris, R. H. A Study of Thermistor Performance within a Textile Structure. Sensors 2017, 17 (8). https://doi.org/10.3390/s17081804.

(37) Lugoda, P.; Hughes-Riley, T.; Morris, R.; Dias, T. A Wearable Textile Thermograph. Sensors 2018, 18 (7). https://doi.org/10.3390/s18072369.

(38) Blasdel, N. J.; Wujcik, E. K.; Carletta, J. E.; Lee, K.-S.; Monty, C. N. Fabric Nanocomposite Resistance Temperature Detector. IEEE Sens. J. 2015, 15 (1), 300–306. https://doi.org/10.1109/JSEN.2014.2341915.

(39) Yokota, T.; Inoue, Y.; Terakawa, Y.; Reeder, J.; Kaltenbrunner, M.; Ware, T.; Yang, K.; Mabuchi, K.; Murakawa, T.; Sekino, M.; Voit, W.; Sekitani, T.; Someya, T. Ultraflexible, Large-Area, Physiological Temperature Sensors for Multipoint Measurements. Proc. Natl. Acad. Sci. 2015, 112 (47), 14533–14538. https://doi.org/10.1073/pnas.1515650112.

(40) Ramachandran, T.; Vigneswaran, C. Design and Development of Copper Core Conductive Fabrics for Smart Textiles. J. Ind. Text. 2009, 39 (1), 81–93. https://doi.org/10.1177/1528083709103317.

(41) Sibinski, M.; Jakubowska, M.; Sloma, M. Flexible Temperature Sensors on Fibers. Sensors 2010, 10 (9), 7934–7946. https://doi.org/10.3390/s100907934.

(42) Bielska, S.; Sibinski, M.; Lukasik, A. Polymer Temperature Sensor for Textronic Applications. Mater. Sci. Eng. B 2009, 165 (1), 50–52. https://doi.org/10.1016/j.mseb.2009.07.014.

(43) Daoud, W. A.; Xin, J. H.; Szeto, Y. S. Polyethylenedioxythiophene Coatings for Humidity, Temperature and Strain Sensing Polyamide Fibers. Sens. Actuators B Chem. 2005, 109 (2), 329–333. https://doi.org/10.1016/j.snb.2004.12.067.

(44) Wang, H.; Ail, U.; Gabrielsson, R.; Berggren, M.; Crispin, X. Ionic Seebeck Effect in Conducting Polymers. Adv. Energy Mater. 2015, 5 (11), 1500044. https://doi.org/10.1002/aenm.201500044.

Chapter 5

THE THERMOELECTRIC PROPERTIES OF VAPOR PRINTED PEDOT-CL TEXTILES AND THEIR APPLICATIONS IN WEARABLES

5.1 Introduction

In Chapter 4 the relationship between the electrical resistance of PEDOT-Cl and heat was explored. In Chapter 5 we will expand on that concept by introducing the concept of non-uniform heating to create a temperature gradient within the polymer film. This results in the redistribution of charge carriers in the film, known as the thermoelectric effect.

The thermoelectric effect can be utilized to convert lost body heat to a source of power by taking advantage of a temperature differential between the body and cooler ambient air.[1–86] Materials with high electrical conductivities and low thermal conductivities, known as thermoelectric materials, demonstrate the ability to produce power when exposed to a temperature gradient. The low thermal conductivity of the material prevents the dissociation of heat, which creates an inequity of energy. This disparity in energy induces the migration of charges within the material toward the colder side.[48,87–89] Reports have demonstrated that up to 5 mW of power can be harvested from a normal human body after an eight-hour workday in an indoor environment, through the use

of silicone thermopiles.[90] However, the form factor, weight, and breathability of these thermopiles needs much optimization before largescale adoption can be expected.[91,92]

Additionally, the availability of materials must be considered when constructing a thermoelectric device. The most efficient body-mounted thermoelectric generators are composed of Bi_2Te_3.[93–96] However, tellurium is a rare earth chalcogenide with limited availability, restricting the scalability of this material.[97] Silicon devices do not face this hurdle but do demonstrate significantly lower thermoelectric harvesting efficiencies and poor flexibility.[98,99] Alternatively, conjugated polymers are low-density, biocompatible, flexible, lightweight, and comprised of earth abundant elements, perfectly positioning them for integration with body-worn electronics. However, to date, the observed thermoelectric performance of typical, solution-processed polymers have not been significant enough to warrant widespread investigation.[100–103] In Chapter 5 we discuss the thermoelectric efficiencies for a conductive polymer synthesized using the CVD technique. We investigate the use of these vapor printed PEDOT-Cl in the production of an all-fabric wearable thermoelectric generator (TEG) with high outputs using the human body as a heat source. We show techniques to optimize device efficiencies through architectural design as well as the integration of devices in the form of a TEG array into a variety of garments. We also show the on-body device outputs of several garments.

In this work, we show that the use of CVD to vapor print persistently *p*-doped PEDOT-Cl onto one face of commercial fabrics, such as cotton, created highly-efficient fabric thermopiles that maintained their function in the presence of sweat.[104] Further, by integrating this one-side-coated cotton thermopile into a knitted armband, we created an

all-fabric, wearable thermoelectric generator that produces Seebeck voltages of up to 23 mV when worn on the body (ΔT = 30 ºC). We show the process of optimizing thermoelectric generators through the choice of substrate and architectural considerations. Here, we present a method for creating arrays of polymer-coated fabric thermopiles, and the design and optimization of thermoelectric garments containing these all-fabric TEGs. We observe notable power outputs of up to 2 μW from a person wearing a three-quarter zip jacket containing a six-leg TEG array.

5.2 Results and Discussion

5.2.1 Textile Characterization

As discussed in Chapter 1, conductive polymers exhibit inherently low thermal conductivities and high electrical conductivities, making them ideal candidates for thermoelectric materials. Additionally, the use of fabric as a substrate largely influences the material efficiencies. Fabrics have inherently low thermal conductivities, so when used as a substrate for a thermoelectrics, the fabric can prevent thermal equilibration, thus allowing for voltage to be constantly generated. The thermal transports of textiles were qualitatively assessed through the means of thermochromic paint (Figure 5.1). The thermochromic paint simulates the PEDOT-Cl coating, as it just coats the surface of the sample. The thermochromic paint appears blue at temperatures below 30 °C, and white at temperatures exceeding 30 °C. Thus, we can qualitatively assess the thermal transport within each fabric sample by measuring the distance of the color change on the samples

from the edge of the heat source. Samples were exposed to a heat source held at 35 °C on the left edge, while the rest of the sample was exposed to ambient air, considered to be 25..°C.

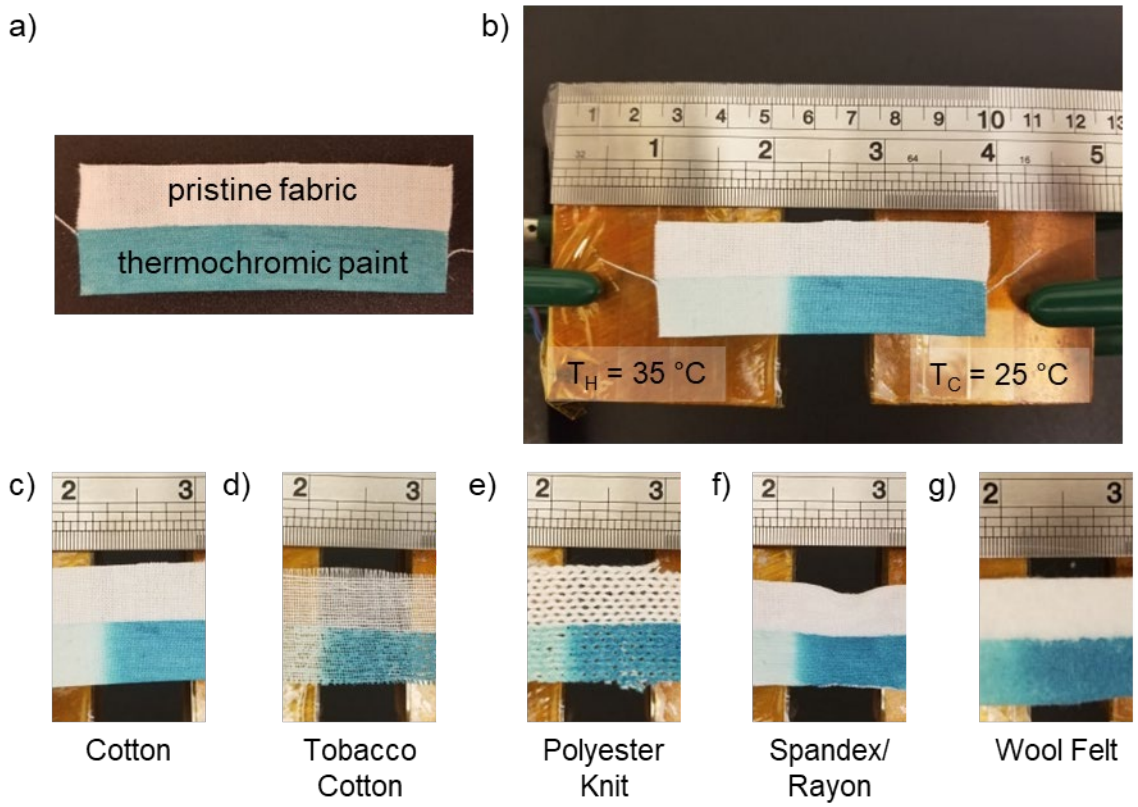

Figure 5.1 a) A sample of cotton with the bottom half coated on one side with thermochromic fabric pain, b) the experimental setup to apply a temperature gradient to the samples, heat transport of c) cotton, d) tobacco cotton, e) polyester knit, f) spandex/rayon blend, and f) wool felt.

The sample shown in Figure 5.1b was held at this temperature gradient for over 24 hours and showed no change in the distance of the color change from the heat source. This suggests that thermoelectric generators made from textiles can be exposed to a temperature gradient indefinitely without reaching thermal equilibrium. Figure 5.1c-g show the results

of cotton, tobacco cotton, polyester knit, spandex/rayon blend, and wool felt when exposed to the temperature gradient for 2 hours each. These results showed that the thickness of the textile, as well as the weave porosity play a role in dictating the thermal transport. The cotton and tobacco cotton were relatively the same thickness; however, the tobacco cotton shows almost no color change from the edge of the heat source. This is because the tobacco cotton has a much looser weave, and the heat is able to escape in the gaps between the fibers more easily than the tight weaved cotton. Additionally, the polyester knit, and wool felt show a slight discoloration of the thermochromic paint on the part of the sample that is in direct contact with the heat source. This suggests that the heat transport in these textiles is so low that the heat is having trouble traveling in the longitudinal direction and the coating on the textiles are not receiving as much heat as the side in direct contact with the heat source. This information also allows us to select the correct substrate for the application we are seeking.

5.2.2 Thermoelectric Efficiencies of PEDOT-Cl

Thermoelectric efficiencies are classically characterized through the Seebeck coefficient (S), $S=(dV/dT)_{I=0}$, where dV is the output voltage and dT is the difference in temperature between the hot side and the cold side of the material, and the power factor $PF=S^2\sigma$, where σ is the electrical conductivity. The power factor is considered a more observable value.

For a 1 μm thick film of PEDOT-Cl prepared on standard cotton, the Seebeck was found to be 18 $\mu V\ K^{-1}$ and the power factor was calculated to be 0.35 $\mu W\ m^{-1}\ K^{-2}$ (Figure

5.2a). We compared this to a sample of PEDOT:PSS coated cotton and found that the power factor value for the PEDOT-Cl is over two orders of magnitude greater than that of PEDOT:PSS, which demonstrated a power factor of 0.0032 μW m^{-1} K^{-2} and a Seebeck of 31 μV K^{-2}.

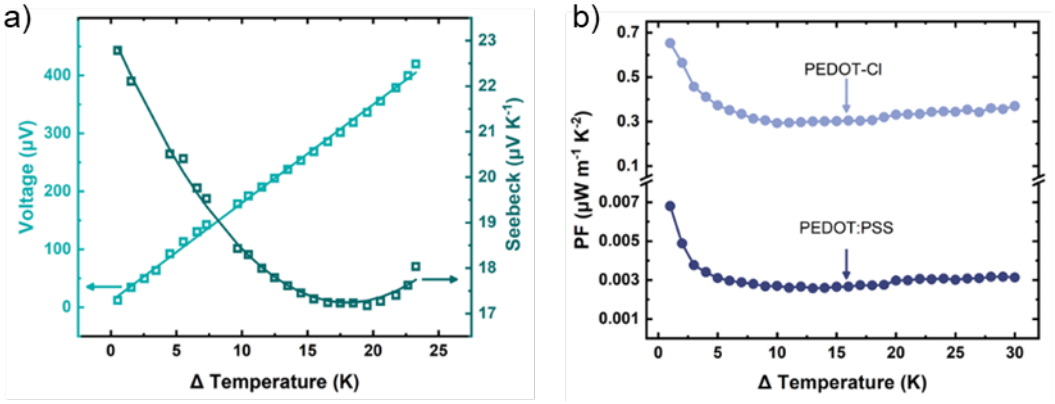

Figure 5.2 (a) The output voltage and calculated Seebeck coefficient of PEDOT-Cl on cotton for a given temperature difference. (b) The power factors of PEDOT-Cl on cotton and PEDOT:PSS on cotton for a given temperature difference.

5.3 First Generation of Thermoelectric Generator Devices

5.3.1 First Generation TEG Device Design

The initial, or first generation, thermoelectric generator device design is shown in Figure 5.3. The PEDOT-Cl was deposited onto a textile mapped with Kapton Tape to create 2 legs both 5 mm wide and 45 mm in length. On both ends of each thermoelectric leg, a square (5 mm x 5 mm) of silver-plated Lycra was hand sewn to act as a charge collector.

The second thermoelectric material was a carbon fiber that was sewn directly onto the silver Lycra in a way that bridges the two legs together.

It is important to note that we started by making a proof-of-concept TEG design. In this iteration of devices, silver paste was used as a charge collector. This was changed to silver-plated Lycra in the first generation, which proved to be a more robust material for use on wearables. Additionally, this was done so that an all-fabric device could be produced.

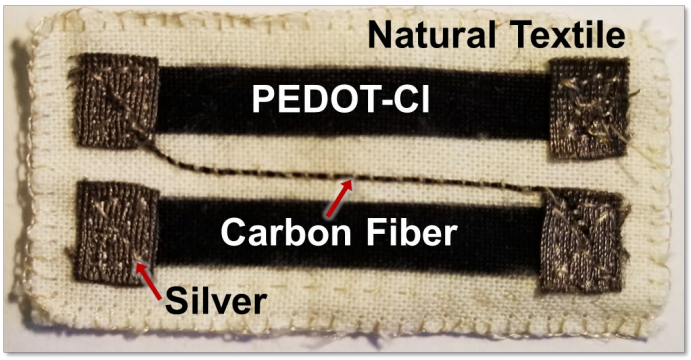

Figure 5.3 The design of the first generation of thermoelectric generator devices.

5.3.2 First Generation TEG Device Characterization

The device outputs for the first-generation TEGs were obtained using the thermoelectric measurement setup shown in Figure 5.4a. The influence of textile weave density on the device performance was investigated by assembling devices on a standard cotton of medium density as well as a loose weave tobacco cotton. Silver paste was used as the conductive connector for these devices as they were proof-of-concept. The resulting output voltages are shown in Figure 5.4b, which show that a two-leg device on standard

cotton can produce up to 1.2 mV at a temperature difference of 30 K. The ouputs of the cotton and the tobacco cotton devices were close in value and showed good repeatability with for both. Ultimately cotton was used predominantly moving forward to the first-generation devices due to the fact that it is a more robust fabric than the tobacco cotton. Furthermore, these results show that efficient devices can be produced on textiles with a variety of porosities using the RVD technique.

The tobacco cotton device demonstrates lower electrical resistances for the PEDOT-Cl leg, when measured end to end (20 kΩ), in comparison to the standard cotton (150 kΩ), allowing for the output currents to be measured for the tobacco cotton device. The comparison of the power and voltage outputs for the tobacco cotton device are shown in Figure 5.4c and demonstrate that 4.5 nW of power are able to be generated at a temperature difference of 30 K when measured with a multi-meter.

Additionally, during this experiment the resistivity of the PEDOT-Cl legs were monitored, in order to determine if the polymer was degrading under heat from the measurements. The temperature range was chosen in order to simulate possible temperature differences the average garment would be exposed to. The PEDOT-Cl showed no changes in resistance at the conclusion of all measurements, which suggests the polymer is stable under normal wear conditions. The voltage outputs of the first-generation TEGs were comparable to the silver paste.

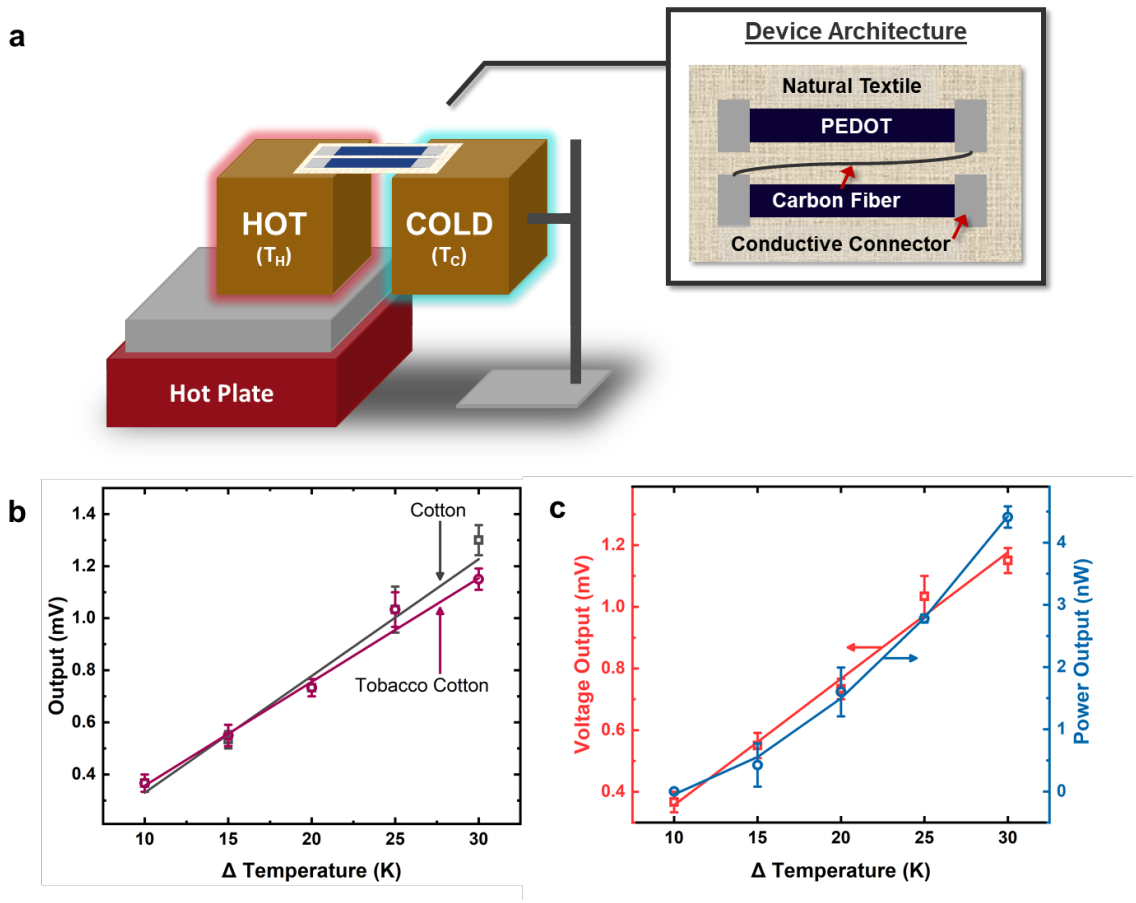

Figure 5.4 a) The thermoelectric measurement setup and architecture of cotton TEGs, b) the voltage outputs for a TEG on standard cotton and tobacco cotton, and c) the power and voltage outputs for a tobacco cotton TEG.

5.3.3 The Integration of First-Generation TEGs into a Wearable Garment

A wearable thermoelectric garment was designed such that a first-generation TEG was mounted into a wearable band (Figure 5.5). The TEG was sewn into a thick knitted band in such a way that one side was only exposed to ambient air, while the other side was exposed to body heat and warm still air trapped between the body and the garment. We

chose a lateral device design, so the device must be sewed in such a way that the device passed through the knitted band. This wearable device was designed to exploit body heat lost on either the inside of the wrist or the upper arm as a heat source, areas chosen based on temperatures observed with thermal imaging. However, during data collection these areas resulted in poor thermal contact between the heat source and the device. Alternatively, when used on the palm of the hand, which has a notably lower temperature, the contact between the heat source and the TEG was able to be optimized and higher output voltages were observed. This finding emphasizes the need for a thermoelectric device to be in direct contact with the heat source in order to obtain the highest possible outputs.

The voltage outputs of this TEG armband were obtained using multiple human subjects, both indoors ($T_C = 25\ °C$) and outdoors on a cold day ($T_C = 2\ °C$), where ΔT is the difference between the subject's palm and the ambient air (Figure 5.5b). These results demonstrate that substantially higher output voltages can be obtained from the same device when the body was used as a heat source compared to the use of temperature-controlled copper blocks. Additionally, the outputs measured with a larger temperature difference, outdoors, were generally higher than those recorded inside. This is to be expected as higher temperature differences resulted in higher output values when the devices were tested on the copper blocks. However, the temperature difference does not seem to be the dominating factor that determines voltage output of a body mounted device.

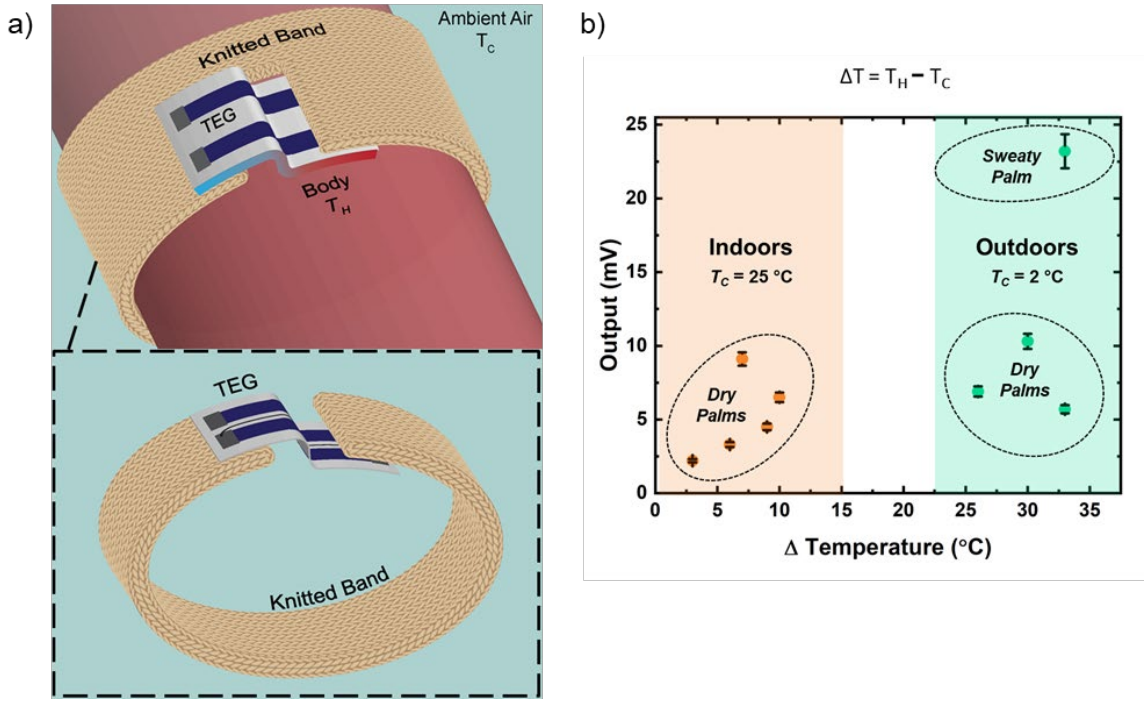

Figure 5.5 a) The design for a body-mounted, all-fabric TEG knitted band, b) the voltage outputs for a knitted band TEG using humans as heat sources, where ΔT is the difference between the subject's palm and the ambient air both indoors (T_C = 25 °C) and outdoors on a cold day (T_C = 2 °C)

The majority of data points in Figure 5.5b were measured on dry palms of participants. However, one of the participants tested had perspiration on their palm during the time the measurement was taken. The subject with perspiration on their palm was able to produce up to 24 mV, while the next closest output was 10 mV. This increase in efficiency can partially be attributed to the increased thermal contact that the sweat provided between the hand and the device. Although, the dominant reason for this increase in efficiency with perspiration can be ascribed to ionic interactions between the skin and the device. This is illustrated in Figure 5.6a where the thermoelectric output voltages were measured on a participant's bare skin. The measurement was taken on the same participant

wearing a layer of plastic wrap between the skin and the device. This scenario allows for thermal contact between the body but prevents the device from coming in contact with moisture on the skin. And finally, the same participant wearing a neoprene glove between the skin and the device, which prevents the device from being exposed to both thermal contact and moisture from the skin. We saw that the outputs for the bare skin measured ~9 mV, but when the plastic wrap was introduced, this value dropped significantly to ~0.2 mV. When the neoprene glove was worn, the voltage dropped to 0, effectively turning off the device. This confirms that the large increase in efficiencies is likely due to an interaction occurring between moist skin and the PEDOT-Cl in the device.

As discussed in Chapter 3, the PEDOT-Cl is a mixed ionic-electronic polymer conductor as it has a moisture dependent conductivity. When the polymer is exposed to moisture, the ions within the film have a higher mobility and an ionic conductivity is increased. We hypothesize that this large increase in thermoelectric efficiencies is likely due to the Soret Effect. The Soret Effect works in the same way as the thermoelectric effect, except that it is ions instead of charge carriers that are moving in the polymer material.

To further test this hypothesis, we tested the thermoelectric arm band on a participant with several different moisture conditions. The first was by spraying the skin with water, second was by spraying the skin with a solution of NaCl in water (0.1 M) to simulate sweat, next was by applying a layer of lotion to the skin, and finally by applying a layer of lotion to the skin and spraying the solution of NaCl on top. We found that water did increase the output voltages confirming that the moisture was changing the thermoelectric properties. Additionally, we found that the output voltages increased even

further when lotion and salt water were introduced. Both of these scenarios introduce moisture, but they also introduce additional ions onto the skin. Thus, supporting the theory that the large increase in thermoelectric efficiencies is coming from the Soret effect.

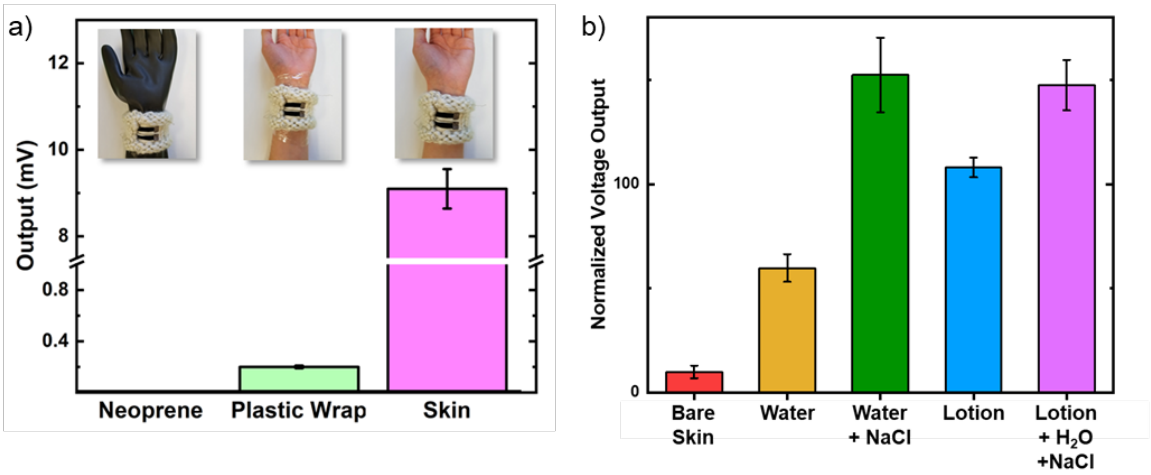

Figure 5.6 a) The voltage outputs of the TEG arm band of a participant's bare skin, while wearing plastic wrap between the skin and the device, and while wearing a neoprene glove between the skin and the device, b) normalized voltage outputs of the TEG arm band under varying moisture conditions.

5.4 Second-Generation of Thermoelectric Generator Devices

5.4.1 Second-Generation Thermoelectric Generator Device Design

While the voltage outputs of the first-generation TEG devices proved to be high, the current in these devices were too low to be functional as a trickle charge generator. Thus, we optimized the design to allow for higher current outputs and creating the second-

generation of thermoelectric generator devices. The second-generation device architecture is shown in Figure 5.7.

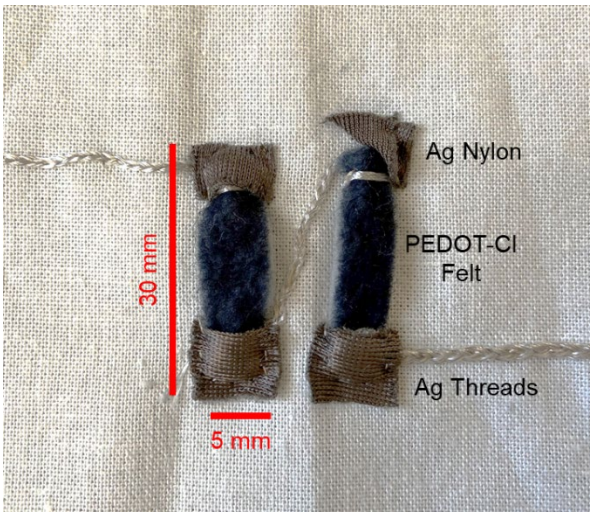

Figure 5.7 The device architecture of second-generation thermoelectric generator devices.

We chose to stick with the lateral architecture used in the first-generation devices, as this type of device architecture has a lower likelihood of causing thermal equilibration across each thermoelectric leg and because the dimensions and constituents of the thermoelectric legs can be independently tuned without adding additional bulk to a garment. Here, modifications were made to this previously reported TEG to increase the power outputs. The carbon fibers previously used as the *n*-type thermoelectric material were replaced with a more robust silver-plated nylon thread. The cotton substrate was exchanged for a wool felt, which is a non-woven material with very low thermal transport. The densely textured, microstructured surface of the wool felt increased the mass loading of the deposited PEDOT-Cl on the fabric surface, as compared to plain-woven cotton,

leading to much higher surface conductivity values. The increased polymer loading on the fabric surface and higher conductivity, coupled with the decreased thermal transport across the wool felt substrate enabled the thermoelectric legs of the device to be shortened, thus increasing the power outputs of an individual thermoelectric leg without sacrificing the effective thermal gradient experienced by the thermopile.

The use of felt also allowed us to create free standing devices, as felt is a non-woven and not susceptible to unravelling. This means we can deposit the PEDOT-Cl on a large surface area and cut the legs out individually as opposed to the previous method of masking the cotton with Kapton Tape. By increasing the sample size, we can more efficiently make larger numbers of devices. The sponge-like texture of the felt and the higher durability of the silver thread allow for the threads to be wrapped tightly around each end of the thermoelectric legs. This creates better electrical contact between the two materials. It also allows for the legs to be connected without sewing, so there is no puncturing of the polymer film needed.

One thermoelectric leg was comprised of a rectangle of PEDOT-Cl coated wool felt contacted to silver-plated nylon threads on either end and the assembly fixed onto a thin backing support fabric using cotton threads. Two thermoelectric legs comprised one TEG unit. Arrays of the two-leg TEGs could be easily created by simple patching the backing fabric onto any desired textile or garment and connecting the TEGs with silver thread embroidery.

5.4.2 Thermoelectric Efficiencies of Second-Generation TEG Devices

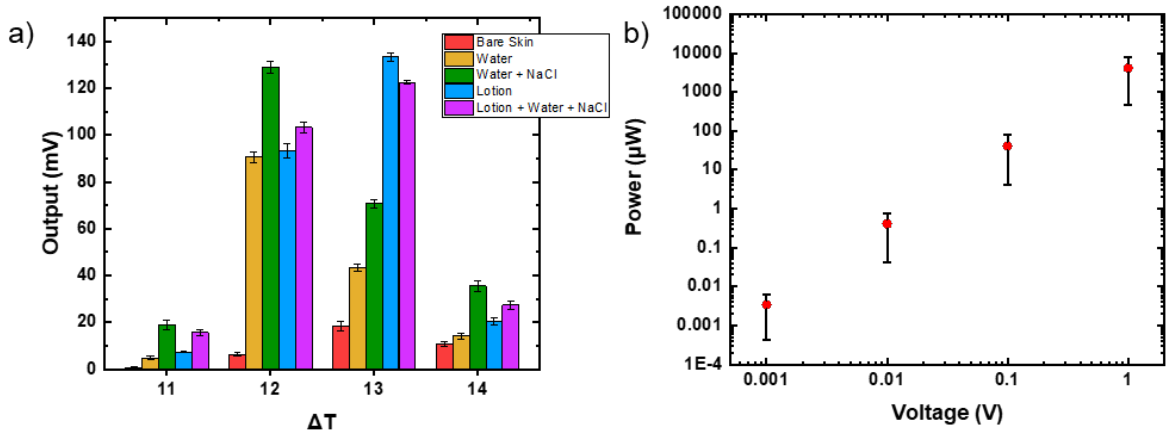

Figure 5.8 a) Output voltages of several body-mounted two-leg TEGs. Each TEG was tested on dry skin as well as skin that was wetted with water, a 1 mM solution of sodium chloride, and commercially available lotion. b) Power outputs recorded from the TEGs at fixed voltage values.

The second-generation TEG device was mounted in the knit arm band, discussed in the first-generation of devices, and was able to reach output voltages as high as 130 mV were recorded at a $\Delta T = 13\ ^{o}C$, particularly when the participant's skin was wetted with lotion and/or saline (Figure 5.8a). We reported a similar observation in our previous work,[17] where the apparent output voltages of all-fabric TEGs were up to an order of magnitude higher on sweaty skin, as compared to a static, dry test station. It is important to note that PEDOT-Cl is a mixed ionic-electronic conductor, and it is known that the increased output voltages are a reflection of the increasing ionic conductivity when the polymer is exposed to moisture.[1] Figure 5.8b shows the device power outputs at fixed voltage values. These voltage values represent the range of possible voltage outputs that

can be produced by the TEGs upon being worn on the body. One TEG produced 3.5 µW at 100 mV, which can be considered the average voltage output of one representative TEG.

5.4.3 The Design and Creation of TEG-Integrated Garments

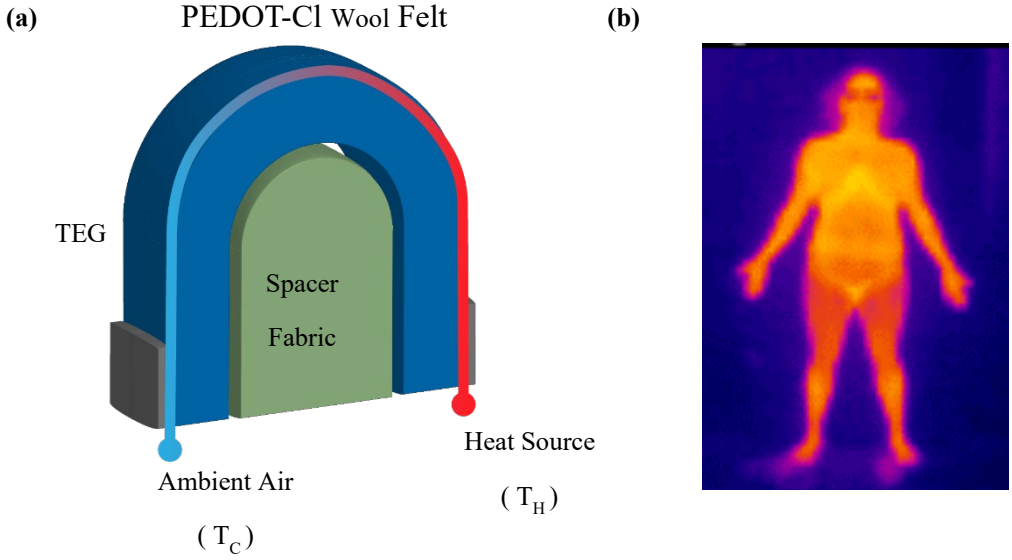

Figure 5.9 a) A diagram of our lateral TEG folded over a spacer fabric such that a thermal gradient is imposed across the TEG, and b) Thermal camera image of a person.

Since our fabric-based TEGs had a lateral architecture, a thermal gradient could be imposed across each thermoelectric leg by simply folding the pliable fabric TEG over a spacer (Figure 5.9a). This meant that our TEGs could be readily integrated to familiar garments at certain points, such as the cuff of a sleeve or the collar, where the TEG arrays would be naturally folded over when the user wears the garment. Folding the TEG around the fabric of the garment exposes the device to both the T_H, body heat, and T_C, ambient air

without sacrificing the comfort or functionality of the garment. In conjunction with optimizing the placement of the TEG on the garment, the placement of the device on the body was also considered in order to maximize the amount of heat transferred from the heat source (the body) to the TEGs. Areas closest to the body's core, along the head, neck and torso, have lower temperature variability than those on the body's extremities, and thus lead to more stable power outputs from the TEGs. Figure 5.9b shows a thermal image of a person, the bright spots representing the hottest areas on the body.

Several proof-of-concept garments were designed where the TEG devices were placed such that they could fold over the edge of the fabric of the garment (Figure 5.10). First, a tee-shirt was created where the TEG devices were mounted along the front of the neck. These devices can then draw heat from the chest, which will have higher temperatures as it is the core of the body. Second, the TEG devices were mounted on a collared shirt. These TEGs were located on the collar at the base of the neck and were designed to be in contact with the upped back/lower neck of the wearer. Again, this will have higher temperatures because it is located in the core of the body. Next, the TEGs were placed at the end of a sleeve. These devices would be in contact with the skin on the wearer's wrist, which will have a lower temperature because they are located on the appendages of the body. Finally, the TEGs were mounted on the top of a neck gaiter. These devices would be in contact with either the skin on the face of the wearer (if the neck gaiter is pulled up) or on the throat (if the neck gaiter is pulled down). The neck and the face should have a similar temperature as the core of the body, and thus should be relatively high.

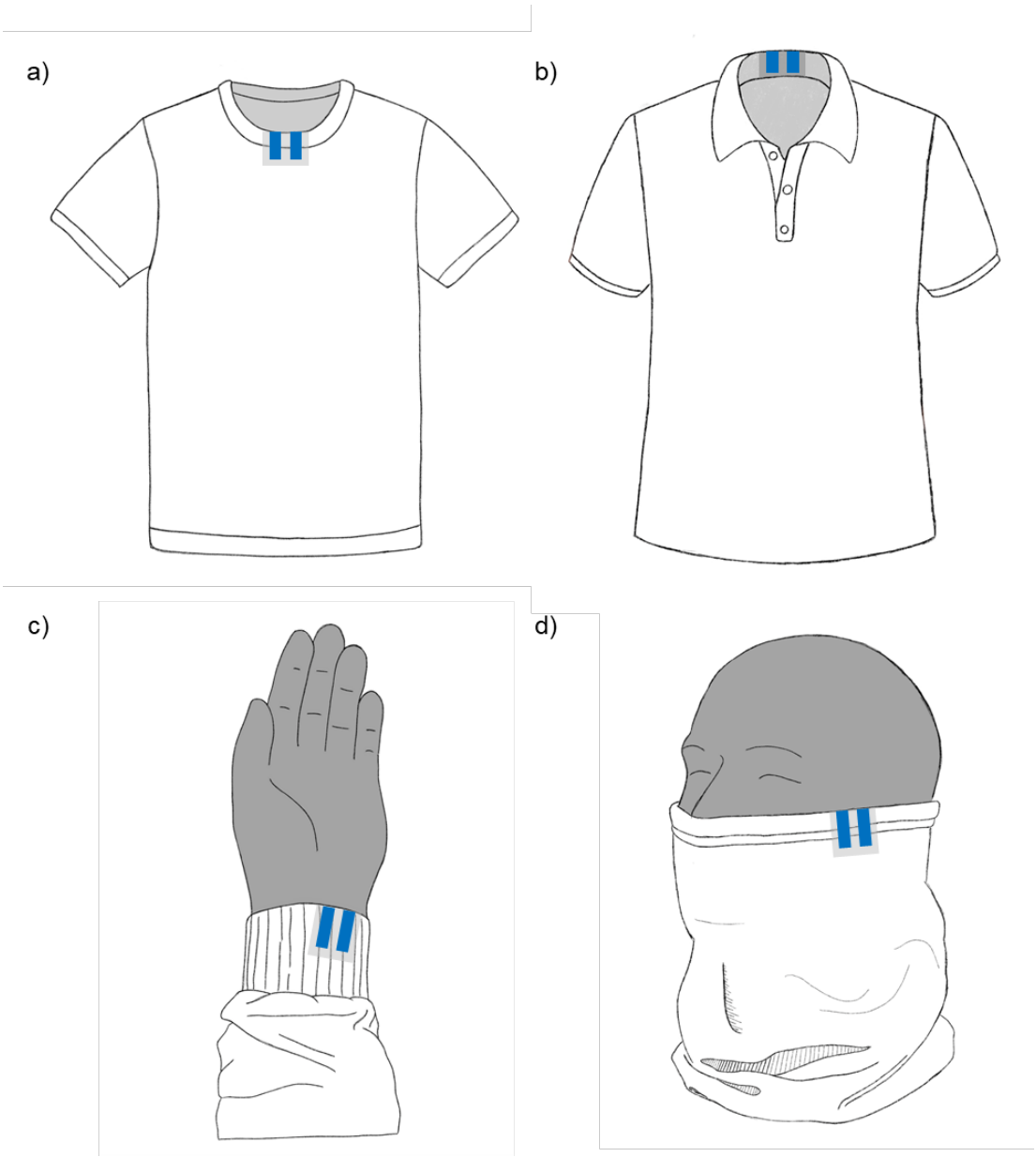

Figure 5.10 The design of a) a tee-shirt b) a collared shirt c) a sleeve, and d) a neck gaiter with TEG devices integrated along the edges. The TEGs are represented by the blue shapes.

Ultimately, for this work, we chose to patch two separate TEG arrays onto the collar of a fleece, three-quarter zip jacket, as depicted in Figure 5.11a. The placement on the collar allows for the TEGs to be in thermal contact with the neck and chest area, which

have low thermal variability. The top of the collar had an array consisting of six PEDOT-Cl thermoelectric legs, while the base of the collar had an array of eight legs. Two separate arrays allowed for thermoelectric body heat harvesting when the jacket was worn either with the collar folded down, or with the collar folder up. The TEGs were connected in series within the array, each array was designed to quick-connect (via snap buttons) to its own modular charge storage device in the future. Silver-plated nylon threads were used to electronically interface the components and therefore create a fabric circuit. Commercially available snap buttons were used as electrical switches, allowing for a modular charge storage device to be connected/disconnected from the TEGs on demand (Figure 5.11b).

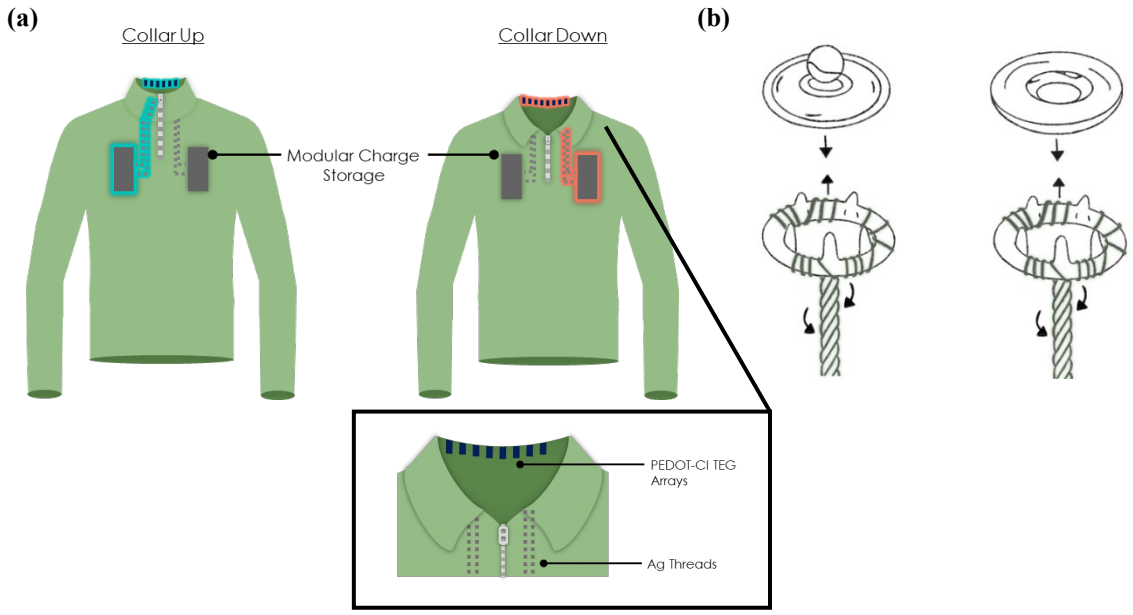

Figure 5.11 a) Design of a three-quarter zip jacket integrated with two separate TEF arrays at the collar b) the mechanism of integrating snap buttons with silver nylon thread.

Figure 5.12a shows the power outputs produced by the eight-leg TEG array at the base of the collar of the fleece zip jacket at room temperature, at fixed voltage values, obtained through chronoamperometry measurements. The data recorded from the six-leg TEG array at the top of the collar is shown in Figure 5.12c-d. The power outputs were recorded at fixed voltage values, where the applied voltage values covered the apparent range of output voltages capable of being produced by our TEGs when worn on the body (see Figure 5.8). Figure 5.12b shows the power outputs as the number of TEGs in the array was increased. The power decreased as more legs were added, which is due to an increase of the overall impedance of the completed circuit, likely due to contact resistance between each of the PEDOT-Cl legs and the silver nylon fabric/thread. It is important to note that the number of TEGs in the array should not exceed the contact area between the jacket with a wearer's neck during regular wear, as this would result in poor thermal contact between the heat source and some of the TEGs, and, therefore, a reduction in the overall efficiency of power generation.

The power and voltage output produced at room temperature by the eight-leg TEG array at the base of the jacket collar when the fleece zip jacket was worn loosely by healthy participants (ΔT = 15 °C) was also recorded, shown in red in Figure 5.12. On-body measurements were taken on lightly dampened skin to simulate perspiration. The output voltage of the device array worn on the body was also independently confirmed using a multimeter and measured to be 112 mV. When worn by a participant at room temperature, a ΔT = 15 °C, the TEG array generated 2 μW, which is currently the highest value reported for a conjugated polymer-based TEG array. These voltage and power output values were

not notably affected by the fit and looseness of the jacket on various participants and were consistently achieved after each participant wore the jacket for at least 15 minutes (to ensure sufficient heat transfer from the wearer's body to the TEG array). Further, due to the low thermal transport property of the wool felt substrate, which prevented complete thermal equilibration across each thermoelectric leg, the TEG array at the base of the jacket collar continuously output 112 mV.

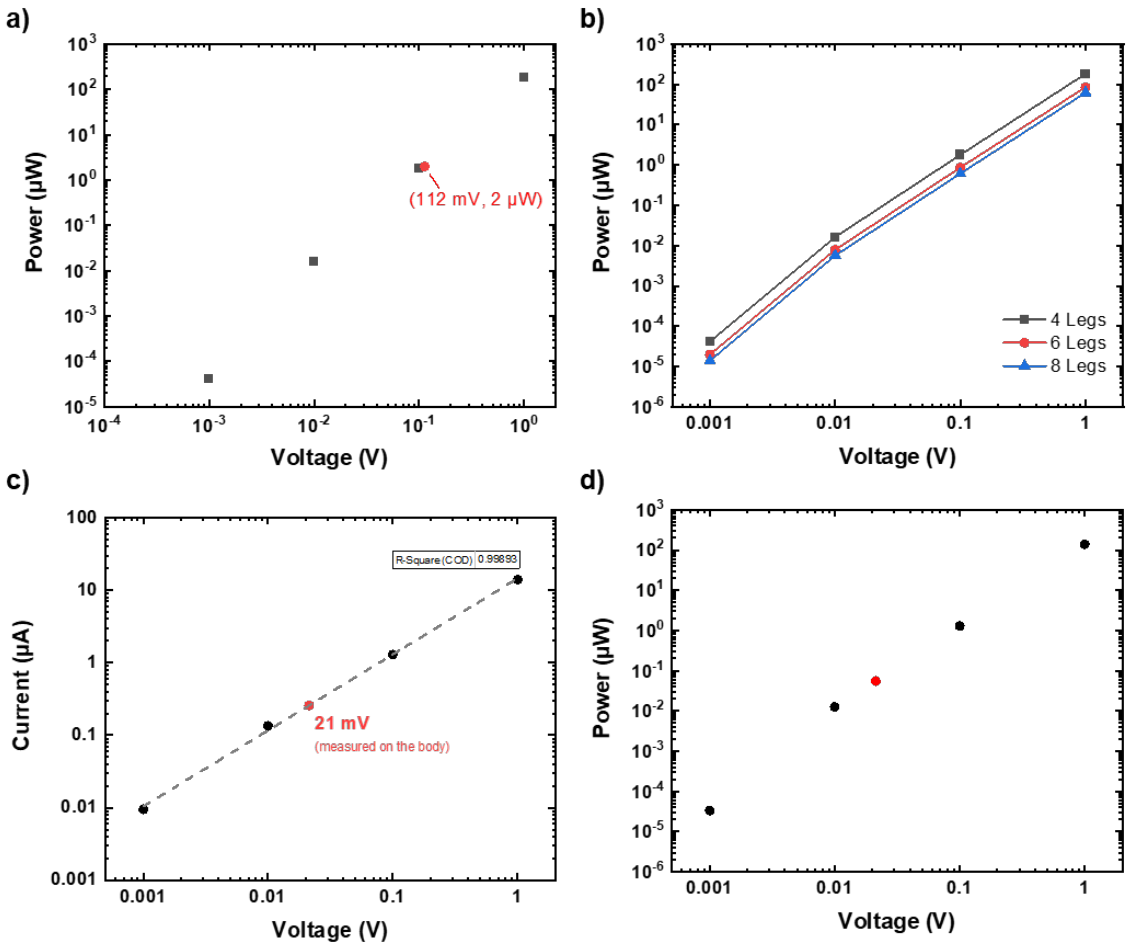

Figure 5.12 a) Power outputs from an eight-leg TEG array located at the base of the collar of a three-quarter zip fleece jacket. Averaged data from three different arrays created on separate garments are presented as black squares; error bars are colored blue. b) the power outputs from the three-quarter zip jacket as more TEGs are added to the array at the base

of the collar, c) The current and d) power outputs of the six-leg TEG array located at the top of the collar of a fleece three-quarter zip jacket. The red data point represents the measurement taken while the jacket was worn by the participant, with the collar folded up.

5.5 Summary

We utilized reactive vapor deposition to coat commercially available wool felt in PEDOT-Cl, which we used to construct an all-fabric thermoelectric generator. We demonstrated that a 2-legged TEG device can generate an average of 3.5 μW at an operating voltage of 100 mV. These TEGS were successfully integrated as arrays into the collar of a three-quarter zip jacket. When worn by a participant the TEGs were able to generate an unprecedented 2 μW of power at room temperatures. Our work reveals pertinent design considerations when integrating thermoelectrics into a garment and also indicates that practical power outputs can be extracted from body-worn polymer-based thermoelectric devices at room temperature. Additionally, this work emphasizes the importance of testing wearable thermoelectrics on a human body to accurately predict the potential power produced by the garment.

5.6 Experimental

5.6.1 Thermoelectric characterization of materials

The conductivity was measured on a 4-probe system and calculated using the formula, $\sigma = G\left(\frac{l}{w \cdot t}\right)$, where G is the slope of the IV curve, l is the distance between the

probes (1.1 cm), *w* is the width of the sample, and *t* is the thickness of the film. Samples were cut into 1.5 cm x 1.5 cm squares.

5.6.2 Device fabrication

For the first-generation devices, using a polyimide tape mask, PEDOT-Cl was deposited on textiles in two rectangles, 45 mm long and 5 mm wide, with a space of 5 mm between them. Silver paste was applied to ends of each leg and dried in ambient conditions for 48 hours, carbon fibers of ~45-50 mm in length were attached using silver paste and dried in the same manner. For all-fabric devices, cotton thread was used to sew silver nylon onto the ends of each leg and embroider on the carbon fibers. For the wearable devices, the band was knit in-house using lion brand acrylic (100%) yarn and the devices were sewn on using cotton thread. For the second-generation devices, the thermoelectric generators were all assembled using commercially available wool felt as a substrate. Silver-plated (76%) nylon (24%) fabrics and silver-plated nylon thread were both purchased from Less EMF Inc.

5.6.3 Voltage Output Characterization of Devices

Thermoelectric properties of devices were characterized in a house-built setup, using copper blocks (2 inch x 2 inch x 2 inch), one held at room temperature (25 °C) and the other controllably heated by a Opti Mag-st heating plate. Blocks were positioned with 1 inch of space between them. All output measurements were taken by connecting the probes of a FLUKE 27 II multimeter to the electrodes on the device. Body mounted device

outputs were measured using alligator clips attached to the probes, taking care to prevent the contact of the metal clip with the skin to avoid false readouts.

5.6.4 Electrical Power Output Characterization of Devices

The power outputs from the TEG array were measured using the "Chronoamperometry" function on an Autolab Potentiostat. The current of the devices were measured under fixed voltage values over a period of 5 minutes at each voltage. The measurements were done both statically at room temperature and ambient humidity, as well as on a participant with damp skin. Voltage outputs (Seebeck voltages) from body-worn devices were measured using a Fluke multimeter.

5.6.5 Infrared (IR) Images

The IR images were taken using a FLIR camera.

5.7 References

(1) Kim, M.-K.; Kim, M.-S.; Lee, S.; Kim, C.; Kim, Y.-J. Wearable Thermoelectric Generator for Harvesting Human Body Heat Energy. Smart Mater. Struct. 2014, 23 (10), 105002. https://doi.org/10.1088/0964-1726/23/10/105002.

(2) Jin Kim, S.; Hyung We, J.; Jin Cho, B. A Wearable Thermoelectric Generator Fabricated on a Glass Fabric. Energy Environ. Sci. 2014, 7 (6), 1959–1965. https://doi.org/10.1039/C4EE00242C.

(3) Hyland, M.; Hunter, H.; Liu, J.; Veety, E.; Vashaee, D. Wearable Thermoelectric Generators for Human Body Heat Harvesting. Appl. Energy 2016, 182, 518–524. https://doi.org/10.1016/j.apenergy.2016.08.150.

(4) Wang, J.; Cai, K.; Shen, S. A Facile Chemical Reduction Approach for Effectively Tuning Thermoelectric Properties of PEDOT Films. Org. Electron. 2015, 17 (Supplement C), 151–158. https://doi.org/10.1016/j.orgel.2014.12.007.
(5) Lund, A.; Tian, Y.; Darabi, S.; Müller, C. A Polymer-Based Textile Thermoelectric Generator for Wearable Energy Harvesting. J. Power Sources 2020, 480, 228836. https://doi.org/10.1016/j.jpowsour.2020.228836.
(6) Goldsmid, H. J. A Simple Technique for Determining the Seebeck Coefficient of Thermoelectric Materials. J. Phys. [E] 1986, 19 (11), 921. https://doi.org/10.1088/0022-3735/19/11/008.
(7) Elmoughni, H. M.; Menon, A. K.; Wolfe, R. M. W.; Yee, S. K. A Textile-Integrated Polymer Thermoelectric Generator for Body Heat Harvesting. Adv. Mater. Technol. 2019, 4 (7), 1800708. https://doi.org/10.1002/admt.201800708.
(8) Yu, C.; Murali, A.; Choi, K.; Ryu, Y. Air-Stable Fabric Thermoelectric Modules Made of N- and P-Type Carbon Nanotubes. Energy Environ. Sci. 2012, 5 (11), 9481–9486. https://doi.org/10.1039/C2EE22838F.
(9) Lee, J. J.; Yoo, D.; Park, C.; Choi, H. H.; Kim, J. H. All Organic-Based Solar Cell and Thermoelectric Generator Hybrid Device System Using Highly Conductive PEDOT:PSS Film as Organic Thermoelectric Generator. Sol. Energy 2016, 134, 479–483. https://doi.org/10.1016/j.solener.2016.05.006.
(10) Oh, J. Y.; Lee, J. H.; Han, S. W.; Chae, S. S.; Bae, E. J.; Kang, Y. H.; Choi, W. J.; Cho, S. Y.; Lee, J.-O.; Baik, H. K.; Lee, T. I. Chemically Exfoliated Transition Metal Dichalcogenide Nanosheet-Based Wearable Thermoelectric Generators. Energy Environ. Sci. 2016, 9 (5), 1696–1705. https://doi.org/10.1039/C5EE03813H.
(11) Zhu, T.; Liu, Y.; Fu, C.; Heremans, J. P.; Snyder, J. G.; Zhao, X. Compromise and Synergy in High-Efficiency Thermoelectric Materials. Adv. Mater. 2017, 29 (14), n/a-n/a. https://doi.org/10.1002/adma.201605884.
(12) Bell, L. E. Cooling, Heating, Generating Power, and Recovering Waste Heat with Thermoelectric Systems. Science 2008, 321 (5895), 1457–1461. https://doi.org/10.1126/science.1158899.
(13) Reenen, S. van; Kemerink, M. Correcting for Contact Geometry in Seebeck Coefficient Measurements of Thin Film Devices. Org. Electron. 2014, 15 (10), 2250–2255. https://doi.org/10.1016/j.orgel.2014.06.018.
(14) Petsagkourakis, I.; Pavlopoulou, E.; Cloutet, E.; Chen, Y. F.; Liu, X.; Fahlman, M.; Berggren, M.; Crispin, X.; Dilhaire, S.; Fleury, G.; Hadziioannou, G. Correlating the Seebeck Coefficient of Thermoelectric Polymer Thin Films to Their Charge Transport Mechanism. Org. Electron. 2018, 52 (Supplement C), 335–341. https://doi.org/10.1016/j.orgel.2017.11.018.
(15) Menon, A. K.; Yee, S. K. Design of a Polymer Thermoelectric Generator Using Radial Architecture. J. Appl. Phys. 2016, 119 (5), 055501. https://doi.org/10.1063/1.4941101.

(16) Rowe, D. M.; Min, G. Design Theory of Thermoelectric Modules for Electrical Power Generation. IEE Proc. - Sci. Meas. Technol. 1996, 143 (6), 351–356. https://doi.org/10.1049/ip-smt:19960714.
(17) Hu, E.; Kaynak, A.; Li, Y. Development of a Cooling Fabric from Conducting Polymer Coated Fibres: Proof of Concept. Synth. Met. 2005, 150 (2), 139–143. https://doi.org/10.1016/j.synthmet.2005.01.018.
(18) Singh, A.; Bhattacharya, S.; Thinaharan, C.; Aswal, D. K.; Gupta, S. K.; Yakhmi, J. V.; Bhanumurthy, K. Development of Low Resistance Electrical Contacts for Thermoelectric Devices Based on N-Type PbTe and p-Type TAGS-85 ((AgSbTe 2) 0.15 (GeTe) 0.85). J. Phys. Appl. Phys. 2009, 42 (1), 015502. https://doi.org/10.1088/0022-3727/42/1/015502.
(19) Zhu, Z.; Liu, C.; Jiang, F.; Xu, J.; Liu, E. Effective Treatment Methods on PEDOT:PSS to Enhance Its Thermoelectric Performance. Synth. Met. 2017, 225, 31–40. https://doi.org/10.1016/j.synthmet.2016.11.011.
(20) Jia, Y.; Li, X.; Jiang, F.; Li, C.; Wang, T.; Jiang, Q.; Hou, J.; Xu, J. Effects of Additives and Post-Treatment on the Thermoelectric Performance of Vapor-Phase Polymerized PEDOT Films. J. Polym. Sci. Part B Polym. Phys. n/a-n/a. https://doi.org/10.1002/polb.24422.
(21) Kim, N.; Lienemann, S.; Petsagkourakis, I.; Alemu Mengistie, D.; Kee, S.; Ederth, T.; Gueskine, V.; Leclère, P.; Lazzaroni, R.; Crispin, X.; Tybrandt, K. Elastic Conducting Polymer Composites in Thermoelectric Modules. Nat. Commun. 2020, 11 (1), 1424. https://doi.org/10.1038/s41467-020-15135-w.
(22) Chung, D. D. L. Electrical Applications of Carbon Materials. J. Mater. Sci. 2004, 39 (8), 2645–2661. https://doi.org/10.1023/B:JMSC.0000021439.18202.ea.
(23) Chang, W. B.; Fang, H.; Liu, J.; Evans, C. M.; Russ, B.; Popere, B. C.; Patel, S. N.; Chabinyc, M. L.; Segalman, R. A. Electrochemical Effects in Thermoelectric Polymers. ACS Macro Lett. 2016, 5 (4), 455–459. https://doi.org/10.1021/acsmacrolett.6b00054.
(24) Wu, H.; Huang, Y.; Xu, F.; Duan, Y.; Yin, Z. Energy Harvesters for Wearable and Stretchable Electronics: From Flexibility to Stretchability. Adv. Mater. 2016, 28 (45), 9881–9919. https://doi.org/10.1002/adma.201602251.
(25) Wang, J.; Cai, K.; Shen, S. Enhanced Thermoelectric Properties of Poly(3,4-Ethylenedioxythiophene) Thin Films Treated with H2SO4. Org. Electron. 2014, 15 (11), 3087–3095. https://doi.org/10.1016/j.orgel.2014.09.012.
(26) Luo, J.; Billep, D.; Waechtler, T.; Otto, T.; Toader, M.; Gordan, O.; Sheremet, E.; Martin, J.; Hietschold, M.; Zahn, D. R. T.; Gessner, T. Enhancement of the Thermoelectric Properties of PEDOT:PSS Thin Films by Post-Treatment. J. Mater. Chem. A 2013, 1 (26), 7576–7583. https://doi.org/10.1039/C3TA11209H.
(27) He, H.; Ouyang, J. Enhancements in the Mechanical Stretchability and Thermoelectric Properties of PEDOT:PSS for Flexible Electronics Applications.

Acc. Mater. Res. 2020, 1 (2), 146–157. https://doi.org/10.1021/accountsmr.0c00021.

(28) Wei, Q.; Mukaida, M.; Kirihara, K.; Ishida, T. Experimental Studies on the Anisotropic Thermoelectric Properties of Conducting Polymer Films. ACS Macro Lett. 2014, 3 (9), 948–952. https://doi.org/10.1021/mz500446z.

(29) Saxena, N.; Keilhofer, J.; Maurya, A. K.; Fortunato, G.; Overbeck, J.; Müller-Buschbaum, P. Facile Optimization of Thermoelectric Properties in PEDOT:PSS Thin Films through Acido-Base and Redox Dedoping Using Readily Available Salts. ACS Appl. Energy Mater. 2018, 1 (2), 336–342. https://doi.org/10.1021/acsaem.7b00334.

(30) Zhang, F.; Zang, Y.; Huang, D.; Di, C.; Zhu, D. Flexible and Self-Powered Temperature–Pressure Dual-Parameter Sensors Using Microstructure-Frame-Supported Organic Thermoelectric Materials. Nat. Commun. 2015, 6, 8356. https://doi.org/10.1038/ncomms9356.

(31) Park, T.; Park, C.; Kim, B.; Shin, H.; Kim, E. Flexible PEDOT Electrodes with Large Thermoelectric Power Factors to Generate Electricity by the Touch of Fingertips. Energy Environ. Sci. 2013, 6 (3), 788–792. https://doi.org/10.1039/C3EE23729J.

(32) Kim, S. L.; Choi, K.; Tazebay, A.; Yu, C. Flexible Power Fabrics Made of Carbon Nanotubes for Harvesting Thermoelectricity. ACS Nano 2014, 8 (3), 2377–2386. https://doi.org/10.1021/nn405893t.

(33) Dun, C.; Hewitt, C. A.; Huang, H.; Montgomery, D. S.; Xu, J.; Carroll, D. L. Flexible Thermoelectric Fabrics Based on Self-Assembled Tellurium Nanorods with a Large Power Factor. Phys. Chem. Chem. Phys. 2015, 17 (14), 8591–8595. https://doi.org/10.1039/C4CP05390G.

(34) Ito, M.; Koizumi, T.; Kojima, H.; Saito, T.; Nakamura, M. From Materials to Device Design of a Thermoelectric Fabric for Wearable Energy Harvesters. J. Mater. Chem. A 2017, 5 (24), 12068–12072. https://doi.org/10.1039/C7TA00304H.

(35) Zuo, G.; Andersson, O.; Abdalla, H.; Kemerink, M. High Thermoelectric Power Factor from Multilayer Solution-Processed Organic Films. Appl. Phys. Lett. 2018, 112 (8), 083303. https://doi.org/10.1063/1.5016908.

(36) Thielen, M.; Sigrist, L.; Magno, M.; Hierold, C.; Benini, L. Human Body Heat for Powering Wearable Devices: From Thermal Energy to Application. Energy Convers. Manag. 2016, 131. https://doi.org/10.1016/j.enconman.2016.11.005.

(37) Kim, G.-H.; Kim, J.; Pipe, K. P. Humidity-Dependent Thermoelectric Properties of Poly(3,4-Ethylenedioxythiophene):Poly(Styrene Sulfonate). Appl. Phys. Lett. 2016, 108 (9), 093301. https://doi.org/10.1063/1.4942598.

(38) Glaudell, A. M.; Cochran, J. E.; Patel, S. N.; Chabinyc, M. L. Impact of the Doping Method on Conductivity and Thermopower in Semiconducting Polythiophenes. Adv. Energy Mater. 2015, 5 (4), n/a-n/a. https://doi.org/10.1002/aenm.201401072.

(39) Patel, S. N.; Glaudell, A. M.; Kiefer, D.; Chabinyc, M. L. Increasing the Thermoelectric Power Factor of a Semiconducting Polymer by Doping from the Vapor Phase. ACS Macro Lett. 2016, 5 (3), 268–272. https://doi.org/10.1021/acsmacrolett.5b00887.
(40) Wang, H.; Ail, U.; Gabrielsson, R.; Berggren, M.; Crispin, X. Ionic Seebeck Effect in Conducting Polymers. Adv. Energy Mater. 2015, 5 (11), 1500044. https://doi.org/10.1002/aenm.201500044.
(41) Zhao, D.; Wang, H.; U. Khan, Z.; C. Chen, J.; Gabrielsson, R.; P. Jonsson, M.; Berggren, M.; Crispin, X. Ionic Thermoelectric Supercapacitors. Energy Environ. Sci. 2016, 9 (4), 1450–1457. https://doi.org/10.1039/C6EE00121A.
(42) Yu, C.; Choi, K.; Yin, L.; Grunlan, J. C. Light-Weight Flexible Carbon Nanotube Based Organic Composites with Large Thermoelectric Power Factors. ACS Nano 2011, 5 (10), 7885–7892. https://doi.org/10.1021/nn202868a.
(43) Ryan, J. D.; Mengistie, D. A.; Gabrielsson, R.; Lund, A.; Müller, C. Machine-Washable PEDOT:PSS Dyed Silk Yarns for Electronic Textiles. ACS Appl. Mater. Interfaces 2017, 9 (10), 9045–9050. https://doi.org/10.1021/acsami.7b00530.
(44) Komatsu, N.; Ichinose, Y.; Dewey, O. S.; Taylor, L. W.; Trafford, M. A.; Yomogida, Y.; Wehmeyer, G.; Pasquali, M.; Yanagi, K.; Kono, J. Macroscopic Weavable Fibers of Carbon Nanotubes with Giant Thermoelectric Power Factor. Nat. Commun. 2021, 12 (1), 4931. https://doi.org/10.1038/s41467-021-25208-z.
(45) Hewitt, C. A.; Kaiser, A. B.; Roth, S.; Craps, M.; Czerw, R.; Carroll, D. L. Multilayered Carbon Nanotube/Polymer Composite Based Thermoelectric Fabrics. Nano Lett. 2012, 12 (3), 1307–1310. https://doi.org/10.1021/nl203806q.
(46) Dresselhaus, M. S.; Chen, G.; Tang, M. Y.; Yang, R. G.; Lee, H.; Wang, D. Z.; Ren, Z. F.; Fleurial, J.-P.; Gogna, P. New Directions for Low-Dimensional Thermoelectric Materials. Adv. Mater. 2007, 19 (8), 1043–1053. https://doi.org/10.1002/adma.200600527.
(47) Bubnova, O.; Khan, Z. U.; Malti, A.; Braun, S.; Fahlman, M.; Berggren, M.; Crispin, X. Optimization of the Thermoelectric Figure of Merit in the Conducting Polymer Poly(3,4-Ethylenedioxythiophene). Nat. Mater. 2011, 10 (6), 429–433. https://doi.org/10.1038/nmat3012.
(48) Russ, B.; Glaudell, A.; Urban, J. J.; Chabinyc, M. L.; Segalman, R. A. Organic Thermoelectric Materials for Energy Harvesting and Temperature Control. Nat. Rev. Mater. 2016, 1 (10), 16050. https://doi.org/10.1038/natrevmats.2016.50.
(49) Zhang, Q.; Sun, Y.; Xu, W.; Zhu, D. Organic Thermoelectric Materials: Emerging Green Energy Materials Converting Heat to Electricity Directly and Efficiently. Adv. Mater. 2014, 26 (40), 6829–6851. https://doi.org/10.1002/adma.201305371.
(50) Li, Y.; Du, Y.; Dou, Y.; Cai, K.; Xu, J. PEDOT-Based Thermoelectric Nanocomposites – A Mini-Review. Synth. Met. 2017, 226, 119–128. https://doi.org/10.1016/j.synthmet.2017.02.007.

(51) Park, T.; Na, J.; Kim, B.; Kim, Y.; Shin, H.; Kim, E. Photothermally Activated Pyroelectric Polymer Films for Harvesting of Solar Heat with a Hybrid Energy Cell Structure. ACS Nano 2015, 9 (12), 11830–11839. https://doi.org/10.1021/acsnano.5b04042.

(52) Petsagkourakis, I.; Kim, N.; Tybrandt, K.; Zozoulenko, I.; Crispin, X. Poly(3,4-Ethylenedioxythiophene): Chemical Synthesis, Transport Properties, and Thermoelectric Devices. Adv. Electron. Mater. 0 (0), 1800918. https://doi.org/10.1002/aelm.201800918.

(53) Mukaida, M.; Wei, Q.; Ishida, T. Polymer Thermoelectric Devices Prepared by Thermal Lamination. Synth. Met. 2017, 225, 64–69. https://doi.org/10.1016/j.synthmet.2016.11.016.

(54) Wei, Q.; Mukaida, M.; Kirihara, K.; Naitoh, Y.; Ishida, T. Polymer Thermoelectric Modules Screen-Printed on Paper. RSC Adv. 2014, 4 (54), 28802–28806. https://doi.org/10.1039/C4RA04946B.

(55) Zaia, E. W.; Gordon, M. P.; Yuan, P.; Urban, J. J. Progress and Perspective: Soft Thermoelectric Materials for Wearable and Internet-of-Things Applications. Adv. Electron. Mater. 2019, 5 (11), 1800823. https://doi.org/10.1002/aelm.201800823.

(56) Stepien, L.; Roch, A.; Tkachov, R.; Gedrange, T. Progress in Polymer Thermoelectrics. 2016. https://doi.org/10.5772/66196.

(57) Gueye, M. N.; Carella, A.; Faure-Vincent, J.; Demadrille, R.; Simonato, J.-P. Progress in Understanding Structure and Transport Properties of PEDOT-Based Materials: A Critical Review. Prog. Mater. Sci. 2020, 108, 100616. https://doi.org/10.1016/j.pmatsci.2019.100616.

(58) Menon, A. K.; Meek, O.; Eng, A. J.; Yee, S. K. Radial Thermoelectric Generator Fabricated from N- and p-Type Conducting Polymers. J. Appl. Polym. Sci. 2017, 134 (3), n/a-n/a. https://doi.org/10.1002/app.44060.

(59) Yao, H.; Fan, Z.; Cheng, H.; Guan, X.; Wang, C.; Sun, K.; Ouyang, J. Recent Development of Thermoelectric Polymers and Composites. Macromol. Rapid Commun. 2018, 39 (6), 1700727. https://doi.org/10.1002/marc.201700727.

(60) Wei, Q.; Mukaida, M.; Kirihara, K.; Naitoh, Y.; Ishida, T. Recent Progress on PEDOT-Based Thermoelectric Materials. Materials 2015, 8 (2), 732–750. https://doi.org/10.3390/ma8020732.

(61) Thomas, E. M.; Popere, B. C.; Fang, H.; Chabinyc, M. L.; Segalman, R. A. Role of Disorder Induced by Doping on the Thermoelectric Properties of Semiconducting Polymers. Chem. Mater. 2018, 30 (9), 2965–2972. https://doi.org/10.1021/acs.chemmater.8b00394.

(62) Guan, X.; Cheng, H.; Ouyang, J. Significant Enhancement in the Seebeck Coefficient and Power Factor of Thermoelectric Polymers by the Soret Effect of Polyelectrolytes. J. Mater. Chem. A 2018, 6 (40), 19347–19352. https://doi.org/10.1039/C8TA08387H.

(63) Wang, J.; Cai, K.; Song, H.; Shen, S. Simultaneously Enhanced Electrical Conductivity and Seebeck Coefficient in Poly (3,4-Ethylenedioxythiophene) Films Treated with Hydroiodic Acid. Synth. Met. 2016, 220 (Supplement C), 585–590. https://doi.org/10.1016/j.synthmet.2016.07.023.

(64) Rull-Bravo, M.; Moure, A.; Fernández, J. F.; Martín-González, M. Skutterudites as Thermoelectric Materials: Revisited. RSC Adv. 2015, 5 (52), 41653–41667. https://doi.org/10.1039/C5RA03942H.

(65) Gordon, M. P.; Zaia, E. W.; Zhou, P.; Russ, B.; Coates, N. E.; Sahu, A.; Urban, J. J. Soft PEDOT:PSS Aerogel Architectures for Thermoelectric Applications. J. Appl. Polym. Sci. 2017, 134 (3). https://doi.org/10.1002/app.44070.

(66) Mazaheripour, A.; Majumdar, S.; Hanemann-Rawlings, D.; Thomas, E. M.; McGuiness, C.; d'Alencon, L.; Chabinyc, M. L.; Segalman, R. A. Tailoring the Seebeck Coefficient of PEDOT:PSS by Controlling Ion Stoichiometry in Ionic Liquid Additives. Chem. Mater. 2018, 30 (14), 4816–4822. https://doi.org/10.1021/acs.chemmater.8b02114.

(67) Faleev, S. V. Theory of Enhancement of Thermoelectric Properties of Materials with Nanoinclusions. Phys. Rev. B 2008, 77 (21). https://doi.org/10.1103/PhysRevB.77.214304.

(68) Liu, J.; Wang, X.; Li, D.; Coates, N. E.; Segalman, R. A.; Cahill, D. G. Thermal Conductivity and Elastic Constants of PEDOT:PSS with High Electrical Conductivity. Macromolecules 2015, 48 (3), 585–591. https://doi.org/10.1021/ma502099t.

(69) Moriarty Gregory P.; De Sukanta; King Paul J.; Khan Umar; Via Michael; King Julia A.; Coleman Jonathan N.; Grunlan Jaime C. Thermoelectric Behavior of Organic Thin Film Nanocomposites. J. Polym. Sci. Part B Polym. Phys. 2012, 51 (2), 119–123. https://doi.org/10.1002/polb.23186.

(70) Kim, S. L.; Hsu, J.-H.; Yu, C. Thermoelectric Effects in Solid-State Polyelectrolytes. Org. Electron. 2018, 54, 231–236. https://doi.org/10.1016/j.orgel.2017.12.021.

(71) Nozariasbmarz, A.; Suarez, F.; Dycus, J. H.; Cabral, M. J.; LeBeau, J. M.; Öztürk, M. C.; Vashaee, D. Thermoelectric Generators for Wearable Body Heat Harvesting: Material and Device Concurrent Optimization. Nano Energy 2019, 104265. https://doi.org/10.1016/j.nanoen.2019.104265.

(72) Kim, G.; Pipe, K. P. Thermoelectric Model to Characterize Carrier Transport in Organic Semiconductors. Phys. Rev. B 2012, 86 (8), 085208. https://doi.org/10.1103/PhysRevB.86.085208.

(73) Kong, F.; Liu, C.; Xu, J.; Huang, Y.; Wang, J.; Sun, Z. Thermoelectric Performance Enhancement of Poly(3,4-Ethylenedioxythiophene):Poly(Styrenesulfonate) Composite Films by Addition of Dimethyl Sulfoxide and Urea. J. Electron. Mater. 2012, 41 (9), 2431–2438. https://doi.org/10.1007/s11664-012-2162-y.

(74) Chabinyc, M. Thermoelectric Polymers: Behind Organics' Thermopower. Nat. Mater. 2014, 13 (2), 119–121. https://doi.org/10.1038/nmat3859.
(75) Kirihara, K.; Wei, Q.; Mukaida, M.; Ishida, T. Thermoelectric Power Generation Using Nonwoven Fabric Module Impregnated with Conducting Polymer PEDOT:PSS. Synth. Met. https://doi.org/10.1016/j.synthmet.2017.01.001.
(76) Du, Y.; Xu, J.; Wang, Y.; Lin, T. Thermoelectric Properties of Graphite-PEDOT:PSS Coated Flexible Polyester Fabrics. J. Mater. Sci. Mater. Electron. 2016, 1–6. https://doi.org/10.1007/s10854-016-6250-2.
(77) Zhang, L.; Goto, T.; Imae, I.; Sakurai, Y.; Harima, Y. Thermoelectric Properties of PEDOT Films Prepared by Electrochemical Polymerization. J. Polym. Sci. Part B Polym. Phys. 2017, n/a-n/a. https://doi.org/10.1002/polb.24299.
(78) Ail, U.; Jafari, M. J.; Wang, H.; Ederth, T.; Berggren, M.; Crispin, X. Thermoelectric Properties of Polymeric Mixed Conductors. Adv. Funct. Mater. 2016, 26 (34), 6288–6296. https://doi.org/10.1002/adfm.201601106.
(79) Wang, J.; Cai, K.; Yin, J.; Shen, S. Thermoelectric Properties of the PEDOT/SWCNT Composite Films Prepared by a Vapor Phase Polymerization. Synth. Met. 2017, 224, 27–32. https://doi.org/10.1016/j.synthmet.2016.11.031.
(80) Reddy, P.; Jang, S.-Y.; Segalman, R. A.; Majumdar, A. Thermoelectricity in Molecular Junctions. Science 2007, 315 (5818), 1568–1571. https://doi.org/10.1126/science.1137149.
(81) Pu Xiong; Hu Weiguo; Wang Zhong Lin. Toward Wearable Self-Charging Power Systems: The Integration of Energy-Harvesting and Storage Devices. Small 2017, 14 (1), 1702817. https://doi.org/10.1002/smll.201702817.
(82) Bubnova, O.; Berggren, M.; Crispin, X. Tuning the Thermoelectric Properties of Conducting Polymers in an Electrochemical Transistor. J. Am. Chem. Soc. 2012, 134 (40), 16456–16459. https://doi.org/10.1021/ja305188r.
(83) Hu, X.; Chen, G.; Wang, X.; Wang, H. Tuning Thermoelectric Performance by Nanostructure Evolution of a Conducting Polymer. J. Mater. Chem. A 2015, 3 (42), 20896–20902. https://doi.org/10.1039/C5TA07381B.
(84) Wu, Q.; Hu, J. Waterborne Polyurethane Based Thermoelectric Composites and Their Application Potential in Wearable Thermoelectric Textiles. Compos. Part B Eng. 2016, 107, 59–66. https://doi.org/10.1016/j.compositesb.2016.09.068.
(85) Kim, M. K.; Kim, M. S.; Jo, S. E.; Kim, H. L.; Lee, S. M.; Kim, Y. J. Wearable Thermoelectric Generator for Human Clothing Applications. In 2013 Transducers Eurosensors XXVII: The 17th International Conference on Solid-State Sensors, Actuators and Microsystems (TRANSDUCERS EUROSENSORS XXVII); 2013; pp 1376–1379. https://doi.org/10.1109/Transducers.2013.6627034.
(86) Lee, J. A.; Aliev, A. E.; Bykova, J. S.; Andrade, M. J. de; Kim, D.; Sim, H. J.; Lepró, X.; Zakhidov, A. A.; Lee, J.-B.; Spinks, G. M.; Roth, S.; Kim, S. J.; Baughman, R. H. Woven-Yarn Thermoelectric Textiles. Adv. Mater. 2016, 28 (25), 5038–5044. https://doi.org/10.1002/adma.201600709.

(87) Bubnova, O.; Crispin, X. Towards Polymer-Based Organic Thermoelectric Generators. Energy Environ. Sci. 2012, 5 (11), 9345–9362. https://doi.org/10.1039/C2EE22777K.
(88) Peng, S.; Wang, D.; Lu, J.; He, M.; Xu, C.; Li, Y.; Zhu, S. A Review on Organic Polymer-Based Thermoelectric Materials. J. Polym. Environ. 2017, 25 (4), 1208–1218. https://doi.org/10.1007/s10924-016-0895-z.
(89) Snyder, G. J.; Toberer, E. S. Complex Thermoelectric Materials. Nat. Mater. 2008, 7 (2), 105–114. https://doi.org/10.1038/nmat2090.
(90) Leonov, V. Thermoelectric Energy Harvesting of Human Body Heat for Wearable Sensors. IEEE Sens. J. 2013, 13 (6), 2284–2291. https://doi.org/10.1109/JSEN.2013.2252526.
(91) Siddique, A. R. M.; Mahmud, S.; Heyst, B. V. A Review of the State of the Science on Wearable Thermoelectric Power Generators (TEGs) and Their Existing Challenges. Renew. Sustain. Energy Rev. 2017, 73, 730–744. https://doi.org/10.1016/j.rser.2017.01.177.
(92) Wang, Z.; Leonov, V.; Fiorini, P.; Van Hoof, C. Realization of a Wearable Miniaturized Thermoelectric Generator for Human Body Applications. Sens. Actuators Phys. 2009, 156 (1), 95–102. https://doi.org/10.1016/j.sna.2009.02.028.
(93) K. Yee, S.; E. Coates, N.; Majumdar, A.; J. Urban, J.; A. Segalman, R. Thermoelectric Power Factor Optimization in PEDOT:PSS Tellurium Nanowire Hybrid Composites. Phys. Chem. Chem. Phys. 2013, 15 (11), 4024–4032. https://doi.org/10.1039/C3CP44558E.
(94) Lu, Z.; Zhang, H.; Mao, C.; Li, C. M. Silk Fabric-Based Wearable Thermoelectric Generator for Energy Harvesting from the Human Body. Appl. Energy 2016, 164, 57–63. https://doi.org/10.1016/j.apenergy.2015.11.038.
(95) Francioso, L.; Pascali, C. D.; Farella, I.; Martucci, C.; Cretì, P.; Siciliano, P.; Perrone, A. Flexible Thermoelectric Generator for Wearable Biometric Sensors. In 2010 IEEE Sensors; 2010; pp 747–750. https://doi.org/10.1109/ICSENS.2010.5690757.
(96) Cao, Z.; Koukharenko, E.; Tudor, M. J.; Torah, R. N.; Beeby, S. P. Screen Printed Flexible Bi 2 Te 3 -Sb 2 Te 3 Based Thermoelectric Generator. J. Phys. Conf. Ser. 2013, 476 (1), 012031. https://doi.org/10.1088/1742-6596/476/1/012031.
(97) Rare Earth Elements—Critical Resources for High Technology | USGS Fact Sheet 087-02 https://pubs.usgs.gov/fs/2002/fs087-02/ (accessed 2018 -06 -26).
(98) Leonov, V. Thermoelectric Energy Harvester on the Heated Human Machine. J. Micromechanics Microengineering 2011, 21 (12), 125013. https://doi.org/10.1088/0960-1317/21/12/125013.
(99) Jung, S.; Lauterbach, C.; Strasser, M.; Weber, W. Enabling Technologies for Disappearing Electronics in Smart Textiles. In 2003 IEEE International Solid-State Circuits Conference, 2003. Digest of Technical Papers. ISSCC.; 2003; pp 386–387 vol.1. https://doi.org/10.1109/ISSCC.2003.1234347.

(100) Chen, Y.; Zhao, Y.; Liang, Z. Solution Processed Organic Thermoelectrics: Towards Flexible Thermoelectric Modules. Energy Environ. Sci. 2015, 8 (2), 401–422. https://doi.org/10.1039/C4EE03297G.
(101) Yue, R.; Xu, J. Poly(3,4-Ethylenedioxythiophene) as Promising Organic Thermoelectric Materials: A Mini-Review. Synth. Met. 2012, 162 (11), 912–917. https://doi.org/10.1016/j.synthmet.2012.04.005.
(102) Cho, C.; Wallace, K. L.; Tzeng, P.; Hsu, J.-H.; Yu, C.; Grunlan, J. C. Outstanding Low Temperature Thermoelectric Power Factor from Completely Organic Thin Films Enabled by Multidimensional Conjugated Nanomaterials. Adv. Energy Mater. 2016, 6 (7), n/a-n/a. https://doi.org/10.1002/aenm.201502168.
(103) Du, Y.; Cai, K.; Chen, S.; Wang, H.; Shen, S. Z.; Donelson, R.; Lin, T. Thermoelectric Fabrics: Toward Power Generating Clothing. Sci. Rep. 2015, 5, 6411. https://doi.org/10.1038/srep06411.
(104) Allison, L. K.; Andrew, T. L. A Wearable All-Fabric Thermoelectric Generator. Adv. Mater. Technol. 0 (0), 1800615. https://doi.org/10.1002/admt.201800615.

Chapter 6

FUTURE WORK

The work explored within this dissertation focused on utilizing the oxidative chemical vapor deposition (oCVD) technique to produce Poly(3,4-ethylenedioxythiophene) (PEDOT-Cl) coated textiles. Through this research we were able to create a method of exploring the electronic and ionic properties of these textiles. The work of designing wearables to optimize the performance of the electronics can act as a foundation for other future projects.

With respect to the PEDOT-Cl textiles described in Chapter 2, initiated chemical vapor deposition (iCVD) could provide a method of encapsulating the coated textiles without changing the look or feel of the textiles, and maintaining the electronic properties of the PEDOT-Cl. iCVD, which is a vapor coating technique similarly related to oCVD, can be used to deposit a coating of protective acrylate-based polymers. These coating will protect the PEDOT-Cl from environmental conditions that could lead to degradation such as extended washing, rubbing, and exposure to moisture. By optimizing a technique for depositing acrylate-based polymers on textiles already coated with PEDOT-Cl could lead to taking the next step in commercializing these textiles for a variety of applications.

Concerning the humidity sensors described in Chapter 3, we were able to design a mask that is able to monitor respiration based on the hygroresistive properties of the PEDOT-Cl. Currently this measurement setup requires the participant to be manually

attached to the electrical board in order to monitor the user's respiration. By incorporating a Bluetooth-enabled circuit component, the user would no longer need to be attached to the electrical board. Instead, the participants would be able to record respiration measurements remotely.

With respect to Chapter 4, we explored the thermoresistive properties of various textiles coated with PEDOT-Cl. As is, these thermistors are not ideal for use in wearables due to the fact that the hygroresistive and thermoresistive properties are strongly coupled. This can be improved by utilizing iCVD to coat these samples with a hydrophobic coating. This coating would need to be optimized to ensure that it is not too thermally insulating and thus preventing the PEDOT-Cl coating is able to accurately measure the temperature of the heat source.

Finally, regarding the thermoelectric generators depicted in Chapter 5, we described the process of creating thermoelectric generators (TEGs) using PEDOT-Cl coated fabrics and the design considerations when integrating these devices into a wearable garment. These devices are designed to work in conjunction with a charge storage mechanism, to create a self-charging system. In order to achieve this, a charge storage mechanism, such as fabric super-capacitors, need to be introduced into this circuit. The TEGs should be optimized to work with these specific charge storage devices so that the TEG garments can trickle charge the supercapacitors. Therefore, more research could certainly lead to improved versions of the devices reported in this dissertation.

WORKS CITED

Chapter 1

(1) Patel, S.; Park, H.; Bonato, P.; Chan, L.; Rodgers, M. A Review of Wearable Sensors and Systems with Application in Rehabilitation. J. NeuroEngineering Rehabil. 2012, 9, 21. https://doi.org/10.1186/1743-0003-9-21.

(2) Herbert, R.; Jeong, J.-W.; Yeo, W.-H. Soft Material-Enabled Electronics for Medicine, Healthcare, and Human-Machine Interfaces. Materials 2020, 13 (3), 517. https://doi.org/10.3390/ma13030517.

(3) Son, D.; Lee, J.; Qiao, S.; Ghaffari, R.; Kim, J.; Lee, J. E.; Song, C.; Kim, S. J.; Lee, D. J.; Jun, S. W.; Yang, S.; Park, M.; Shin, J.; Do, K.; Lee, M.; Kang, K.; Hwang, C. S.; Lu, N.; Hyeon, T.; Kim, D.-H. Multifunctional Wearable Devices for Diagnosis and Therapy of Movement Disorders. Nat. Nanotechnol. 2014, 9 (5), 397–404. https://doi.org/10.1038/nnano.2014.38.

(4) Jung, S.; Hong, S.; Kim, J.; Lee, S.; Hyeon, T.; Lee, M.; Kim, D.-H. Wearable Fall Detector Using Integrated Sensors and Energy Devices. Sci. Rep. 2015, 5 (1), 17081. https://doi.org/10.1038/srep17081.

(5) Merritt, C. R.; Troy Nagle, H.; Grant, E. Fabric-Based Active Electrode Design and Fabrication for Health Monitoring Clothing. IEEE Trans. Inf. Technol. Biomed. 2009, 13 (2), 274–280. https://doi.org/10.1109/TITB.2009.2012408.

(6) Pang, Y.; Jian, J.; Tu, T.; Yang, Z.; Ling, J.; Li, Y.; Wang, X.; Qiao, Y.; Tian, H.; Yang, Y.; Ren, T.-L. Wearable Humidity Sensor Based on Porous Graphene Network for Respiration Monitoring. Biosens. Bioelectron. 2018, 116, 123–129. https://doi.org/10.1016/j.bios.2018.05.038.

(7) Dinh, T.; Nguyen, T.; Phan, H.-P.; Nguyen, N.-T.; Dao, D. V.; Bell, J. Stretchable Respiration Sensors: Advanced Designs and Multifunctional Platforms for Wearable Physiological Monitoring. Biosens. Bioelectron. 2020, 166, 112460. https://doi.org/10.1016/j.bios.2020.112460.

(8) Wang, Y.; Zhang, L.; Zhang, Z.; Sun, P.; Chen, H. High-Sensitivity Wearable and Flexible Humidity Sensor Based on Graphene Oxide/Non-Woven Fabric for Respiration Monitoring. Langmuir 2020, 36 (32), 9443–9448. https://doi.org/10.1021/acs.langmuir.0c01315.

(9) Hughes-Riley, T.; Dias, T.; Cork, C. A Historical Review of the Development of Electronic Textiles. Fibers 2018, 6 (2), 34. https://doi.org/10.3390/fib6020034.

(10) Pu Xiong; Hu Weiguo; Wang Zhong Lin. Toward Wearable Self-Charging Power Systems: The Integration of Energy-Harvesting and Storage Devices. Small 2017, 14 (1), 1702817. https://doi.org/10.1002/smll.201702817.

(11) Fan Feng Ru; Tang Wei; Wang Zhong Lin. Flexible Nanogenerators for Energy Harvesting and Self-Powered Electronics. Adv. Mater. 2016, 28 (22), 4283–4305. https://doi.org/10.1002/adma.201504299.
(12) Kim, M. K.; Kim, M. S.; Jo, S. E.; Kim, H. L.; Lee, S. M.; Kim, Y. J. Wearable Thermoelectric Generator for Human Clothing Applications. In 2013 Transducers Eurosensors XXVII: The 17th International Conference on Solid-State Sensors, Actuators and Microsystems (TRANSDUCERS EUROSENSORS XXVII); 2013; pp 1376–1379. https://doi.org/10.1109/Transducers.2013.6627034.
(13) Hussain, A. M.; Ghaffar, F. A.; Park, S. I.; Rogers, J. A.; Shamim, A.; Hussain, M. M. Metal/Polymer Based Stretchable Antenna for Constant Frequency Far-Field Communication in Wearable Electronics. Adv. Funct. Mater. 2015, 25 (42), 6565–6575. https://doi.org/10.1002/adfm.201503277.
(14) Vilkhu, R.; Thio, W. J.-C.; Das Ghatak, P.; Sen, C. K.; Co, A. C.; Kiourti, A. Power Generation for Wearable Electronics: Designing Electrochemical Storage on Fabrics. IEEE Access 2018, 6, 28945–28950. https://doi.org/10.1109/ACCESS.2018.2839078.
(15) Vilkhu, R.; DeLong, B.; Kiourti, A.; Das Ghatak, P.; Mathew-Steiner, S.; Sen, C. K. Power Harvesting for Wearable Electronics Using Fabric Electrochemistry. In 2017 IEEE International Symposium on Antennas and Propagation USNC/URSI National Radio Science Meeting; 2017; pp 213–214. https://doi.org/10.1109/APUSNCURSINRSM.2017.8072149.
(16) Li, J.; Xin, M.; Ma, Z.; Shi, Y.; Pan, L. Nanomaterials and Their Applications on Bio-Inspired Wearable Electronics. Nanotechnology 2021, 32 (47), 472002. https://doi.org/10.1088/1361-6528/abe6c7.
(17) Wu, H.; Huang, Y.; Xu, F.; Duan, Y.; Yin, Z. Energy Harvesters for Wearable and Stretchable Electronics: From Flexibility to Stretchability. Adv. Mater. 2016, 28 (45), 9881–9919. https://doi.org/10.1002/adma.201602251.
(18) Siddique, A. R. M.; Mahmud, S.; Heyst, B. V. A Review of the State of the Science on Wearable Thermoelectric Power Generators (TEGs) and Their Existing Challenges. Renew. Sustain. Energy Rev. 2017, 73, 730–744. https://doi.org/10.1016/j.rser.2017.01.177.
(19) Lugoda, P.; Hughes-Riley, T.; Morris, R.; Dias, T. A Wearable Textile Thermograph. Sensors 2018, 18 (7). https://doi.org/10.3390/s18072369.
(20) Fan, X.; Liu, B.; Ding, J.; Deng, Y.; Han, X.; Hu, W.; Zhong, C. Flexible and Wearable Power Sources for Next-Generation Wearable Electronics. Batter. Supercaps 2020, 3 (12), 1262–1274. https://doi.org/10.1002/batt.202000115.
(21) Zhong, J.; Zhang, Y.; Zhong, Q.; Hu, Q.; Hu, B.; Wang, Z. L.; Zhou, J. Fiber-Based Generator for Wearable Electronics and Mobile Medication. ACS Nano 2014, 8 (6), 6273–6280. https://doi.org/10.1021/nn501732z.
(22) Zeng, W.; Shu, L.; Li, Q.; Chen, S.; Wang, F.; Tao, X.-M. Fiber-Based Wearable Electronics: A Review of Materials, Fabrication, Devices, and Applications. Adv. Mater. 2014, 26 (31), 5310–5336. https://doi.org/10.1002/adma.201400633.
(23) Qiu, Q.; Zhu, M.; Li, Z.; Qiu, K.; Liu, X.; Yu, J.; Ding, B. Highly Flexible, Breathable, Tailorable and Washable Power Generation Fabrics for Wearable

Electronics. Nano Energy 2019, 58, 750–758. https://doi.org/10.1016/j.nanoen.2019.02.010.
(24) Ling, Y.; An, T.; Yap, L. W.; Zhu, B.; Gong, S.; Cheng, W. Disruptive, Soft, Wearable Sensors. Adv. Mater. 2020, 32 (18), 1904664. https://doi.org/10.1002/adma.201904664.
(25) Qu, H.; Semenikhin, O.; Skorobogatiy, M. Flexible Fiber Batteries for Applications in Smart Textiles. Smart Mater. Struct. 2015, 24 (2), 025012. https://doi.org/10.1088/0964-1726/24/2/025012.
(26) Wu, Q.; Hu, J. Waterborne Polyurethane Based Thermoelectric Composites and Their Application Potential in Wearable Thermoelectric Textiles. Compos. Part B Eng. 2016, 107, 59–66. https://doi.org/10.1016/j.compositesb.2016.09.068.
(27) Hu, E.; Kaynak, A.; Li, Y. Development of a Cooling Fabric from Conducting Polymer Coated Fibres: Proof of Concept. Synth. Met. 2005, 150 (2), 139–143. https://doi.org/10.1016/j.synthmet.2005.01.018.
(28) Leonov, V. Thermoelectric Energy Harvesting of Human Body Heat for Wearable Sensors. IEEE Sens. J. 2013, 13 (6), 2284–2291. https://doi.org/10.1109/JSEN.2013.2252526.
(29) Jafar-Zanjani, S.; Salary, M. M.; Mosallaei, H. Metafabrics for Thermoregulation and Energy-Harvesting Applications. ACS Photonics 2017, 4 (4), 915–927. https://doi.org/10.1021/acsphotonics.6b01005.
(30) Zhang, L.; Baima, M.; Andrew, T. L. Transforming Commercial Textiles and Threads into Sewable and Weavable Electric Heaters. ACS Appl. Mater. Interfaces 2017, 9 (37), 32299–32307. https://doi.org/10.1021/acsami.7b10514.
(31) Allison, L.; Hoxie, S.; Andrew, T. L. Towards Seamlessly-Integrated Textile Electronics: Methods to Coat Fabrics and Fibers with Conducting Polymers for Electronic Applications. Chem. Commun. 2017, 53 (53), 7182–7193. https://doi.org/10.1039/C7CC02592K.
(32) Zhang Lushuai; Fairbanks Marianne; Andrew Trisha L. Rugged Textile Electrodes for Wearable Devices Obtained by Vapor Coating Off-the-Shelf, Plain-Woven Fabrics. Adv. Funct. Mater. 2017, 27 (24), 1700415. https://doi.org/10.1002/adfm.201700415.
(33) Ryan, J. D.; Mengistie, D. A.; Gabrielsson, R.; Lund, A.; Müller, C. Machine-Washable PEDOT:PSS Dyed Silk Yarns for Electronic Textiles. ACS Appl. Mater. Interfaces 2017, 9 (10), 9045–9050. https://doi.org/10.1021/acsami.7b00530.
(34) Wawro, D.; Stęplewski, W. Producing of Continuous Cellulose Fibres Modified with Plant Proteins. Fibres Text. East. Eur. 2010, Nr 6 (83).
(35) Knittel, D.; Schollmeyer, E. Electrically High-Conductive Textiles. Synth. Met. 2009, 159 (14), 1433–1437. https://doi.org/10.1016/j.synthmet.2009.03.021.
(36) Ding, Y.; Invernale, M. A.; Sotzing, G. A. Conductivity Trends of PEDOT-PSS Impregnated Fabric and the Effect of Conductivity on Electrochromic Textile. ACS Appl. Mater. Interfaces 2010, 2 (6), 1588–1593. https://doi.org/10.1021/am100036n.
(37) Lee, J. A.; Aliev, A. E.; Bykova, J. S.; Andrade, M. J. de; Kim, D.; Sim, H. J.; Lepró, X.; Zakhidov, A. A.; Lee, J.-B.; Spinks, G. M.; Roth, S.; Kim, S. J.;

Baughman, R. H. Woven-Yarn Thermoelectric Textiles. Adv. Mater. 2016, 28 (25), 5038–5044. https://doi.org/10.1002/adma.201600709.
(38) Jung, S.; Lauterbach, C.; Strasser, M.; Weber, W. Enabling Technologies for Disappearing Electronics in Smart Textiles. In 2003 IEEE International Solid-State Circuits Conference, 2003. Digest of Technical Papers. ISSCC.; 2003; pp 386–387 vol.1. https://doi.org/10.1109/ISSCC.2003.1234347.
(39) Glampedaki, P.; Calvimontes, A.; Dutschk, V.; Warmoeskerken, M. M. C. G. Polyester Textile Functionalization through Incorporation of PH/Thermo-Responsive Microgels. Part II: Polyester Functionalization and Characterization. J. Mater. Sci. 2012, 47 (5), 2078–2087. https://doi.org/10.1007/s10853-011-6006-6.
(40) Husain, M. D.; Kennon, R.; Dias, T. Design and Fabrication of Temperature Sensing Fabric. J. Ind. Text. 2014, 44 (3), 398–417. https://doi.org/10.1177/1528083713495249.
(41) Lee, J.-W.; Han, D.-C.; Shin, H.-J.; Yeom, S.-H.; Ju, B.-K.; Lee, W. PEDOT:PSS-Based Temperature-Detection Thread for Wearable Devices. Sensors 2018, 18 (9). https://doi.org/10.3390/s18092996.
(42) Castano, L. M.; Flatau, A. B. Smart Fabric Sensors and E-Textile Technologies: A Review. Smart Mater. Struct. 2014, 23 (5), 053001. https://doi.org/10.1088/0964-1726/23/5/053001.
(43) Bhat, N. V.; Seshadri, D. T.; Nate, M. M.; Gore, A. V. Development of Conductive Cotton Fabrics for Heating Devices. J. Appl. Polym. Sci. 2006, 102 (5), 4690–4695. https://doi.org/10.1002/app.24708.
(44) Bielska, S.; Sibinski, M.; Lukasik, A. Polymer Temperature Sensor for Textronic Applications. Mater. Sci. Eng. B 2009, 165 (1), 50–52. https://doi.org/10.1016/j.mseb.2009.07.014.
(45) Enzo Pasquale Scilingo; Lorussi, F.; Mazzoldi, A.; De Rossi, D. Strain-Sensing Fabrics for Wearable Kinaesthetic-like Systems. IEEE Sens. J. 2003, 3 (4), 460–467. https://doi.org/10.1109/JSEN.2003.815771.
(46) He, Y.; Gui, Q.; Liao, S.; Jia, H.; Wang, Y. Coiled Fiber-Shaped Stretchable Thermal Sensors for Wearable Electronics. Adv. Mater. Technol. 2016, 1 (8), 1600170. https://doi.org/10.1002/admt.201600170.
(47) Kim, J.; Cho, G. Thermal Storage/Release, Durability, and Temperature Sensing Properties of Thermostatic Fabrics Treated with Octadecane-Containing Microcapsules. Text. Res. J. 2002, 72 (12), 1093–1098. https://doi.org/10.1177/004051750207201209.
(48) Lim, Z. H.; Chia, Z. X.; Kevin, M.; Wong, A. S. W.; Ho, G. W. A Facile Approach towards ZnO Nanorods Conductive Textile for Room Temperature Multifunctional Sensors. Sens. Actuators B Chem. 2010, 151 (1), 121–126. https://doi.org/10.1016/j.snb.2010.09.037.
(49) Sibinski, M.; Jakubowska, M.; Sloma, M. Flexible Temperature Sensors on Fibers. Sensors 2010, 10 (9), 7934–7946. https://doi.org/10.3390/s100907934.
(50) Ramachandran, T.; Vigneswaran, C. Design and Development of Copper Core Conductive Fabrics for Smart Textiles. J. Ind. Text. 2009, 39 (1), 81–93. https://doi.org/10.1177/1528083709103317.

(51) Hughes-Riley, T.; Lugoda, P.; Dias, T.; Trabi, C. L.; Morris, R. H. A Study of Thermistor Performance within a Textile Structure. Sensors 2017, 17 (8). https://doi.org/10.3390/s17081804.
(52) Agcayazi, T.; Chatterjee, K.; Bozkurt, A.; Ghosh, T. K. Flexible Interconnects for Electronic Textiles. Adv. Mater. Technol. 2018, 3 (10), 1700277. https://doi.org/10.1002/admt.201700277.
(53) Yang, J.-H.; Cho, H.-S.; Kwak, H.; Chae, J.-W.; Lee, H.-J.; Lee, J.-W.; Oh, S.; Lee, J.-H. Sensing Efficiency of Three-Dimensional Textile Sensors with an Open-and-Close Structure for Respiration Rate Detection. Text. Res. J. 2020, 90 (19–20), 2258–2274. https://doi.org/10.1177/0040517520915846.
(54) Catarino, A.; Carvalho, H.; Dias, M. J.; Pereira, T.; Postolache, O.; Girão, P. S. Continuous Health Monitoring Using E-Textile Integrated Biosensors. In 2012 International Conference and Exposition on Electrical and Power Engineering; 2012; pp 605–609. https://doi.org/10.1109/ICEPE.2012.6463867.
(55) Carvalho, H.; Catarino, A. P.; Rocha, A.; Postolache, O. Health Monitoring Using Textile Sensors and Electrodes: An Overview and Integration of Technologies. In 2014 IEEE International Symposium on Medical Measurements and Applications (MeMeA); 2014; pp 1–6. https://doi.org/10.1109/MeMeA.2014.6860033.
(56) Rai, P.; Kumar, P. S.; Oh, S.; Kwon, H.; Mathur, G. N.; Varadan, V. K.; Agarwal, M. P. Smart Healthcare Textile Sensor System for Unhindered-Pervasive Health Monitoring. In Nanosensors, Biosensors, and Info-Tech Sensors and Systems 2012; International Society for Optics and Photonics, 2012; Vol. 8344, p 83440E. https://doi.org/10.1117/12.921253.
(57) Rai, P.; Oh, S.; Shyamkumar, P.; Ramasamy, M.; Harbaugh, R. E.; Varadan, V. K. Nano- Bio- Textile Sensors with Mobile Wireless Platform for Wearable Health Monitoring of Neurological and Cardiovascular Disorders. J. Electrochem. Soc. 2013, 161 (2), B3116. https://doi.org/10.1149/2.012402jes.
(58) Kiaghadi, A.; Homayounfar, S. Z.; Gummeson, J.; Andrew, T.; Ganesan, D. Phyjama: Physiological Sensing via Fiber-Enhanced Pyjamas. Proc. ACM Interact. Mob. Wearable Ubiquitous Technol. 2019, 3 (3), 89:1-89:29. https://doi.org/10.1145/3351247.
(59) Lund, A.; Tian, Y.; Darabi, S.; Müller, C. A Polymer-Based Textile Thermoelectric Generator for Wearable Energy Harvesting. J. Power Sources 2020, 480, 228836. https://doi.org/10.1016/j.jpowsour.2020.228836.
(60) Elmoughni, H. M.; Menon, A. K.; Wolfe, R. M. W.; Yee, S. K. A Textile-Integrated Polymer Thermoelectric Generator for Body Heat Harvesting. Adv. Mater. Technol. 2019, 4 (7), 1800708. https://doi.org/10.1002/admt.201800708.
(61) Komatsu, N.; Ichinose, Y.; Dewey, O. S.; Taylor, L. W.; Trafford, M. A.; Yomogida, Y.; Wehmeyer, G.; Pasquali, M.; Yanagi, K.; Kono, J. Macroscopic Weavable Fibers of Carbon Nanotubes with Giant Thermoelectric Power Factor. Nat. Commun. 2021, 12 (1), 4931. https://doi.org/10.1038/s41467-021-25208-z.
(62) Carbon Nanotubes.

(63) Gordon, M. P.; Zaia, E. W.; Zhou, P.; Russ, B.; Coates, N. E.; Sahu, A.; Urban, J. J. Soft PEDOT:PSS Aerogel Architectures for Thermoelectric Applications. J. Appl. Polym. Sci. 2017, 134 (3). https://doi.org/10.1002/app.44070.
(64) Elschner, A.; Kirchmeyer, S.; Lovenich, W.; Merker, U.; Reuter, K. PEDOT: Principles and Applications of an Intrinsically Conductive Polymer; CRC Press, 2010.
(65) Åkerfeldt, M.; Strååt, M.; Walkenström, P. Influence of Coating Parameters on Textile and Electrical Properties of a Poly(3,4-Ethylene Dioxythiophene):Poly(Styrene Sulfonate)/Polyurethane-Coated Textile. Text. Res. J. 2013, 83 (20), 2164–2176. https://doi.org/10.1177/0040517513487786.
(66) Luo, J.; Billep, D.; Waechtler, T.; Otto, T.; Toader, M.; Gordan, O.; Sheremet, E.; Martin, J.; Hietschold, M.; Zahn, D. R. T.; Gessner, T. Enhancement of the Thermoelectric Properties of PEDOT:PSS Thin Films by Post-Treatment. J. Mater. Chem. A 2013, 1 (26), 7576–7583. https://doi.org/10.1039/C3TA11209H.
(67) Zhu, Z.; Liu, C.; Jiang, F.; Xu, J.; Liu, E. Effective Treatment Methods on PEDOT:PSS to Enhance Its Thermoelectric Performance. Synth. Met. 2017, 225, 31–40. https://doi.org/10.1016/j.synthmet.2016.11.011.
(68) Bubnova, O.; Crispin, X. Towards Polymer-Based Organic Thermoelectric Generators. Energy Environ. Sci. 2012, 5 (11), 9345–9362. https://doi.org/10.1039/C2EE22777K.
(69) Ail, U.; Jafari, M. J.; Wang, H.; Ederth, T.; Berggren, M.; Crispin, X. Thermoelectric Properties of Polymeric Mixed Conductors. Adv. Funct. Mater. 2016, 26 (34), 6288–6296. https://doi.org/10.1002/adfm.201601106.
(70) Daoud, W. A.; Xin, J. H.; Szeto, Y. S. Polyethylenedioxythiophene Coatings for Humidity, Temperature and Strain Sensing Polyamide Fibers. Sens. Actuators B Chem. 2005, 109 (2), 329–333. https://doi.org/10.1016/j.snb.2004.12.067.
(71) Wang, H.; Ail, U.; Gabrielsson, R.; Berggren, M.; Crispin, X. Ionic Seebeck Effect in Conducting Polymers. Adv. Energy Mater. 2015, 5 (11), 1500044. https://doi.org/10.1002/aenm.201500044.
(72) Verma, A. K.; Dash, R. R.; Bhunia, P. A Review on Chemical Coagulation/Flocculation Technologies for Removal of Colour from Textile Wastewaters. J. Environ. Manage. 2012, 93 (1), 154–168. https://doi.org/10.1016/j.jenvman.2011.09.012.
(73) Kant, R. Textile Dyeing Industry an Environmental Hazard. Nat. Sci. 2011, 04 (01), 22. https://doi.org/10.4236/ns.2012.41004.
(74) Chelawat, H.; Vaddiraju, S.; Gleason, K. Conformal, Conducting Poly(3,4-Ethylenedioxythiophene) Thin Films Deposited Using Bromine as the Oxidant in a Completely Dry Oxidative Chemical Vapor Deposition Process. Chem. Mater. 2010, 22 (9), 2864–2868. https://doi.org/10.1021/cm100092c.
(75) Goktas, H.; Wang, X.; Boscher, N. D.; Torosian, S.; Gleason, K. K. Functionalizable and Electrically Conductive Thin Films Formed by Oxidative Chemical Vapor Deposition (OCVD) from Mixtures of 3-Thiopheneethanol (3TE) and Ethylene Dioxythiophene (EDOT). J. Mater. Chem. C 2016, 4 (16), 3403–3414. https://doi.org/10.1039/C6TC00567E.

(76) Goktas, H.; Wang, X.; Ugur, A.; Gleason, K. K. Water-Assisted Vapor Deposition of PEDOT Thin Film. Macromol. Rapid Commun. 2015, 36 (13), 1283–1289. https://doi.org/10.1002/marc.201500069.
(77) Chen, N.; Kim, D. H.; Kovacik, P.; Sojoudi, H.; Wang, M.; Gleason, K. K. Polymer Thin Films and Surface Modification by Chemical Vapor Deposition: Recent Progress. Annu. Rev. Chem. Biomol. Eng. 2016, 7 (1), 373–393. https://doi.org/10.1146/annurev-chembioeng-080615-033524.
(78) Chen, N.; Wang, X.; Gleason, K. K. Conformal Single-Layer Encapsulation of PEDOT at Low Substrate Temperature. Appl. Surf. Sci. 2014, 323, 2–6. https://doi.org/10.1016/j.apsusc.2014.06.123.
(79) Tenhaeff Wyatt E.; Gleason Karen K. Initiated and Oxidative Chemical Vapor Deposition of Polymeric Thin Films: ICVD and OCVD. Adv. Funct. Mater. 2008, 18 (7), 979–992. https://doi.org/10.1002/adfm.200701479.
(80) Wang, X.; Zhang, X.; Sun, L.; Lee, D.; Lee, S.; Wang, M.; Zhao, J.; Shao-Horn, Y.; Dincă, M.; Palacios, T.; Gleason, K. K. High Electrical Conductivity and Carrier Mobility in OCVD PEDOT Thin Films by Engineered Crystallization and Acid Treatment. Sci. Adv. 2018, 4 (9), eaat5780. https://doi.org/10.1126/sciadv.aat5780.
(81) Gueye, M. N.; Carella, A.; Faure-Vincent, J.; Demadrille, R.; Simonato, J.-P. Progress in Understanding Structure and Transport Properties of PEDOT-Based Materials: A Critical Review. Prog. Mater. Sci. 2020, 108, 100616. https://doi.org/10.1016/j.pmatsci.2019.100616.
(82) Stepien, L.; Roch, A.; Tkachov, R.; Gedrange, T. Progress in Polymer Thermoelectrics. 2016. https://doi.org/10.5772/66196.
(83) Wang, J.; Cai, K.; Shen, S. A Facile Chemical Reduction Approach for Effectively Tuning Thermoelectric Properties of PEDOT Films. Org. Electron. 2015, 17 (Supplement C), 151–158. https://doi.org/10.1016/j.orgel.2014.12.007.
(84) Snyder, G. J.; Toberer, E. S. Complex Thermoelectric Materials. Nat. Mater. 2008, 7 (2), 105–114. https://doi.org/10.1038/nmat2090.
(85) Zhu, T.; Liu, Y.; Fu, C.; Heremans, J. P.; Snyder, J. G.; Zhao, X. Compromise and Synergy in High-Efficiency Thermoelectric Materials. Adv. Mater. 2017, 29 (14), n/a-n/a. https://doi.org/10.1002/adma.201605884.
(86) Bell, L. E. Cooling, Heating, Generating Power, and Recovering Waste Heat with Thermoelectric Systems. Science 2008, 321 (5895), 1457–1461. https://doi.org/10.1126/science.1158899.
(87) Petsagkourakis, I.; Pavlopoulou, E.; Cloutet, E.; Chen, Y. F.; Liu, X.; Fahlman, M.; Berggren, M.; Crispin, X.; Dilhaire, S.; Fleury, G.; Hadziioannou, G. Correlating the Seebeck Coefficient of Thermoelectric Polymer Thin Films to Their Charge Transport Mechanism. Org. Electron. 2018, 52 (Supplement C), 335–341. https://doi.org/10.1016/j.orgel.2017.11.018.
(88) Menon, A. K.; Yee, S. K. Design of a Polymer Thermoelectric Generator Using Radial Architecture. J. Appl. Phys. 2016, 119 (5), 055501. https://doi.org/10.1063/1.4941101.

(89) Rowe, D. M.; Min, G. Design Theory of Thermoelectric Modules for Electrical Power Generation. IEE Proc. - Sci. Meas. Technol. 1996, 143 (6), 351–356. https://doi.org/10.1049/ip-smt:19960714.
(90) Chang, W. B.; Fang, H.; Liu, J.; Evans, C. M.; Russ, B.; Popere, B. C.; Patel, S. N.; Chabinyc, M. L.; Segalman, R. A. Electrochemical Effects in Thermoelectric Polymers. ACS Macro Lett. 2016, 5 (4), 455–459. https://doi.org/10.1021/acsmacrolett.6b00054.
(91) Patel, S. N.; Glaudell, A. M.; Kiefer, D.; Chabinyc, M. L. Increasing the Thermoelectric Power Factor of a Semiconducting Polymer by Doping from the Vapor Phase. ACS Macro Lett. 2016, 5 (3), 268–272. https://doi.org/10.1021/acsmacrolett.5b00887.
(92) Dresselhaus, M. S.; Chen, G.; Tang, M. Y.; Yang, R. G.; Lee, H.; Wang, D. Z.; Ren, Z. F.; Fleurial, J.-P.; Gogna, P. New Directions for Low-Dimensional Thermoelectric Materials. Adv. Mater. 2007, 19 (8), 1043–1053. https://doi.org/10.1002/adma.200600527.
(93) Yao, H.; Fan, Z.; Cheng, H.; Guan, X.; Wang, C.; Sun, K.; Ouyang, J. Recent Development of Thermoelectric Polymers and Composites. Macromol. Rapid Commun. 2018, 39 (6), 1700727. https://doi.org/10.1002/marc.201700727.
(94) Chen, Y.; Zhao, Y.; Liang, Z. Solution Processed Organic Thermoelectrics: Towards Flexible Thermoelectric Modules. Energy Environ. Sci. 2015, 8 (2), 401–422. https://doi.org/10.1039/C4EE03297G.
(95) Faleev, S. V. Theory of Enhancement of Thermoelectric Properties of Materials with Nanoinclusions. Phys. Rev. B 2008, 77 (21). https://doi.org/10.1103/PhysRevB.77.214304.
(96) Moriarty Gregory P.; De Sukanta; King Paul J.; Khan Umar; Via Michael; King Julia A.; Coleman Jonathan N.; Grunlan Jaime C. Thermoelectric Behavior of Organic Thin Film Nanocomposites. J. Polym. Sci. Part B Polym. Phys. 2012, 51 (2), 119–123. https://doi.org/10.1002/polb.23186.
(97) Chabinyc, M. Thermoelectric Polymers: Behind Organics' Thermopower. Nat. Mater. 2014, 13 (2), 119–121. https://doi.org/10.1038/nmat3859.
(98) Reddy, P.; Jang, S.-Y.; Segalman, R. A.; Majumdar, A. Thermoelectricity in Molecular Junctions. Science 2007, 315 (5818), 1568–1571. https://doi.org/10.1126/science.1137149.

Chapter 2

(1) Kim, D.-H.; Lu, N.; Ma, R.; Kim, Y.-S.; Kim, R.-H.; Wang, S.; Wu, J.; Won, S. M.; Tao, H.; Islam, A.; Yu, K. J.; Kim, T.; Chowdhury, R.; Ying, M.; Xu, L.; Li, M.; Chung, H.-J.; Keum, H.; McCormick, M.; Liu, P.; Zhang, Y.-W.; Omenetto, F. G.; Huang, Y.; Coleman, T.; Rogers, J. A. Epidermal Electronics. Science 2011, 333 (6044), 838–843. https://doi.org/10.1126/science.1206157.

(2) Mostafalu, P.; Akbari, M.; Alberti, K. A.; Xu, Q.; Khademhosseini, A.; Sonkusale, S. R. A Toolkit of Thread-Based Microfluidics, Sensors, and Electronics for 3D Tissue Embedding for Medical Diagnostics. Microsyst. Nanoeng. 2016, 2 (1), 1–10. https://doi.org/10.1038/micronano.2016.39.

(3) Schwartz, G.; Tee, B. C.-K.; Mei, J.; Appleton, A. L.; Kim, D. H.; Wang, H.; Bao, Z. Flexible Polymer Transistors with High Pressure Sensitivity for Application in Electronic Skin and Health Monitoring. Nat. Commun. 2013, 4 (1), 1859. https://doi.org/10.1038/ncomms2832.

(4) O'Connor, T. F.; Zaretski, A. V.; Savagatrup, S.; Printz, A. D.; Wilkes, C. D.; Diaz, M. I.; Sawyer, E. J.; Lipomi, D. J. Wearable Organic Solar Cells with High Cyclic Bending Stability: Materials Selection Criteria. Sol. Energy Mater. Sol. Cells 2016, 144, 438–444. https://doi.org/10.1016/j.solmat.2015.09.049.

(5) Jost, K.; Dion, G.; Gogotsi, Y. Textile Energy Storage in Perspective. J. Mater. Chem. A 2014, 2 (28), 10776–10787. https://doi.org/10.1039/C4TA00203B.

(6) Kaltenbrunner, M.; White, M. S.; Głowacki, E. D.; Sekitani, T.; Someya, T.; Sariciftci, N. S.; Bauer, S. Ultrathin and Lightweight Organic Solar Cells with High Flexibility. Nat. Commun. 2012, 3, 770. https://doi.org/10.1038/ncomms1772.

(7) Kaltenbrunner, M.; Sekitani, T.; Reeder, J.; Yokota, T.; Kuribara, K.; Tokuhara, T.; Drack, M.; Schwödiauer, R.; Graz, I.; Bauer-Gogonea, S.; Bauer, S.; Someya, T. An Ultra-Lightweight Design for Imperceptible Plastic Electronics. Nature 2013, 499 (7459), 458–463. https://doi.org/10.1038/nature12314.

(8) White, M. S.; Kaltenbrunner, M.; Głowacki, E. D.; Gutnichenko, K.; Kettlgruber, G.; Graz, I.; Aazou, S.; Ulbricht, C.; Egbe, D. A. M.; Miron, M. C.; Major, Z.; Scharber, M. C.; Sekitani, T.; Someya, T.; Bauer, S.; Sariciftci, N. S. Ultrathin, Highly Flexible and Stretchable PLEDs. Nat. Photonics 2013, 7 (10), 811–816. https://doi.org/10.1038/nphoton.2013.188.

(9) Hamedi, M.; Forchheimer, R.; Inganäs, O. Towards Woven Logic from Organic Electronic Fibres. Nat. Mater. 2007, 6 (5), 357–362. https://doi.org/10.1038/nmat1884.

(10) Yang, Z.; Deng, J.; Chen, X.; Ren, J.; Peng, H. A Highly Stretchable, Fiber-Shaped Supercapacitor. Angew. Chem. 2013, 125 (50), 13695–13699. https://doi.org/10.1002/ange.201307619.

(11) Lee, M. R.; Eckert, R. D.; Forberich, K.; Dennler, G.; Brabec, C. J.; Gaudiana, R. A. Solar Power Wires Based on Organic Photovoltaic Materials. Science 2009, 324 (5924), 232–235. https://doi.org/10.1126/science.1168539.

(12) Cai, Z.; Li, L.; Ren, J.; Qiu, L.; Lin, H.; Peng, H. Flexible, Weavable and Efficient Microsupercapacitor Wires Based on Polyaniline Composite Fibers Incorporated with Aligned Carbon Nanotubes. J. Mater. Chem. A 2012, 1 (2), 258–261. https://doi.org/10.1039/C2TA00274D.

(13) Zheng, L.; Zhang, X.; Li, Q.; Chikkannanavar, S. B.; Li, Y.; Zhao, Y.; Liao, X.; Jia, Q.; Doorn, S. K.; Peterson, D. E.; Zhu, Y. Carbon-Nanotube Cotton for Large-

Scale Fibers. Adv. Mater. 2007, 19 (18), 2567–2570. https://doi.org/10.1002/adma.200602648.

(14) Ma, R.; Lee, J.; Choi, D.; Moon, H.; Baik, S. Knitted Fabrics Made from Highly Conductive Stretchable Fibers. Nano Lett. 2014, 14 (4), 1944–1951. https://doi.org/10.1021/nl404801t.

(15) Lee, J. A.; Shin, M. K.; Kim, S. H.; Cho, H. U.; Spinks, G. M.; Wallace, G. G.; Lima, M. D.; Lepró, X.; Kozlov, M. E.; Baughman, R. H.; Kim, S. J. Ultrafast Charge and Discharge Biscrolled Yarn Supercapacitors for Textiles and Microdevices. Nat. Commun. 2013, 4 (1), 1970. https://doi.org/10.1038/ncomms2970.

(16) Peng, M.; Zou, D. Flexible Fiber/Wire-Shaped Solar Cells in Progress: Properties, Materials, and Designs. J. Mater. Chem. A 2015, 3 (41), 20435–20458. https://doi.org/10.1039/C5TA03731J.

(17) Jost, K.; R. Perez, C.; K. McDonough, J.; Presser, V.; Heon, M.; Dion, G.; Gogotsi, Y. Carbon Coated Textiles for Flexible Energy Storage. Energy Environ. Sci. 2011, 4 (12), 5060–5067. https://doi.org/10.1039/C1EE02421C.

(18) Hu, L.; Pasta, M.; La Mantia, F.; Cui, L.; Jeong, S.; Deshazer, H. D.; Choi, J. W.; Han, S. M.; Cui, Y. Stretchable, Porous, and Conductive Energy Textiles. Nano Lett. 2010, 10 (2), 708–714. https://doi.org/10.1021/nl903949m.

(19) Koncar, V. Smart Textiles and Their Applications; Woodhead Publishing, 2016.

(20) Ding, Y.; Invernale, M. A.; Sotzing, G. A. Conductivity Trends of PEDOT-PSS Impregnated Fabric and the Effect of Conductivity on Electrochromic Textile. ACS Appl. Mater. Interfaces 2010, 2 (6), 1588–1593. https://doi.org/10.1021/am100036n.

(21) Amba Sankar K., N.; Mohanta, K. Dwindling the Resistance Value of PEDOT:PSS - Coated on Fabric Yarns. 2016, 1731, 120019. https://doi.org/10.1063/1.4948091.

(22) Yeon, C.; Kim, G.; W. Lim, J.; J. Yun, S. Highly Conductive PEDOT:PSS Treated by Sodium Dodecyl Sulfate for Stretchable Fabric Heaters. RSC Adv. 2017, 7 (10), 5888–5897. https://doi.org/10.1039/C6RA24749K.

(23) Wu, Q.; Hu, J. Waterborne Polyurethane Based Thermoelectric Composites and Their Application Potential in Wearable Thermoelectric Textiles. Compos. Part B Eng. 2016, 107, 59–66. https://doi.org/10.1016/j.compositesb.2016.09.068.

(24) Åkerfeldt, M.; Strååt, M.; Walkenström, P. Influence of Coating Parameters on Textile and Electrical Properties of a Poly(3,4-Ethylene Dioxythiophene):Poly(Styrene Sulfonate)/Polyurethane-Coated Textile. Text. Res. J. 2013, 83 (20), 2164–2176. https://doi.org/10.1177/0040517513487786.

(25) Ryan, J. D.; Mengistie, D. A.; Gabrielsson, R.; Lund, A.; Müller, C. Machine-Washable PEDOT:PSS Dyed Silk Yarns for Electronic Textiles. ACS Appl. Mater. Interfaces 2017, 9 (10), 9045–9050. https://doi.org/10.1021/acsami.7b00530.

(26) Kirihara, K.; Wei, Q.; Mukaida, M.; Ishida, T. Thermoelectric Power Generation Using Nonwoven Fabric Module Impregnated with Conducting Polymer PEDOT:PSS. Synth. Met. https://doi.org/10.1016/j.synthmet.2017.01.001.

(27) Du, Y.; Cai, K.; Chen, S.; Wang, H.; Shen, S. Z.; Donelson, R.; Lin, T. Thermoelectric Fabrics: Toward Power Generating Clothing. Sci. Rep. 2015, 5, 6411. https://doi.org/10.1038/srep06411.

(28) Müller, C.; Jansson, R.; Elfwing, A.; Askarieh, G.; Karlsson, R.; Hamedi, M.; Rising, A.; Johansson, J.; Inganäs, O.; Hedhammar, M. Functionalisation of Recombinant Spider Silk with Conjugated Polyelectrolytes. J. Mater. Chem. 2011, 21 (9), 2909–2915. https://doi.org/10.1039/C0JM03270K.

(29) Müller, C.; Hamedi, M.; Karlsson, R.; Jansson, R.; Marcilla, R.; Hedhammar, M.; Inganäs, O. Woven Electrochemical Transistors on Silk Fibers. Adv. Mater. 2011, 23 (7), 898–901. https://doi.org/10.1002/adma.201003601.

(30) Tarabella, G.; Villani, M.; Calestani, D.; Mosca, R.; Iannotta, S.; Zappettini, A.; Coppedè, N. A Single Cotton Fiber Organic Electrochemical Transistor for Liquid Electrolyte Saline Sensing. J. Mater. Chem. 2012, 22 (45), 23830–23834. https://doi.org/10.1039/C2JM34898E.

(31) Coppedè, N.; Tarabella, G.; Villani, M.; Calestani, D.; Iannotta, S.; Zappettini, A. Human Stress Monitoring through an Organic Cotton-Fiber Biosensor. J. Mater. Chem. B 2014, 2 (34), 5620–5626. https://doi.org/10.1039/C4TB00317A.

(32) Zhang, L.; Yu, Y.; Eyer, G. P.; Suo, G.; Kozik, L. A.; Fairbanks, M.; Wang, X.; Andrew, T. L. All-Textile Triboelectric Generator Compatible with Traditional Textile Process. Adv. Mater. Technol. 2016, 1 (9), 1600147. https://doi.org/10.1002/admt.201600147.

(33) Sadki, S.; Schottland, P.; Brodie, N.; Sabouraud, G. The Mechanisms of Pyrrole Electropolymerization. Chem. Soc. Rev. 2000, 29 (5), 283–293. https://doi.org/10.1039/A807124A.

(34) Subianto, S.; Will, GeoffreyD.; Kokot, S. Electropolymerization of Pyrrole on Cotton Fabrics. Int. J. Polym. Mater. 2005, 54 (2), 141–150. https://doi.org/10.1080/00914030390246252.

(35) Bhadani, S. N.; Kumari, M.; Gupta, S. K. S.; Sahu, G. C. Preparation of Conducting Fibers via the Electrochemical Polymerization of Pyrrole. J. Appl. Polym. Sci. 1997, 64 (6), 1073–1077. https://doi.org/10.1002/(SICI)1097-4628(19970509)64:6<1073::AID-APP6>3.0.CO;2-I.

(36) Molina, J.; del Río, A. I.; Bonastre, J.; Cases, F. Electrochemical Polymerisation of Aniline on Conducting Textiles of Polyester Covered with Polypyrrole/AQSA. Eur. Polym. J. 2009, 45 (4), 1302–1315. https://doi.org/10.1016/j.eurpolymj.2008.11.003.

(37) Molina, J.; del Río, A. I.; Bonastre, J.; Cases, F. Chemical and Electrochemical Polymerisation of Pyrrole on Polyester Textiles in Presence of Phosphotungstic

Acid. Eur. Polym. J. 2008, 44 (7), 2087–2098. https://doi.org/10.1016/j.eurpolymj.2008.04.007.

(38) Severt, S. Y.; Ostrovsky-Snider, N. A.; Leger, J. M.; Murphy, A. R. Versatile Method for Producing 2D and 3D Conductive Biomaterial Composites Using Sequential Chemical and Electrochemical Polymerization. ACS Appl. Mater. Interfaces 2015, 7 (45), 25281–25288. https://doi.org/10.1021/acsami.5b07332.

(39) Maziz, A.; Concas, A.; Khaldi, A.; Stålhand, J.; Persson, N.-K.; Jager, E. W. H. Knitting and Weaving Artificial Muscles. Sci. Adv. 3 (1), e1600327. https://doi.org/10.1126/sciadv.1600327.

(40) Das, C.; Jain, B.; Krishnamoorthy, K. Phenols from Green Tea as a Dual Functional Coating to Prepare Devices for Energy Storage and Molecular Separation. Chem. Commun. 2015, 51 (58), 11662–11664. https://doi.org/10.1039/C5CC03108G.

(41) Molina, J.; del Río, A. I.; Bonastre, J.; Cases, F. Influence of the Scan Rate on the Morphology of Polyaniline Grown on Conducting Fabrics. Centipede-like Morphology. Synth. Met. 2010, 160 (1), 99–107. https://doi.org/10.1016/j.synthmet.2009.10.012.

(42) Hong, K. H.; Oh, K. W.; Kang, T. J. Preparation and Properties of Electrically Conducting Textiles by in Situ Polymerization of Poly(3,4-Ethylenedioxythiophene). J. Appl. Polym. Sci. 2005, 97 (3), 1326–1332. https://doi.org/10.1002/app.21835.

(43) Varesano, A.; Aluigi, A.; Florio, L.; Fabris, R. Multifunctional Cotton Fabrics. Synth. Met. 2009, 159 (11), 1082–1089. https://doi.org/10.1016/j.synthmet.2009.01.036.

(44) Xu, J.; Wang, D.; Fan, L.; Yuan, Y.; Wei, W.; Liu, R.; Gu, S.; Xu, W. Fabric Electrodes Coated with Polypyrrole Nanorods for Flexible Supercapacitor Application Prepared via a Reactive Self-Degraded Template. Org. Electron. 2015, 26, 292–299. https://doi.org/10.1016/j.orgel.2015.07.054.

(45) Akşit, A. C.; Onar, N.; Ebeoglugil, M. F.; Birlik, I.; Celik, E.; Ozdemir, I. Electromagnetic and Electrical Properties of Coated Cotton Fabric with Barium Ferrite Doped Polyaniline Film. J. Appl. Polym. Sci. 2009, 113 (1), 358–366. https://doi.org/10.1002/app.29856.

(46) Maráková, N.; Humpolíček, P.; Kašpárková, V.; Capáková, Z.; Martinková, L.; Bober, P.; Trchová, M.; Stejskal, J. Antimicrobial Activity and Cytotoxicity of Cotton Fabric Coated with Conducting Polymers, Polyaniline or Polypyrrole, and with Deposited Silver Nanoparticles. Appl. Surf. Sci. 2017, 396, 169–176. https://doi.org/10.1016/j.apsusc.2016.11.024.

(47) Sarvi, A.; Silva, A. B.; Bretas, R. E.; Sundararaj, U. A New Approach for Conductive Network Formation in Electrospun Poly(Vinylidene Fluoride) Nanofibers. Polym. Int. 2015, 64 (9), 1262–1267. https://doi.org/10.1002/pi.4915.

(48) Ding, B.; Wang, M.; Wang, X.; Yu, J.; Sun, G. Electrospun Nanomaterials for Ultrasensitive Sensors. Mater. Today 2010, 13 (11), 16–27. https://doi.org/10.1016/S1369-7021(10)70200-5.
(49) Ye, W.; Zhu, J.; Liao, X.; Jiang, S.; Li, Y.; Fang, H.; Hou, H. Hierarchical Three-Dimensional Micro/Nano-Architecture of Polyaniline Nanowires Wrapped-on Polyimide Nanofibers for High Performance Lithium-Ion Battery Separators. J. Power Sources 2015, 299, 417–424. https://doi.org/10.1016/j.jpowsour.2015.09.037.
(50) Alf, M. E.; Asatekin, A.; Barr, M. C.; Baxamusa, S. H.; Chelawat, H.; Ozaydin-Ince, G.; Petruczok, C. D.; Sreenivasan, R.; Tenhaeff, W. E.; Trujillo, N. J.; Vaddiraju, S.; Xu, J.; Gleason, K. K. Chemical Vapor Deposition of Conformal, Functional, and Responsive Polymer Films. Adv. Mater. 2010, 22 (18), 1993–2027. https://doi.org/10.1002/adma.200902765.
(51) Bhattacharyya, D.; Howden, R. M.; Borrelli, D. C.; Gleason, K. K. Vapor Phase Oxidative Synthesis of Conjugated Polymers and Applications. J. Polym. Sci. Part B Polym. Phys. 2012, 50 (19), 1329–1351. https://doi.org/10.1002/polb.23138.
(52) Tenhaeff Wyatt E.; Gleason Karen K. Initiated and Oxidative Chemical Vapor Deposition of Polymeric Thin Films: ICVD and OCVD. Adv. Funct. Mater. 2008, 18 (7), 979–992. https://doi.org/10.1002/adfm.200701479.
(53) Vaeth, K. M.; Jensen, K. F. Selective Growth of Poly(p-Phenylene Vinylene) Prepared by Chemical Vapor Deposition. Adv. Mater. 1999, 11 (10), 814–820. https://doi.org/10.1002/(SICI)1521-4095(199907)11:10<814::AID-ADMA814>3.0.CO;2-Z.
(54) Lau, K. K. S.; Gleason, K. K. Initiated Chemical Vapor Deposition (ICVD) of Poly(Alkyl Acrylates): An Experimental Study. Macromolecules 2006, 39 (10), 3688–3694. https://doi.org/10.1021/ma0601619.
(55) Allison, L. K.; Andrew, T. L. A Wearable All-Fabric Thermoelectric Generator. Adv. Mater. Technol. 2019, 4 (5), 1800615. https://doi.org/10.1002/admt.201800615.
(56) Choy, K. L. Chemical Vapour Deposition of Coatings. Prog. Mater. Sci. 2003, 48 (2), 57–170. https://doi.org/10.1016/S0079-6425(01)00009-3.
(57) Dall'Acqua, L.; Tonin, C.; Varesano, A.; Canetti, M.; Porzio, W.; Catellani, M. Vapour Phase Polymerisation of Pyrrole on Cellulose-Based Textile Substrates. Synth. Met. 2006, 156 (5), 379–386. https://doi.org/10.1016/j.synthmet.2005.12.021.
(58) Shang, S.; Yang, X.; Tao, X.; Lam, S. S. Vapor-Phase Polymerization of Pyrrole on Flexible Substrate at Low Temperature and Its Application in Heat Generation. Polym. Int. 2010, 59 (2), 204–211. https://doi.org/10.1002/pi.2709.
(59) Bashir, T.; Ali, M.; Cho, S.-W.; Persson, N.-K.; Skrifvars, M. OCVD Polymerization of PEDOT: Effect of Pre-Treatment Steps on PEDOT-Coated Conductive Fibers and a Morphological Study of PEDOT Distribution on Textile

Yarns. Polym. Adv. Technol. 2013, 24 (2), 210–219. https://doi.org/10.1002/pat.3073.
(60) Laforgue, A.; Robitaille, L. Production of Conductive PEDOT Nanofibers by the Combination of Electrospinning and Vapor-Phase Polymerization. Macromolecules 2010, 43 (9), 4194–4200. https://doi.org/10.1021/ma9027678.
(61) Laforgue, A. Electrically Controlled Colour-Changing Textiles Using the Resistive Heating Properties of PEDOT Nanofibers. J. Mater. Chem. 2010, 20 (38), 8233–8235. https://doi.org/10.1039/C0JM02307H.
(62) Bashir, T.; Naeem, J.; Skrifvars, M.; Persson, N.-K. Synthesis of Electro-Active Membranes by Chemical Vapor Deposition (CVD) Process. Polym. Adv. Technol. 2014, 25 (12), 1501–1508. https://doi.org/10.1002/pat.3392.
(63) Kovacik, P.; Hierro, G. del; Livernois, W.; Gleason, K. K. Scale-up of OCVD: Large-Area Conductive Polymer Thin Films for next-Generation Electronics. Mater. Horiz. 2015, 2 (2), 221–227. https://doi.org/10.1039/C4MH00222A.
(64) Park, J.-H.; Sudarshan, T. S. Chemical Vapor Deposition; ASM International, 2001.
(65) Rajendran, S.; Nguyen, T. A.; Kakooei, S.; Li, Y.; Yeganeh, M. Corrosion Protection at the Nanoscale; Elsevier, 2020.
(66) Im, S. G.; Kusters, D.; Choi, W.; Baxamusa, S. H.; van de Sanden, M. C. M.; Gleason, K. K. Conformal Coverage of Poly(3,4-Ethylenedioxythiophene) Films with Tunable Nanoporosity via Oxidative Chemical Vapor Deposition. ACS Nano 2008, 2 (9), 1959–1967. https://doi.org/10.1021/nn800380e.
(67) Chen, N.; Wang, X.; Gleason, K. K. Conformal Single-Layer Encapsulation of PEDOT at Low Substrate Temperature. Appl. Surf. Sci. 2014, 323, 2–6. https://doi.org/10.1016/j.apsusc.2014.06.123.
(68) Chelawat, H.; Vaddiraju, S.; Gleason, K. Conformal, Conducting Poly(3,4-Ethylenedioxythiophene) Thin Films Deposited Using Bromine as the Oxidant in a Completely Dry Oxidative Chemical Vapor Deposition Process. Chem. Mater. 2010, 22 (9), 2864–2868. https://doi.org/10.1021/cm100092c.
(69) Barr Miles C.; Rowehl Jill A.; Lunt Richard R.; Xu Jingjing; Wang Annie; Boyce Christopher M.; Im Sung Gap; Bulović Vladimir; Gleason Karen K. Direct Monolithic Integration of Organic Photovoltaic Circuits on Unmodified Paper. Adv. Mater. 2011, 23 (31), 3500–3505. https://doi.org/10.1002/adma.201101263.
(70) Goktas, H.; Wang, X.; Boscher, N. D.; Torosian, S.; Gleason, K. K. Functionalizable and Electrically Conductive Thin Films Formed by Oxidative Chemical Vapor Deposition (OCVD) from Mixtures of 3-Thiopheneethanol (3TE) and Ethylene Dioxythiophene (EDOT). J. Mater. Chem. C 2016, 4 (16), 3403–3414. https://doi.org/10.1039/C6TC00567E.
(71) Howden, R. M.; McVay, E. D.; Gleason, K. K. OCVD Poly(3,4-Ethylenedioxythiophene) Conductivity and Lifetime Enhancement via Acid Rinse

Dopant Exchange. J. Mater. Chem. A 2012, 1 (4), 1334–1340. https://doi.org/10.1039/C2TA00321J.

(72) Chen, N.; Kim, D. H.; Kovacik, P.; Sojoudi, H.; Wang, M.; Gleason, K. K. Polymer Thin Films and Surface Modification by Chemical Vapor Deposition: Recent Progress. Annu. Rev. Chem. Biomol. Eng. 2016, 7 (1), 373–393. https://doi.org/10.1146/annurev-chembioeng-080615-033524.

(73) Im, S. G.; Gleason, K. K. Systematic Control of the Electrical Conductivity of Poly(3,4-Ethylenedioxythiophene) via Oxidative Chemical Vapor Deposition. Macromolecules 2007, 40 (18), 6552–6556. https://doi.org/10.1021/ma0628477.

(74) Goktas, H.; Wang, X.; Ugur, A.; Gleason, K. K. Water-Assisted Vapor Deposition of PEDOT Thin Film. Macromol. Rapid Commun. 2015, 36 (13), 1283–1289. https://doi.org/10.1002/marc.201500069.

(75) Li, Y.; Cheng, X. Y.; Leung, M. Y.; Tsang, J.; Tao, X. M.; Yuen, M. C. W. A Flexible Strain Sensor from Polypyrrole-Coated Fabrics. Synth. Met. 2005, 155 (1), 89–94. https://doi.org/10.1016/j.synthmet.2005.06.008.

(76) Hilt, F.; Boscher, N. D.; Duday, D.; Desbenoit, N.; Levalois-Grützmacher, J.; Choquet, P. Atmospheric Pressure Plasma-Initiated Chemical Vapor Deposition (AP-PiCVD) of Poly(Diethylallylphosphate) Coating: A Char-Forming Protective Coating for Cellulosic Textile. ACS Appl. Mater. Interfaces 2014, 6 (21), 18418–18422. https://doi.org/10.1021/am504892q.

(77) Abessolo Ondo, D.; Loyer, F.; Werner, F.; Leturcq, R.; Dale, P. J.; Boscher, N. D. Atmospheric-Pressure Synthesis of Atomically Smooth, Conformal, and Ultrathin Low-k Polymer Insulating Layers by Plasma-Initiated Chemical Vapor Deposition. ACS Appl. Polym. Mater. 2019, 1 (12), 3304–3312. https://doi.org/10.1021/acsapm.9b00759.

(78) Mohammadi, A.; Hasan, M.-A.; Liedberg, B.; Lundström, I.; Salaneck, W. R. Chemical Vapour Deposition (CVD) of Conducting Polymers: Polypyrrole. Synth. Met. 1986, 14 (3), 189–197. https://doi.org/10.1016/0379-6779(86)90183-9.

(79) Zhang, L.; Andrew, T. L. Deposition Dependent Ion Transport in Doped Conjugated Polymer Films: Insights for Creating High-Performance Electrochemical Devices. Adv. Mater. Interfaces 2017, 4 (23), n/a-n/a. https://doi.org/10.1002/admi.201700873.

(80) Wang, X.; Zhang, X.; Sun, L.; Lee, D.; Lee, S.; Wang, M.; Zhao, J.; Shao-Horn, Y.; Dincă, M.; Palacios, T.; Gleason, K. K. High Electrical Conductivity and Carrier Mobility in OCVD PEDOT Thin Films by Engineered Crystallization and Acid Treatment. Sci. Adv. 2018, 4 (9), eaat5780. https://doi.org/10.1126/sciadv.aat5780.

(81) Smolin, Yuriy. Y.; Soroush, M.; Lau, K. K. S. Influence of OCVD Polyaniline Film Chemistry in Carbon-Based Supercapacitors. Ind. Eng. Chem. Res. 2017, 56 (21), 6221–6228. https://doi.org/10.1021/acs.iecr.7b00441.

(82) Bhattacharya, S.; Datta, A.; Berg, J. M.; Gangopadhyay, S. Studies on Surface Wettability of Poly(Dimethyl) Siloxane (PDMS) and Glass under Oxygen-Plasma Treatment and Correlation with Bond Strength. J. Microelectromechanical Syst. 2005, 14 (3), 590–597. https://doi.org/10.1109/JMEMS.2005.844746.
(83) Bilger, D.; Homayounfar, S. Z.; Andrew, T. L. A Critical Review of Reactive Vapor Deposition for Conjugated Polymer Synthesis. J. Mater. Chem. C 2019, 7 (24), 7159–7174. https://doi.org/10.1039/C9TC01388A.
(84) Kim, J. J.; Allison, L. K.; Andrew, T. L. Vapor-Printed Polymer Electrodes for Long-Term, on-Demand Health Monitoring. Sci. Adv. 2019, 5 (3), eaaw0463. https://doi.org/10.1126/sciadv.aaw0463.
(85) Atanasov, S. E.; Losego, M. D.; Gong, B.; Sachet, E.; Maria, J.-P.; Williams, P. S.; Parsons, G. N. Highly Conductive and Conformal Poly(3,4-Ethylenedioxythiophene) (PEDOT) Thin Films via Oxidative Molecular Layer Deposition. Chem. Mater. 2014, 26 (11), 3471–3478. https://doi.org/10.1021/cm500825b.
(86) Lock, J. P.; Im, S. G.; Gleason, K. K. Oxidative Chemical Vapor Deposition of Electrically Conducting Poly(3,4-Ethylenedioxythiophene) Films. Macromolecules 2006, 39 (16), 5326–5329. https://doi.org/10.1021/ma060113o.
(87) Zhang, L.; Baima, M.; Andrew, T. L. Transforming Commercial Textiles and Threads into Sewable and Weavable Electric Heaters. ACS Appl. Mater. Interfaces 2017, 9 (37), 32299–32307. https://doi.org/10.1021/acsami.7b10514.
(88) Zhang Lushuai; Fairbanks Marianne; Andrew Trisha L. Rugged Textile Electrodes for Wearable Devices Obtained by Vapor Coating Off-the-Shelf, Plain-Woven Fabrics. Adv. Funct. Mater. 2017, 27 (24), 1700415. https://doi.org/10.1002/adfm.201700415.
(89) Zhang, L.; Andrew, T. Vapor-Coated Monofilament Fibers for Embroidered Electrochemical Transistor Arrays on Fabrics. Adv. Electron. Mater. 2018, 4 (9), 1800271. https://doi.org/10.1002/aelm.201800271.
(90) Allison, L.; Hoxie, S.; Andrew, T. L. Towards Seamlessly-Integrated Textile Electronics: Methods to Coat Fabrics and Fibers with Conducting Polymers for Electronic Applications. Chem. Commun. 2017, 53 (53), 7182–7193. https://doi.org/10.1039/C7CC02592K.

Chapter 3

(1) Chu, M.; Nguyen, T.; Pandey, V.; Zhou, Y.; Pham, H. N.; Bar-Yoseph, R.; Radom-Aizik, S.; Jain, R.; Cooper, D. M.; Khine, M. Respiration Rate and Volume Measurements Using Wearable Strain Sensors. Npj Digit. Med. 2019, 2 (1), 1–9. https://doi.org/10.1038/s41746-019-0083-3.

(2) Jortberg, E.; Silva, I.; Bhatkar, V.; McGinnis, R. S.; Sen-Gupta, E.; Morey, B.; Wright, J. A.; Pindado, J.; Bianchi, M. T. A Novel Adhesive Biosensor System for Detecting Respiration, Cardiac, and Limb Movement Signals during Sleep: Validation with Polysomnography. Nat. Sci. Sleep 2018, 10, 397–408. https://doi.org/10.2147/NSS.S179588.

(3) Raziq, A.; Kidakova, A.; Boroznjak, R.; Reut, J.; Öpik, A.; Syritski, V. Development of a Portable MIP-Based Electrochemical Sensor for Detection of SARS-CoV-2 Antigen. Biosens. Bioelectron. 2021, 178, 113029. https://doi.org/10.1016/j.bios.2021.113029.

(4) Jayarathna, T.; Gargiulo, G. D.; Breen, P. P. Continuous Vital Monitoring During Sleep and Light Activity Using Carbon-Black Elastomer Sensors. Sensors 2020, 20 (6). https://doi.org/10.3390/s20061583.

(5) Zhou, C.; Zhang, X.; Tang, N.; Fang, Y.; Zhang, H.; Duan, X. Rapid Response Flexible Humidity Sensor for Respiration Monitoring Using Nano-Confined Strategy. Nanotechnology 2020, 31 (12), 125302. https://doi.org/10.1088/1361-6528/ab5cda.

(6) Dai, J.; Zhao, H.; Lin, X.; Liu, S.; Fei, T.; Zhang, T. Design Strategy for Ultrafast-Response Humidity Sensors Based on Gel Polymer Electrolytes and Application for Detecting Respiration. Sens. Actuators B Chem. 2020, 304, 127270. https://doi.org/10.1016/j.snb.2019.127270.

(7) Dai, J.; Zhao, H.; Lin, X.; Liu, S.; Liu, Y.; Liu, X.; Fei, T.; Zhang, T. Ultrafast Response Polyelectrolyte Humidity Sensor for Respiration Monitoring. ACS Appl. Mater. Interfaces 2019, 11 (6), 6483–6490. https://doi.org/10.1021/acsami.8b18904.

(8) Wu, Z.; Yang, J.; Sun, X.; Wu, Y.; Wang, L.; Meng, G.; Kuang, D.; Guo, X.; Qu, W.; Du, B.; Liang, C.; Fang, X.; Tang, X.; He, Y. An Excellent Impedance-Type Humidity Sensor Based on Halide Perovskite CsPbBr3 Nanoparticles for Human Respiration Monitoring. Sens. Actuators B Chem. 2021, 337, 129772. https://doi.org/10.1016/j.snb.2021.129772.

(9) Guan, Y.; Le, X.; Hu, M.; Liu, W.; Xie, J. A Noninvasive Method for Monitoring Respiratory Rate of Rats Based on a Microcantilever Resonant Humidity Sensor. J. Micromechanics Microengineering 2019, 29 (12), 125001. https://doi.org/10.1088/1361-6439/ab43e8.

(10) Güder, F.; Ainla, A.; Redston, J.; Mosadegh, B.; Glavan, A.; Martin, T. J.; Whitesides, G. M. Paper-Based Electrical Respiration Sensor. Angew. Chem. Int. Ed. 2016, 55 (19), 5727–5732. https://doi.org/10.1002/anie.201511805.

(11) Wang, S.; Jiang, Y.; Tai, H.; Liu, B.; Duan, Z.; Yuan, Z.; Pan, H.; Xie, G.; Du, X.; Su, Y. An Integrated Flexible Self-Powered Wearable Respiration Sensor. Nano Energy 2019, 63, 103829. https://doi.org/10.1016/j.nanoen.2019.06.025.

(12) Min, S. D.; Yun, Y.; Shin, H. Simplified Structural Textile Respiration Sensor Based on Capacitive Pressure Sensing Method. IEEE Sens. J. 2014, 14 (9), 3245–3251. https://doi.org/10.1109/JSEN.2014.2327991.
(13) Guay, P.; Gorgutsa, S.; LaRochelle, S.; Messaddeq, Y. Wearable Contactless Respiration Sensor Based on Multi-Material Fibers Integrated into Textile. Sensors 2017, 17 (5), 1050. https://doi.org/10.3390/s17051050.
(14) Kano, S.; Dobashi, Y.; Fujii, M. Silica Nanoparticle-Based Portable Respiration Sensor for Analysis of Respiration Rate, Pattern, and Phase During Exercise. IEEE Sens. Lett. 2018, 2 (1), 1–4. https://doi.org/10.1109/LSENS.2017.2787099.
(15) Kano, S.; Fujii, M. All-Painting Process To Produce Respiration Sensor Using Humidity-Sensitive Nanoparticle Film and Graphite Trace. ACS Sustain. Chem. Eng. 2018, 6 (9), 12217–12223. https://doi.org/10.1021/acssuschemeng.8b02550.
(16) Jin, H.; Tao, X.; Dong, S.; Qin, Y.; Yu, L.; Luo, J.; Deen, M. J. Flexible Surface Acoustic Wave Respiration Sensor for Monitoring Obstructive Sleep Apnea Syndrome. J. Micromechanics Microengineering 2017, 27 (11), 115006. https://doi.org/10.1088/1361-6439/aa8ae0.
(17) Improving the Accuracy and Efficiency of Respiratory Rate Measurements in Children Using Mobile Devices https://journals.plos.org/plosone/article?id=10.1371/journal.pone.0099266 (accessed 2020 -09 -22).
(18) Mauri, T.; Turrini, C.; Eronia, N.; Grasselli, G.; Volta, C. A.; Bellani, G.; Pesenti, A. Physiologic Effects of High-Flow Nasal Cannula in Acute Hypoxemic Respiratory Failure. Am. J. Respir. Crit. Care Med. 2016, 195 (9), 1207–1215. https://doi.org/10.1164/rccm.201605-0916OC.
(19) Current evidence for the effectiveness of heated and humidified high flow nasal cannula supportive therapy in adult patients with respiratory failure | SpringerLink https://link.springer.com/article/10.1186/s13054-016-1263-z (accessed 2020 -09 -22).
(20) Zhang, H.; Zhang, J.; Hu, Z.; Quan, L.; Shi, L.; Chen, J.; Xuan, W.; Zhang, Z.; Dong, S.; Luo, J. Waist-Wearable Wireless Respiration Sensor Based on Triboelectric Effect. Nano Energy 2019, 59, 75–83. https://doi.org/10.1016/j.nanoen.2019.01.063.
(21) Dinh, T.; Nguyen, T.; Phan, H.-P.; Nguyen, N.-T.; Dao, D. V.; Bell, J. Stretchable Respiration Sensors: Advanced Designs and Multifunctional Platforms for Wearable Physiological Monitoring. Biosens. Bioelectron. 2020, 166, 112460. https://doi.org/10.1016/j.bios.2020.112460.
(22) Borini, S.; White, R.; Wei, D.; Astley, M.; Haque, S.; Spigone, E.; Harris, N.; Kivioja, J.; Ryhänen, T. Ultrafast Graphene Oxide Humidity Sensors. ACS Nano 2013, 7 (12), 11166–11173. https://doi.org/10.1021/nn404889b.
(23) Wang, Y.; Zhang, L.; Zhang, Z.; Sun, P.; Chen, H. High-Sensitivity Wearable and Flexible Humidity Sensor Based on Graphene Oxide/Non-Woven Fabric for

Respiration Monitoring. Langmuir 2020, 36 (32), 9443–9448. https://doi.org/10.1021/acs.langmuir.0c01315.
(24) Pang, Y.; Jian, J.; Tu, T.; Yang, Z.; Ling, J.; Li, Y.; Wang, X.; Qiao, Y.; Tian, H.; Yang, Y.; Ren, T.-L. Wearable Humidity Sensor Based on Porous Graphene Network for Respiration Monitoring. Biosens. Bioelectron. 2018, 116, 123–129. https://doi.org/10.1016/j.bios.2018.05.038.
(25) Allison, L. K.; Andrew, T. L. A Wearable All-Fabric Thermoelectric Generator. Adv. Mater. Technol. 0 (0), 1800615. https://doi.org/10.1002/admt.201800615.
(26) Zhang Lushuai; Fairbanks Marianne; Andrew Trisha L. Rugged Textile Electrodes for Wearable Devices Obtained by Vapor Coating Off-the-Shelf, Plain-Woven Fabrics. Adv. Funct. Mater. 2017, 27 (24), 1700415. https://doi.org/10.1002/adfm.201700415.
(27) Wang, H.; Ail, U.; Gabrielsson, R.; Berggren, M.; Crispin, X. Ionic Seebeck Effect in Conducting Polymers. Adv. Energy Mater. 2015, 5 (11), 1500044. https://doi.org/10.1002/aenm.201500044.

Chapter 4

(1) Chen, Z.; Zhao, D.; Ma, R.; Zhang, X.; Rao, J.; Yin, Y.; Wang, X.; Yi, F. Flexible Temperature Sensors Based on Carbon Nanomaterials. J. Mater. Chem. B 2021, 9 (8), 1941–1964. https://doi.org/10.1039/D0TB02451A.
(2) Koo, J.; Lee, C.; Chu, C. R.; Kang, S.-K.; Lee, H. M. Integration of Ultrathin Silicon and Metal Nanowires for High-Performance Transparent Electronics. Adv. Mater. Technol. 2020, 5 (4), 1900962. https://doi.org/10.1002/admt.201900962.
(3) Shin, J.; Jeong, B.; Kim, J.; Nam, V. B.; Yoon, Y.; Jung, J.; Hong, S.; Lee, H.; Eom, H.; Yeo, J.; Choi, J.; Lee, D.; Ko, S. H. Sensitive Wearable Temperature Sensor with Seamless Monolithic Integration. Adv. Mater. 2020, 32 (2), 1905527. https://doi.org/10.1002/adma.201905527.
(4) Yang, Q.; Wang, X.; Ding, X.; Li, Q. Fabrication and Characterization of Wrapped Metal Yarns-Based Fabric Temperature Sensors. Polymers 2019, 11 (10), 1549. https://doi.org/10.3390/polym11101549.
(5) Yan, C.; Wang, J.; Lee, P. S. Stretchable Graphene Thermistor with Tunable Thermal Index. ACS Nano 2015, 9 (2), 2130–2137. https://doi.org/10.1021/nn507441c.
(6) Agcayazi, T.; Chatterjee, K.; Bozkurt, A.; Ghosh, T. K. Flexible Interconnects for Electronic Textiles. Adv. Mater. Technol. 2018, 3 (10), 1700277. https://doi.org/10.1002/admt.201700277.

(7) Castano, L. M.; Flatau, A. B. Smart Fabric Sensors and E-Textile Technologies: A Review. Smart Mater. Struct. 2014, 23 (5), 053001. https://doi.org/10.1088/0964-1726/23/5/053001.
(8) Chen, N.; Kim, D. H.; Kovacik, P.; Sojoudi, H.; Wang, M.; Gleason, K. K. Polymer Thin Films and Surface Modification by Chemical Vapor Deposition: Recent Progress. Annu. Rev. Chem. Biomol. Eng. 2016, 7 (1), 373–393. https://doi.org/10.1146/annurev-chembioeng-080615-033524.
(9) Menon, A. K.; Meek, O.; Eng, A. J.; Yee, S. K. Radial Thermoelectric Generator Fabricated from N- and p-Type Conducting Polymers. J. Appl. Polym. Sci. 2017, 134 (3), n/a-n/a. https://doi.org/10.1002/app.44060.
(10) Kim, J.; Cho, G. Thermal Storage/Release, Durability, and Temperature Sensing Properties of Thermostatic Fabrics Treated with Octadecane-Containing Microcapsules. Text. Res. J. 2002, 72 (12), 1093–1098. https://doi.org/10.1177/004051750207201209.
(11) Catarino, A.; Carvalho, H.; Dias, M. J.; Pereira, T.; Postolache, O.; Girão, P. S. Continuous Health Monitoring Using E-Textile Integrated Biosensors. In 2012 International Conference and Exposition on Electrical and Power Engineering; 2012; pp 605–609. https://doi.org/10.1109/ICEPE.2012.6463867.
(12) Carvalho, H.; Catarino, A. P.; Rocha, A.; Postolache, O. Health Monitoring Using Textile Sensors and Electrodes: An Overview and Integration of Technologies. In 2014 IEEE International Symposium on Medical Measurements and Applications (MeMeA); 2014; pp 1–6. https://doi.org/10.1109/MeMeA.2014.6860033.
(13) Rai, P.; Kumar, P. S.; Oh, S.; Kwon, H.; Mathur, G. N.; Varadan, V. K.; Agarwal, M. P. Smart Healthcare Textile Sensor System for Unhindered-Pervasive Health Monitoring. In Nanosensors, Biosensors, and Info-Tech Sensors and Systems 2012; International Society for Optics and Photonics, 2012; Vol. 8344, p 83440E. https://doi.org/10.1117/12.921253.
(14) Rai, P.; Oh, S.; Shyamkumar, P.; Ramasamy, M.; Harbaugh, R. E.; Varadan, V. K. Nano- Bio- Textile Sensors with Mobile Wireless Platform for Wearable Health Monitoring of Neurological and Cardiovascular Disorders. J. Electrochem. Soc. 2013, 161 (2), B3116. https://doi.org/10.1149/2.012402jes.
(15) Merritt, C. R.; Troy Nagle, H.; Grant, E. Fabric-Based Active Electrode Design and Fabrication for Health Monitoring Clothing. IEEE Trans. Inf. Technol. Biomed. 2009, 13 (2), 274–280. https://doi.org/10.1109/TITB.2009.2012408.
(16) Kiaghadi, A.; Homayounfar, S. Z.; Gummeson, J.; Andrew, T.; Ganesan, D. Phyjama: Physiological Sensing via Fiber-Enhanced Pyjamas. Proc. ACM Interact. Mob. Wearable Ubiquitous Technol. 2019, 3 (3), 89:1-89:29. https://doi.org/10.1145/3351247.
(17) High Energy Density, Super-Deformable, Garment-Integrated Microsupercapacitors for Powering Wearable Electronics | ACS Applied Materials

& Interfaces https://pubs.acs.org/doi/full/10.1021/acsami.8b08408 (accessed 2020 -10 -15).

(18) Heikenfeld, J.; Jajack, A.; Rogers, J.; Gutruf, P.; Tian, L.; Pan, T.; Li, R.; Khine, M.; Kim, J.; Wang, J.; Kim, J. Wearable Sensors: Modalities, Challenges, and Prospects. Lab. Chip 2018, 18 (2), 217–248. https://doi.org/10.1039/C7LC00914C.

(19) Lim, Z. H.; Chia, Z. X.; Kevin, M.; Wong, A. S. W.; Ho, G. W. A Facile Approach towards ZnO Nanorods Conductive Textile for Room Temperature Multifunctional Sensors. Sens. Actuators B Chem. 2010, 151 (1), 121–126. https://doi.org/10.1016/j.snb.2010.09.037.

(20) Li, Y.; Cheng, X. Y.; Leung, M. Y.; Tsang, J.; Tao, X. M.; Yuen, M. C. W. A Flexible Strain Sensor from Polypyrrole-Coated Fabrics. Synth. Met. 2005, 155 (1), 89–94. https://doi.org/10.1016/j.synthmet.2005.06.008.

(21) Kano, S.; Fujii, M. All-Painting Process To Produce Respiration Sensor Using Humidity-Sensitive Nanoparticle Film and Graphite Trace. ACS Sustain. Chem. Eng. 2018, 6 (9), 12217–12223. https://doi.org/10.1021/acssuschemeng.8b02550.

(22) Wu, Z.; Yang, J.; Sun, X.; Wu, Y.; Wang, L.; Meng, G.; Kuang, D.; Guo, X.; Qu, W.; Du, B.; Liang, C.; Fang, X.; Tang, X.; He, Y. An Excellent Impedance-Type Humidity Sensor Based on Halide Perovskite CsPbBr3 Nanoparticles for Human Respiration Monitoring. Sens. Actuators B Chem. 2021, 337, 129772. https://doi.org/10.1016/j.snb.2021.129772.

(23) Krucińska, I.; Surma, B.; Chrzanowski, M.; Skrzetuska, E.; Puchalski, M. Application of Melt-Blown Technology for the Manufacture of Temperature-Sensitive Nonwoven Fabrics Composed of Polymer Blends PP/PCL Loaded with Multiwall Carbon Nanotubes. J. Appl. Polym. Sci. 2013, 127 (2), 869–878. https://doi.org/10.1002/app.37834.

(24) Huynh, T.-P.; Haick, H. Autonomous Flexible Sensors for Health Monitoring. Adv. Mater. 0 (0), 1802337. https://doi.org/10.1002/adma.201802337.

(25) Chen, Y.; Lu, B.; Chen, Y.; Feng, X. Breathable and Stretchable Temperature Sensors Inspired by Skin. Sci. Rep. 2015, 5 (1), 11505. https://doi.org/10.1038/srep11505.

(26) Im, S. G.; Kusters, D.; Choi, W.; Baxamusa, S. H.; van de Sanden, M. C. M.; Gleason, K. K. Conformal Coverage of Poly(3,4-Ethylenedioxythiophene) Films with Tunable Nanoporosity via Oxidative Chemical Vapor Deposition. ACS Nano 2008, 2 (9), 1959–1967. https://doi.org/10.1021/nn800380e.

(27) Husain, M. D.; Kennon, R.; Dias, T. Design and Fabrication of Temperature Sensing Fabric. J. Ind. Text. 2014, 44 (3), 398–417. https://doi.org/10.1177/1528083713495249.

(28) Bhat, N. V.; Seshadri, D. T.; Nate, M. M.; Gore, A. V. Development of Conductive Cotton Fabrics for Heating Devices. J. Appl. Polym. Sci. 2006, 102 (5), 4690–4695. https://doi.org/10.1002/app.24708.

(29) Tang, K.-P. M.; Kan, C.-W.; Fan, J. Evaluation of Water Absorption and Transport Property of Fabrics. Text. Prog. 2014, 46 (1), 1–132. https://doi.org/10.1080/00405167.2014.942582.
(30) Zhong, J.; Zhang, Y.; Zhong, Q.; Hu, Q.; Hu, B.; Wang, Z. L.; Zhou, J. Fiber-Based Generator for Wearable Electronics and Mobile Medication. ACS Nano 2014, 8 (6), 6273–6280. https://doi.org/10.1021/nn501732z.
(31) Zhang, F.; Zang, Y.; Huang, D.; Di, C.; Zhu, D. Flexible and Self-Powered Temperature–Pressure Dual-Parameter Sensors Using Microstructure-Frame-Supported Organic Thermoelectric Materials. Nat. Commun. 2015, 6, 8356. https://doi.org/10.1038/ncomms9356.
(32) Khan, Y.; Garg, M.; Gui, Q.; Schadt, M.; Gaikwad, A.; Han, D.; Yamamoto, N. A. D.; Hart, P.; Welte, R.; Wilson, W.; Czarnecki, S.; Poliks, M.; Jin, Z.; Ghose, K.; Egitto, F.; Turner, J.; Arias, A. C. Flexible Hybrid Electronics: Direct Interfacing of Soft and Hard Electronics for Wearable Health Monitoring. Adv. Funct. Mater. 2016, 26 (47), 8764–8775. https://doi.org/10.1002/adfm.201603763.
(33) Kim, S. L.; Choi, K.; Tazebay, A.; Yu, C. Flexible Power Fabrics Made of Carbon Nanotubes for Harvesting Thermoelectricity. ACS Nano 2014, 8 (3), 2377–2386. https://doi.org/10.1021/nn405893t.
(34) Lee, J.-W.; Han, D.-C.; Shin, H.-J.; Yeom, S.-H.; Ju, B.-K.; Lee, W. PEDOT:PSS-Based Temperature-Detection Thread for Wearable Devices. Sensors 2018, 18 (9). https://doi.org/10.3390/s18092996.
(35) Strümpler, R. Polymer Composite Thermistors for Temperature and Current Sensors. J. Appl. Phys. 1996, 80 (11), 6091–6096. https://doi.org/10.1063/1.363682.
(36) Hughes-Riley, T.; Lugoda, P.; Dias, T.; Trabi, C. L.; Morris, R. H. A Study of Thermistor Performance within a Textile Structure. Sensors 2017, 17 (8). https://doi.org/10.3390/s17081804.
(37) Lugoda, P.; Hughes-Riley, T.; Morris, R.; Dias, T. A Wearable Textile Thermograph. Sensors 2018, 18 (7). https://doi.org/10.3390/s18072369.
(38) Blasdel, N. J.; Wujcik, E. K.; Carletta, J. E.; Lee, K.-S.; Monty, C. N. Fabric Nanocomposite Resistance Temperature Detector. IEEE Sens. J. 2015, 15 (1), 300–306. https://doi.org/10.1109/JSEN.2014.2341915.
(39) Yokota, T.; Inoue, Y.; Terakawa, Y.; Reeder, J.; Kaltenbrunner, M.; Ware, T.; Yang, K.; Mabuchi, K.; Murakawa, T.; Sekino, M.; Voit, W.; Sekitani, T.; Someya, T. Ultraflexible, Large-Area, Physiological Temperature Sensors for Multipoint Measurements. Proc. Natl. Acad. Sci. 2015, 112 (47), 14533–14538. https://doi.org/10.1073/pnas.1515650112.
(40) Ramachandran, T.; Vigneswaran, C. Design and Development of Copper Core Conductive Fabrics for Smart Textiles. J. Ind. Text. 2009, 39 (1), 81–93. https://doi.org/10.1177/1528083709103317.

(41) Sibinski, M.; Jakubowska, M.; Sloma, M. Flexible Temperature Sensors on Fibers. Sensors 2010, 10 (9), 7934–7946. https://doi.org/10.3390/s100907934.
(42) Bielska, S.; Sibinski, M.; Lukasik, A. Polymer Temperature Sensor for Textronic Applications. Mater. Sci. Eng. B 2009, 165 (1), 50–52. https://doi.org/10.1016/j.mseb.2009.07.014.
(43) Daoud, W. A.; Xin, J. H.; Szeto, Y. S. Polyethylenedioxythiophene Coatings for Humidity, Temperature and Strain Sensing Polyamide Fibers. Sens. Actuators B Chem. 2005, 109 (2), 329–333. https://doi.org/10.1016/j.snb.2004.12.067.
(44) Wang, H.; Ail, U.; Gabrielsson, R.; Berggren, M.; Crispin, X. Ionic Seebeck Effect in Conducting Polymers. Adv. Energy Mater. 2015, 5 (11), 1500044. https://doi.org/10.1002/aenm.201500044.

Chapter 5

(1) Kim, M.-K.; Kim, M.-S.; Lee, S.; Kim, C.; Kim, Y.-J. Wearable Thermoelectric Generator for Harvesting Human Body Heat Energy. Smart Mater. Struct. 2014, 23 (10), 105002. https://doi.org/10.1088/0964-1726/23/10/105002.
(2) Jin Kim, S.; Hyung We, J.; Jin Cho, B. A Wearable Thermoelectric Generator Fabricated on a Glass Fabric. Energy Environ. Sci. 2014, 7 (6), 1959–1965. https://doi.org/10.1039/C4EE00242C.
(3) Hyland, M.; Hunter, H.; Liu, J.; Veety, E.; Vashaee, D. Wearable Thermoelectric Generators for Human Body Heat Harvesting. Appl. Energy 2016, 182, 518–524. https://doi.org/10.1016/j.apenergy.2016.08.150.
(4) Wang, J.; Cai, K.; Shen, S. A Facile Chemical Reduction Approach for Effectively Tuning Thermoelectric Properties of PEDOT Films. Org. Electron. 2015, 17 (Supplement C), 151–158. https://doi.org/10.1016/j.orgel.2014.12.007.
(5) Lund, A.; Tian, Y.; Darabi, S.; Müller, C. A Polymer-Based Textile Thermoelectric Generator for Wearable Energy Harvesting. J. Power Sources 2020, 480, 228836. https://doi.org/10.1016/j.jpowsour.2020.228836.
(6) Goldsmid, H. J. A Simple Technique for Determining the Seebeck Coefficient of Thermoelectric Materials. J. Phys. [E] 1986, 19 (11), 921. https://doi.org/10.1088/0022-3735/19/11/008.
(7) Elmoughni, H. M.; Menon, A. K.; Wolfe, R. M. W.; Yee, S. K. A Textile-Integrated Polymer Thermoelectric Generator for Body Heat Harvesting. Adv. Mater. Technol. 2019, 4 (7), 1800708. https://doi.org/10.1002/admt.201800708.
(8) Yu, C.; Murali, A.; Choi, K.; Ryu, Y. Air-Stable Fabric Thermoelectric Modules Made of N- and P-Type Carbon Nanotubes. Energy Environ. Sci. 2012, 5 (11), 9481–9486. https://doi.org/10.1039/C2EE22838F.

(9) Lee, J. J.; Yoo, D.; Park, C.; Choi, H. H.; Kim, J. H. All Organic-Based Solar Cell and Thermoelectric Generator Hybrid Device System Using Highly Conductive PEDOT:PSS Film as Organic Thermoelectric Generator. Sol. Energy 2016, 134, 479–483. https://doi.org/10.1016/j.solener.2016.05.006.

(10) Oh, J. Y.; Lee, J. H.; Han, S. W.; Chae, S. S.; Bae, E. J.; Kang, Y. H.; Choi, W. J.; Cho, S. Y.; Lee, J.-O.; Baik, H. K.; Lee, T. I. Chemically Exfoliated Transition Metal Dichalcogenide Nanosheet-Based Wearable Thermoelectric Generators. Energy Environ. Sci. 2016, 9 (5), 1696–1705. https://doi.org/10.1039/C5EE03813H.

(11) Zhu, T.; Liu, Y.; Fu, C.; Heremans, J. P.; Snyder, J. G.; Zhao, X. Compromise and Synergy in High-Efficiency Thermoelectric Materials. Adv. Mater. 2017, 29 (14), n/a-n/a. https://doi.org/10.1002/adma.201605884.

(12) Bell, L. E. Cooling, Heating, Generating Power, and Recovering Waste Heat with Thermoelectric Systems. Science 2008, 321 (5895), 1457–1461. https://doi.org/10.1126/science.1158899.

(13) Reenen, S. van; Kemerink, M. Correcting for Contact Geometry in Seebeck Coefficient Measurements of Thin Film Devices. Org. Electron. 2014, 15 (10), 2250–2255. https://doi.org/10.1016/j.orgel.2014.06.018.

(14) Petsagkourakis, I.; Pavlopoulou, E.; Cloutet, E.; Chen, Y. F.; Liu, X.; Fahlman, M.; Berggren, M.; Crispin, X.; Dilhaire, S.; Fleury, G.; Hadziioannou, G. Correlating the Seebeck Coefficient of Thermoelectric Polymer Thin Films to Their Charge Transport Mechanism. Org. Electron. 2018, 52 (Supplement C), 335–341. https://doi.org/10.1016/j.orgel.2017.11.018.

(15) Menon, A. K.; Yee, S. K. Design of a Polymer Thermoelectric Generator Using Radial Architecture. J. Appl. Phys. 2016, 119 (5), 055501. https://doi.org/10.1063/1.4941101.

(16) Rowe, D. M.; Min, G. Design Theory of Thermoelectric Modules for Electrical Power Generation. IEE Proc. - Sci. Meas. Technol. 1996, 143 (6), 351–356. https://doi.org/10.1049/ip-smt:19960714.

(17) Hu, E.; Kaynak, A.; Li, Y. Development of a Cooling Fabric from Conducting Polymer Coated Fibres: Proof of Concept. Synth. Met. 2005, 150 (2), 139–143. https://doi.org/10.1016/j.synthmet.2005.01.018.

(18) Singh, A.; Bhattacharya, S.; Thinaharan, C.; Aswal, D. K.; Gupta, S. K.; Yakhmi, J. V.; Bhanumurthy, K. Development of Low Resistance Electrical Contacts for Thermoelectric Devices Based on N-Type PbTe and p-Type TAGS-85 ((AgSbTe 2) 0.15 (GeTe) 0.85). J. Phys. Appl. Phys. 2009, 42 (1), 015502. https://doi.org/10.1088/0022-3727/42/1/015502.

(19) Zhu, Z.; Liu, C.; Jiang, F.; Xu, J.; Liu, E. Effective Treatment Methods on PEDOT:PSS to Enhance Its Thermoelectric Performance. Synth. Met. 2017, 225, 31–40. https://doi.org/10.1016/j.synthmet.2016.11.011.

(20) Jia, Y.; Li, X.; Jiang, F.; Li, C.; Wang, T.; Jiang, Q.; Hou, J.; Xu, J. Effects of Additives and Post-Treatment on the Thermoelectric Performance of Vapor-Phase Polymerized PEDOT Films. J. Polym. Sci. Part B Polym. Phys. n/a-n/a. https://doi.org/10.1002/polb.24422.

(21) Kim, N.; Lienemann, S.; Petsagkourakis, I.; Alemu Mengistie, D.; Kee, S.; Ederth, T.; Gueskine, V.; Leclère, P.; Lazzaroni, R.; Crispin, X.; Tybrandt, K. Elastic Conducting Polymer Composites in Thermoelectric Modules. Nat. Commun. 2020, 11 (1), 1424. https://doi.org/10.1038/s41467-020-15135-w.

(22) Chung, D. D. L. Electrical Applications of Carbon Materials. J. Mater. Sci. 2004, 39 (8), 2645–2661. https://doi.org/10.1023/B:JMSC.0000021439.18202.ea.

(23) Chang, W. B.; Fang, H.; Liu, J.; Evans, C. M.; Russ, B.; Popere, B. C.; Patel, S. N.; Chabinyc, M. L.; Segalman, R. A. Electrochemical Effects in Thermoelectric Polymers. ACS Macro Lett. 2016, 5 (4), 455–459. https://doi.org/10.1021/acsmacrolett.6b00054.

(24) Wu, H.; Huang, Y.; Xu, F.; Duan, Y.; Yin, Z. Energy Harvesters for Wearable and Stretchable Electronics: From Flexibility to Stretchability. Adv. Mater. 2016, 28 (45), 9881–9919. https://doi.org/10.1002/adma.201602251.

(25) Wang, J.; Cai, K.; Shen, S. Enhanced Thermoelectric Properties of Poly(3,4-Ethylenedioxythiophene) Thin Films Treated with H2SO4. Org. Electron. 2014, 15 (11), 3087–3095. https://doi.org/10.1016/j.orgel.2014.09.012.

(26) Luo, J.; Billep, D.; Waechtler, T.; Otto, T.; Toader, M.; Gordan, O.; Sheremet, E.; Martin, J.; Hietschold, M.; Zahn, D. R. T.; Gessner, T. Enhancement of the Thermoelectric Properties of PEDOT:PSS Thin Films by Post-Treatment. J. Mater. Chem. A 2013, 1 (26), 7576–7583. https://doi.org/10.1039/C3TA11209H.

(27) He, H.; Ouyang, J. Enhancements in the Mechanical Stretchability and Thermoelectric Properties of PEDOT:PSS for Flexible Electronics Applications. Acc. Mater. Res. 2020, 1 (2), 146–157. https://doi.org/10.1021/accountsmr.0c00021.

(28) Wei, Q.; Mukaida, M.; Kirihara, K.; Ishida, T. Experimental Studies on the Anisotropic Thermoelectric Properties of Conducting Polymer Films. ACS Macro Lett. 2014, 3 (9), 948–952. https://doi.org/10.1021/mz500446z.

(29) Saxena, N.; Keilhofer, J.; Maurya, A. K.; Fortunato, G.; Overbeck, J.; Müller-Buschbaum, P. Facile Optimization of Thermoelectric Properties in PEDOT:PSS Thin Films through Acido-Base and Redox Dedoping Using Readily Available Salts. ACS Appl. Energy Mater. 2018, 1 (2), 336–342. https://doi.org/10.1021/acsaem.7b00334.

(30) Zhang, F.; Zang, Y.; Huang, D.; Di, C.; Zhu, D. Flexible and Self-Powered Temperature–Pressure Dual-Parameter Sensors Using Microstructure-Frame-Supported Organic Thermoelectric Materials. Nat. Commun. 2015, 6, 8356. https://doi.org/10.1038/ncomms9356.

(31) Park, T.; Park, C.; Kim, B.; Shin, H.; Kim, E. Flexible PEDOT Electrodes with Large Thermoelectric Power Factors to Generate Electricity by the Touch of Fingertips. Energy Environ. Sci. 2013, 6 (3), 788–792. https://doi.org/10.1039/C3EE23729J.

(32) Kim, S. L.; Choi, K.; Tazebay, A.; Yu, C. Flexible Power Fabrics Made of Carbon Nanotubes for Harvesting Thermoelectricity. ACS Nano 2014, 8 (3), 2377–2386. https://doi.org/10.1021/nn405893t.

(33) Dun, C.; Hewitt, C. A.; Huang, H.; Montgomery, D. S.; Xu, J.; Carroll, D. L. Flexible Thermoelectric Fabrics Based on Self-Assembled Tellurium Nanorods with a Large Power Factor. Phys. Chem. Chem. Phys. 2015, 17 (14), 8591–8595. https://doi.org/10.1039/C4CP05390G.

(34) Ito, M.; Koizumi, T.; Kojima, H.; Saito, T.; Nakamura, M. From Materials to Device Design of a Thermoelectric Fabric for Wearable Energy Harvesters. J. Mater. Chem. A 2017, 5 (24), 12068–12072. https://doi.org/10.1039/C7TA00304H.

(35) Zuo, G.; Andersson, O.; Abdalla, H.; Kemerink, M. High Thermoelectric Power Factor from Multilayer Solution-Processed Organic Films. Appl. Phys. Lett. 2018, 112 (8), 083303. https://doi.org/10.1063/1.5016908.

(36) Thielen, M.; Sigrist, L.; Magno, M.; Hierold, C.; Benini, L. Human Body Heat for Powering Wearable Devices: From Thermal Energy to Application. Energy Convers. Manag. 2016, 131. https://doi.org/10.1016/j.enconman.2016.11.005.

(37) Kim, G.-H.; Kim, J.; Pipe, K. P. Humidity-Dependent Thermoelectric Properties of Poly(3,4-Ethylenedioxythiophene):Poly(Styrene Sulfonate). Appl. Phys. Lett. 2016, 108 (9), 093301. https://doi.org/10.1063/1.4942598.

(38) Glaudell, A. M.; Cochran, J. E.; Patel, S. N.; Chabinyc, M. L. Impact of the Doping Method on Conductivity and Thermopower in Semiconducting Polythiophenes. Adv. Energy Mater. 2015, 5 (4), n/a-n/a. https://doi.org/10.1002/aenm.201401072.

(39) Patel, S. N.; Glaudell, A. M.; Kiefer, D.; Chabinyc, M. L. Increasing the Thermoelectric Power Factor of a Semiconducting Polymer by Doping from the Vapor Phase. ACS Macro Lett. 2016, 5 (3), 268–272. https://doi.org/10.1021/acsmacrolett.5b00887.

(40) Wang, H.; Ail, U.; Gabrielsson, R.; Berggren, M.; Crispin, X. Ionic Seebeck Effect in Conducting Polymers. Adv. Energy Mater. 2015, 5 (11), 1500044. https://doi.org/10.1002/aenm.201500044.

(41) Zhao, D.; Wang, H.; U. Khan, Z.; C. Chen, J.; Gabrielsson, R.; P. Jonsson, M.; Berggren, M.; Crispin, X. Ionic Thermoelectric Supercapacitors. Energy Environ. Sci. 2016, 9 (4), 1450–1457. https://doi.org/10.1039/C6EE00121A.

(42) Yu, C.; Choi, K.; Yin, L.; Grunlan, J. C. Light-Weight Flexible Carbon Nanotube Based Organic Composites with Large Thermoelectric Power Factors. ACS Nano 2011, 5 (10), 7885–7892. https://doi.org/10.1021/nn202868a.

(43) Ryan, J. D.; Mengistie, D. A.; Gabrielsson, R.; Lund, A.; Müller, C. Machine-Washable PEDOT:PSS Dyed Silk Yarns for Electronic Textiles. ACS Appl. Mater. Interfaces 2017, 9 (10), 9045–9050. https://doi.org/10.1021/acsami.7b00530.
(44) Komatsu, N.; Ichinose, Y.; Dewey, O. S.; Taylor, L. W.; Trafford, M. A.; Yomogida, Y.; Wehmeyer, G.; Pasquali, M.; Yanagi, K.; Kono, J. Macroscopic Weavable Fibers of Carbon Nanotubes with Giant Thermoelectric Power Factor. Nat. Commun. 2021, 12 (1), 4931. https://doi.org/10.1038/s41467-021-25208-z.
(45) Hewitt, C. A.; Kaiser, A. B.; Roth, S.; Craps, M.; Czerw, R.; Carroll, D. L. Multilayered Carbon Nanotube/Polymer Composite Based Thermoelectric Fabrics. Nano Lett. 2012, 12 (3), 1307–1310. https://doi.org/10.1021/nl203806q.
(46) Dresselhaus, M. S.; Chen, G.; Tang, M. Y.; Yang, R. G.; Lee, H.; Wang, D. Z.; Ren, Z. F.; Fleurial, J.-P.; Gogna, P. New Directions for Low-Dimensional Thermoelectric Materials. Adv. Mater. 2007, 19 (8), 1043–1053. https://doi.org/10.1002/adma.200600527.
(47) Bubnova, O.; Khan, Z. U.; Malti, A.; Braun, S.; Fahlman, M.; Berggren, M.; Crispin, X. Optimization of the Thermoelectric Figure of Merit in the Conducting Polymer Poly(3,4-Ethylenedioxythiophene). Nat. Mater. 2011, 10 (6), 429–433. https://doi.org/10.1038/nmat3012.
(48) Russ, B.; Glaudell, A.; Urban, J. J.; Chabinyc, M. L.; Segalman, R. A. Organic Thermoelectric Materials for Energy Harvesting and Temperature Control. Nat. Rev. Mater. 2016, 1 (10), 16050. https://doi.org/10.1038/natrevmats.2016.50.
(49) Zhang, Q.; Sun, Y.; Xu, W.; Zhu, D. Organic Thermoelectric Materials: Emerging Green Energy Materials Converting Heat to Electricity Directly and Efficiently. Adv. Mater. 2014, 26 (40), 6829–6851. https://doi.org/10.1002/adma.201305371.
(50) Li, Y.; Du, Y.; Dou, Y.; Cai, K.; Xu, J. PEDOT-Based Thermoelectric Nanocomposites – A Mini-Review. Synth. Met. 2017, 226, 119–128. https://doi.org/10.1016/j.synthmet.2017.02.007.
(51) Park, T.; Na, J.; Kim, B.; Kim, Y.; Shin, H.; Kim, E. Photothermally Activated Pyroelectric Polymer Films for Harvesting of Solar Heat with a Hybrid Energy Cell Structure. ACS Nano 2015, 9 (12), 11830–11839. https://doi.org/10.1021/acsnano.5b04042.
(52) Petsagkourakis, I.; Kim, N.; Tybrandt, K.; Zozoulenko, I.; Crispin, X. Poly(3,4-Ethylenedioxythiophene): Chemical Synthesis, Transport Properties, and Thermoelectric Devices. Adv. Electron. Mater. 0 (0), 1800918. https://doi.org/10.1002/aelm.201800918.
(53) Mukaida, M.; Wei, Q.; Ishida, T. Polymer Thermoelectric Devices Prepared by Thermal Lamination. Synth. Met. 2017, 225, 64–69. https://doi.org/10.1016/j.synthmet.2016.11.016.
(54) Wei, Q.; Mukaida, M.; Kirihara, K.; Naitoh, Y.; Ishida, T. Polymer Thermoelectric Modules Screen-Printed on Paper. RSC Adv. 2014, 4 (54), 28802–28806. https://doi.org/10.1039/C4RA04946B.

(55) Zaia, E. W.; Gordon, M. P.; Yuan, P.; Urban, J. J. Progress and Perspective: Soft Thermoelectric Materials for Wearable and Internet-of-Things Applications. Adv. Electron. Mater. 2019, 5 (11), 1800823. https://doi.org/10.1002/aelm.201800823.
(56) Stepien, L.; Roch, A.; Tkachov, R.; Gedrange, T. Progress in Polymer Thermoelectrics. 2016. https://doi.org/10.5772/66196.
(57) Gueye, M. N.; Carella, A.; Faure-Vincent, J.; Demadrille, R.; Simonato, J.-P. Progress in Understanding Structure and Transport Properties of PEDOT-Based Materials: A Critical Review. Prog. Mater. Sci. 2020, 108, 100616. https://doi.org/10.1016/j.pmatsci.2019.100616.
(58) Menon, A. K.; Meek, O.; Eng, A. J.; Yee, S. K. Radial Thermoelectric Generator Fabricated from N- and p-Type Conducting Polymers. J. Appl. Polym. Sci. 2017, 134 (3), n/a-n/a. https://doi.org/10.1002/app.44060.
(59) Yao, H.; Fan, Z.; Cheng, H.; Guan, X.; Wang, C.; Sun, K.; Ouyang, J. Recent Development of Thermoelectric Polymers and Composites. Macromol. Rapid Commun. 2018, 39 (6), 1700727. https://doi.org/10.1002/marc.201700727.
(60) Wei, Q.; Mukaida, M.; Kirihara, K.; Naitoh, Y.; Ishida, T. Recent Progress on PEDOT-Based Thermoelectric Materials. Materials 2015, 8 (2), 732–750. https://doi.org/10.3390/ma8020732.
(61) Thomas, E. M.; Popere, B. C.; Fang, H.; Chabinyc, M. L.; Segalman, R. A. Role of Disorder Induced by Doping on the Thermoelectric Properties of Semiconducting Polymers. Chem. Mater. 2018, 30 (9), 2965–2972. https://doi.org/10.1021/acs.chemmater.8b00394.
(62) Guan, X.; Cheng, H.; Ouyang, J. Significant Enhancement in the Seebeck Coefficient and Power Factor of Thermoelectric Polymers by the Soret Effect of Polyelectrolytes. J. Mater. Chem. A 2018, 6 (40), 19347–19352. https://doi.org/10.1039/C8TA08387H.
(63) Wang, J.; Cai, K.; Song, H.; Shen, S. Simultaneously Enhanced Electrical Conductivity and Seebeck Coefficient in Poly (3,4-Ethylenedioxythiophene) Films Treated with Hydroiodic Acid. Synth. Met. 2016, 220 (Supplement C), 585–590. https://doi.org/10.1016/j.synthmet.2016.07.023.
(64) Rull-Bravo, M.; Moure, A.; Fernández, J. F.; Martín-González, M. Skutterudites as Thermoelectric Materials: Revisited. RSC Adv. 2015, 5 (52), 41653–41667. https://doi.org/10.1039/C5RA03942H.
(65) Gordon, M. P.; Zaia, E. W.; Zhou, P.; Russ, B.; Coates, N. E.; Sahu, A.; Urban, J. J. Soft PEDOT:PSS Aerogel Architectures for Thermoelectric Applications. J. Appl. Polym. Sci. 2017, 134 (3). https://doi.org/10.1002/app.44070.
(66) Mazaheripour, A.; Majumdar, S.; Hanemann-Rawlings, D.; Thomas, E. M.; McGuiness, C.; d'Alencon, L.; Chabinyc, M. L.; Segalman, R. A. Tailoring the Seebeck Coefficient of PEDOT:PSS by Controlling Ion Stoichiometry in Ionic Liquid Additives. Chem. Mater. 2018, 30 (14), 4816–4822. https://doi.org/10.1021/acs.chemmater.8b02114.

(67) Faleev, S. V. Theory of Enhancement of Thermoelectric Properties of Materials with Nanoinclusions. Phys. Rev. B 2008, 77 (21). https://doi.org/10.1103/PhysRevB.77.214304.
(68) Liu, J.; Wang, X.; Li, D.; Coates, N. E.; Segalman, R. A.; Cahill, D. G. Thermal Conductivity and Elastic Constants of PEDOT:PSS with High Electrical Conductivity. Macromolecules 2015, 48 (3), 585–591. https://doi.org/10.1021/ma502099t.
(69) Moriarty Gregory P.; De Sukanta; King Paul J.; Khan Umar; Via Michael; King Julia A.; Coleman Jonathan N.; Grunlan Jaime C. Thermoelectric Behavior of Organic Thin Film Nanocomposites. J. Polym. Sci. Part B Polym. Phys. 2012, 51 (2), 119–123. https://doi.org/10.1002/polb.23186.
(70) Kim, S. L.; Hsu, J.-H.; Yu, C. Thermoelectric Effects in Solid-State Polyelectrolytes. Org. Electron. 2018, 54, 231–236. https://doi.org/10.1016/j.orgel.2017.12.021.
(71) Nozariasbmarz, A.; Suarez, F.; Dycus, J. H.; Cabral, M. J.; LeBeau, J. M.; Öztürk, M. C.; Vashaee, D. Thermoelectric Generators for Wearable Body Heat Harvesting: Material and Device Concurrent Optimization. Nano Energy 2019, 104265. https://doi.org/10.1016/j.nanoen.2019.104265.
(72) Kim, G.; Pipe, K. P. Thermoelectric Model to Characterize Carrier Transport in Organic Semiconductors. Phys. Rev. B 2012, 86 (8), 085208. https://doi.org/10.1103/PhysRevB.86.085208.
(73) Kong, F.; Liu, C.; Xu, J.; Huang, Y.; Wang, J.; Sun, Z. Thermoelectric Performance Enhancement of Poly(3,4-Ethylenedioxythiophene):Poly(Styrenesulfonate) Composite Films by Addition of Dimethyl Sulfoxide and Urea. J. Electron. Mater. 2012, 41 (9), 2431–2438. https://doi.org/10.1007/s11664-012-2162-y.
(74) Chabinyc, M. Thermoelectric Polymers: Behind Organics' Thermopower. Nat. Mater. 2014, 13 (2), 119–121. https://doi.org/10.1038/nmat3859.
(75) Kirihara, K.; Wei, Q.; Mukaida, M.; Ishida, T. Thermoelectric Power Generation Using Nonwoven Fabric Module Impregnated with Conducting Polymer PEDOT:PSS. Synth. Met. https://doi.org/10.1016/j.synthmet.2017.01.001.
(76) Du, Y.; Xu, J.; Wang, Y.; Lin, T. Thermoelectric Properties of Graphite-PEDOT:PSS Coated Flexible Polyester Fabrics. J. Mater. Sci. Mater. Electron. 2016, 1–6. https://doi.org/10.1007/s10854-016-6250-2.
(77) Zhang, L.; Goto, T.; Imae, I.; Sakurai, Y.; Harima, Y. Thermoelectric Properties of PEDOT Films Prepared by Electrochemical Polymerization. J. Polym. Sci. Part B Polym. Phys. 2017, n/a-n/a. https://doi.org/10.1002/polb.24299.
(78) Ail, U.; Jafari, M. J.; Wang, H.; Ederth, T.; Berggren, M.; Crispin, X. Thermoelectric Properties of Polymeric Mixed Conductors. Adv. Funct. Mater. 2016, 26 (34), 6288–6296. https://doi.org/10.1002/adfm.201601106.

(79) Wang, J.; Cai, K.; Yin, J.; Shen, S. Thermoelectric Properties of the PEDOT/SWCNT Composite Films Prepared by a Vapor Phase Polymerization. Synth. Met. 2017, 224, 27–32. https://doi.org/10.1016/j.synthmet.2016.11.031.
(80) Reddy, P.; Jang, S.-Y.; Segalman, R. A.; Majumdar, A. Thermoelectricity in Molecular Junctions. Science 2007, 315 (5818), 1568–1571. https://doi.org/10.1126/science.1137149.
(81) Pu Xiong; Hu Weiguo; Wang Zhong Lin. Toward Wearable Self-Charging Power Systems: The Integration of Energy-Harvesting and Storage Devices. Small 2017, 14 (1), 1702817. https://doi.org/10.1002/smll.201702817.
(82) Bubnova, O.; Berggren, M.; Crispin, X. Tuning the Thermoelectric Properties of Conducting Polymers in an Electrochemical Transistor. J. Am. Chem. Soc. 2012, 134 (40), 16456–16459. https://doi.org/10.1021/ja305188r.
(83) Hu, X.; Chen, G.; Wang, X.; Wang, H. Tuning Thermoelectric Performance by Nanostructure Evolution of a Conducting Polymer. J. Mater. Chem. A 2015, 3 (42), 20896–20902. https://doi.org/10.1039/C5TA07381B.
(84) Wu, Q.; Hu, J. Waterborne Polyurethane Based Thermoelectric Composites and Their Application Potential in Wearable Thermoelectric Textiles. Compos. Part B Eng. 2016, 107, 59–66. https://doi.org/10.1016/j.compositesb.2016.09.068.
(85) Kim, M. K.; Kim, M. S.; Jo, S. E.; Kim, H. L.; Lee, S. M.; Kim, Y. J. Wearable Thermoelectric Generator for Human Clothing Applications. In 2013 Transducers Eurosensors XXVII: The 17th International Conference on Solid-State Sensors, Actuators and Microsystems (TRANSDUCERS EUROSENSORS XXVII); 2013; pp 1376–1379. https://doi.org/10.1109/Transducers.2013.6627034.
(86) Lee, J. A.; Aliev, A. E.; Bykova, J. S.; Andrade, M. J. de; Kim, D.; Sim, H. J.; Lepró, X.; Zakhidov, A. A.; Lee, J.-B.; Spinks, G. M.; Roth, S.; Kim, S. J.; Baughman, R. H. Woven-Yarn Thermoelectric Textiles. Adv. Mater. 2016, 28 (25), 5038–5044. https://doi.org/10.1002/adma.201600709.
(87) Bubnova, O.; Crispin, X. Towards Polymer-Based Organic Thermoelectric Generators. Energy Environ. Sci. 2012, 5 (11), 9345–9362. https://doi.org/10.1039/C2EE22777K.
(88) Peng, S.; Wang, D.; Lu, J.; He, M.; Xu, C.; Li, Y.; Zhu, S. A Review on Organic Polymer-Based Thermoelectric Materials. J. Polym. Environ. 2017, 25 (4), 1208–1218. https://doi.org/10.1007/s10924-016-0895-z.
(89) Snyder, G. J.; Toberer, E. S. Complex Thermoelectric Materials. Nat. Mater. 2008, 7 (2), 105–114. https://doi.org/10.1038/nmat2090.
(90) Leonov, V. Thermoelectric Energy Harvesting of Human Body Heat for Wearable Sensors. IEEE Sens. J. 2013, 13 (6), 2284–2291. https://doi.org/10.1109/JSEN.2013.2252526.
(91) Siddique, A. R. M.; Mahmud, S.; Heyst, B. V. A Review of the State of the Science on Wearable Thermoelectric Power Generators (TEGs) and Their Existing

Challenges. Renew. Sustain. Energy Rev. 2017, 73, 730–744. https://doi.org/10.1016/j.rser.2017.01.177.
(92) Wang, Z.; Leonov, V.; Fiorini, P.; Van Hoof, C. Realization of a Wearable Miniaturized Thermoelectric Generator for Human Body Applications. Sens. Actuators Phys. 2009, 156 (1), 95–102. https://doi.org/10.1016/j.sna.2009.02.028.
(93) K. Yee, S.; E. Coates, N.; Majumdar, A.; J. Urban, J.; A. Segalman, R. Thermoelectric Power Factor Optimization in PEDOT:PSS Tellurium Nanowire Hybrid Composites. Phys. Chem. Chem. Phys. 2013, 15 (11), 4024–4032. https://doi.org/10.1039/C3CP44558E.
(94) Lu, Z.; Zhang, H.; Mao, C.; Li, C. M. Silk Fabric-Based Wearable Thermoelectric Generator for Energy Harvesting from the Human Body. Appl. Energy 2016, 164, 57–63. https://doi.org/10.1016/j.apenergy.2015.11.038.
(95) Francioso, L.; Pascali, C. D.; Farella, I.; Martucci, C.; Cretì, P.; Siciliano, P.; Perrone, A. Flexible Thermoelectric Generator for Wearable Biometric Sensors. In 2010 IEEE Sensors; 2010; pp 747–750. https://doi.org/10.1109/ICSENS.2010.5690757.
(96) Cao, Z.; Koukharenko, E.; Tudor, M. J.; Torah, R. N.; Beeby, S. P. Screen Printed Flexible Bi 2 Te 3 -Sb 2 Te 3 Based Thermoelectric Generator. J. Phys. Conf. Ser. 2013, 476 (1), 012031. https://doi.org/10.1088/1742-6596/476/1/012031.
(97) Rare Earth Elements—Critical Resources for High Technology | USGS Fact Sheet 087-02 https://pubs.usgs.gov/fs/2002/fs087-02/ (accessed 2018 -06 -26).
(98) Leonov, V. Thermoelectric Energy Harvester on the Heated Human Machine. J. Micromechanics Microengineering 2011, 21 (12), 125013. https://doi.org/10.1088/0960-1317/21/12/125013.
(99) Jung, S.; Lauterbach, C.; Strasser, M.; Weber, W. Enabling Technologies for Disappearing Electronics in Smart Textiles. In 2003 IEEE International Solid-State Circuits Conference, 2003. Digest of Technical Papers. ISSCC.; 2003; pp 386–387 vol.1. https://doi.org/10.1109/ISSCC.2003.1234347.
(100) Chen, Y.; Zhao, Y.; Liang, Z. Solution Processed Organic Thermoelectrics: Towards Flexible Thermoelectric Modules. Energy Environ. Sci. 2015, 8 (2), 401–422. https://doi.org/10.1039/C4EE03297G.
(101) Yue, R.; Xu, J. Poly(3,4-Ethylenedioxythiophene) as Promising Organic Thermoelectric Materials: A Mini-Review. Synth. Met. 2012, 162 (11), 912–917. https://doi.org/10.1016/j.synthmet.2012.04.005.
(102) Cho, C.; Wallace, K. L.; Tzeng, P.; Hsu, J.-H.; Yu, C.; Grunlan, J. C. Outstanding Low Temperature Thermoelectric Power Factor from Completely Organic Thin Films Enabled by Multidimensional Conjugated Nanomaterials. Adv. Energy Mater. 2016, 6 (7), n/a-n/a. https://doi.org/10.1002/aenm.201502168.
(103) Du, Y.; Cai, K.; Chen, S.; Wang, H.; Shen, S. Z.; Donelson, R.; Lin, T. Thermoelectric Fabrics: Toward Power Generating Clothing. Sci. Rep. 2015, 5, 6411. https://doi.org/10.1038/srep06411.

(104) Allison, L. K.; Andrew, T. L. A Wearable All-Fabric Thermoelectric Generator. Adv. Mater. Technol. 0 (0), 1800615. https://doi.org/10.1002/admt.201800615.